Publication No. FHWA- RD-91-123
August 1992

Chemical Modification of Asphalts

U.S. Department of Transportation
Federal Highway Administration

Research and Development
Turner-Fairbank Highway Research Center
6300 Georgetown Pike
McLean, Virginia 22101-2296

FOREWORD

This report presents the findings of a laboratory study examining chemical modifications to asphalt and its effects on performance parameters. The study compares modified asphalt to virgin asphalt using standard performance parameters in hopes of reducing cracking and rutting in highway asphalt concretes. This report will be of interest to research and operations personnel involved with pavement mixtures involving modified asphalt binders.

Thomas J Pasko

Thomas J. Pasko Jr., P.E.
Director, Office of Engineering and
Highway Operations Research and
Development.

Technical Report Documentation Page

1. Report No. FHWA-RD-91-123	2. PB93-105955	3. Recipient's Catalog No.

4. Title and Subtitle
CHEMICAL MODIFICATION OF ASPHALTS

5. Report Date
August 1992

6. Performing Organization Code

7. Author's: D. Kumari, B. H. Chollar
J. A. Zenewitz and J. G. Boone

8. Performing Organization Report No.

9. Performing Organization Name and Address
Office of Engineering and Highway Operation R&D
Federal Highway Adminstration
6300 Georgetown pike
McLean, VA 22101-2296

10. Work Unit No. (TRAIS)
NCP 2E1A1011

11. Contract or Grant No.
In-House Report

12. Sponsoring Agency Name and Address
Office of Engineering and Highway Operation R&D
Federal Highway Adminstration
6300 Georgetown pike
McLean, VA 22101-2296

13. Type of Report and Period Covered
Final Report
Oct. 1988-Sept. 1991

14. Sponsoring Agency Code

15. Supplementary Notes
Viscoelastic properties were measured by Richard A. Sadar of Rheometrics, Inc., Piscataway, NJ. Drs N.Shashidhar and G.M.Memon assisted with data analysis and report editing. FHWA project Manager: Dr. Brian H. Chollar, HNR-30.

16. Abstract
Prominent among the damages occurring to asphalt cement concrete pavements are cracking and rutting. The occurrence of such damage is dependent upon many factors including the properties of the asphalt, which are, in turn, dependent upon its molecular structure. Experiments to test this hypothesis have been performed; these experiments include the modification of asphalt cements by reacting them separately with maleic anhydride, chromium trioxide and furfural in the presence of hydrochloric acid. Six different asphalts were used in these exploratory reactions. The original and chemically modified asphalts were subjected to laboratory tests to obtain such comparative parameters as penetration-viscosity number (PVN), penetration index (PI), limiting stiffness temperature (LST), aging index (AI), complex viscosity (η^*), storage modulus (G'), loss modulus (G''), complex modulus (G) and tan delta (tanδ). These data show that the chemically modified asphalts have potential for use in the highway pavements to help avoid cracking and rutting in such pavements. The adhesion to aggregate by the modified Wyoming pedestal test was performed. The chemical modification of asphalts improves the adhesive bond between asphalt and aggregate in an asphalt mixture implying an increased resistance to stripping. The presence of polar and polymerizing groups in the modified asphalts play a major role in controlling the adhesion to aggregate. The infrared spectra (IR) and high pressure-gel permeation chromatography (HP-GPC) support this hypothesis.

17. Key Words
Chemical modification of asphalts, MAH, CrO_3, furfural, temperature susceptibility, stripping test

18. Distribution Statement
No restrictions. This document is available to the public through the NTIS springfield, Virginia 22161.

19. Security Classif. (of this report) Unclassified	20. Security Classif. (of this page) Unclassified	21. No. of Pages 155	22. Price

Form DOT F 1700.7 (8-72)

Reproduction of completed page authorized

SI* (MODERN METRIC) CONVERSION FACTORS

APPROXIMATE CONVERSIONS TO SI UNITS

Symbol	When You Know	Multiply By	To Find	Symbol
		LENGTH		
in	inches	25.4	millimeters	mm
ft	feet	0.305	meters	m
yd	yards	0.914	meters	m
mi	miles	1.61	kilometers	km
		AREA		
in^2	square inches	645.2	millimeters squared	mm^2
ft^2	square feet	0.093	meters squared	m^2
yd^2	square yards	0.836	meters squared	m^2
ac	acres	0.405	hectares	ha
mi^2	square miles	2.59	kilometers squared	km^2
		VOLUME		
fl oz	fluid ounces	29.57	milliliters	ml
gal	gallons	3.785	liters	l
ft^3	cubic feet	0.028	meters cubed	m^3
yd^3	cubic yards	0.765	meters cubed	m^3
NOTE: Volumes greater than 1000 l shall be shown in m^3.				
		MASS		
oz	ounces	28.35	grams	g
lb	pounds	0.454	kilograms	kg
T	short tons (2000 lb)	0.907	megagrams	Mg
		TEMPERATURE (exact)		
°F	Fahrenheit temperature	5(F-32)/9 or (F-32)/1.8	Celcius temperature	°C
		ILLUMINATION		
fc	foot-candles	10.76	lux	l
fl	foot-Lamberts	3.426	candela/m^2	cd/m^2
		FORCE and PRESSURE or STRESS		
lbf	poundforce	4.45	newtons	N
psi	poundforce per square inch	6.89	kilopascals	kPa

APPROXIMATE CONVERSIONS FROM SI UNITS

Symbol	When You Know	Multiply By	To Find	Symbol
		LENGTH		
mm	millimeters	0.039	inches	in
m	meters	3.28	feet	ft
m	meters	1.09	yards	yd
km	kilometers	0.621	miles	mi
		AREA		
mm^2	millimeters squared	0.0016	square inches	in^2
m^2	meters squared	10.764	square feet	ft^2
m^2	meters squared	1.195	square yards	ac
ha	hectares	2.47	acres	mi^2
km^2	kilometers squared	0.386	square miles	
		VOLUME		
ml	milliliters	0.034	fluid ounces	fl oz
l	liters	0.264	gallons	gal
m^3	meters cubed	35.71	cubic feet	ft^3
m^3	meters cubed	1.307	cubic yards	yd^3
		MASS		
g	grams	0.035	ounces	oz
kg	kilograms	2.202	pounds	lb
Mg	megagrams	1.103	short tons (2000 lb)	T
		TEMPERATURE (exact)		
°C	Celcius temperature	1.8C + 32	Fahrenheit temperature	°F
		ILLUMINATION		
lx	lux	0.0929	foot-candles	fc
cd/m^2	candela/m^2	0.2919	foot-Lamberts	fl
		FORCE and PRESSURE or STRESS		
N	newtons	0.225	poundforce	lbf
kPa	kilopascals	0.145	poundforce per square inch	psi

* SI is the symbol for the International System of Units

(Revised January 1992)

TABLE OF CONTENTS

TABLE OF CONTENTS

Section Page

LIST OF FIGURES

LIST OF FIGURES (continued)

LIST OF FIGURES (continued)

LIST OF TABLES

LIST OF TABLES

Table Page

INTRODUCTION

BACKGROUND

Today, two of the most serious problems with asphalt pavements are cracking and rutting.(1-5) These decrease the lives of pavements and also result in increased rehabilitation costs. Over the years, researchers have classified cracking into two phenomenological categories: load associated and non-load associated.(1-3) The principal type of load associated cracking is fatigue cracking, the phenomenon of fracture under repeated or cyclic stress having a maximum value of less than the tensile strength of the material. The non-load associated cracks manifest themselves in the form of low-temperature shrinkage cracks.(3) Cracking of flexible pavements can occur when low winter temperatures induce tensile forces in asphalt concrete, which exceed the tensile strength of the material. Thermal cycling covering a wide, intermediate temperature range can also lead to a gradual pavement failure through thermal fatigue cracking. The magnitude of these stresses from thermal shrinkage is dependent on the rate of temperature drop and on the viscoelastic properties of the asphalt material at these low temperatures. Most low-temperature pavement failures are due to a combination of sudden, severe thermal stresses, thermal fatigue, and fatigue due to vehicular loads.(1-3) Asphalt is a material with thermoplastic properties, being solid or semi-solid at normal temperatures but softening and flowing when heat is applied and hardening when the temperature is lowered. Thus, at low temperatures, if asphalt receives a sudden impact, it breaks into pieces, and at a high temperature it softens and liquifies.

Excessive rutting in a highway pavement can create a serious safety hazard and can accelerate structural deterioration. A modified asphalt is needed that does not have an excessive stiffness at low temperatures so it can sustain severe thermal stress and resist thermal cracking and at the same time maintain a high stiffness at high temperatures to resist rutting. Very little work has been done on the modification of asphalts by means of chemical reactions. Nadkarni et al. have demonstrated that the modification of asphalt with maleic anhydride results in significant improvement in both the low temperature cracking resistance and the high temperature cohesive strength.(6) Recently, numerous papers have been published by Southwestern Laboratories and the FHWA on the chemical modification of asphalts.(7-10)

OBJECTIVE

The objective of the current research program is to modify asphalts by chemical means to produce asphalts which will have the potential for reducing both rutting and cracking when used in asphalt pavement construction. These asphalts would have a reduced stiffness at low temperatures and an adequate stiffness at high temperatures. These changes in properties would be accomplished by decreasing the asphalts' temperature susceptibility. Secondary aims are to produce asphalts with an improved adhesion to aggregates.

APPROACH

Asphalts with improved temperature susceptibilities and adhesion to aggregates can be obtained by introducing polar groups into candidate asphalts and also by increasing the size of their molecules by polymerization (by chemical reaction); both desirable attributes brought about by a change of the chemical makeup of the available candidate asphalts. It has been shown that the additions of polar groups to asphalts will help to promote the adhesion of such asphalts to aggregates in the presence of water and also retard oxidative hardening of such chemically treated asphalts.(11-15) In the present study, polar groups have been introduced by reacting asphalts with reagents such as maleic anhydride (MAH), chromium trioxide (CrO_3), hydrogen chloride gas (HCl), a nitrating mixture (HNO_3:H_2SO_4, 1:1, volume/volume), and sulfuric acid (H_2SO_4). Polymerizing groups (higher molecular size groups) and polar groups have been introduced in the asphalt by reacting samples with MAH, CrO_3 and furfural. Condensation reactions using potassium hydroxide (KOH) and triethylamine [$(CH_3CH_2)_3N$] have been evaluated. These preliminary reactions were performed with an AC-5 grade of asphalt (B-5901) to obtain a measurable change in an asphalt's properties, e.g., viscosity, penetration, softening point, but essentially a reduced temperature susceptibility and a resistance to stripping; all are due to our specific chemical reaction(s). This approach indicated that the reaction of an asphalt with MAH, CrO_3, and furfural produced improved and desirable characteristics in the modified asphalt. This judgement is based on the resultant viscosities, penetrations, softening points, temperature susceptibilities (PI, PVN, LST and various moduli) and stripping tests. The three successful reactions were then tried with five additional AC-5 grade asphalts to establish whether the same trend of modification was attainable. Here again, the desired improvements were attained. Next, it was decided to prepare AC-20 type of modified asphalts using these reactions with AC-5 grade asphalt and to compare the properties of the modified asphalts with those of an unmodified AC-20 asphalt with similar chemistry. An AC-5 and an AC-20 grade asphalt from the same refinery were used. These asphalts originated from the same crude oil using essentially the same distillation process. In order to change the AC-5 to an AC-20 grade asphalt for comparative purposes, it was reacted systematically with either 4% MAH, 1.5% CrO_3 or 1 ml furfural plus 5 ml of hydrochloric acid per 200 g of asphalt to obtain comparative AC-20 grade asphalt materials.

EXPERIMENTAL MATERIALS AND REACTION PROCEDURES

MATERIALS

Asphalts: The asphalt cements used in this study are identified in table 1.

Aggregates: A fine aggregate consisting of crushed granite and approximately 5 percent of slightly weathered material, and a aggregate consisting of angular and rounded quartz aggregate and a quartzite sand were used. These two kinds of sands were mixed in the ratio of 1:1. The sands also contained a small amount (< 3 percent) of sandstone. Both types, supplied by Julian, Inc., in northeast Maryland, were mixed in equal weight amounts and used for the pedestal test.

All reagents were of analytical grade from Baxter Scientific Products, Mcgaw Park, IL. unless other specified.

Table 1. Virgin asphalts used in the study.

FHWA ID	Grade	supplier
B-5901	AC-5	Chevron, Mobile, AL
C-9041	AC-5	Marathon Oil Co., detroit, MI
C-8613	120/150 Pen	Ashland, St. Paul, MN
C-8615	120/150 Pen	Murphy Oil Corp., Superior, WI
C-8561	AC-5	Marathon Oil Co., Cleveland, OH
C-9040	AC-5	SHRP, AAV
C-9042	AC-20	Marathon Oil Co., Detroit, MI

REACTION PROCEDURES

Reactions were performed using six AC-5 grade asphalts and a number of reagents under varied but controlled conditions. In some instances, reactions with each reagent were run in triplicate, and in some, just once (preliminary reactions). The physical and chemical test properties were measured and noted for each of the modified asphalts.

Maleic Anhydride (MAH) Reaction: The reaction apparatus consisted of a 500 ml three-necked round-bottomed flask, fitted with a mechanical stirrer, thermometer, gas inlet and gas outlet. A 200 g sample of asphalt was placed in the flask, and heated to 302 °F (150 °C) or, in some instances, to either 347 °F (175 °C) or 212 °F (100 °C) while flushing the system with either nitrogen or compressed air. A 20 g sample of maleic anhydride (10%) was then added to the asphalt through the gas outlet during the next 30 minutes. During this addition and for the next 6 h, the mixture was stirred continuously and the nitrogen or air flushing maintained. After 6.5 h, the reaction was terminated and the product was poured into an 8-oz metal container. This reaction was also performed using 6, 4, 3, and 2 percent of maleic anhydride.

Control Sample Conditions for the Maleic Anhydride (NOMAH) Reaction: Conditions were the same as in the maleic anhydride reaction omitting the MAH additive.

Chromium Trioxide (CrO_3) Reaction: A solution of 8 g of chromium trioxide (4 percent of the asphalt weight) in 16 ml of acetic anhydride and 64 ml of acetic acid was added to a 3-l, round-bottomed flask containing a solution of 200 g asphalt in 500 ml of methylene chloride. The mixture was stirred by a magnetic stirrer at room temperature for either 24 h or 72 h. The methylene chloride, acetic anhydride and acetic acid were removed by distillation. The modified asphalt product was recovered from the remaining methylene chloride, acetic anhydride and acetic acid by the Abson Method of recovery (ASTM D-1856). This reaction plus recovery was also performed with 2, 1.5, 1, and 0.5 percent of chromium trioxide reagent.

Chromium Trioxide (CrO_3) Reaction, Neat: The reaction apparatus consisted of a 500 ml, three-necked round-bottomed flask, fitted with a mechanical stirrer and a thermometer. A 200-g sample of asphalt was placed in the flask and heated to 180 °F (82.22 °C). A 3-g sample of chromium trioxide (1.5 percent of the asphalt weight) was added, then 3 ml of acetic acid was added in the next 10 minutes. The temperature of the asphalt was brought to 302 °F (150 °C) where it was kept for the next 6 h with continuous stirring. Finally the contents of the flask were poured into an 8-oz metal container.

Control Sample Conditions for the Chromium Trioxide ($NOCrO_3$) Reaction: A solution of 200-g asphalt in 500 ml of methylene chloride was stirred at room temperature for 24 h. The asphaltic reaction product was recovered by the Abson Method of recovery (ASTM D-1856).

Hydrogen Chloride Gas (HCl) Reaction: The hydrogen chloride gas was produced by reacting 156 g of sodium chloride with 131 g of concentrated sulfuric acid. The concentrated sulfuric acid was added dropwise through a dropping funnel on the solid sodium chloride. The gas was dried by passing it through concentrated sulfuric acid. A 200-g asphalt sample was dissolved in 500 ml of methylene chloride in a 3-l round-bottomed flask. Dry hydrogen chloride gas was bubbled through the solution for about 4 h with continuous stirring at room temperature. The solution was allowed to stand overnight at room temperature. The modified asphalt product was recovered by the Abson Method of recovery (ASTM D-1856).

Control Sample Conditions for the Hydrogen Chloride Gas (NOHCl) Reaction: Conditions were the same as for the control sample conditions for the chromium trioxide reaction ($NOCrO_3$).

Hydrochloric Acid (HCl) Reaction: To a 500-ml three-necked round-bottomed flask equipped with a thermometer and a mechanical stirrer, a 200-g asphalt sample was added and heated to 180 °F (82.22 °C). At this point, concentrated hydrochloric acid (1 ml or 5 ml) was added within a 5-min period. The contents of the flask were then heated to a temperature of 212 °F (100 °C) and were kept at this temperature for 4 h. The reaction product was then poured into a metal container of 200 g capacity.

Furfural Reaction: To a 500-ml three-necked round-bottomed flask equipped with a mechanical stirrer and a thermometer, were added 200 g of asphalt. The asphalt was heated to 210 °F (98.89 °C); furfural (2 ml) was added dropwise with continuous stirring. Hydrochloric acid (5 ml) was then added during the next 10 minutes. The contents of the flask were then heated to 240 °F (115.56 °C) and continuously stirred for an additional 4 h. The various concentrations of furfural and hydrochloric acid used per 200 g of asphalt have been varied and are given below for the various trials:

Table 2. Concentrations of Furfural and Hydrochloric Acid

Furfural	Hydrochloric Acid	Sample Designate
2 ml	2.5 ml	Furfural 2:2.5
2 ml	5 ml	Furfural 2:5
1 ml	5 ml	Furfural 1:5
0.75 ml	4 ml	Furfural 0.75:4
0.5 ml	2.5 ml	Furfural 0.5:2.5
0.5 ml	1.0 ml	Furfural 0.5:1

The reactions were also performed using 2 ml of furfural and 5 ml of ammonium hydroxide or 10 g of oxalic acid per 200 g of asphalt.

Oxalic Acid Reaction: To a 500-ml, three-necked, round-bottomed flask equipped with a thermometer, a mechanical stirrer, and a gas inlet and outlet tube for adding nitrogen during the reaction, a 200-g sample of asphalt was added and heated to 302 °F (150 °C). Ten grams of oxalic acid (5 percent of the asphalt weight) were added into the flask during the following 15 minutes. The contents of the flask were stirred at 302 °F (150 °C) for an additional 6 h, under nitrogen. The final product was poured into a 200-g capacity metal container.

Nitration Reaction, Neat: To a 500-ml three-necked, round-bottomed flask, equipped with a mechanical stirrer and a thermometer were added 200-g of asphalt. The asphalt was heated to 200 °F (93.33 °C). Dropwise, a solution mixture of 1 ml sulfuric and 1 ml nitric acid, i.e., 2 ml nitrating mixture was added to the asphalt within a 10-min period while stirring. The temperature of the reactants was then raised to 270 °F (132.22 °C). The contents were then continuously stirred at this temperature for an additional 3 h, after which, the resultant product was poured into a 200-g capacity metal can. In some samples the amount of the nitrating mixture added was varied using 0.5, 1, and 2 ml.

Nitration Reaction, Abson Method: To a 200-g sample of asphalt dissolved in 600 ml of methylene chloride in a 3-l flask, 2-ml of nitrating mixture was added. The contents of the flask were stirred by a magnetic stirrer at room temperature for the next 24 h. The product was recovered using the Abson Method (ASTM D-1856). The final product was poured into a 200-g capacity metal can. In one reaction, before performing an Abson recovery, 0.5 g of calcium oxide (CaO) was added to neutralize the excess of nitrating mixture.

Nitration-Reduction Reaction: Two hundred grams of asphalt was dissolved in 600 ml of methylene chloride. To this solution, 2-ml of nitrating mixture (1 ml sulfuric and 1 ml nitric acid) was added. It was stirred for 2 h, then 0.5 g of zinc and 1.5 ml of hydrochloric acid were added. The contents of the flask were stirred for about 20 h at room temperature. The modified product was recovered by the Abson Method. The final product was poured into a 200-g capacity metal can.

Sulfonation Reaction: To a 500-ml three-necked round-bottomed flask equipped with a mechanical stirrer and a thermometer, 200-g of asphalt was added. The asphalt was heated to a temperature of 200 °F (93.33 °C). Two milliliters of sulfuric acid was added drop by drop in a 10-min period while stirring. The contents of the flask were heated to 275 °F (135 °C), and kept at this temperature for an additional 3 h while stirring. The final product was poured into a 200-g capacity metal can. The reaction was also performed using 1 ml and 0.5 ml of sulfuric acid.

Sulfonation Reaction, Abson Method: To a 200-g sample of asphalt dissolved in 600 ml methylene chloride in a 3-l flask was added 1 ml conc. sulfuric acid. The contents of the flask were stirred at room temperature for 24 h with a magnetic stirrer. The modified product was recovered by the Abson Method. The final product was poured into a 200-g capacity metal can.

Condensation with Potassium Hydroxide (KOH) Reaction: To a 3-l round-bottomed flask equipped with a reflux condenser and a teflon magnetic bar, 200-g of asphalt was added. The asphalt was then dissolved with 600-ml of methylene chloride. A solution of either 1, 4 or 7.5 percent KOH (by weight of the asphalt) in methanol (100 ml) was added to the flask. The mixture was stirred and refluxed continuously for 6 h. After which, the modified resultant product was recovered by the Abson Method of recovery (ASTM D-1856). In one of the 4 percent reactions, the mixture was not refluxed, but kept with continuous stirring at room temperature for the 24 h. The product was recovered by an Abson Method.

Sulfanilic Acid Reaction: To a 500-ml three-necked round-bottomed flask equipped with a thermometer, mechanical stirrer, and gas inlet and outlet tubes, a 200-g sample of asphalt was added and heated to 302 °F (150 °C). Ten grams of sulfanilic acid was then added into the flask during the next 15 min. The contents of the flask were then heated for an additional 6 h at 302 °F (150 °C), under nitrogen while stirring. Finally the contents of the flask were poured into a 200-g capacity metal can.

Triethylamine Reaction: To a 200-g sample of asphalt dissolved in 600 ml of methylene chloride in a 3-l flask, 15 ml of triethylamine was added. The contents of the flask were refluxed for 6 h and then the product was recovered by the Abson Method. In a second reaction, after adding 15 ml of triethylamine; the solution was continuously stirred by magnetic stirrer at room temperature for 24 h. Finally the product was recovered using the Abson Method (ASTM D-1856).

TEST METHODS

Penetrations (Pen):(16,17) Penetration is defined as the depth, measured in dmm, that a standardized needle penetrates into an asphalt surface under a constant load (100 g) in a specified time (5 sec). Penetrations of virgin and modified asphalts were obtained at 77, 60 and 50 °F (25, 15.55 and 10 °C). The procedure is described in ASTM-D5 and AASHTO-T49.

Kinematic and Absolute Viscosities (Visc.):(18-21) The procedures in AASHTO-T201, ASTM-D2170, AASHTO-T202 and ASTM-D2171 were used to obtain the kinematic viscosities at 275 °F (135 °C) and the absolute viscosities at 140 °F (60 °C) of the virgin and modified asphalts.

Softening Point, Ring and Ball:(22) The softening point temperature was measured with a ring and ball apparatus. It is the temperature at which asphalt material becomes soft so that a steel ball of a standard dimension and weight (13.5 g) placed on the top surface of the asphalt specimen in a brass ring causes a prescribed deformation. The standard method is described in ASTM-D36.

Cone and Plate Viscosities:(23) The viscosity vs shear rate measurements were obtained for virgin and modified asphalts by using a Cone and Plate Viscometer obtained from the Cannon Instrument Company, PA. The instrument was operated at various temperatures over a wide range of shear rates. Comparative viscosities were used and reported at only two shear rates, viz. 0.05 and 0.01 sec^{-1}. A constant temperature bath was maintained by circulating water. Viscosities of virgin and modified asphalts were measured at various temperatures and shear rates according to the procedures given in ASTM-D3205.

Thin Film Oven Test (TFOT):(24,25) Asphalt (50 g) was poured into a specified dish. This thin film of asphalt was heated to and maintained at 325 °F (163 °C) for 5 h. Data for the loss on heating were obtained from this test. The test detects asphalts with volatile components that may be lost during the hot mix operation. Volatile loss leads to undesirable hardening of the asphalt. In this TFOT, the asphalt hardens from both the loss of light ends and from air oxidation during the 5 h period of heating. This test has been carried out according to the directions of ASTM-T1754 and AASHTO-T179.

Abson Method:(26) This method was used to recover asphalt from methylene chloride solutions and is the recommended recovery method of asphalt from a solution. The solvent is removed from the reacted asphalt by distillation. Carbon dioxide is used in the distillation process to provide agitation and to prevent foaming. This standard method is reported in ASTM-D1856.

Pen-Vis Number (PVN):(27,28) A penetration-viscosity number (pen-vis number), a measure of temperature-flow susceptibility of an asphalt, has been derived for each of the virgin asphalts and their chemically modified products. It is based on the penetration of an asphalt cement at 77 °F (25 °C) and its viscosity at 275 °F (135 °C) in centistokes or at 140 °F (60 °C) in poises.

PVN (77-275 °F) and PVN′ (77-140 °F) were computed by using the following equations:

PVN (77-275 °F) = $[(4.258 - 0.7967 \log P - \log X)/(0.79510 - 0.1858 \log P)](-1.5)$
P is penetration at 77 °F in decimillimeters and X is the viscosity at 275 °F in centistokes.

PVN′ (77-140 °F) = $[(6.489 - 1.590 \log P - \log X')/(1.050 - 0.2234 \log P)](-1.5)$
P is penetration at 77 °F in decimillimeters and X′ is viscosity at 140 °F in poises

A lower PVN (or PVN′) indicates a greater temperature susceptibility.

The Penetration Index (PI):(28,29) This is an index figure introduced by Pfeiffer and Van Doormaal to indicate the temperature susceptibility of an asphalt by using the equation: $PI = (20 - 500S)/(1 + 50S)$, where S is the slope and is developed with the equation, $S = d \log pen/dT$, from the penetrations at 50 °F (10 °C), 60 °F (15.55 °C) and 77 °F (25 °C).(29) The PI is thus a simple function of S, which in turn is a coefficient that describes the sensitivity of the penetration to changes with temperature. The value of S, and hence that of the PI, depends to some extent on the temperatures at which the penetrations are measured. A lower PI indicates a greater temperature susceptibility.

Limiting Stiffness Temperature (LST):(30) The limiting stiffness temperature (i.e., the predicted cracking temperature) is based on the hypothesis that a pavement cracks at a temperature where asphalt loses its viscous nature and becomes elastically hard. The LST predicts the minimum temperature below which cracking can be expected. It is calculated according to a procedure developed by the Asphalt Institute.(30) The equations used to calculate the LST are given below:

$$\log pen = ST + C$$

Where:
S = slope of the graphical plot of log pen vs temperature, and C is the Y intercept (log pen, where T = 0 °C).

Using the preceding equation and penetrations at three temperatures, both the C and S were calculated.

The softening point temperature T_{800}, was calculated by using the following equation:

$$T_{800} = \frac{\log 800 - C}{S}$$

It is assumed that the penetration at the softening point is 800 dmm. T_{800} is the temperature where the penetration is 800 dmm.

The temperature difference (ΔT) was calculated using the following equation taken from the plot of penetration index (PI) vs temperature difference (ΔT) in the Asphalt institute's procedure.(30)

$$\Delta T = \frac{PI+7.14}{0.069}$$

By subtracting ΔT from T_{800}, the LST has been calculated.

$$LST = T_{800} - \Delta T$$

ΔT, T_{800} and LST are in degrees celsius.

Aging Index:(32) Aging index is defined as a ratio of absolute viscosities.

Aging index = $Visc_{140}$ aged sample/$Visc_{140}$ unaged sample (by TFOT)

Since the viscosity normally increases with aging, the aging index, defined as a ratio of the viscosity after aging (using TFO test) to the viscosity before aging is always greater than 1. The interaction of an asphalt cement with its environment is considered the main cause of the hardening and the subsequent deterioration of the material with time. The phenomenon, known as age-hardening, is believed to be primarily due to an oxidation of the material. Oxidative hardening is an irreversible chemical reaction involving the components of an asphalt cement and environmental oxygen.

High-Pressure Liquid Chromatography (HPLC): Gel permeation chromatography (GPC), also called size exclusion chromatography (SEC), is a form of high pressure liquid chromatography (HPLC) that separates sample molecules on the basis of their hydrodynamic volume, or effective molecular size in solution. GPC is a non-interactive, nondestructive technique in which a separation is effected as sample molecules are forced through a rigid, highly porous, polymeric gel material packed in a stainless steel column. In GPC, large molecules elute (are removed) first due to restricted access to the pore structure in the packing material, whereas smaller molecules with greater access elute later. GPC is unique in its ability to furnish molecular size distribution (MSD) information.

The high pressure liquid chromatography data were obtained with a Waters 600E solvent delivery system equipped with a 990 Photodiode Array detector. One hundred microliters of sample was injected into the HPLC device which contains three columns containing polymeric gel material with decreasing pore sizes as follows: 1000°A, 500°A and 100°A. Tetrahydrofuran (THF) (from Baxter Health care Corp., Burdick and Jackson Division, Muschegan, Mich.), distilled from sodium metal and benzophenone under argon, was pumped at a rate of 1 ml/min as an eluant. The area of each of the chromatographs was partitioned into three sections representing large molecular size (LMS), medium molecular size (MMS) and small molecular size (SMS) components with the use of a UV detector at 340 nm.(33) Each sample was monitored with a Photodiode Array detector in the UV range of 200 to 600 nm. A typical HP-GPC chromatogram is shown in figure 1.

Infrared Spectroscopy (IR): Considering all of the measurable analytical responses of an organic compound, the single characteristic providing the most information about the compound's structure is its infrared spectrum. A molecule is constantly vibrating, its bonds stretch, contract, and bend with respect to each other. Changes in the vibrations of a molecule are caused by the absorption of infrared light; light lying beyond (lower frequency, longer wavelength, less energy) the red of the visible spectrum. An infrared spectrum is referred to either by its wavelength or preferably by its frequency. The wavelength is expressed in microns, μ ($1\mu = 10^{-4}$ cm). Frequency is expressed in wavenumber, cm^{-1}, often called reciprocal centimeters; the wavenumber is simply the number of waves per centimeter, and is equal to the reciprocal of the wavelength in centimeters. The infrared spectrum helps to reveal the structure of a compound by determining the groups that are present in or absent from the molecule. A particular group of atoms gives rise to characteristic absorption bands; that is to say, a particular group absorbs light of certain frequencies that are much the same from compound to compound.

The infrared spectrum of each sample was obtained using a Nicolet 10 DX spectrometer. Ten scans of a sample were taken and the data averaged. Hot asphalt was applied as a film on a KBr plate with a spatula. Some of the samples were prepared as KBr discs. Ten mg of asphalt and 250 mg of dried KBr were mixed mechanically for 5 min. The powder was transferred to a steel die and pressed under a vacuum with 15 tons/in^2 of pressure for 2 min. Using tweezers, the disc was then placed in the sample holder of the spectrometer. An infrared spectrum was obtained for the frequency range from 4600 - 400 cm^{-1}.

Determination of Viscoelastic Properties: Asphalts are viscoelastic materials. Hence their mechanical properties exhibit a pronounced dependence on the rate of loading. They also exhibit severe temperature dependency. In studying the viscoelastic response of asphalts, our tool of choice is dynamic mechanical analysis (DMA) which can be run either in a temperature sweep at a fixed frequency (rate of deformation) or in a frequency sweep at a fixed temperature.

The complex shear modulus, G^*, can be represented as

$$G^* = G' + iG''$$

where G' and G'' are termed the storage modulus and loss modulus, respectively. G' represents the elastic material response related to the potential energy stored by the asphalt under deformation, whereas the viscous response of the asphalt is characterized in terms of G'', which signifies the dissipation of energy as heat during deformation. The ratio of the two moduli is represented as

$$\text{tan delta}\ (\tan\delta) = G''/G'$$

where tan delta $(\tan\delta)$ represents the internal friction or dampening and is termed as a loss factor. The mathematical relationships between the parameters are well described in the literature.(34,35) All the parameters described in the immediate foregoing are ultimately related to the asphaltic molecular structure and to its molecular motions under stress, and therefore should yield useful information about the asphalt structures. These parameters, G', G'', and tan delta, are sensitive to the molecular structure of the asphalt. The value of the storage modulus, G', signifies the rigidity of the asphalt. The variation of G'' and tan delta with temperature provide information about the energy dissipated in the molecular motions and thereby the impact resistance of the asphalt.

Viscoelastic properties were determined by a dynamic method in which stress and strain follow the sinusoidal pattern as shown in figure 2. The ratio of the maximum stress to the maximum strain is the absolute value of the complex modulus, $|G^*|$. The time difference between input and output, called phase angle (δ). It is also called delta or phase lag. Storage modulus (G') and loss modulus (G'') are calculated from the phase angle, δ as follows:

$$G' = |G^*| \cos\delta$$

$$G'' = |G^*| \sin\delta$$

Complex viscosity (η^*) is defined as follows:

$$\eta^* = \frac{\sqrt{(G')^2 + (G'')^2}}{\omega} = \frac{G^*}{\omega}$$

Where ω is the frequency in radians/second.

The Rheometrics Dynamic Analyzer (RDA): The viscoelastic properties of the control and the chemically modified asphalts were measured with a Rheometrics Dynamic Analyzer (RDA). Rheological data were obtained over a range of frequencies from 0.1 to 100 radians/second and at 18 °F (10 °C) temperature intervals from -58 to 176 °F (-50 to 80 °C). Parallel plate and torsion rectangular geometry were used, employing a 2 by 10 by 1/2-cm bar of asphalt from -58 to -4 °F (-50 to -20 °C), a 3.95 mm radius plate from 14 to 68 °F (-10 to 20 °C), and a 12.5 mm radius plate from 86 to 176 °F (30 to 80 °C). Sample thickness between the parallel plates (gap) was usually 1 mm to 2 mm.

A sample is sinusoidally strained at a controlled amplitude and frequency. A torque transducer measures the resulting sinusoidal force that is transmitted through the sample. These oscillations are analyzed electronically. When the two waves superimpose, the material is purely elastic as shown in figure 3, when they are displaced by a phase angle of 90°, the material is purely viscous as shown in figure 4. An asphalt material is viscoelastic and has a phase angle between 0° and 90°. In general, rheological properties may vary with amplitude, frequency and temperature.

Rheological parameters, such as complex viscosity (η^*), complex modulus (G^*), storage modulus (G'), loss modulus (G''), and tan delta ($\tan\delta$) are measured simultaneously.

Freeze-Thaw Pedestal Test: The asphalt-aggregate bond in asphalt pavements can be weakened or destroyed in wet environments, especially if the moisture penetrates into the asphalt concrete. The effects of water damage include stripping of the asphalt cement from the aggregate, flushing of the asphalt cement, and various localized structural failures. Stripping also occurs when moisture enters the asphalt aggregate interface regions and disrupts the mechanical and chemical bond formed between the asphalt and aggregate. This process may weaken the adhesive bond without actually stripping the asphalt from the aggregate's surface and may, in fact, be the most common form of moisture-induced pavement distress.

A water susceptibility test for asphalt mixtures developed by Plancher et al., a pedestal test, was used in this study.(36) For this, briquets were made by heating an aggregate (150 g) in an oven for 3 h at 302 °F (150 °C) and heating asphalt (10.5 g) at 302 °F (150 °C) for 30 minutes. The hot asphalt was then poured onto the aggregate and stirred continuously with a spatula until all of the aggregate was thoroughly coated with asphalt. The mixture was then split into three equal portions by weight. Each portion was placed in the oven at 302 °F (150 °C) for 20 minutes and then immediately poured into a mold, and compacted into a briquet. The briquets used in this study are 0.750 in (1.905 cm) thick and 1.627 in (4.133 cm) in diameter and weigh approximately 50 g. The three prepared briquets were cured at room temperature overnight before testing. The briquets were subjected to 23 h of freezing at -11 °F (-25 °C), a 1-h thawing in a water bath at 125.6 °F (52 °C) and 23 h of further thaw conditioning in an oven at 140 °F (60 °C). Failure and termination were determined when briquets exhibited a splitting exfoliation.

Chromatographic Analysis of the Chemically Modified Asphalts:(37) The asphalts, virgin (B-5901) and its various resultant products from reactions with maleic anhydride, chromium trioxide, and furfural, were each separated into four distinct chemical fractions by the use of a method described in ASTM D-4124. An asphaltene fraction was the first obtainable by precipitation with n-heptane. The n-heptane soluble material, the maltenes, was then separated into three fractions, the saturates, the naphthene-aromatics and the polar-aromatics by elution through an alumina column; the saturates were eluted from the column with heptane, the naphthene-aromatics by toluene and the polar-aromatics with toluene and methanol. The amounts of each of the components thus obtained for the virgin and its various reacted versions are reported in table 3.

Table 3. Compositional analyses of the B-5901 virgin asphalt and its chemically modified versions.

Sample	Asphaltenes %	Saturates %	Naphthene Aromatics %	Polar Aromatics %
B-5901 Virgin	11.26	15.74	27.92	45.07
MAH 10% N_2	24.81	18.06	34.92	22.20
CrO_3 4%	26.36	26.45	34.80	12.37
Furfural 2:5	14.71	21.75	32.70	30.82

RESULTS AND DISCUSSION

PHYSICAL PROPERTIES

Table 4 presents the consistency properties, penetration at 77 °F (25 °C), viscosity at 140 °F (60 °C) and softening point of the B-5901 virgin asphalt and its chemically-modified versions. It shows the dramatic decrease in penetration at 77 °F (25 °C) and an increase in viscosity at 140 °F (60 °C) and softening point, which occur when the asphalt is reacted with maleic anhydride (MAH), chromium trioxide (CrO_3), furfural, hydrogen chloride gas (HCl), nitrating mixture, sulfuric acid and potassium hydroxide (KOH). The increase in viscosity at 140 °F (60 °C) and softening point indicate a better resistance to high-temperature flow and rutting.(38) Table 5 presents the properties of the thin film oven test residues. It shows that the modified asphalts have higher viscosities as compared to that of the virgin asphalt.

Penetration-viscosity number (PVN) at 25-60 °C (77-140 °F), penetration index (PI), the limiting stiffness temperature (LST) and aging index are presented in table 6. PVN and PI are measures of temperature susceptibility, the rate at which the consistency of an asphalt cement changes with temperature. PVN provides a quantitative measure of the variation in temperature susceptibilities of asphalt cements.

McLeod used the PVN to select asphalts for use in pavements.(27,39) According to McLeod asphalts with PVN values greater than -0.5 can be used in pavements for all traffic situations; values between -1.0 and -0.5 indicate an asphalt suitable for pavements in moderate traffic; and PVN values less than -1.0 suitable for only those pavements with low traffic situations. PVN values in table 6 for almost all the modified asphalt's are higher than that of the B-5901 virgin asphalt and therefore indicate that these products have a lower temperature susceptibility than the virgin asphalt, which enables the pavement with this asphaltic product to resist rutting and cracking simultaneously. Pfeiffer and Van Doormaal expressed the temperature susceptibility quantitatively as penetration index PI and mentioned that the pavements with asphalts having higher PI's have generally shown lesser tendency to crack than those made with asphalts having low PI's.(29) Fromm and Phang have recommended use of an asphalt with a PI of zero or greater to avoid cracking at low temperatures in a bituminous pavement.(40)

Cracking resistance of a pavement at low temperatures increases as the limiting stiffness temperature (LST) value of its asphalt decreases. Almost all the PI values in table 6 for the modified asphalt products are higher and almost all the LST values with the exception of CrO_3 for the modified asphalt products are lower than those of the virgin or control asphalts. This indicates that pavements made with these products may have a lesser tendency to crack at lower temperatures than pavements made with the virgin asphalts.

The modified products from the maleic anhydride, chromium trioxide or furfural reactions appear to be greatly improved (with a few exceptions) since they have positive PVN and PI values. The LST of the MAH and furfural modified asphalts were also lower than that of the unmodified asphalt. The aging indices of the modified asphalts are higher than that of the B-5901 virgin asphalt except for those products from the furfural, potassium hydroxide, hydrogen chloride gas reacted asphalts and products from the low concentrations of CrO_3, which have lower or equal aging indices. Findings from the pedestal test are reported in table 7. The maleic anhydride, chromium trioxide and furfural reacted asphalts again showed much better performances than that of the B-5901 virgin asphalt.

Table 4. Penetrations, viscosities and softening points of the B-5901 virgin asphalt and its chemically modified versions.

Sample	Pen. 77 °F dmm SD	Visc. 140 °F poise SD	Soft. Point °F SD
B-5901 Virgin	139 ± 7	613 ± 14	114.33 ± 1.2
CrO_3 0.5%	88 ± 16	1688 ± 532	123.5 ± 6.4
CrO_3 1%	96	1140	120
CrO_3 2%	65 ± 11.31	3000 ± 1400	130.5 ± 6.4
CrO_3 4%	41 ± 6.5	12428 ± 4830	144 ± 4.3
CrO_3 4% 72 Hrs	54	14156	142
CrO_3 4% Neat	161	-----	114
Furfural-Oxalic Acid	151	832	117
Furfural-NH_4OH	153	604	115
Furfural 0.5:1	100 ± 13	1579 ± 750	123.5 ± 4.9
Furfural 0.5:2.5	72	3050	131
Furfural 1:1	94	1517	123
Furfural 1:5	67	3432	131
Furfural 2:5	53 ± 5	10200 ± 3500	141.33 ± 2.1
HCl acid 5 ml	74	2592	124
HCl acid 1 ml	93	1368	124
HCl gas	83 ± 12	3800 ± 3200	125 ± 6
KOH 1%	92	1372	125
KOH 4% A 24 h	97	1298	122
KOH 4% R 6 h	58	8552	139
KOH 7.5% R 6 h	82	10025	139
MAH 10% 175 °C	54	13012	147
MAH 10% Air	58	11394	140
MAH 10% N_2	60 ± 4	7697 ± 2585	140.5 ± 2.5
MAH 2.5% N_2 100 °C	94	1550	126
MAH 2%	88	1800	125
MAH 5%	65	4871	136
Nitration 1:1 Abson	56 ± 5	12000 ± 6900	142.3 ± 4.4
Nitration 1:1 3 h Heat	67	6380	136
Nitration CaO Abson	68	3904	131
Nitration Neat 2 ml	104	1085	122
Nitration-reduction	43	42374	153
$NOCrO_3$	121.7 ± 11	840 ± 62	116.3 ± 2.1
NOMAH 175 °C	138	637	113
NOMAH AIR 150 °C	108	756	116
NOMAH N_2 150 °C	126 ± 7	707 ± 97	115.7 ± 1.2

Table 4. Penetrations, viscosities and softening points of the B-5901 virgin asphalt and its chemically modified versions (continued).

Sample	Pen. 77 °F dmm DS	Visc. 140 °F poise DS	Soft. Point °F DS
Oxalic acid	135 ± 11	661 ± 83	113 ± 1.4
Sulfonation 0.5 ml	112	1161	120
Sulfonation 1 ml Abson	89	2712	127
Sulfonation 1 ml Heat	64	8785	141
Sulfonation 2 ml Heat	46	95195	161
Sulphanilic acid	150	650	114
Triethylamine 6 hrs H	107	977	119
Triethylamine 24 hrs A	106	1014	119

Table 5. Thin film oven test data of the B-5901 virgin asphalt and its chemically modified versions.

Sample	TFOT Loss %	Pen. 77 °F dmm	Visc. 140 °F poise
B-5901 Virgin	0.12 ± 0.02	85 ± 1.5	1433 ± 167
CrO_3 0.5%	0.35 ± 0.25	54 ± 1.4	4716 ± 31.8
CrO_3 1%	0.28	49	6063
CrO_3 2%	0.50 ± 0.30	43 ± 0.71	9636 ± 893
CrO_3 4%	0.48 ± 0.33	28 ± 0.58	67072 ± 9011
CrO_3 4% 72 h	0.98	28	67753
CrO_3 4% Neat	0.17	95	1265
Furfural-Oxalic Acid	0.25	94	2047
Furfural-NH_4OH	0.16	91	1354
Furfural 0.5:1	0.29 ± 0.10	72 ± 6.4	4357 ± 2705
Furfural 0.5:2.5	0.38	66	4753
Furfural 1:1	0.16	70	3294
Furfural 1:5	0.24	58	8255
Furfural 2:5	0.42 ± 0.04	55 ± 3.5	15447 ± 2579
HCl acid 5 ml	0.37	70	3734
HCl acid 1 ml	0.26	75	2680
HCl gas	0.38 ± 0.22	59 ± 12	6588 ± 3724
KOH 1%	0.15	71	2301
KOH 4% A 24 h	0.25	77	2187
KOH 4% R 6 h	0.15	57	4749
KOH 7.5% R 6 h	0.25	54	12440

Table 5. Thin film oven test data of the B-5901 virgin asphalt and its chemically modified versions (continued).

Sample	TFOT Loss %	Pen. 77 °F dmm	Visc. 140 °F poise
MAH 10% 175 °C	0.22	45	31519
MAH 10% Air	0.33	42	43558
MAH 10% N_2 150 °C	0.57 ± 0.23	46 ± 0.58	25363 ± 19893
MAH 2.5% 100 °C	1.04	61	4546
MAH 2%	0.28	62	4074
MAH 5%	0.47	50	15018
Nitration 1:1 Abson	0.21 ± 0.04	42 ± 2.5	40555 ± 23671
Nitration 1:1 3 h Heat	0.52	49	35967
Nitration CaO A	0.13	49	12242
Nitration Neat 2 ml	0.56	53	4664
Nitration-Reduction	0.24	36	189892
$NOCrO_3$	0.26 ± 0.16	75 ± 0	1996 ± 264
NOMAH 175 °C	0.023	88	1456
NOMAH Air 150 °C	0.02	79	1568
NOMAH N_2 150 °C	0.06 ± 0.01	79 ± 6.7	1645 ± 250
Oxalic acid	0.23 ± 0.01	85 ± 0.0	1542 ± 44
Sulfonation 0.5 ml	0.17	72	3074
Sulfonation 1 ml Abson	0.33	56	7452
Sulfonation 1 ml Heat	0.68	53	20329
Sulfonation 2 ml Heat	0.96	39	177450
Sulphanilic acid	0.61	92	1261
Triethylamine 6 h Heat	0.14	72	2069
Triethylamine 24 h A	0.20	73	2439

Table 6. Calculated data for the B-5901 virgin asphalt and its chemically modified versions.

Sample	PVN (77-140 °F)	PI	LST °C	Aging Index Visc. ratio 140 °F
B-5901 Virgin	-0.77 ± 0.10	-1.05 ± 0.40	-46.99 ± 4.48	2.34 ± 0.29
CrO_3 0.5%	-0.46 ± 0.05	-0.21 ± 0.92	-51.80 ± 8.31	2.94 ± 0.95
CrO_3 1%	-0.69	-1.51	-38.11	5.32
CrO_3 2%	-0.39 ± 0.23	0.2 ± 0.10	-52.84 ± 8.62	3.58 ± 1.41
CrO_3 4%	0.29 ± 0.24	0.65 ± 0.60	-52.00 ± 4.53	6.69 ± 2.26
CrO_3 4% 72 h	0.94	0.08	-50.16	4.79
CrO_3 4% Neat	----	-1.31	-45.16	----
Furfural-Oxalic Acid	-0.21	-0.27	-52.60	2.15
Furfural-NH_4OH	-0.63	-0.92	-49.55	2.24
Furfural 0.5:1	-0.35 ± 0.33	0.11 ± 0.30	-56.95 ± 1.75	2.65 ± 0.45
Furfural 0.5:2.5	-0.12	0.53	-57.87	1.56
Furfural 1:1	-0.42	0.10	-56.32	2.17
Furfural 1:5	-0.12	1.01	-61.68	2.41
Furfural 2:5	0.54 ± 0.19	1.54 ± 0.40	-63.73 ± 2.53	1.61 ± 0.48
HCl acid 5 ml	-0.24	0.64	-59.31	1.44
HCl acid 1 ml	-0.55	0.37	-59.06	1.96
HCl gas	0.04 ± 0.82	0.04 ± 0.21	-54.24 ± 1.77	2.10 ± 1.03
KOH 1%	-0.56	0.18	-56.94	1.68
KOH 4% A 24 h	-0.54	-0.25	-52.71	1.68
KOH 4% R 6 h	0.56	4.06	-84.35	0.56
KOH 7.5% R 6 h	1.34	0.03	-54.18	1.24
MAH 10% 175 °C	0.86	1.22	-61.19	2.42
MAH 10% Air	0.85	0.85	-58.41	3.82
MAH 10% N_2	0.47 ± 0.27	-0.38 ± 1.12	-45.91 ± 12.10	3.86 ± 2.57
MAH 2.5% N_2 100 °C	-0.40	-0.06	-54.42	2.93
MAH 2%	-0.35	-0.06	-53.92	2.26
MAH 5%	0.19	0.73	-58.80	3.08
Nitration 1:1 Abson	0.74 ± 0.37	1.82 ± 0.70	-67.14 ± 7.81	3.33 ± 0.19
Nitration 1:1 3 h Heat	0.51	1.19	-63.68	5.64
Nitration CaO Abson	0.04	0.33	-55.01	3.14
Nitration Neat 2 ml H	-0.62	-0.51	-50.40	4.30
Nitration-Reduction A	1.61	1.88	-64.08	4.48

Table 6. Calculated data for the B-5901 virgin asphalt and its chemically modified versions (continued).

Sample	PVN′ (77-140 °F)	PI	LST °C	Aging Index Visc. ratio 140 °F
NOCrO$_3$	-0.64 ± 0.06	-0.76 ± 0.09	-49.21 ± 2.00	2.37 ± 0.06
NOMAH 175 °C	-0.74	-0.93	-48.48	2.29
NOMAH Air 150 °C	-0.95	-0.49	-51.05	2.07
NOMAH N$_2$ 150 °C	-0.78 ± 0.10	-0.68 ± 0.15	-50.46 ± 1.52	2.32 ± 0.09
Oxalic acid	-0.75 ± 0.28	-0.66 ± 0.57	-51.33 ± 5.81	2.35 ± 0.23
Sulfonation 0.5 ml H	-0.42	-0.16	-55.28	2.65
Sulfonation 1 ml Abson	0.11	0.33	-58.29	2.75
Sulfonation 1 ml Heat	0.76	1.22	-63.29	2.31
Sulfonation 2 ml Heat	2.51	2.64	-71.77	1.86
Sulphanilic acid Heat	-0.57	-0.97	-48.70	1.94
Triethylamine 6 h H	-0.68	-0.19	-54.55	2.12
Triethylamine 24 h A	-0.67	-0.45	-51.38	2.44

Table 7. Pedestal test results (cycles to failure) of the B-5901 virgin asphalt and its chemically modified versions.

Sample	A Cycles	B Cycles	C Cycles	AVE Cycles	SD Cycles
B-5901 Virgin	8	8	9	8	0.6
B-5901 Virgin TFOT	11	11	15	12	2.3
CrO_3 0.5%	--	--	--	--	--
CrO_3 1%	--	--	--	--	--
CrO_3 2%	--	--	--	--	--
CrO_3 4%	25	34	44	34	9.5
CrO_3 4% 72 h	--	--	--	--	--
CrO_3 4% Neat	--	--	--	--	--
Furfural-NH_4OH	--	--	--	--	--
Furfural 0.5:1	--	--	--	--	--
Furfural 0.5:2.5	--	--	--	--	--
Furfural 1:1	--	--	--	--	--
Furfural 1:5	50	61	90	67	21
Furfural 2:5	43	53	59	52	8.1
HCl acid 5 ml	--	--	--	--	--
HCl acid 1 ml	--	--	--	--	--
HCl gas	18	18	19	18	0.6
KOH 1%	--	--	--	--	--
KOH 4%	--	--	--	--	--
KOH 7.5% R 6 h	8	8	8	8	0.0
MAH 10% 175 °C	--	--	--	--	--
MAH 10% Air	26	26	26	26	0.0
MAH 10% N_2	40+	40+	40+	40+	--
MAH 10% N_2 60 °C	9	9	10	9	0.6
MAH 2.5% 100 °C	--	--	--	--	--
MAH 2%	--	--	--	--	--
MAH 5%	--	--	--	--	--
Nitration 1:1	7	7	7	7	0.0
Nitration 0.5:1	5	5	7	6	1.2
Nitration CaO A	2	2	1	2	0.6
Nitration Neat 2 ml	--	--	--	--	--
Nitration-reduction	6	6	6	6	0.0
$NOCrO_3$	13	15	20	16	3.6
NOMAH 175 °C	--	--	--	--	--
NOMAH Air	--	--	--	--	--
NOMAH Air 150 °C	--	--	--	--	--
NOMAH N_2 150 °C	8	9	11	9	1.5
Oxalic acid	12	11	15	13	2.1
Sulfonation 0.5 ml H	3	3	4	3	0.6
Sulfonation 1 ml A	--	--	--	--	--
Sulfonation 1 ml H	5	6	6	6	0.6
Sulfonation 2 ml H	--	--	--	--	--
Sulphanilic acid	--	--	--	--	--
Triethylamine 6 h H	4	2	4	3	1.2
Triethylamine 24 h A	5	5	5	5	0.0

These three reactions with furfural, chromium trioxide, and maleic anhydride produced the most improved asphalts from the B-5901 virgin asphalt. These additives were reacted with five additional AC-5 grade asphalts (C-8613, C-8615, C-8561, C-9040 and C-9041) to establish whether the same trend of desired modification was obtainable. Table 8 presents the properties, penetration at 77 °F (25 °C), viscosity at 140 °F (60 °C) and softening point of all the unmodified virgin asphalts and the chemically modified asphalts with MAH, CrO_3, and furfural reactions in the study. It shows the dramatic increases in viscosity at 140 °F (60 °C) and softening point. The increase in viscosity and softening point denote resistance to flow. Table 9, which presents the thin film oven test data, shows that the modified asphalts have higher viscosities after the TFOT than the original (virgin) asphalts. Table 10 presents the PVN, PI, LST and aging index data of the modified asphalts. PVN and PI values increase in the modified asphalts, except for the C-8561 furfural reacted asphalt which has lower PVN value than that of the virgin asphalt. LST values are also reported in table 10, where the LST values are lower than that of the virgin asphalt, a greater resistance to cracking at low temperature is indicated. The aging index data, also reported in table 10, indicate higher values than that of the virgin asphalt in all of the modified asphalts except for those of furfural, where the aging index was lower. Freeze-thaw pedestal test data are given in table 11. It indicates that the modified asphalts have better adherence to aggregate than the original asphalts.

At this stage, it was decided that a comparison of the various test properties of the modified asphalts to those of their corresponding virgin control asphalts was desirable. The virgin (control) asphalts consisted of the AC-5 (C-9041) and an AC-20 (C-9042) graded material; both asphalts were obtained from the same refinery using the same crude source. The AC-5 (C-9041) asphalt was reacted with a) 4 percent maleic anhydride b) 1.5 percent chromium trioxide and c) furfural (1 ml) plus 5 ml hydrochloric acid per 200 g of asphalt to obtain in each instance a viscosity at 140 °F (60 °C) of approximately 2000 poises i.e., equivalent to an AC-20 asphalt. The viscosity data and associated penetrations for these reaction products are a part of table 8. Other considerations such as PVN, PI, LST and aging index data, developed from test measurements of these products, are contained in table 9. The PVN and PI values of the modified products are greater than that of the virgin asphalt, AC-20 (C-9042). The LST values are lower than that of the corresponding virgin asphalt, AC-20 (C-9042). The aging indices of the MAH and CrO_3 products are generally equivalent to that of the virgin asphalt (C-9042); the aging index for the furfural reacted asphalt is lower. All the raw data and calculated variables (PVN, PI, LST and aging index) of all the virgin asphalts and their modified versions used in the study are presented in appendix A of this report.

Table 8. Penetrations, viscosities and softening points of all the virgin asphalts and their modified versions used in the study.

Sample		Pen. 77 °F dmm	Visc. 140 °F poise	Soft. point °F
B-5901	Virgin	139 ± 6.6	613 ± 14	114.33 ±1.15
	MAH 10% N_2	60 ± 3.6	7697 ± 2585	140.5 ± 2.51
	CrO_3 4%	41 ± 6.5	12428 ± 4830	144 ± 4.34
	Furfural 2:5	53 ± 5.0	10187 ± 3516	141.33 ±2.08
C-8613	Virgin	112	763	121
	MAH 10% N_2	53	6113	141
	CrO_3 4%	49	4925	138
	Furfural 2:5	59	3075	132
C-8615	Virgin	102	804	123
	MAH 10% N_2	53	4740	140
	CrO_3 4%	35	12629	147
	Furfural 2:5	48	5707	141
C-8561	Virgin	157	665	113
	MAH 10% N_2	70	4283	135
	CrO_3 4%	35	17465	148
	Furfural 2:5	60	2433	127
C-9040	Virgin	137	610	116
	MAH 10% N_2	67	2385	128
	CrO_3 4%	34	13389	143
	Furfural 2:5	52	3078	131
C-9042	Virgin, AC-20	78	1923	125
C-9041	Virgin	212	411	108
	MAH 10% N_2	71	12228	144
	MAH 6% N_2 L.Sc.	100	2313	127
	MAH 4% N_2	103 ± 11.3	1724 ± 680	123.5 ± 2.12
	MAH 4% N_2 L. Sc.	102	1966	124
	MAH 3% N_2	117	1132	121
	MAH 2% N_2	126	994	118
	CrO_3 4%	47	11831	143
	CrO_3 2%	70	3379	132
	CrO_3 1.5%	88 ± 3.8	2052 ± 289	127.33 ±3.21
	CrO_3 1.5% Neat	173	476	118
	CrO_3 1%	106	1303	122
	CrO_3 0.5%	109	1492	122
	Furfural 2:5	71 ± 2.6	3992 ± 288	130.75 ±1.26
	Furfural 1:5	85 ± 10.6	2471 ± 1182	126.5 ± 2.12
	Furfural 0.5:2.5	112 ± 0.7	1220 ± 62.2	120 ± 1.41
	Furfural 0.75:4 L.Sc.	71	4019	133

Table 9. Thin film oven test data of all the virgin asphalts and their modified versions used in the study.

Sample	TFOT Loss %	Pen. 77 °F dmm	Visc. 140 °F poise
B-5901 Virgin	0.12 ± 0.02	85 ± 1.5	1423 ± 167
MAH 10% N_2	0.57 ± 0.23	46 ± 0.58	25363 ±19893
CrO_3 4%	0.48 ± 0.33	28 ± 0.58	67072 ± 9011
Furfural 2:5	0.42 ± 0.04	55 ± 3.5	15447 ± 2579
C-8613 Virgin	0.09	71	1555
MAH 10% N_2	0.47	40	23065
CrO_3 4%	1.45	30	29134
Furfural 2:5	0.33	49	5659
C-8615 Virgin	0.17	62	1807
MAH 10% N_2	0.47	40	16907
CrO_3 4%	0.38	28	42015
Furfural 2:5	0.81	45	9719
C-8561 Virgin	0.22	91	1285
MAH 10% N_2	1.04	47	13562
CrO_3 4%	0.28	28	38036
Furfural 2:5	0.55	57	6079
C-9040 Virgin	0.07	87	1070
MAH 10% N_2	0.90	44	5273
CrO_3 4%	0.45	28	23845
Furfural 2:5	0.76	52	4130
C-9042 Virgin, AC-20	0.14	47	5171
C-9041 Virgin	0.27	121	990
MAH 10% N_2	0.74	51	28371
MAH 6% N_2 L. Sc.	0.50	66	7397
MAH 4% N_2	0.48 ± 0.04	69 ± 0.07	5023 ± 2329
MAH 4% N_2 L. Sc.	0.79	65	5439
MAH 3% N_2	0.01	91	1883
MAH 2% N_2	0.43	82	2521
CrO_3 4%	0.48	38	43844
CrO_3 2%	0.25	47	12280
CrO_3 1.5%	0.35 ± 0.10	63 ± 10.9	4816 ± 1934
CrO_3 1.5% Neat	0.30	102	1308
CrO_3 1%	0.40	69	3424
CrO_3 0.5%	0.34	68	3030
Furfural 2:5	0.64 ± 0.20	70 ± 2.2	6619 ± 493
Furfural 1:5	0.55 ± 0.21	75 ± 0.70	3688 ± 264
Furfural 0.5:2.5	0.45 ± 0.07	85 ± 0.70	2544 ± 182
Furfural 0.75:4 L.Sc.	0.94	74	4057

Table 10. Calculated data of all the virgin asphalts and their modified versions used in the study.

Sample		PVN′ (77-140 °F)	PI	LST °C	Aging Index Visc. ratio 140 °F
B-5901	Virgin	-0.77 ± 0.10	-1.05 ± 0.40	-46.99 ± 4.48	2.34 ± 0.29
	MAH 10% N_2	0.47 ± 0.27	-0.38 ± 1.12	-45.91 ± 12.10	3.86 ± 2.57
	CrO_3 4%	0.40 ± 0.06	0.94 ± 0.19	-52.00 ± 4.53	6.69 ± 2.26
	Furfural 2:5	0.54 ± 0.19	1.54 ± 0.40	-63.73 ± 2.53	1.61 ± 0.48
C-8613	Virgin	-0.88	-0.92	-46.65	2.04
	MAH 10% N_2	0.09	-0.11	-47.90	3.77
	CrO_3 4%	-0.24	-0.08	-47.27	5.92
	Furfural 2:5	-0.43	-0.23	-47.72	1.84
C-8615	Virgin	-0.97	-0.93	-45.78	2.25
	MAH 10% N_2	-0.16	0.21	-51.23	3.57
	CrO_3 4%	0.14	-0.37	-40.82	3.33
	Furfural 2:5	-0.13	-0.31	-44.56	1.70
C-8561	Virgin	-0.47	-1.29	-45.28	1.93
	MAH 10% N_2	0.18	0.23	-54.16	3.17
	CrO_3 4%	0.44	1.71	-59.89	2.18
	Furfural 2:5	-0.63	0.93	-59.76	2.50
C-9040	Virgin	-0.80	-3.23	-20.06	1.75
	MAH 10% N_2	-0.49	-2.32	-25.43	2.21
	CrO_3 4%	0.15	1.28	-55.93	1.78
	Furfural 2:5	-0.61	-0.01	-48.66	1.34
C-9042	Virgin, AC-20	-0.47	-3.03	-18.38	2.69
C-9041	Virgin	-0.50	-0.92	-52.56	2.41
	MAH 10% N_2	1.28	1.89	-71.45	2.32
	MAH 6% N_2 L. Sc.	0.14	0.04	-56.19	3.20
	MAH 4% N_2	-0.18 ± 0.25	0.25 ± 0.54	-58.89 ± 4.75	2.88 ± 0.21
	MAH 4% N_2 L. Sc.	-0.00	0.14	-57.55	2.77
	MAH 3% N_2	-0.37	-0.20	-55.22	1.66
	MAH 2% N_2	-0.39	-0.27	-55.36	2.54
	CrO_3 4%	0.54	1.31	-60.22	3.71
	CrO_3 2%	-0.06	-2.78	-20.58	3.63

Table 10. Calculated data of all the virgin asphalts and their modified versions used in the study (continued).

Sample	PVN′ (77-140 °F)	PI	LST °C	Aging Index Visc. ratio 140 °F
CrO_3 1.5%	-0.26 ± 0.10	0.29 ± 0.47	-58.40 ± 2.80	2.64 ± 0.29
CrO_3 1.5% Neat	-0.69	-0.92	-50.69	2.75
CrO_3 1%	-0.39	-1.77	-35.73	2.63
CrO_3 0.5%	-0.19	0.10	-58.02	2.03
Furfural 2:5	0.12 ± 0.06	1.51 ± 0.24	-67.50 ± 2.66	1.61 ± 0.16
Furfural 1:5	-0.16 ± 0.32	0.97 ± 0.08	-64.05 ± 0.78	1.66 ± 0.69
Furfural 0.5:2.5	-0.38 ± 0.05	0.27 ± 0.14	-60.09 ± 1.56	2.08 ± 0.04
Furfural 0.75:4 L.Sc.	0.14	1.68	-69.26	1.01

Freeze-thaw data are shown in table 11. Test briquets prepared with the AC-20 grade product resulting from the treatment of the AC-5 grade (C-9041) asphalt with 1.5 percent CrO_3 survived more than 100 freeze-thaw cycles while a comparative grade AC-20 asphalt (C-9042) from the same refinery which supplied the AC-5 lasted for only 9 cycles of freeze-thaw testing. The furfural reacted asphalt material also showed a much better performance in comparison to that of the virgin asphalt used as a control. On the basis of such test results, it can be claimed that the modified asphalts, developed by reactions with either CrO_3 or furfural, show a much better freeze-thaw test performance than an unreacted virgin asphalt of a like test grade originating from the same refinery. The 4 percent MAH reaction product did not perform as well as the virgin asphalt, AC-20, while the 10 percent MAH did perform as well as the other modified asphalt products in the freeze-thaw testings.

A number of investigators have observed that the water stripping resistance is a function of asphalt composition.(11-15) Further, that polar and polymerized constituents contribute better bridging between asphalt and aggregate. The results of this study show that the water-stripping resistances of the chemically modified asphalts are better than that of the virgin asphalts, since they contain polar and polymerized constituents, i.e., equipped for a better adherence to the aggregate than the virgin asphalt. A large aromatic ring system, which is formed by the reaction of asphalt with MAH and furfural, might be expected to contribute significantly to asphalt aggregate interactions. The surface of the aggregate is known to contain silica (SiO_2), hydroxyl groups of phenols (-OH group) and other electron deficient (acidic) centers that may coordinate with the electron rich (polarizable electrons) in the aromatic ring system.

HP-GPC data are presented in table 12. The data show that there are increases in the LMS of the MAH- and the CrO_3- treated asphalts as compared to that of the virgin asphalts. There is no such significant change observable in the furfural reacted asphalts. It shows that polarization and/or polymerization products have occurred in the asphalts, when reacted with either MAH or CrO_3. In the furfural reacted asphalt entity, a similar type of reaction may have occurred but may have been limited to fewer reactive sites of the asphalt molecules in comparison to that which was afforded to both the MAH and CrO_3 reactions. This premise is supported by such evidence as to greater viscosity and adhesiveness to aggregate properties exhibited by the furfural reacted asphalt. All the data obtained by the HP-GPC of the virgin asphalts and their modified versions in this study are presented in appendix B of this report.

Table 11. Pedestal test findings (cycles to failure) for all the virgin asphalts and their modifications used in the study.

Sample Cycles	A Cycles	B Cycles	C Cycles	AVE Cycles	SD
B-5901 Virgin	8	8	9	8	0.6
MAH 10% N_2	40+	40+	40+	40+	--
CrO_3 4%	25	34	44	34	9.5
Furfural 2:5	43	53	59	52	8.1
C-8613 Virgin	6	4	6	5	1.2
MAH 10% N_2	--	--	--	--	--
CrO_3 4%	--	--	--	--	--
Furfural 2:5	--	--	--	--	--
C-8615 Virgin	5	6	7	6	1.0
MAH 10% N_2	--	--	--	--	--
CrO_3 4%	--	--	--	--	--
Furfural 2:5	--	--	--	--	--
C-8561 Virgin	--	--	--	--	--
MAH 10% N_2	--	--	--	--	--
CrO_3 4%	--	--	--	--	--
Furfural 2:5	--	--	--	--	--
C-9040 Virgin	4	5	5	5	0.6
MAH 10% N_2	6	6	6	6	0.0
CrO_3 4%	26	31	52	36	13
Furfural 2:5	17	19	17	18	1.2
C-9042 Virgin, AC-20	8	9	9	9	0.6
C-9041 Virgin	8	8	9	8	0.6
MAH 10% N_2	19	80+	80+	80+	--
MAH 6% N_2 Lg. Sc.	--	--	--	--	--
MAH 4% N_2	4	6	6	5	1.2
MAH 4% N_2 Lg. Sc.	2	3	4	3	1.0
MAH 3% N_2	--	--	--	--	--
MAH 2% N_2	--	--	--	--	--
CrO_3 4%	--	--	--	--	--
CrO_3 2%	--	--	--	--	--
CrO_3 1.5%	73+	101+	133	100^+	--
CrO_3 1.5% NEAT	30	32	36	33	3.1
CrO_3 1%	--	--	--	--	--
CrO_3 0.5%	--	--	--	--	--
Furfural 2:5	28	37	32	32	4.5
Furfural 1:5	35	36	37	36	1.0
Furfural 0.5:2.5	--	--	--	--	--
Furfural 0.75:4 L.Sc.	35	36	44	38	4.9

Table 12. Gel permeation chromatography data of all the virgin asphalts and their modified versions used in the study.

Sample		LMS ± SD %	MMS ± SD %	SMS ± SD %
B-5901	Virgin	21.97 ± 0.56	45.53 ± 0.29	32.50 ± 0.81
	MAH 10% N_2	25.62 ± 0.32	44.29 ± 0.29	30.10 ± 0.61
	CrO_3 4%	34.43 ± 0.11	39.68 ± 0.01	25.89 ± 0.13
	Furfural 2:5	20.71 ± 0.14	45.41 ± 0.13	33.88 ± 0.10
C-8613	Virgin	21.63 ± 0.29	47.85 ± 0.22	30.52 ± 0.43
	MAH 10% N_2	27.85 ± 0.26	44.54 ± 0.20	27.62 ± 0.37
	CrO_3 4%	31.82 ± 0.39	42.96.0 ± 0.30	25.22 ± 0.15
	Furfural 2:5	19.93 ± 0.27	48.22 ± 0.03	31.84 ± 0.24
C-8615	Virgin	24.23 ± 0.40	43.42 ± 0.29	32.36 ± 0.25
	MAH 10% N_2	25.67 ± 0.63	43.16 ± 0.33	31.23 ± 0.68
	CrO_3 4%	31.99 ± 0.30	39.51 ± 0.41	28.50 ± 0.12
	Furfural 2:5	24.52 ± 0.16	43.08 ± 0.05	32.41 ± 0.16
C-8561	Virgin	22.64 ± 0.25	44.56 ± 0.53	32.80 ± 0.30
	MAH 10% N_2	30.14 ± 0.12	41.26 ± 0.35	28.6 ± 0.29
	CrO_3 4%	32.71 ± 0.72	40.07 ± 0.46	27.22 ± 0.29
	Furfural 2:5	21.83 ± 0.18	44.52 ± 0.08	33.65 ± 0.23
C-9040	Virgin	19.24 ± 0.08	49.12 ± 0.11	31.65 ± 0.06
	MAH 10% N_2	24.24 ± 0.64	47.11 ± 0.62	28.65 ± 0.35
	CrO_3 4%	29.21 ± 0.34	44.47 ± 0.30	26.34 ± 0.26
	Furfural 2:5	20.21 ± 0.89	49.05 ± 0.16	30.74 ± 0.93
C-9041	Virgin	23.45 ± 0.40	44.02 ± 0.35	32.54 ± 0.07
	MAH 10% N_2	32.57 ± 0.44	39.21 ± 0.26	28.22 ± 0.18
	MAH 4% N_2	27.41 ± 0.45	41.67 ± 0.30	30.93 ± 0.21
	MAH 3% N_2	26.64 ± 0.22	42.23 ± 0.20	31.13 ± 0.40
	CrO_3 4%	32.40 ± 0.22	39.05 ± 0.23	28.31 ± 0.43
	CrO_3 2%	29.79 ± 0.20	40.74 ± 0.58	29.47 ± 0.68
	CrO_3 1.5%	27.78 ± 0.35	41.78 ± 0.15	30.44 ± 0.21
	CrO_3 1%	26.88 ± 0.37	42.02 ± 0.36	31.10 ± 0.19
	Furfural 2:5	22.57 ± 0.42	43.98 ± 0.75	33.44 ± 0.39

LMS increases as the agglomerates of the polar and polarizable compounds in asphalt are formed by reacting the asphalt with maleic anhydride and chromium trioxide. These agglomerations depend on the polarity and the dispersing power of the solvating media, although in the virgin asphalt, there is no agglomeration of the molecules.

Figures 5 through 22 show the plots of the viscosities of the virgin and modified asphalts which were measured with a cone and plate viscometer (ASTM D-3205) at temperatures from 60 to 131 °F (15.56 to 55 °C) with low to heavy loadings and absolute viscosity at 140 °F (60 °C) by the (ASTM-D2171) vacuum capillary method. The data show that there are increases of the viscosities of essentially all of the chemically modified asphalts when compared with those of the unmodified asphalt. This range of temperatures encompasses the viscoelastic region, where asphalt becomes fluid. As the viscosities of the modified asphalts increase, the asphalts assume a greater stiffness at higher temperatures; this helps to reduce a rutting problem in pavements, which occurs at such high temperatures. All the viscous data obtained with the cone and plate viscometer at 0.05 $sec.^{-1}$ and 0.01 $sec.^{-1}$ rates of shear of the virgin asphalts and their modified versions in this study are presented in appendix C of this report.

Recent developments in instrumentation have now made it possible to easily measure low temperature viscosities and other stiffness related properties accurately. The mechanical behavior of asphalts can be described at pavement temperatures by such parameters as complex viscosity (η^*), complex modulus (G^*), storage modulus (G'), loss modulus (G'') and tan delta ($\tan\delta$) using a dynamic mechanical analyzer (DMA). All of these properties are dependent on the following three variables:

1. Time of loading or frequency.
2. Temperature.
3. The chemical properties of the asphalt.

The DMA (Rheometrics) instrument gives true viscosities and is able to distinguish smaller existing rheological differences between asphalts. Additional advantages of the DMA instrument over the cone and plate viscometer are the following:

- A small sample size can be used (1 to 2 grams). This small sample size reduces thermal gradients.
- The DMA instrument is more sensitive.
- Viscosities at very low temperatures can be measured. With the cone and plate viscometer, it is not possible to measure viscosities of these asphalts at temperatures much lower than 0 °C.
- The samples are easy to prepare, and the discs are easy to clean.

Figures 23 through 26 show the complex viscosity-temperature plots for the virgin (B-5901), MAH reacted, CrO_3 reacted, and furfural reacted asphalt at frequencies of 100, 10, 1, and 0.1 rad/s. The complex viscosities of MAH reacted, CrO_3 reacted or furfural reacted asphalts are lower at low temperatures and higher at higher temperatures as compared to that of the virgin (B-5901). This viscoelastic response shows that the modified asphalt will flow better than the virgin asphalt at low temperatures, but will also be stiffer and have a lesser tendency to rut at higher temperatures. Therefore, these modified asphalts are less temperature susceptible than the virgin i.e., control asphalt.

The storage moduli (G') of the virgin (B-5901), MAH reacted, CrO_3 reacted and furfural reacted asphalts at frequencies 100, 10, 1, and 0.1 rad/s are shown in figures 27-30. The storage moduli of MAH reacted, CrO_3 reacted and furfural reacted asphalt are lower at low temperatures and higher at high temperatures than the virgin asphalt. The storage modulus is a measure of the amount of energy recovered during a periodic deformation and relates to the elasticity of the tested material. In our results, the virgin (B-5901) asphalt becomes more brittle than the modified asphalts at a low temperature. It indicates that the modified asphalts are better equipped than the virgin asphalt for any low temperature performance.

The loss moduli of the virgin (B-5901), MAH- reacted, CrO_3- reacted and furfural- reacted asphalts are shown in figures 31 through 34. The loss moduli of MAH- reacted, CrO_3- reacted and furfural- reacted asphalt are lower at low temperatures and higher at high temperatures as compared to the loss modulus of the virgin asphalt (B-5901).

The loss modulus (G'') is a measure of the amount of energy dissipated by the asphalt in the form of heat and can be related to the viscous response of the asphalt. The loss modulus is pertinent in respect to low temperature impact and crack resistance, especially since its concern is at the molecular level. Viscoelastic materials such as asphalt when functioning under moderate temperatures and normal use conditions, can (through viscous flow) relieve those stresses caused by temperature changes in the pavement. At low temperatures all asphalts reach a point where viscous flow stops and where their behavior becomes purely elastic. Dynamic rheological testing at such low temperatures provides the best information as to where and when this occurs.

The effect of temperature on the complex moduli at frequencies of 100, 10, 1, and 0.1 rad/s of the virgin (B-5901), MAH- treated, CrO_3- treated, furfural- treated asphalts are shown in figures 35 through 38. These figures indicate that the modified asphalts have lower moduli at low temperatures and higher moduli at high temperatures as compared to the virgin (B-5901) asphalt.

For plots of complex viscosity, η^*, and complex modulus, $|G^*|$ vs

temperature; at temperatures above 10 °C, the slope of the modulus vs temperature line for the modified products is statistically less than that of the virgin asphalt. It is clear on the basis of these test results that the modified asphalts have the potential to provide asphalt cements that are stiffer at high temperatures and more flexible at low temperatures than the virgin i.e., the control (B-5901) asphalt. Hence, the modified asphalts have a greater capability to resist both rutting at high temperatures and thermal cracking at low temperatures.

The tan delta is the ratio of the energy lost to the energy stored in a cyclic deformation; its equation is: tan delta = G"/G'. The tan delta of the virgin (B-5901), MAH- treated, CrO_3- treated and furfural treated asphalt are shown in figures 39 through 42. At higher temperatures, the tan delta value significantly increases for the virgin asphalt as compared to those of the MAH- reacted, CrO_3- reacted, and furfural- reacted asphalts. This indicates that the unmodified i.e., virgin, B-5901 asphalt dissipates much more energy as frictional heat (kinetic energy) than the modified asphalts (MAH- reacted, CrO_3- reacted and furfural- reacted). The attendant raw data obtained for the B-5901 virgin asphalt and its modified versions used in this part of the study are presented in appendix D of this report.

STATISTICAL INTERPRETATION OF DMA RESULTS

The complex storage and loss modulii of virgin and modified asphalts were measured using a rectangular torsion geometry between -50 and 10 °C and parallel plate geometry between 10 and 100 °C. The storage and loss modulii are reportedly independent of the sample geometry. But in some cases, a discontinuity in the data exists probably indicating a need to apply corrections to the geometry used in some cases. This uncontinuity is most obvious in loss modulus data as exemplified by the two curves in figure 43.

In order to show if these data for modified asphalts are significantly different from the virgin asphalt, a statistical analysis was performed. A direct test such as Student's T test can be used only if multiple observations have been recorded at each data point in the curve. In the absence of such data, other means of evaluation of significant differences have to be resorted to.

It is evident that the storage, loss and complex modulii are continuous functions of the temperature. This implies that each of these functions can be approximated by an n^{th} order polynomial. In figures 44 through 49, the curves have been satisfactorily fit with a 4^{th} order polynomial by least squares linear regression. The 95% confidence limit on this regression which is plotted[1] as dotted lines on either sides of the polynomial fit indicates that 95% of the data falls within this region. The confidence limits on the regression have been used to evaluate the significant differences between modified and virgin asphalts.

The interpretation of the complex modulii data as applied to asphalts is not well understood. More work has to be performed in this area to relate these data to pavement performance. The storage modulus represents the in-phase component of the complex modulus and includes the elastic and visco-elastic response of the material. Figures 44 and 45 illustrate the storage modulii dependence on the temperature at 0.1 and 100 radians/second cyclic strains, respectively. At temperatures below freezing, the storage modulii of modified asphalts are lower than virgin asphalt. At -30 °C, the storage

---

[1] The curve-fit and confidence lines were calculated with Sigmaplot, Jandel Systems

modulus of furfural modified asphalt at 100 rad/s is an order-of-magnitude lower than the virgin asphalt while the other modifications show lesser changes. However, the storage modulii of all the modified asphalts are significantly lesser than the virgin asphalt. At 0.1 rad/sec, the storage modulii of furfural-modified asphalt is significantly lower than the virgin asphalt while other modified asphalts are not significantly different.

At 50 °C, the storage modulii of modified asphalts are significantly higher than virgin asphalts up to 2 orders-of-magnitude at 100 rad/sec and 5 orders-of-magnitude at 0.1 rad/s. The CrO_3-modified asphalt shows the highest increase in storage modulii.

The loss modulii is a measure of the energy dissipated or lost as heat per cycle of sinusoidal deformation, when different systems are compared at the same strain amplitude. The loss modulus can be viewed as the ability of a material to relieve stresses by molecular or atomic motions.

At low temperatures, (below freezing) the loss modulus of modified asphalts are lower, but not significantly lower than the virgin asphalt, except for furfural-modified asphalt at 0.1 rad/sec, which is significant (an order-of-magnitude) lower than virgin asphalt at -20 °C. At 60 °C, the loss modulii of modified asphalts are also significantly (1-2 orders-of-magnitude) greater than the virgin asphalt.

In theory composition of the modified asphalts can also be optimized by the use of dynamic mechanical data to get the desired values of η^*, $|G^*|$, G', G'', and tan delta by varying the molecular size, chemical structure and by using ideal amounts of reactant, when reacting a controlled asphalt with a reagent (e.g., MAH, CrO_3, and furfural).

The complex modulus-temperature and complex viscosity-temperature relationships were used in this study to directly measure temperature susceptibility of the chemically modified asphalt products. Complex moduli and viscosities of the MAH-, CrO_3-, and furfural- modified asphalts at low temperatures are less than or almost identical to those of the virgin asphalts but are higher than those of the virgin asphalts at higher temperatures. Modified asphalts show lower slope values i.e., flatter curves than those of the virgin asphalts. Thus, the modified asphalts are less temperature susceptible than the virgin asphalts at normal pavement temperatures.

Nature of Reactions

Changes in the chemical composition of an asphalt will change the physical properties of that asphalt. The chemical reactions conducted in this study did change the overall chemical composition of the virgin asphalt. These reactions developed polar and acidic constituents in the modified asphalts as seen by infra-red spectroscopy. The infra-red spectrum of the B-5901 virgin asphalt and its reacted product with MAH, CrO_3 and furfural are shown in figure 43. The infra-red spectra of the maleic anhydride reacted asphalt (spectrum B) shows the presence of a C=O stretching band around the

1859 and 1784 cm^{-1} region. However, all anhydrides show two carbonyl bands in this region as do the cyclic anhydrides. In addition to the carbonyl absorptions, the spectrum also shows the peak at 1225 cm^{-1} (in the 1175-1278 cm^{-1} region) due to the C-O-C stretching vibration for cyclic molecules in which ring strain is involved.(41) The anhydride C-O stretching vibrations are observed in the 1050-1096 cm^{-1} region. In addition, the cyclic anhydride C-O stretching band is observed in the 896-975 cm^{-1} region for the cyclic 5-membered ring which is conjugated.

The infrared spectra of the chromium trioxide reacted asphalt (spectrum C) in figure 43 shows the formation of an absorbance peak in the 1681-1784 cm^{-1} region, which was not present in the virgin asphalt spectrum. Absorbance in this region is due to the carbonyl group, which indicates the presence of acids. The strong band around 1596-1681 cm^{-1} indicated the presence of keto groups (-CO-). The spectra also shows the formation of an absorbance peak in the region 1500 to 1596 cm^{-1}, which reflects the presence of carboxylate ions (COO$^-$). There is a disappearance of a band in the 1547 to 1656 cm^{-1} region due to the C=C and C=O stretching of the aromatic system. The cyclic ether linkage is observed in the 1218 to 1253 cm^{-1} region. There is a strong band between 1409 to 1496 cm^{-1}, indicating the presence of the carboxylic O-H group. The band in the 1287 to 1362 cm^{-1} region may be due to the presence of methyl ketone. The increases in intensity in the 984 to 1081 cm^{-1} region could be attributed to the COOH dimers and a variety of C-O, C-O-C groups. The number of bands present below 650 cm^{-1} are due to the presence of unreacted CrO_3 or a reduced form of chromium trioxide (CrO_2 or Cr_2O_3). The infrared spectrum of the asphalt reacted with furfural is shown in figure 43 D. It is similar to that of the virgin asphalt. Thus, infrared spectrum does not show any evidence of a reaction between asphalt and furfural.

The infrared spectrum of the nitrated product of the asphalt is shown in figure 44 B. An increase in intensity is observed in the bands near 1525 and 1340 cm^{-1} due to the presence of an asymmetrical and a symmetrical C-NO_2 group. However, an increase in intensity is also observed in a band at 875 cm^{-1}, indicating a C-N stretching vibration of the nitro group. There is also a strong band at 669 cm^{-1}, believed to be a nitro group (-O-N=O) resulting from the interaction of the nitro group and the C-H out-of-plane bending frequencies. The infrared spectrum of the nitrated and reduced entity (reduction product) of an asphalt is shown in figure 44 C. There is a disappearance of a strong peak at 668 cm^{-1}, which is due to the interaction of the nitro group and the C-H bending frequency. It indicates that the nitro group has been converted into an amino group. The IR spectrum of a sulfonated product of asphalt is shown in figure 44 D. It shows a strong band at 1062 cm^{-1} due to the presence of sulfonic acid salts. The presence of sulfonic acids is an increase in the recorded intensity at 1165 cm^{-1}.

For the asphalt reacted with hydrogen chloride gas, spectrum B (figure 45) shows the presence of a C-Cl stretching band at 703 cm^{-1}. The asphalt reacted with oxalic acid spectrum is shown in figure 45 C. It does not show any difference in the scan to that of the virgin asphalt (figure 45 A). It may be a possibility that the oxalic acid when heated to a temperature of 302 °F (150 °C) undergoes a conversion to form carbon dioxide and carbon monoxide and does not react with the asphalt. The IR spectrum of the KOH reacted asphalt is shown in figure 45 D. There is an increase in the absorption in the 1603 cm^{-1} region, which is attributed to the formation of a double bond, which may be due to an aldol condensation. The bands found approximately at 1603 and 1418 cm^{-1}, are due to the formation of carboxylate ions in the asphalt. The strong band at 881 cm^{-1}, appears to be an indication of the out-of-plane bending of two hydrogens of either a terminal methylene group ($=CH_2$) or an epoxide group. The broad spectrum from 1109 to 1220 cm^{-1}, suggests the presence of C-O and C-O-C vibrations of a wide variety of materials such as acids, phenols and ether.

The infrared spectrum of the asphaltene fractions from the virgin (B-5901, control) asphalt, the MAH- reacted, CrO_3- reacted and furfural- reacted asphalts are shown in figure 46. The asphaltene obtained from the virgin (B-5901, control) asphalt is shown in figure 46 A. There is a lack of a band around region 1700 cm^{-1} of the spectrum indicating that carboxylate acid carbonyls are absent from the virgin asphaltene. The infrared spectrum of the maleic anhydride reaction product asphaltene (figure 46 B), shows the formation of absorbance peaks at 1859, 1778, 1744 and 1715 cm^{-1}, such are not found in that of the virgin asphaltene. Such peaks are typical for the cyclic products formed by the reaction of maleic anhydride with asphalt and represents the presence of a keto (C=O) group of a five membered ring. In addition to the carbonyl absorptions, anhydrides also show strong bands due to the C-O-C stretching vibrations which show up as a strong band near 1212 cm^{-1}, it is due to the presence of cyclic materials in which a ring strain is involved. Cyclic anhydride C-O stretching is also shown by the presence of a band at the 931 cm^{-1}. The chromium trioxide reacted asphaltene is shown in figure 46 C. A prominent band is present at 1700 cm^{-1}, indicating the presence of a carboxyl (COOH) group. The ranges, 1500-1630 and 1450-1360 cm^{-1}, are assigned to carboxylate (COO^{-1}) groups. The C-O stretching band is present near 1228 cm^{-1}. The band 956 cm^{-1} is assigned to the presence of acid (COOH) dimer. The furfural reacted asphaltene (figure 46 D) is similar to the virgin asphaltene (i.e., control asphaltene) in all regions.

The infrared spectra of the saturated fractions from all the asphalts i.e., virgin, MAH reacted, CrO_3 reacted and furfural reacted asphalts are shown in figure 47. All the four spectra are similar. Each spectrum shows a strong absorption band near the 1460 cm^{-1}, due to the hydrogen bending vibrations of CH_2 and CH_3 groupings. The strong band at 1377 cm^{-1} is assigned to the symmetrical CH_3 mode in the molecule. A band near the 721 cm^{-1} arises due to the rocking mode of the (CH_2) group, and is mostly present when a long chain of the type $-(CH_2)_n$, (if n=4 or more) is present in a molecule.

The infrared spectra of naphthene aromatics fractions from the virgin, maleic anhydride reacted, chromium trioxide reacted and furfural reacted asphalt are shown in figure 48. The naphthene aromatics fractions show the presence of bands at 1604 and 1459 cm^{-1}, are characteristic bands attributed to the presence of aromatic C=C stretching vibrations. The strong band at 1376 cm^{-1} exhibit absorption due to a methyl symmetrical stretch. The bands around the region 872-700 cm^{-1} are due to the aromatic substitution patterns. It shows that all the naphthene aromatic fractions are similar.

The infrared spectra of the polar aromatic fractions of virgin, maleic anhydride, chromium trioxide and furfural reacted asphalt are shown in figure 49. The presence of absorptions in the vicinity of 1600, 1450, 820, 740, 725, and 700 cm^{-1} in all spectra indicate that asymmetrically substituted aromatic nuclei are major contributors to overall structure. The absorption near the 1496 cm^{-1}, which may be due to aromatic nuclei, is conspicuously weak in the virgin asphalt's spectrum. In all instances, the polar aromatic fractions of virgin, MAH, CrO_3 and furfural- reacted asphalts have a band at approximately 1703 cm^{-1}, implying the presence of a -COOH group (-C=O group of an acid). The other keto (-C=O groups) are present at around 1656 cm^{-1}. Particularly, in the maleic anhydride and chromium trioxide treated asphalts, there is a strong band at 1203 cm^{-1}, it indicates the C-O stretching vibrations formed by the reaction of asphalt with MAH and CrO_3. In the MAH reacted asphalt, the band around 1080 cm^{-1} is due to the C-O and C-O-C groups. In a MAH reacted asphalt, there are strong bands around 700-750 cm^{-1} which are due to the asymmetric and symmetric substituted aromatic nuclei which are the major contributors to the overall structure. These bands are not as strong in other spectrums (e.g., virgin, CrO_3 treated and furfural treated asphalt).

These IR data are consistant with the following reactions: Maleic anhydride forms a Diels Alder product with the polynuclear aromatic hydrocarbons in the asphalt. Chromium trioxide oxidizes the aldehydes, aromatic hydrocarbons, and benzylics; reacts with the double bonds in the asphalt; and forms keto (C=O), acidic (COOH) and epoxy groups in the modified asphalt. The MAH and CrO_3 reacts with the asphalt to form polar molecules. Furfural reacts with the asphalt in the presence of hydrochloric acid which acts as a catalyst, and forms a polar molecule or a larger molecule. The presence of a larger molecule can not be explained by IR, but is shown by an increase in the large molecular size portion of its HP-GPC chromatogram and in the sample viscosity at 140 °F (60 °C). The various typical type of reactions which are assumed to be occurring when asphalt (virgin) is reacted with by each of the following reagents, (MAH, CrO_3 and furfural), are presented in appendix E of this report.

The relationship of polar functional groups and viscosity has been demonstrated by Plancher et al.(42) They have shown that the viscosity of an uncarboxylated asphalt is lower than that of its carboxylated versions. That is why the chemically modified asphalt samples in this study have a higher viscosity than their virgin entities. Chemical modification of asphalts with maleic anhydride, chromium trioxide or furfural increases the oxygen content of the treated asphalts. Hence polarity is increased in the treated asphalt. Polar compounds formed during the chemical modification of asphalts would also be expected to increase the complex modulus of the asphalt at high temperatures.

CONCLUSIONS

A notable increase in viscosity and softening point were observed in the chemically modified asphalts as compared to their virgin asphalts, indicating their greater resistance to flow at higher temperatures. Penetration-viscosity number (PVN) and penetration index (PI) values usually increased and the limiting stiffness temperature (LST) values usually decreased in the modified asphalts. The temperature susceptibility defined by the complex modulus-temperature and complex viscosity-temperature data typically has been reduced in the modified asphalts. The chemical modification of asphalts improved the adhesive bond between asphalt and aggregate in asphalt mixtures implying an increased resistance to stripping. The presence of polar group and polymerizing groups in the modified asphalts played a major role in controlling their viscosities. These data show that the chemically modified asphalts have potential for use in highway pavements to help avoid cracking and rutting in such pavements. However, engineering tests involving correlation between observed pavement rutting and high-temperature stiffness are required to confirm this conclusion. The production of the perfect chemically modified asphalt is, of course, impossible. What has been demonstrated in this research is the improvement of asphalt properties such as viscosity, softening point, PVN, PI, complex modulus, and adhesiveness to aggregate. These characteristics could and should improve pavement performance when such modified asphalts are used in asphalt cement pavement construction. The chemical modification of asphalt with MAH, CrO_3 or furfural is a relatively inexpensive method of converting an asphalt into a powerful modified asphalt product to ameliorate cracking and rutting problems in asphaltic pavements.

RECOMMENDATIONS

1. DMA (using Rheometric Dynamic Analyzer) analyses should be conducted for all the modified asphalts as well as the virgin asphalts. Viscosities, moduli, and tan deltas will give further information about the modified asphalts.
2. An ideal mix design has to be established for the use of the modified asphalts.
3. Marshall stability and flow values have to be determined and specified.
4. Specific gravities and air void analyses should be made on mixes prepared from the chemically modified and unmodified asphalts for comparative purposes.
5. Engineering properties of the mixes made with the modified asphalts have to be determined for the structural considerations. Such properties will include fatigue, permanent deformation, and shrinkage fracture. With the knowledge of such engineering properties, it would be possible to make meaningful comparisons of the mixes prepared with the modified asphalts and virgin i.e., control asphalts.
6. Results and conclusions should be drawn from the low and high temperature studies of the modified asphalt mixes.
7. The potential advantage of the chemically modified asphalts as road construction material should be determined.
8. Finally, if the modified asphalts show better performances in the laboratory and engineering tests, further study should be performed on larger scale with the help of refinery personnels and the State Highway Agencies.
9. The capabilities and limitations of the new products, i.e., chemically modified asphalts, should be reported.

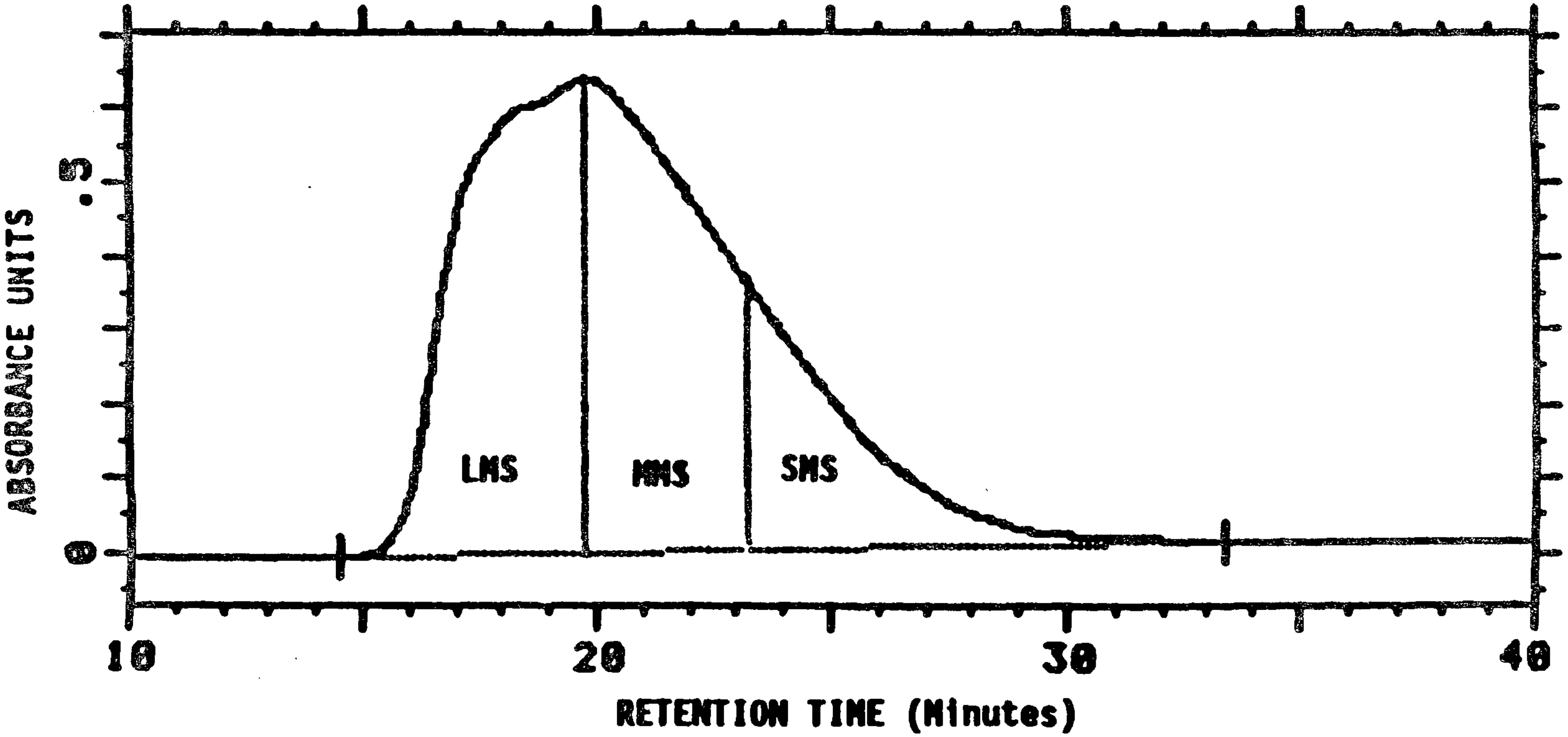

Figure 1. A typical HP-GPC chromatogram of an asphalt.

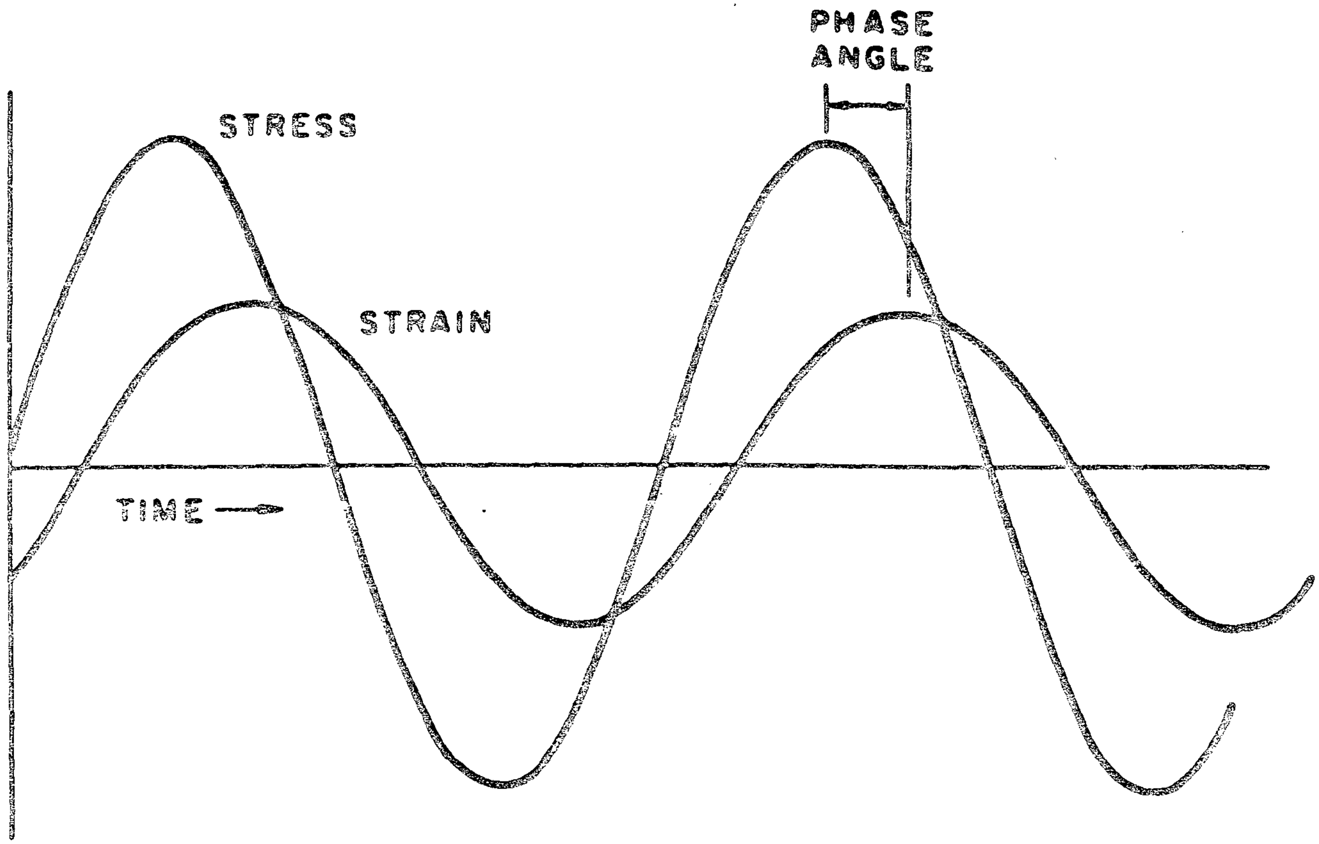

Figure 2. Deformation response of a viscoelastic material to repeated sinusoidal loading.

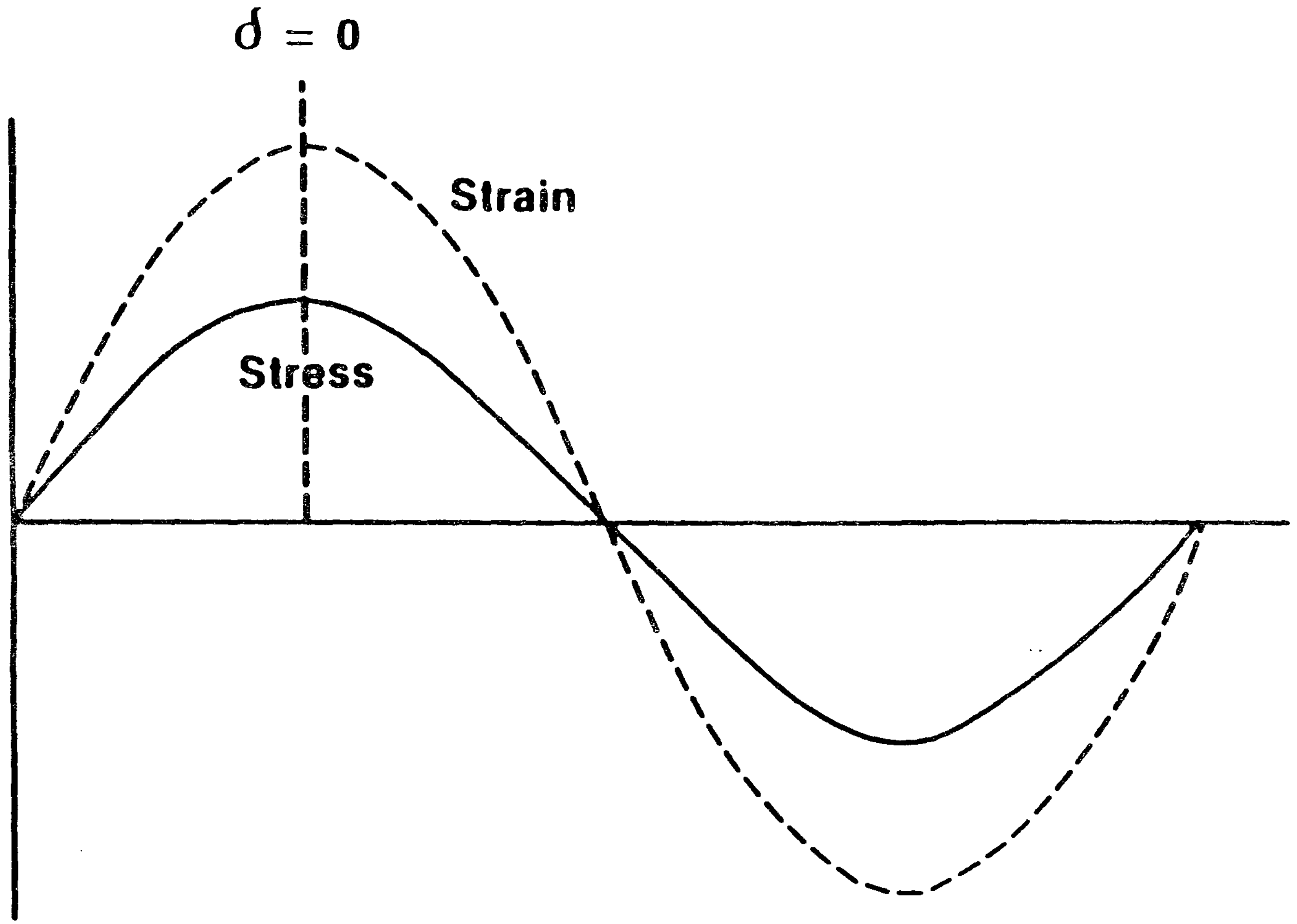

Figure 3. Deformation response of a purely elastic material.

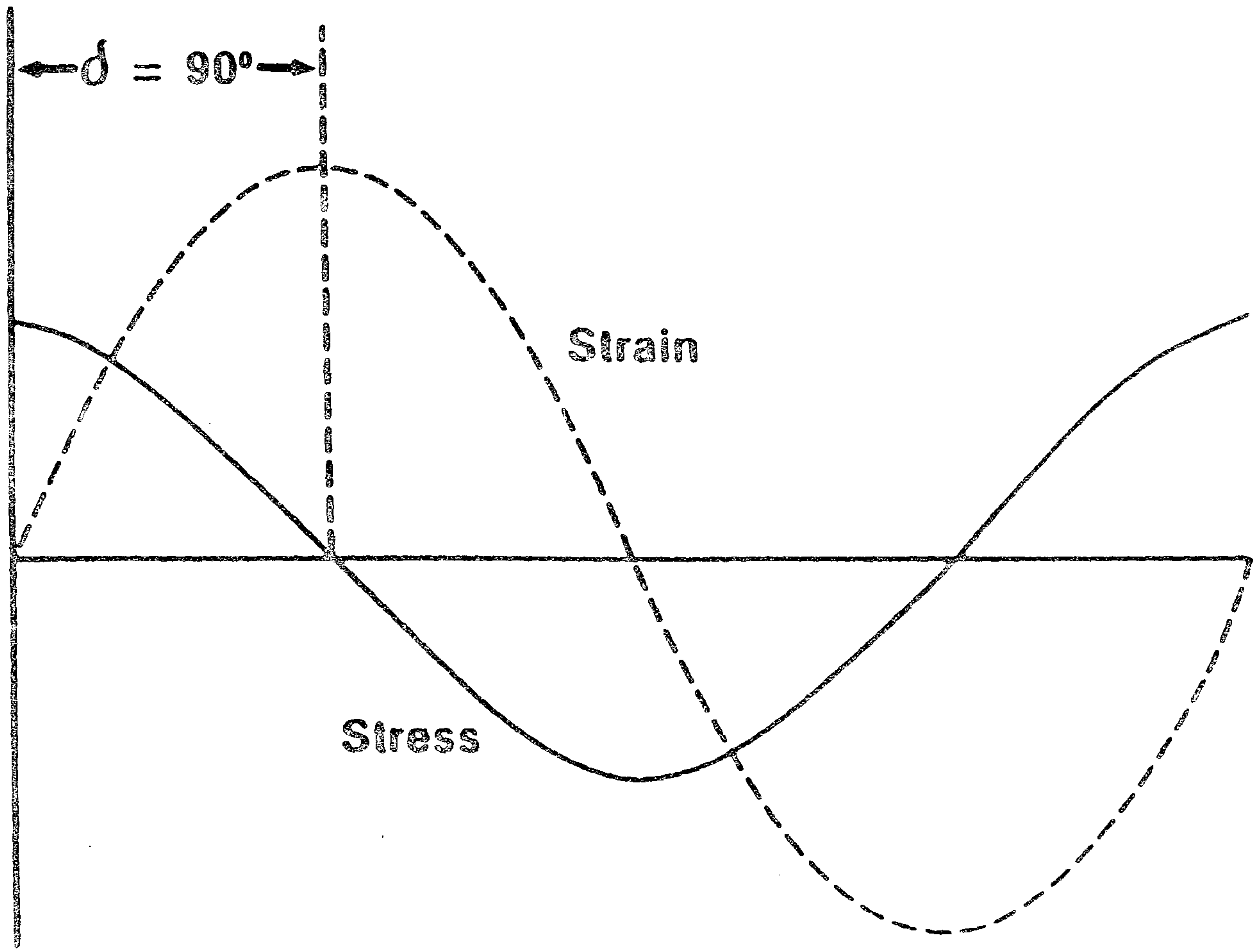

Figure 4. Deformation response of a purely viscous material.

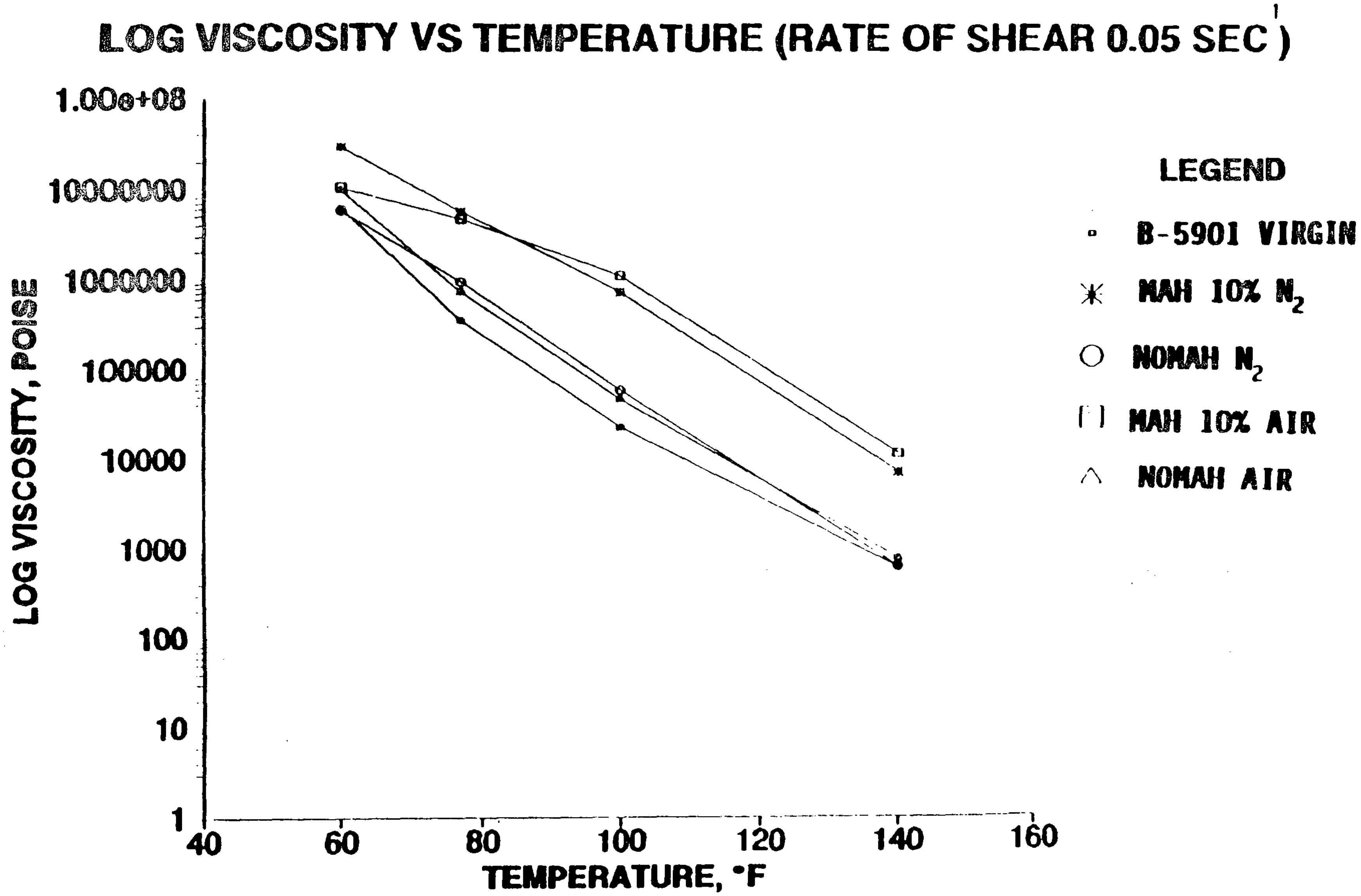

Figure 5. Viscosities at a shear rate of 0.05 sec^{-1} are shown as a function of temperature for the B-5901 virgin asphalt and its reaction with MAH products.

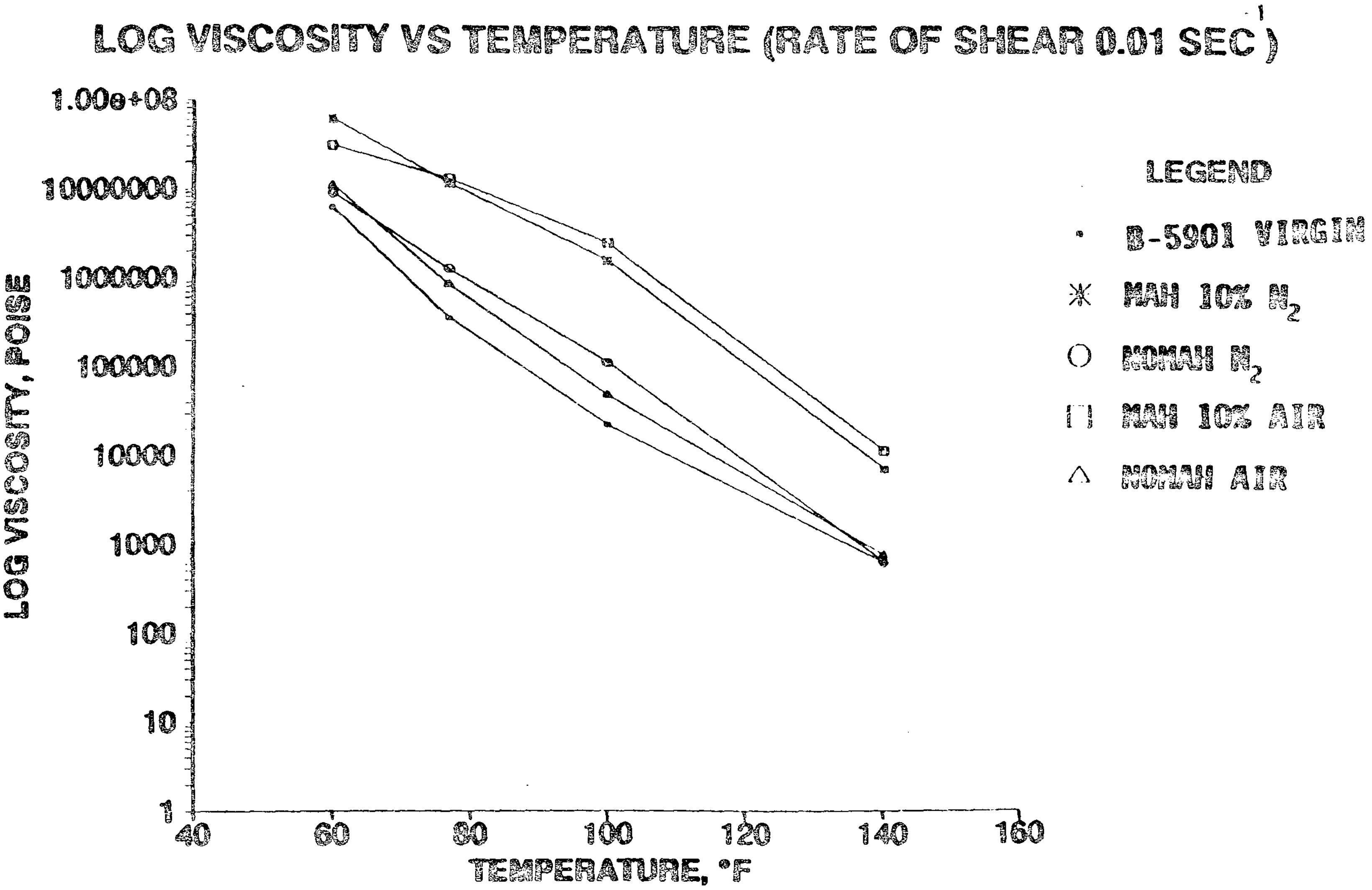

Figure 6. Viscosities at a shear rate of 0.01 sec^{-1} are shown as a function of temperature for the B-5901 virgin asphalt and its reaction with MAH products.

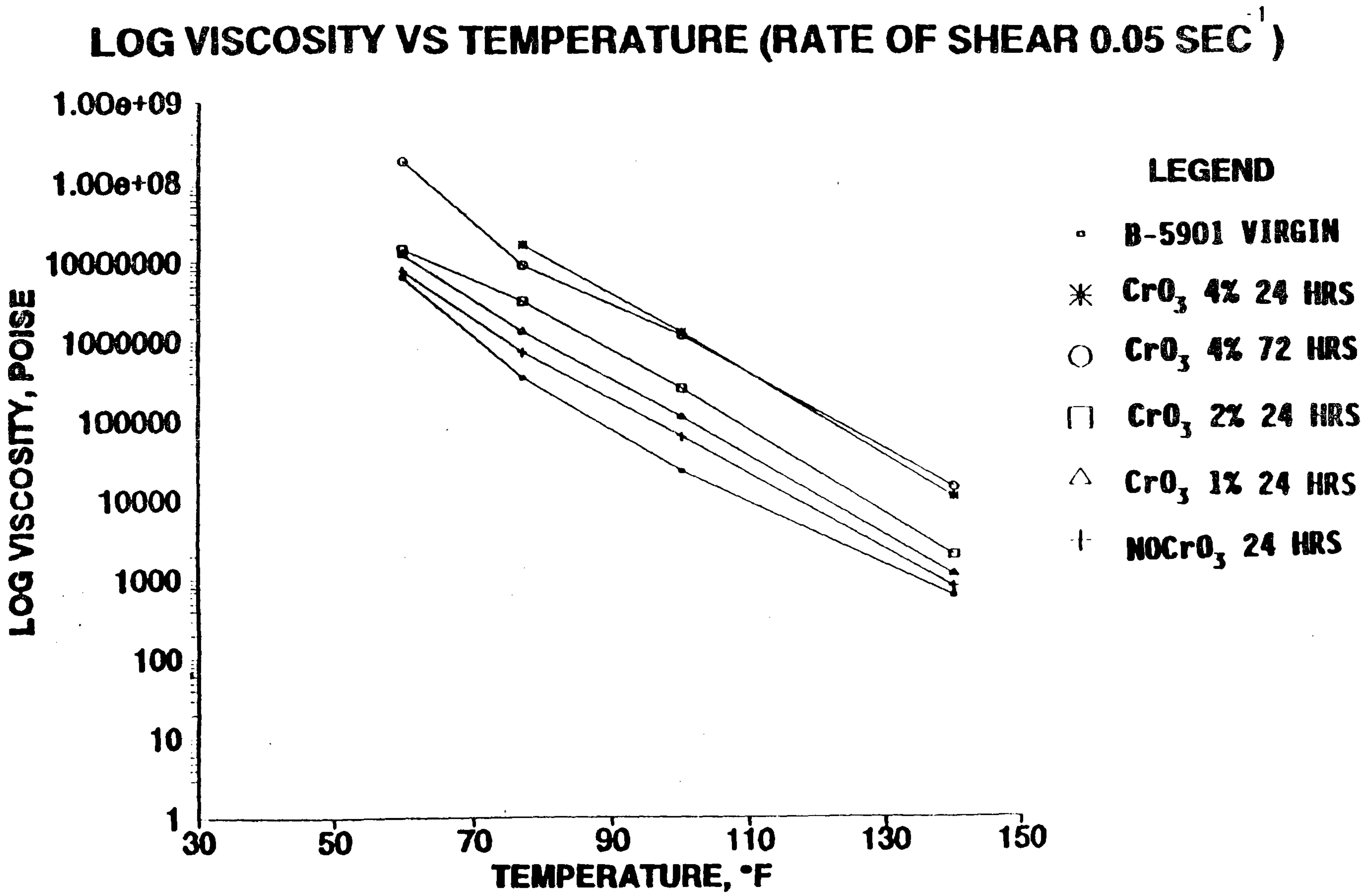

Figure 7. Viscosities at a shear rate of 0.05 sec^{-1} are shown as a function of temperature for the B-5901 virgin asphalt and its reaction with CrO_3 products.

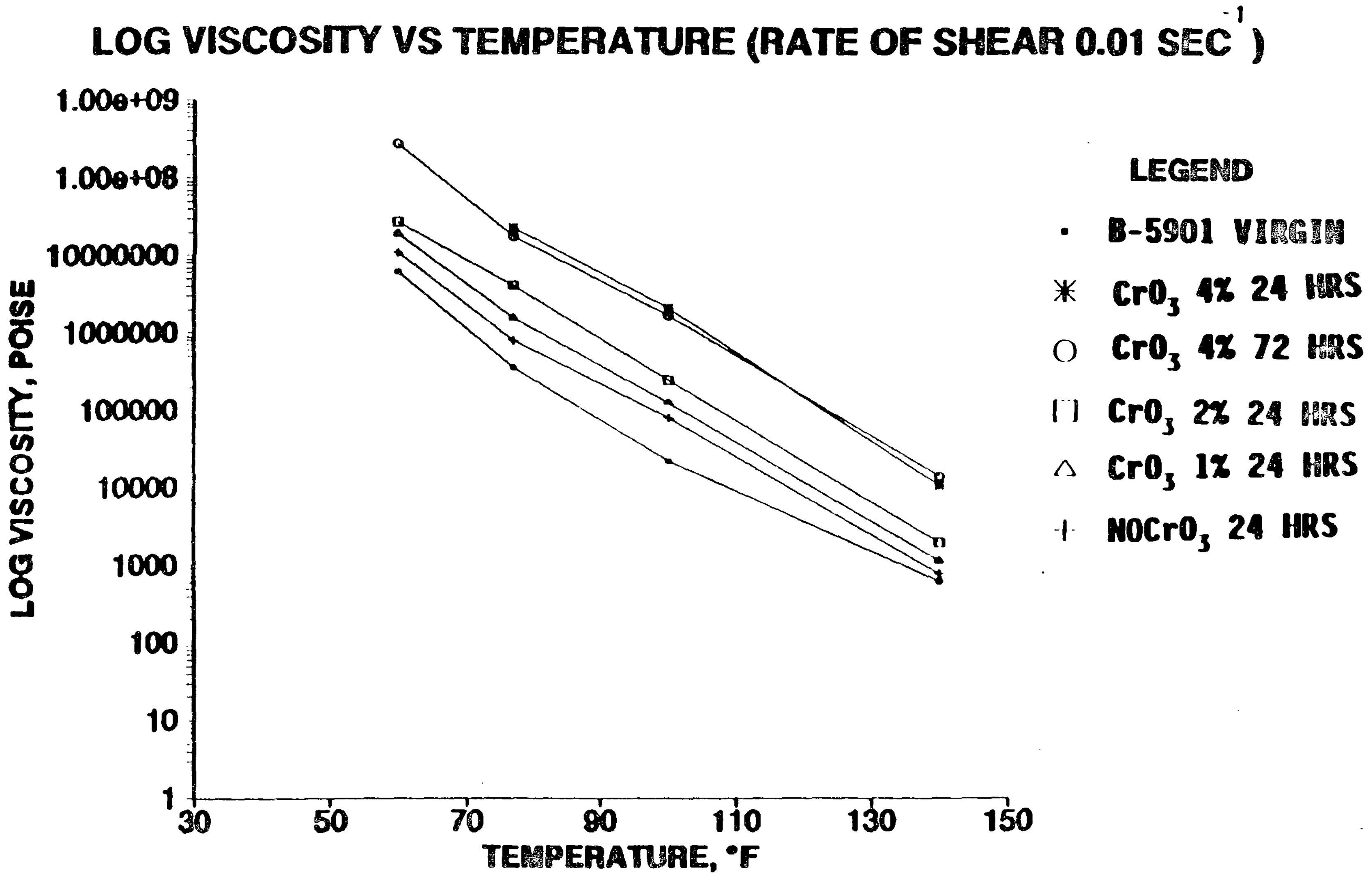

Figure 8. Viscosities at a shear rate of 0.01 sec^{-1} are shown as a function of temperature for the B-5901 virgin asphalt and its reaction with CrO_3 products.

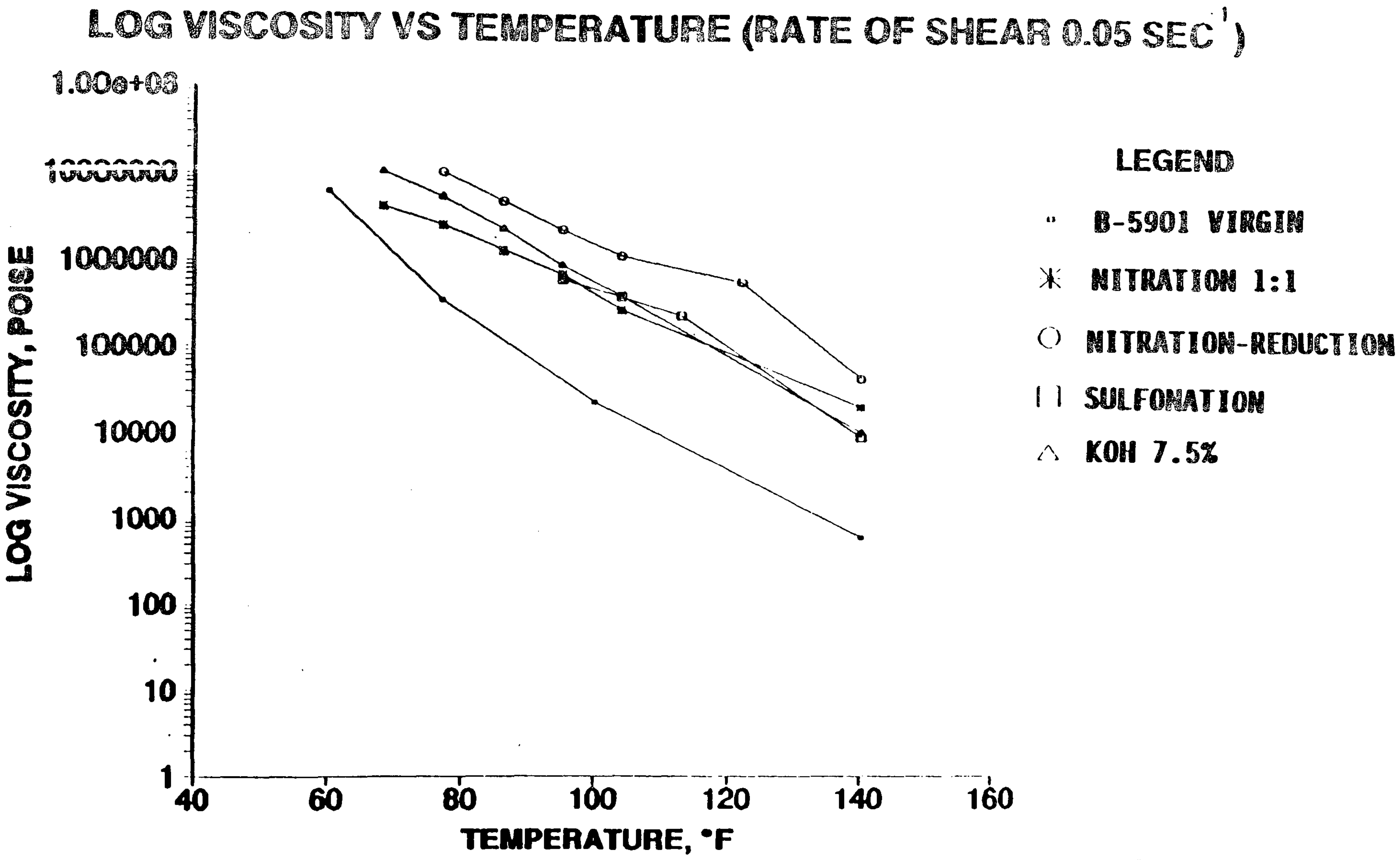

Figure 9. Viscosities at a shear rate of 0.05 sec^{-1} are shown as a function of temperature for the B-5901 virgin asphalt and its nitrated, nitrated-reduced, sulfonated and condensed products.

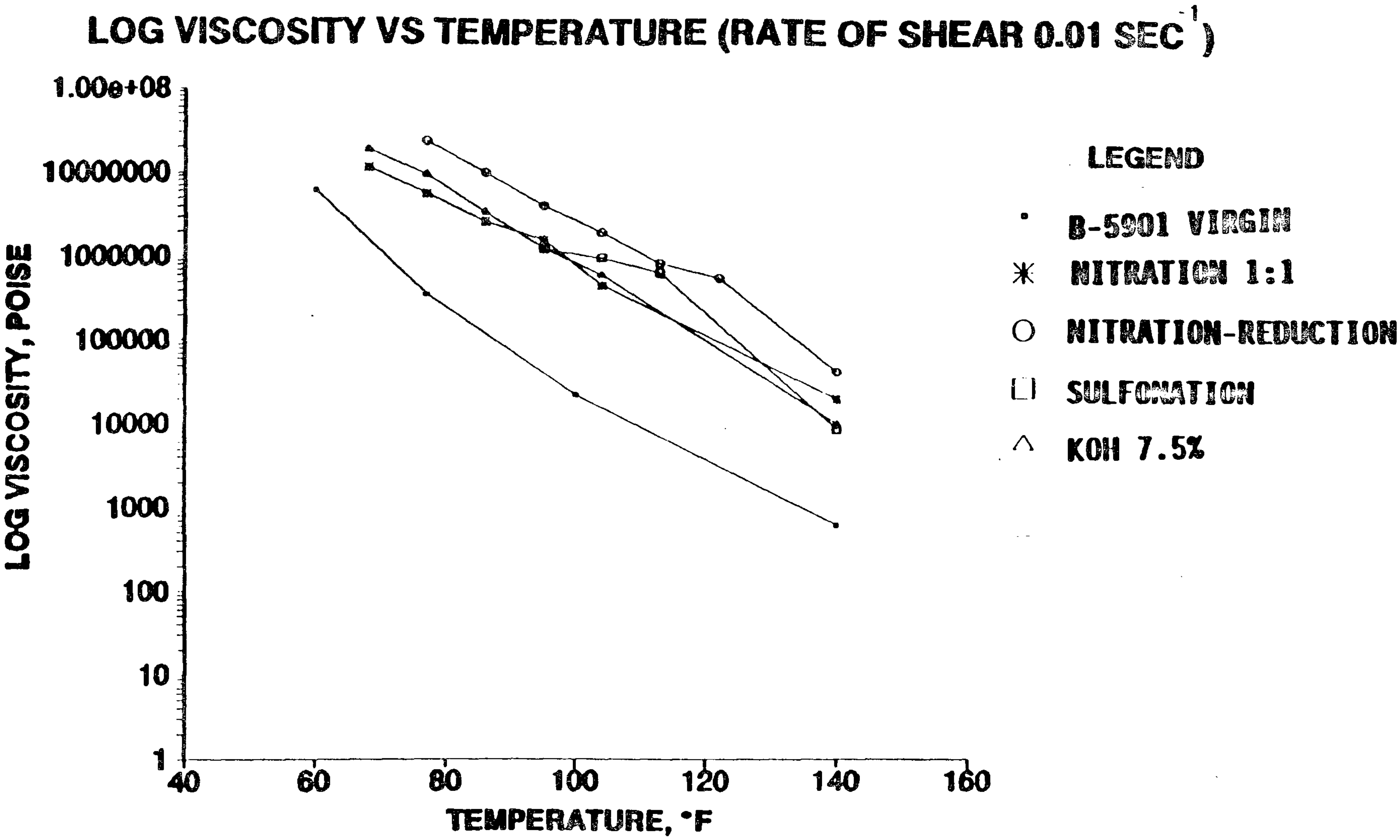

Figure 10. Viscosities at a shear rate of 0.01 sec^{-1} are shown as a function of temperature for the B-5901 virgin asphalt and its nitrated, nitrated-reduced, sulfonated and condensed products.

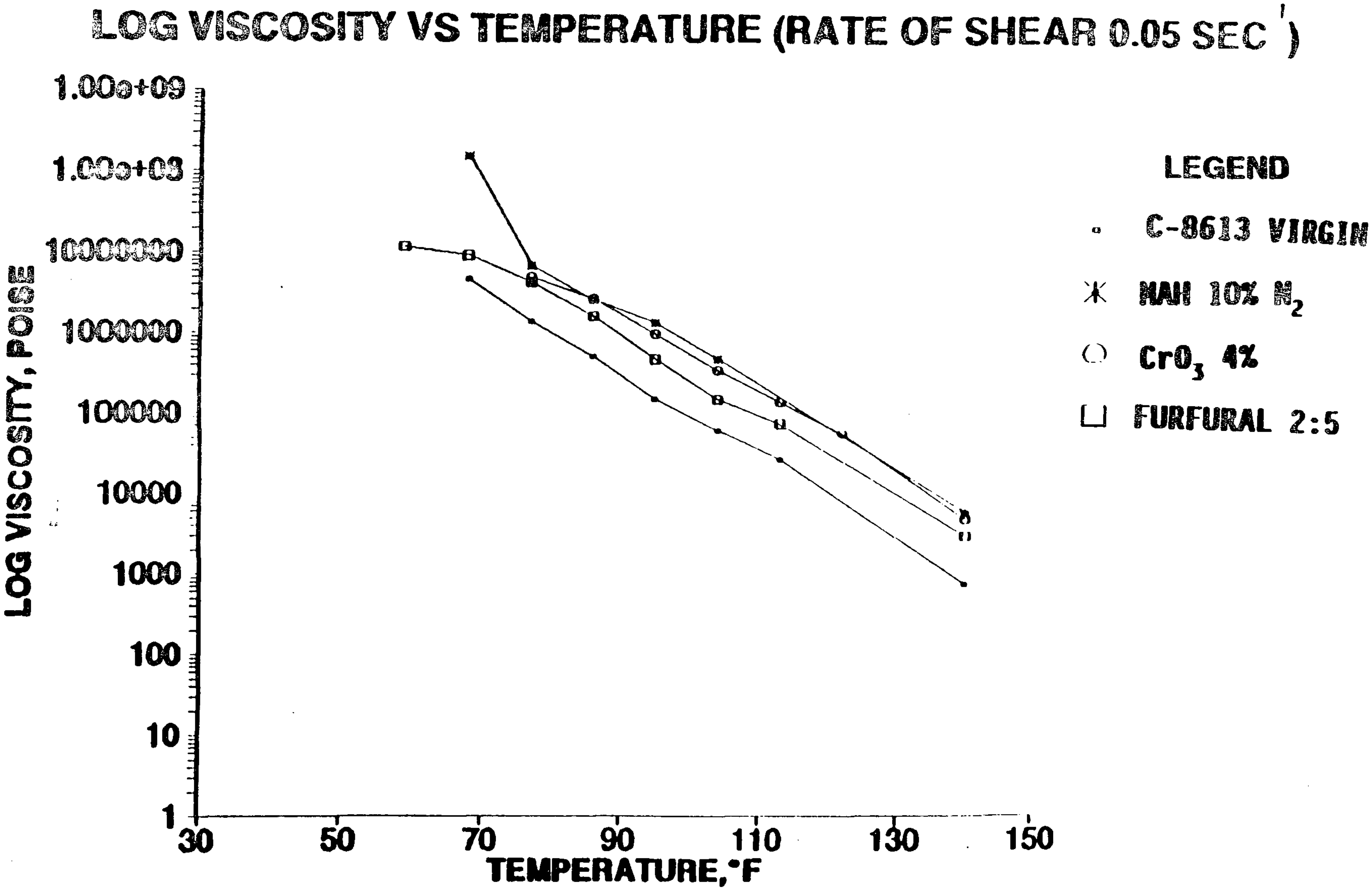

Figure 11. Viscosities at a shear rate of 0.05 sec^{-1} are shown as a function of temperature for the C-8613 virgin asphalt and its chemically modified versions.

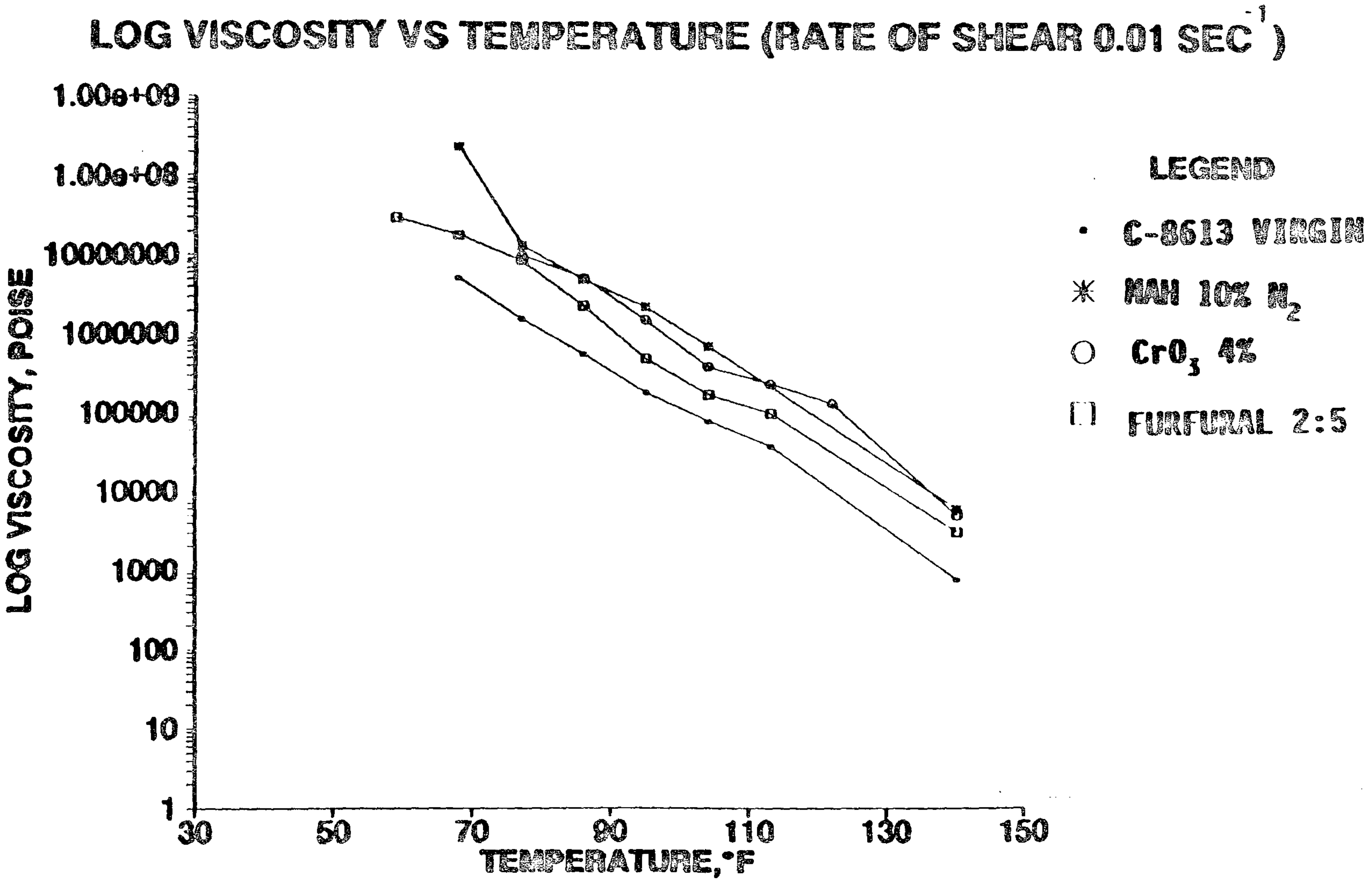

Figure 12. Viscosities at a shear rate of 0.01 sec^{-1} are shown as a function of temperature for the C-8613 virgin asphalt and its chemically modified versions.

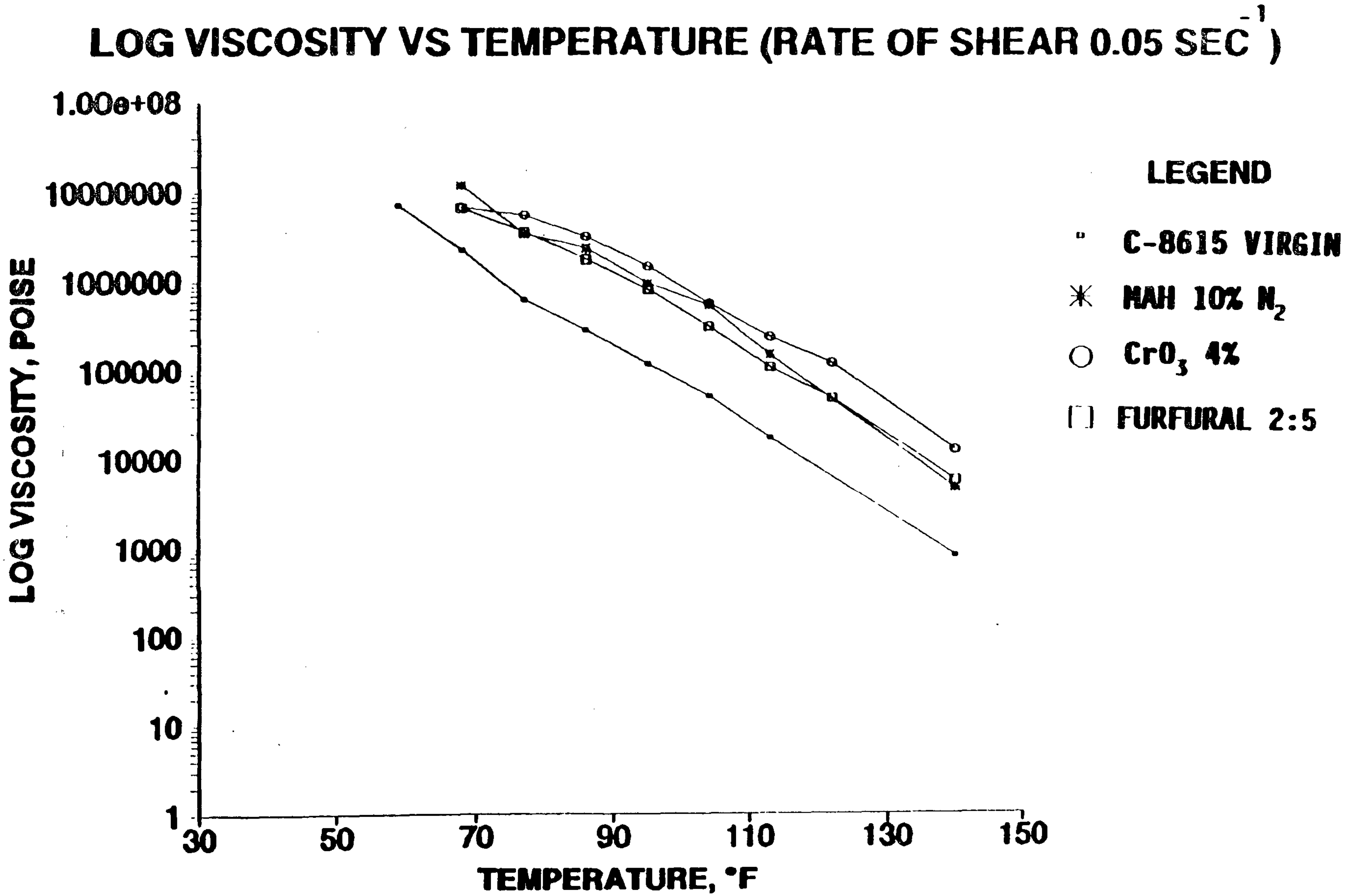

Figure 13. Viscosities at a shear rate of 0.05 sec^{-1} are shown as a function of temperature for the C-8615 virgin asphalt and its chemically modified versions.

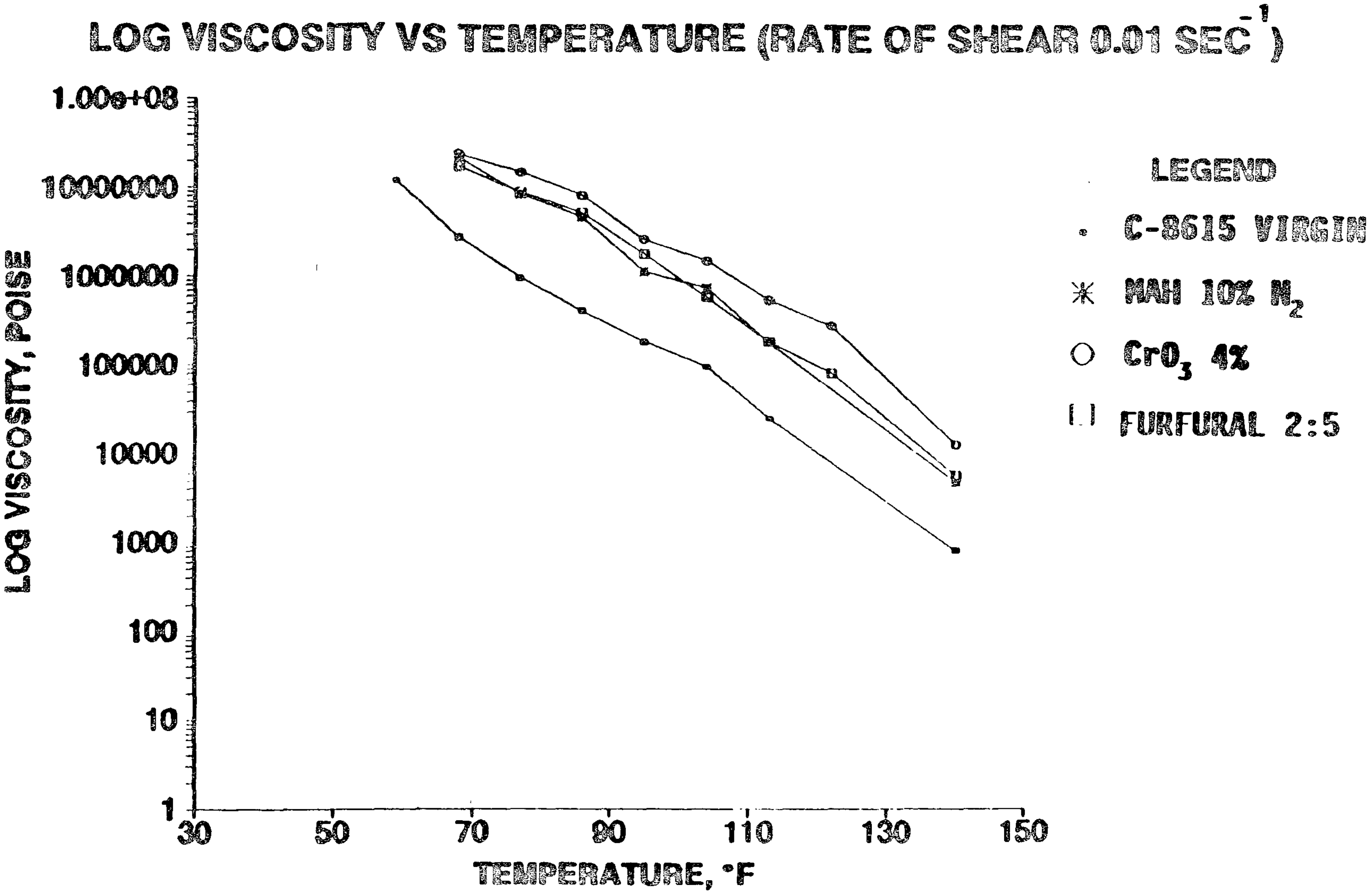

Figure 14. Viscosities at a shear rate of 0.01 sec^{-1} are shown as a function of temperature for the C-8615 virgin asphalt and its chemically modified versions.

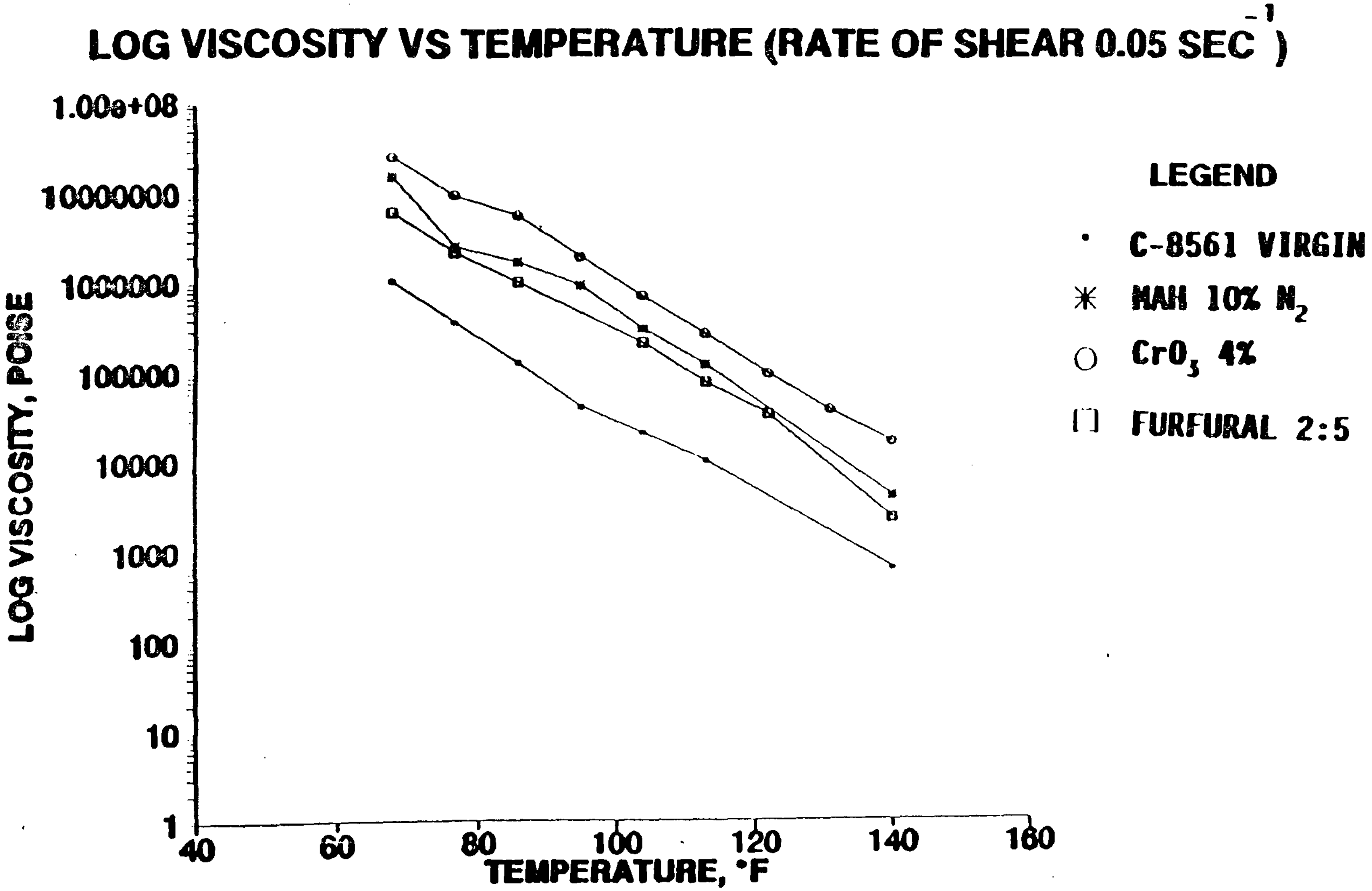

Figure 15. Viscosities at a shear rate of 0.05 sec^{-1} are shown as a function of temperature for the C-8561 virgin asphalt and its chemically modified versions.

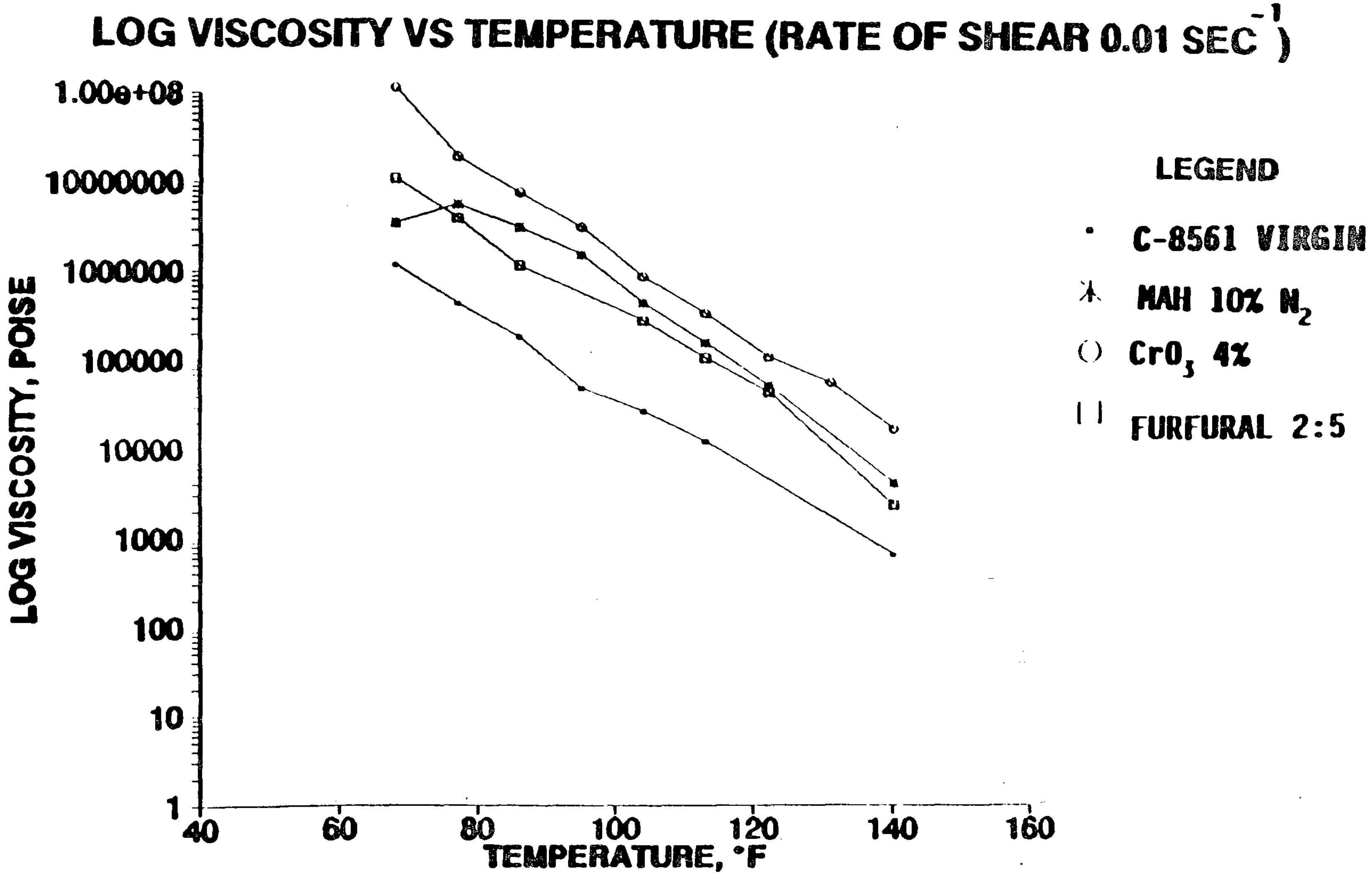

Figure 16. Viscosities at a shear rate of 0.01 sec^{-1} are shown as a function of temperature for the C-8561 virgin asphalt and its chemically modified versions.

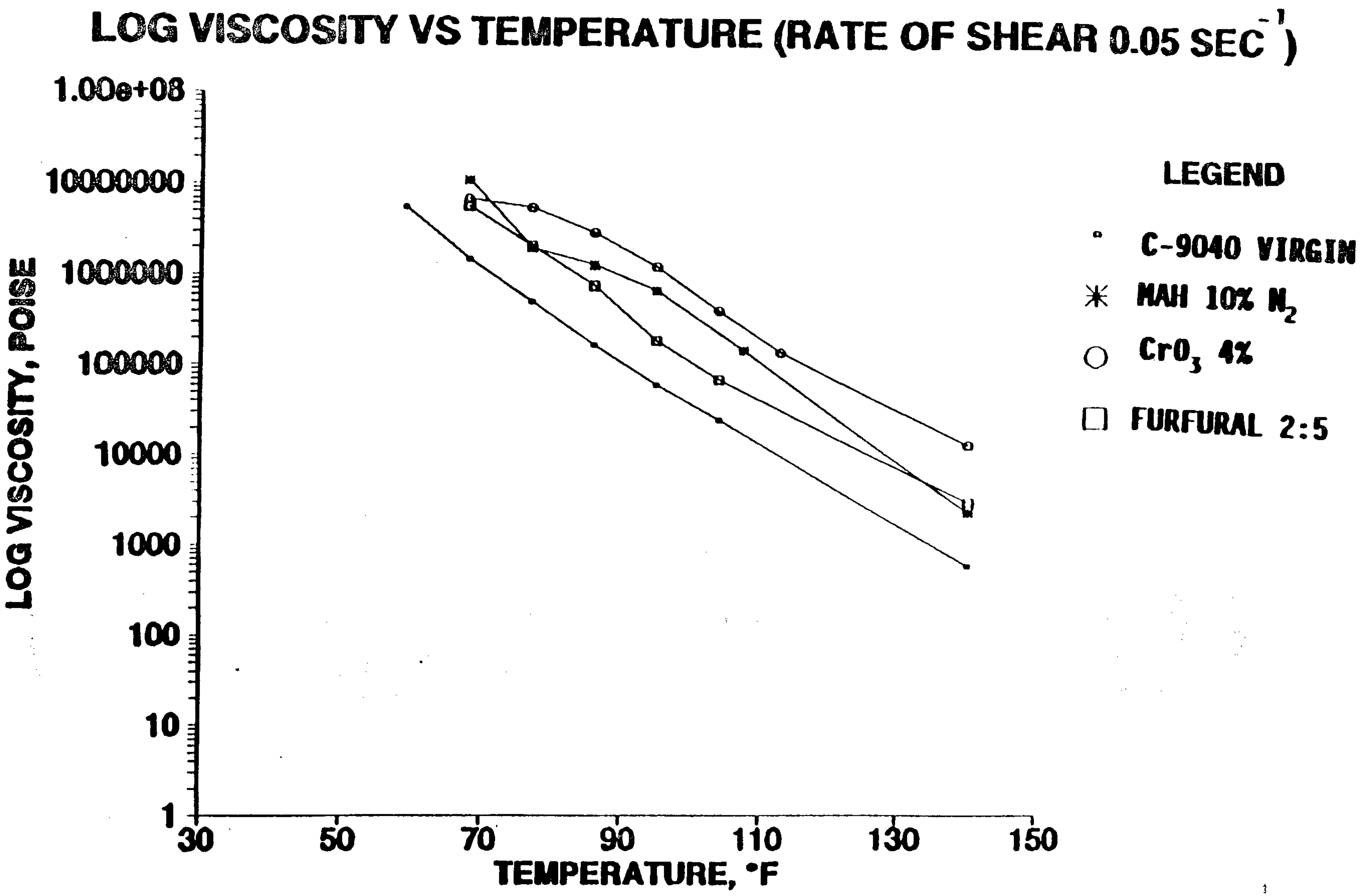

Figure 17. Viscosities at a shear rate of 0.05 sec^{-1} are shown as a function of temperature for the C-9040 virgin asphalt and its chemically modified versions.

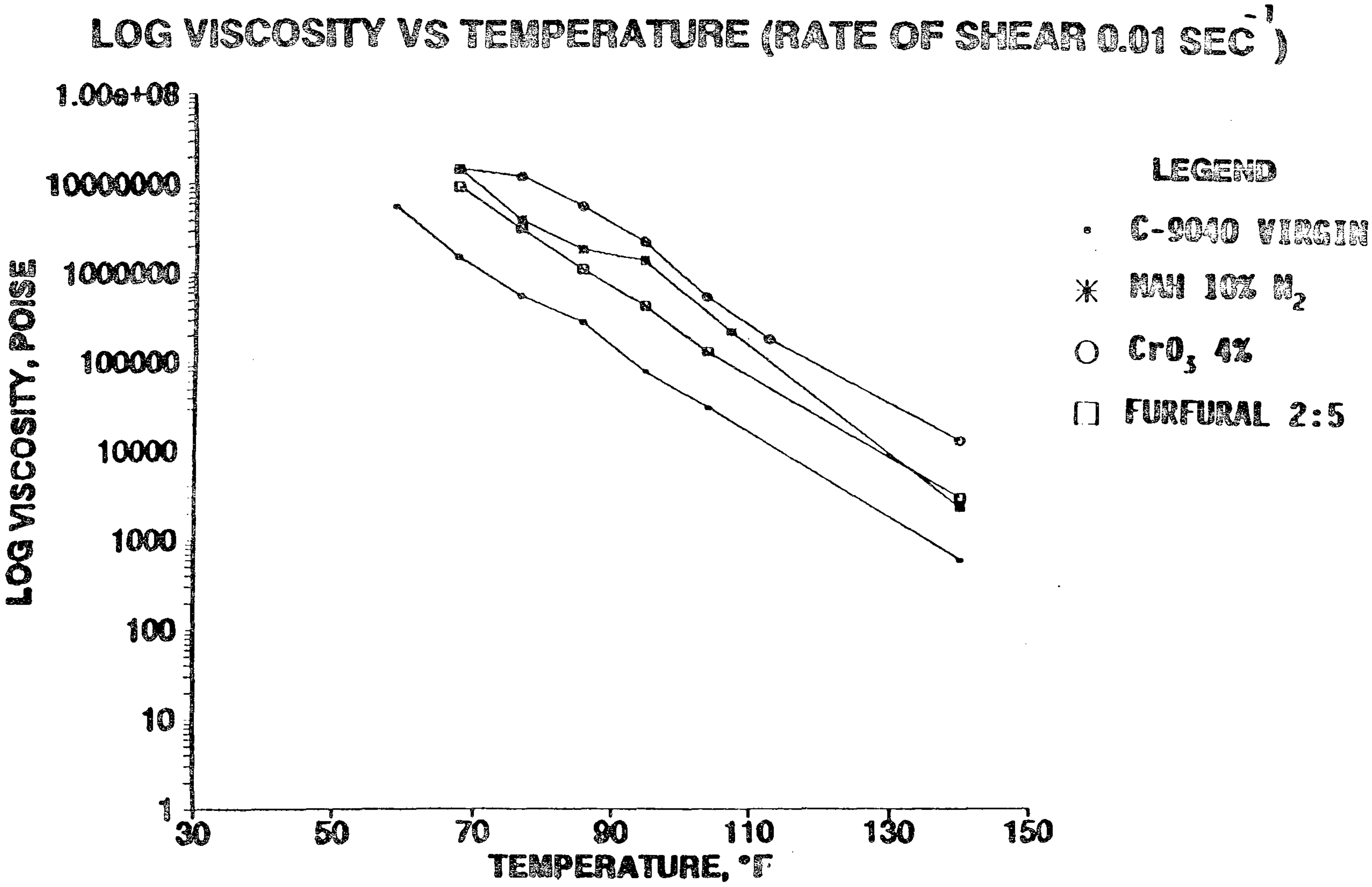

Figure 18. Viscosities at a shear rate of 0.01 sec^{-1} are shown as a function of temperature for the C-9040 virgin asphalt and its chemically modified versions.

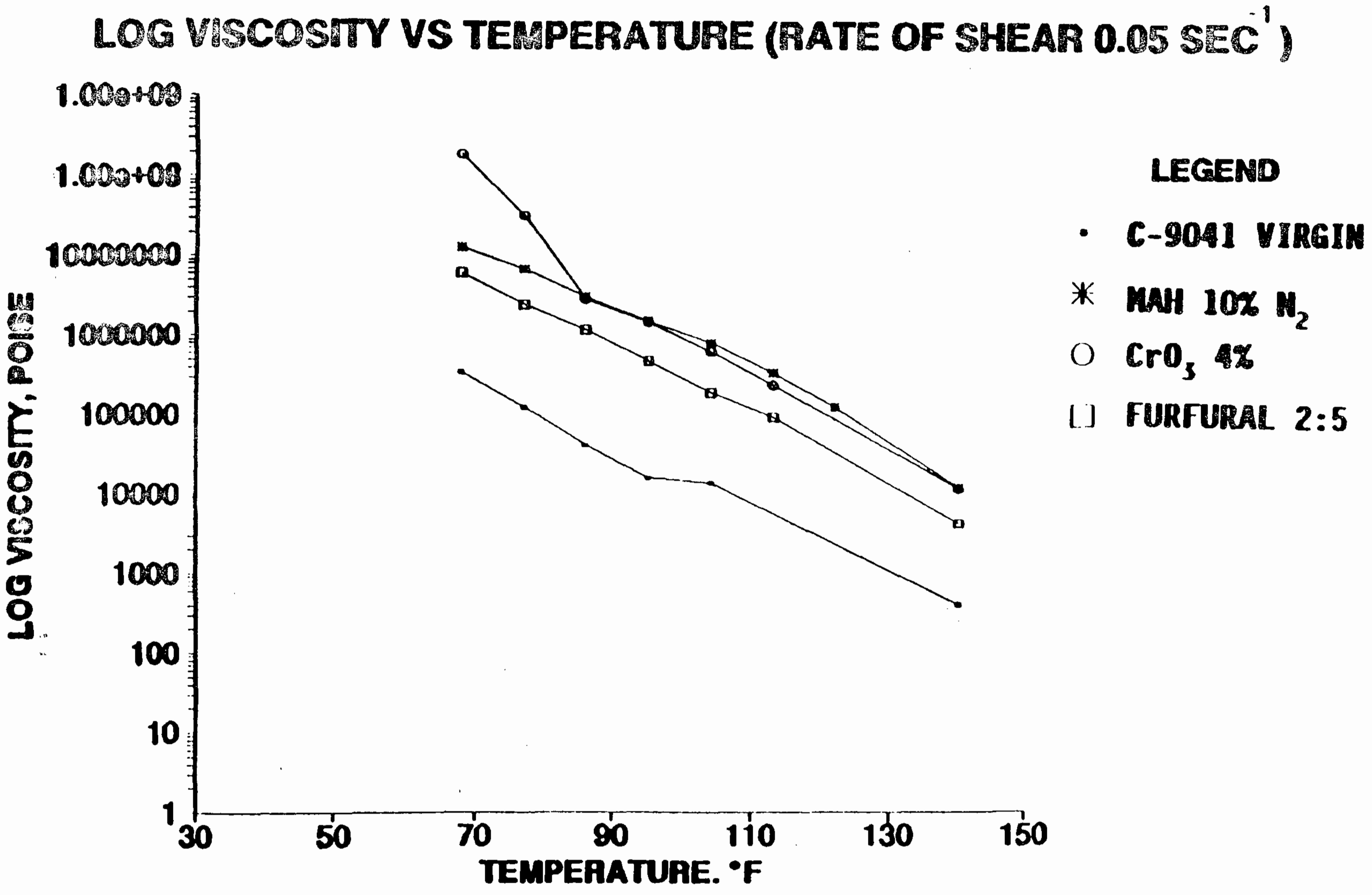

Figure 19. Viscosities at a shear rate of 0.05 sec^{-1} are shown as a function of temperature for the C-9041 virgin asphalt and its chemically modified versions.

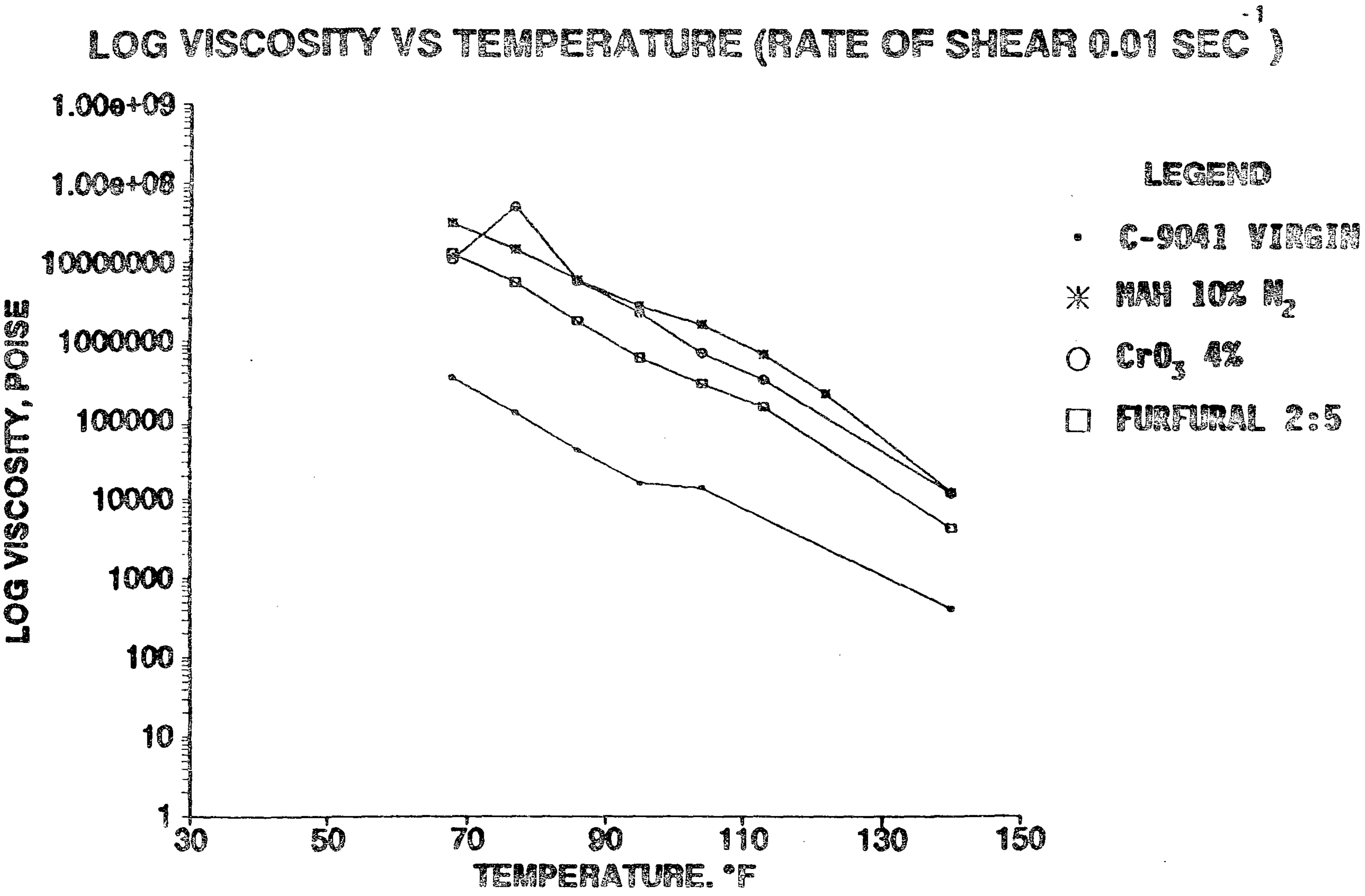

Figure 20. Viscosities at a shear rate of 0.01 sec^{-1} are shown as a function of temperature for the C-9041 virgin asphalt and its chemically modified versions.

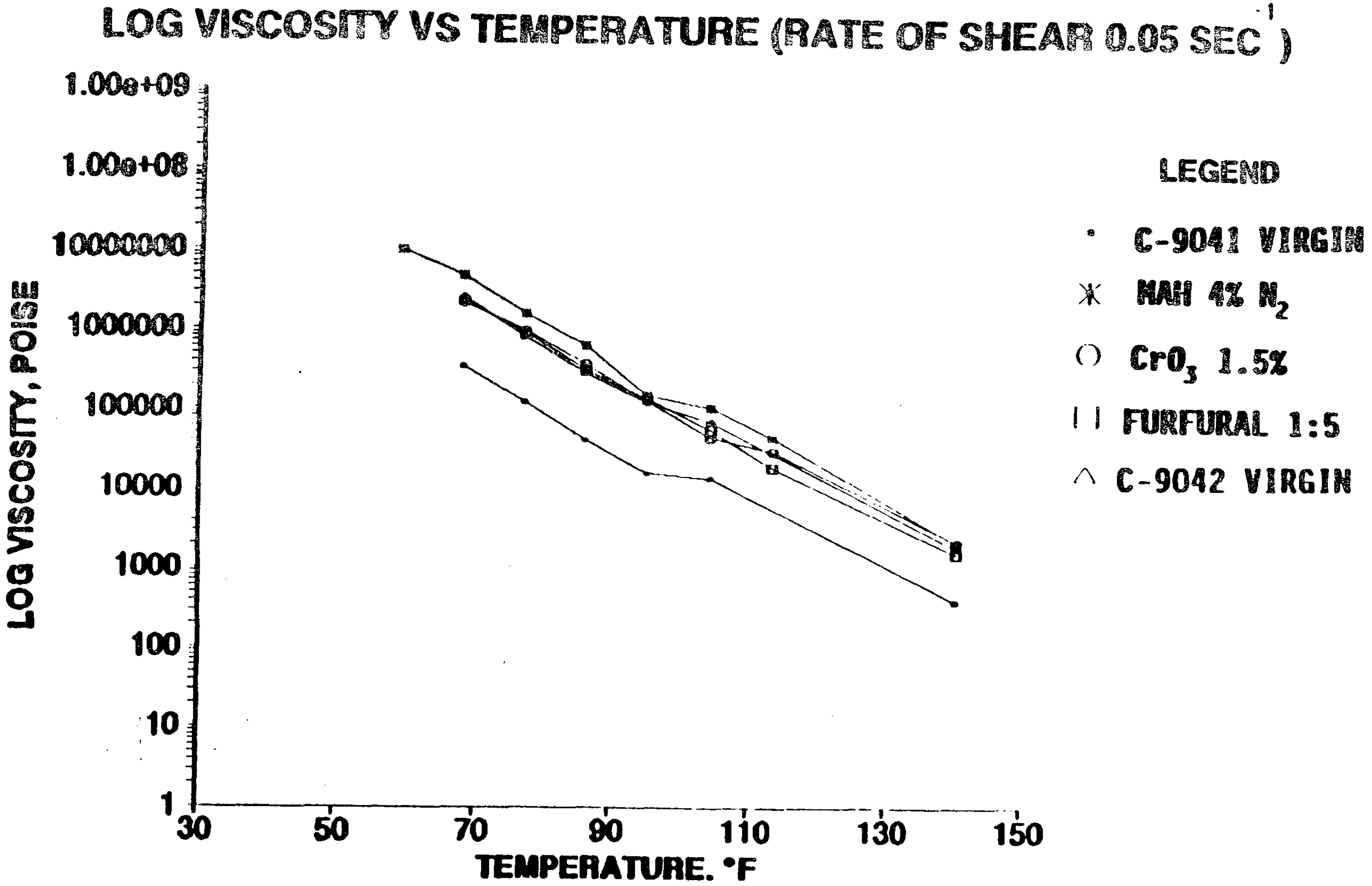

Figure 21. Viscosities at a shear rate of 0.05 sec^{-1} are shown as a function of temperature for the C-9041 virgin asphalt and its chemically modified versions compared to that of the C-9042 virgin asphalt.

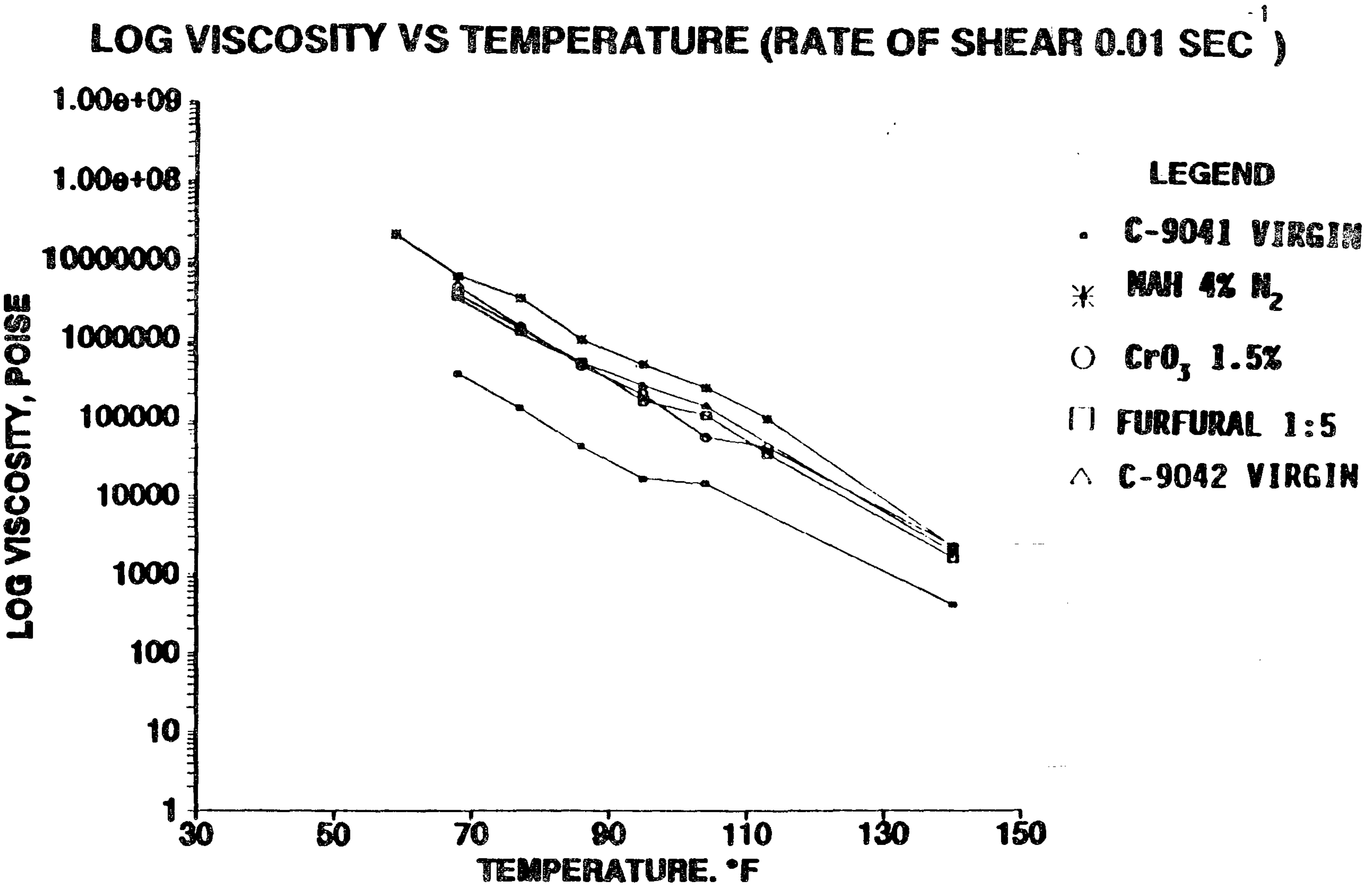

Figure 22. Viscosities at a shear rate of 0.01 sec^{-1} are shown as a function of temperature for the C-9041 virgin asphalt and its chemically modified versions compared to that of the C-9042 virgin asphalt.

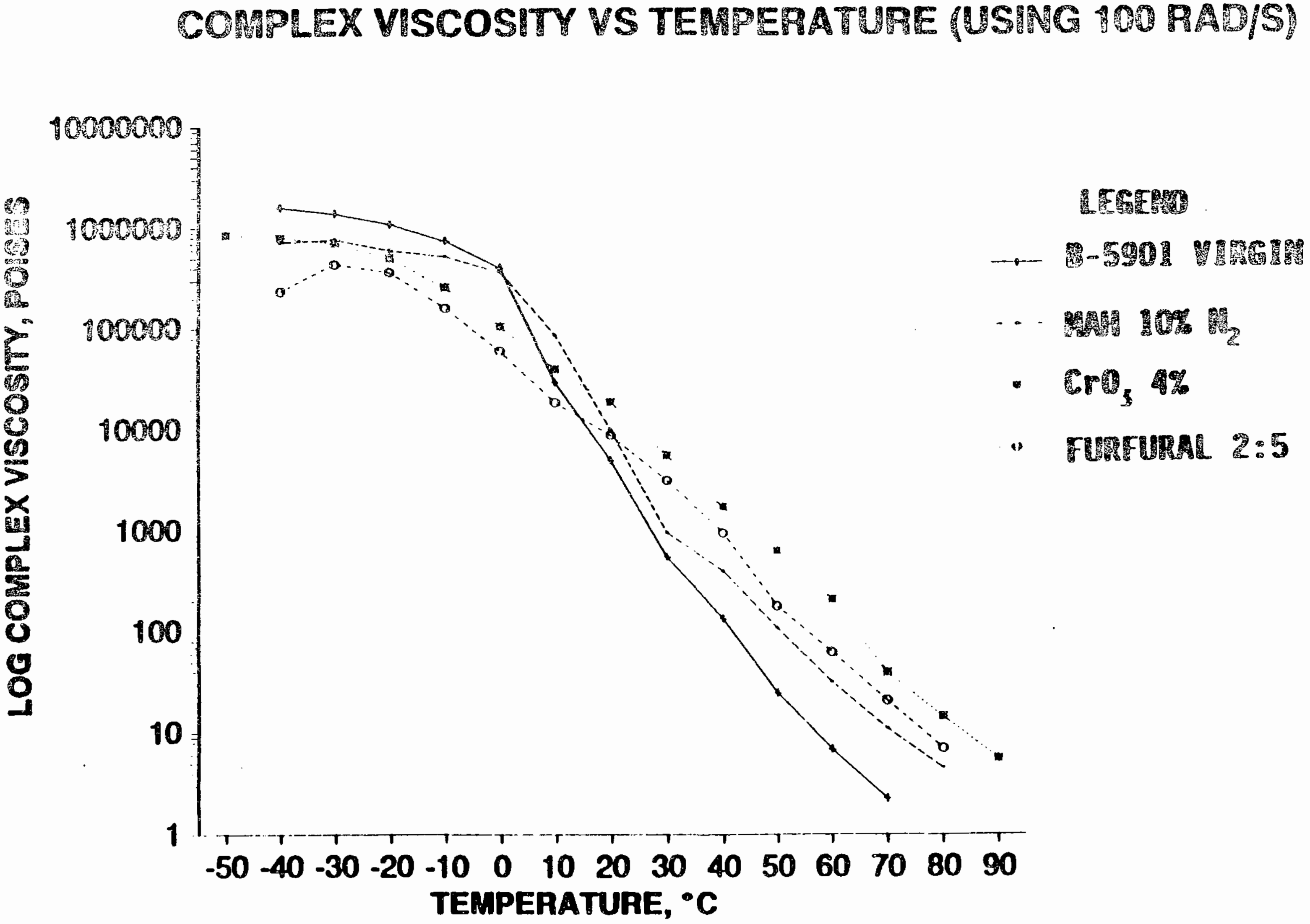

Figure 23. Complex viscosities vs temperature of the B-5901 virgin asphalt and its chemically modified versions at 100 radians/second.

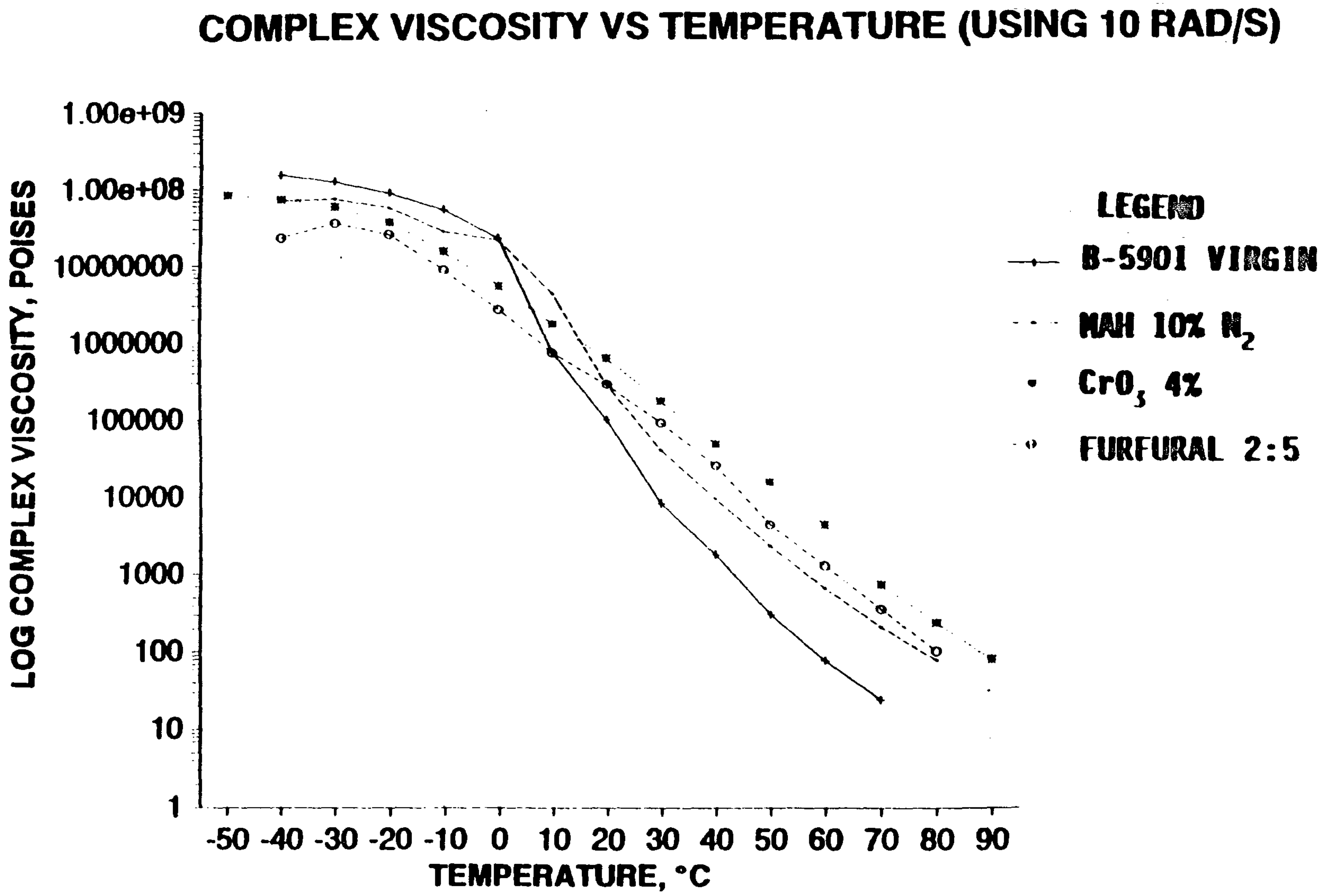

Figure 24. Complex viscosities vs temperature of the B-5901 virgin asphalt and its chemically modified versions at 10 radians/second.

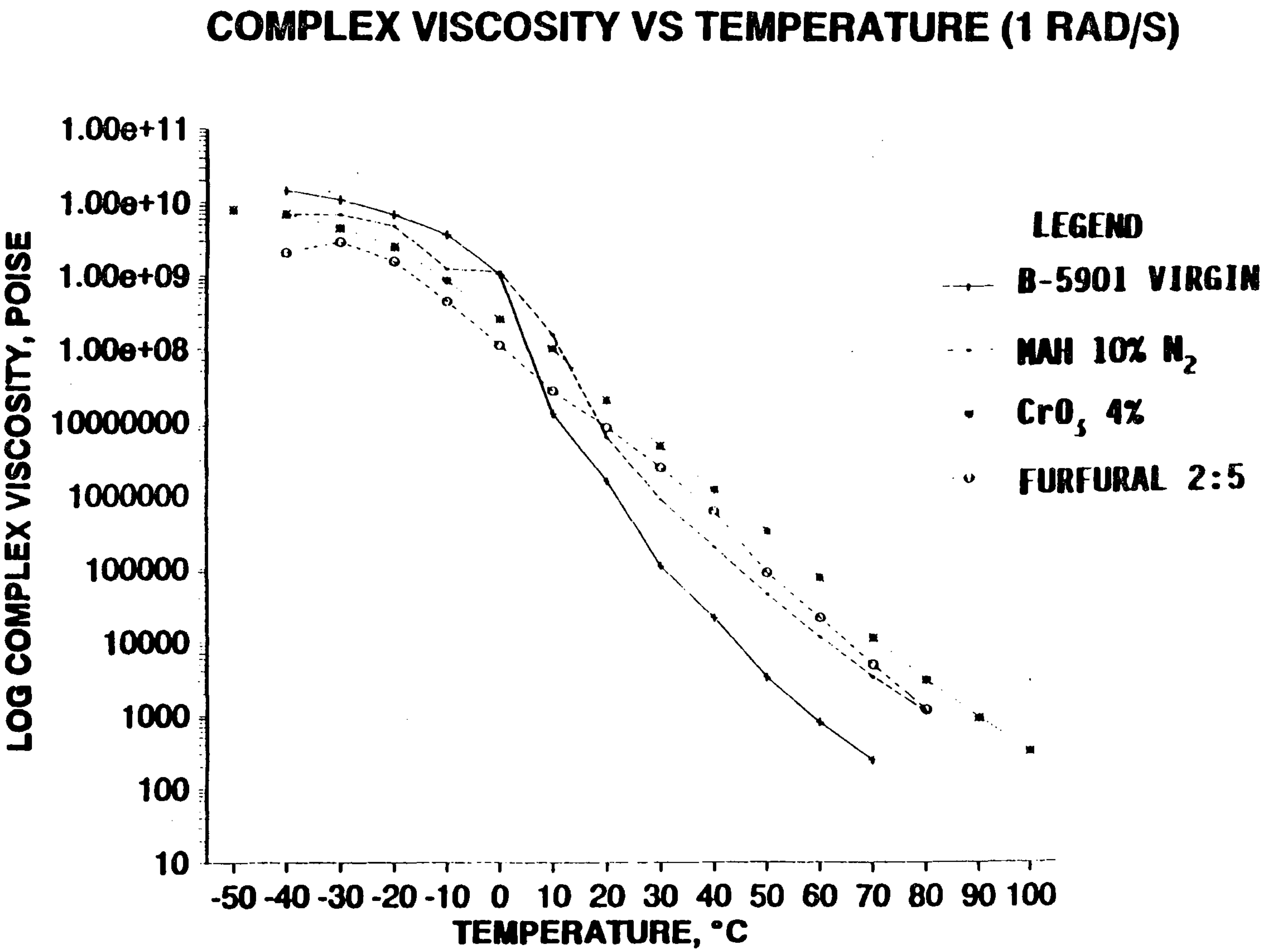

Figure 25. Complex viscosities vs temperature of the B-5901 virgin asphalt and its chemically modified versions at 1 radian/second.

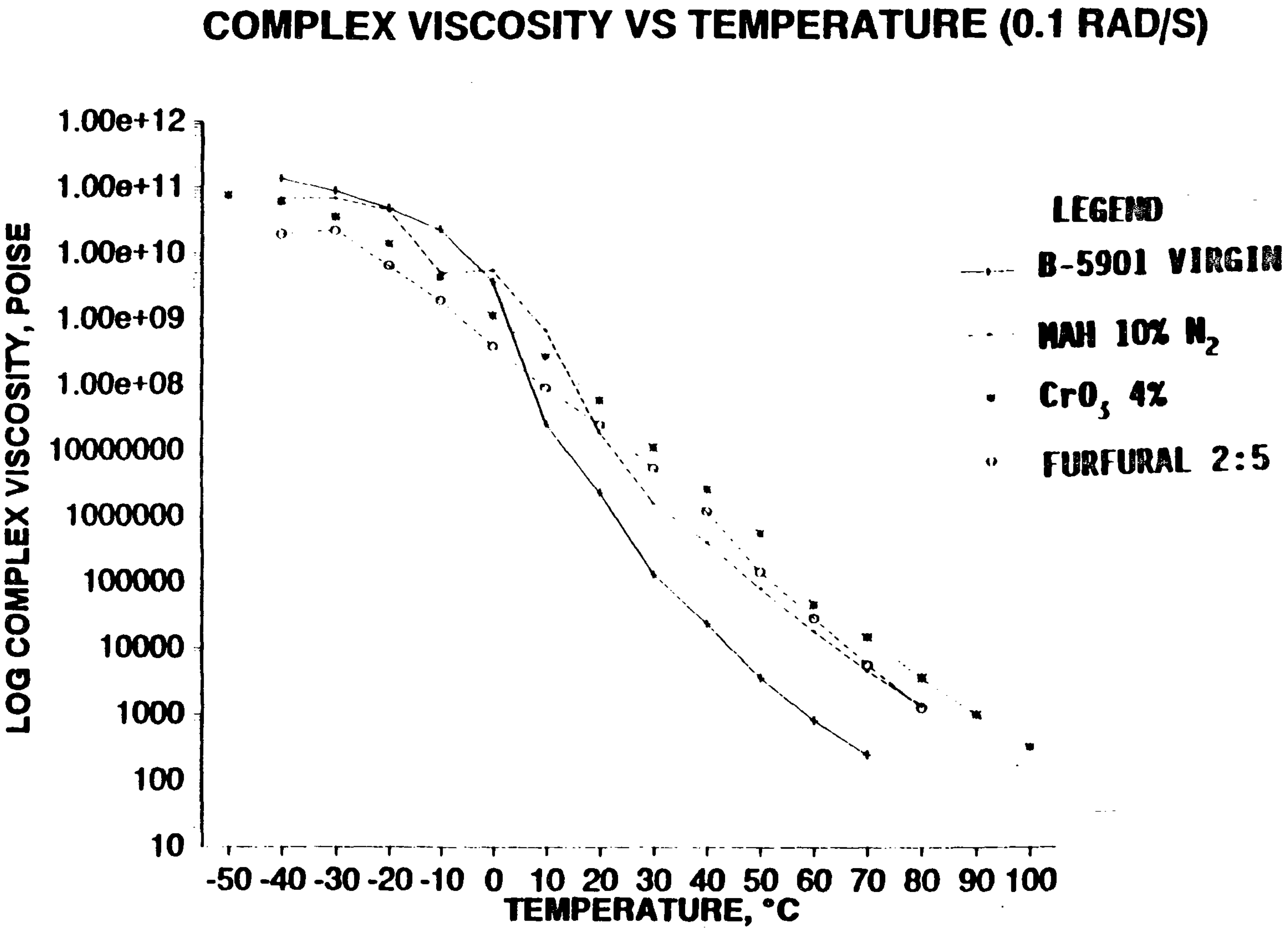

Figure 26. Complex viscosities vs temperature of the B-5901 virgin asphalt and its chemically modified versions at 0.1 radian/second.

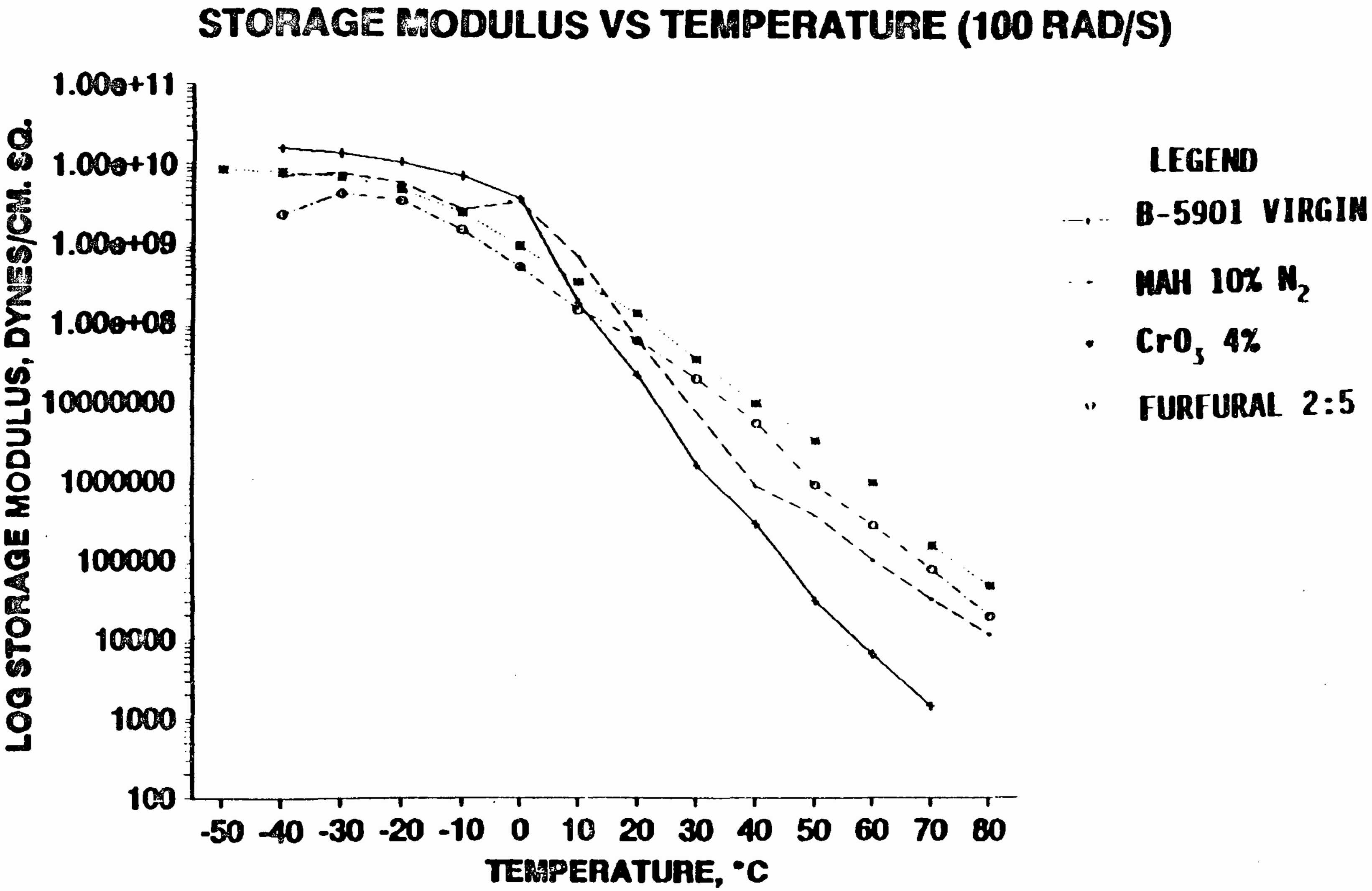

Figure 27. Storage moduli vs temperature of the B-5901 virgin asphalt and its chemically modified versions at 100 radians/second.

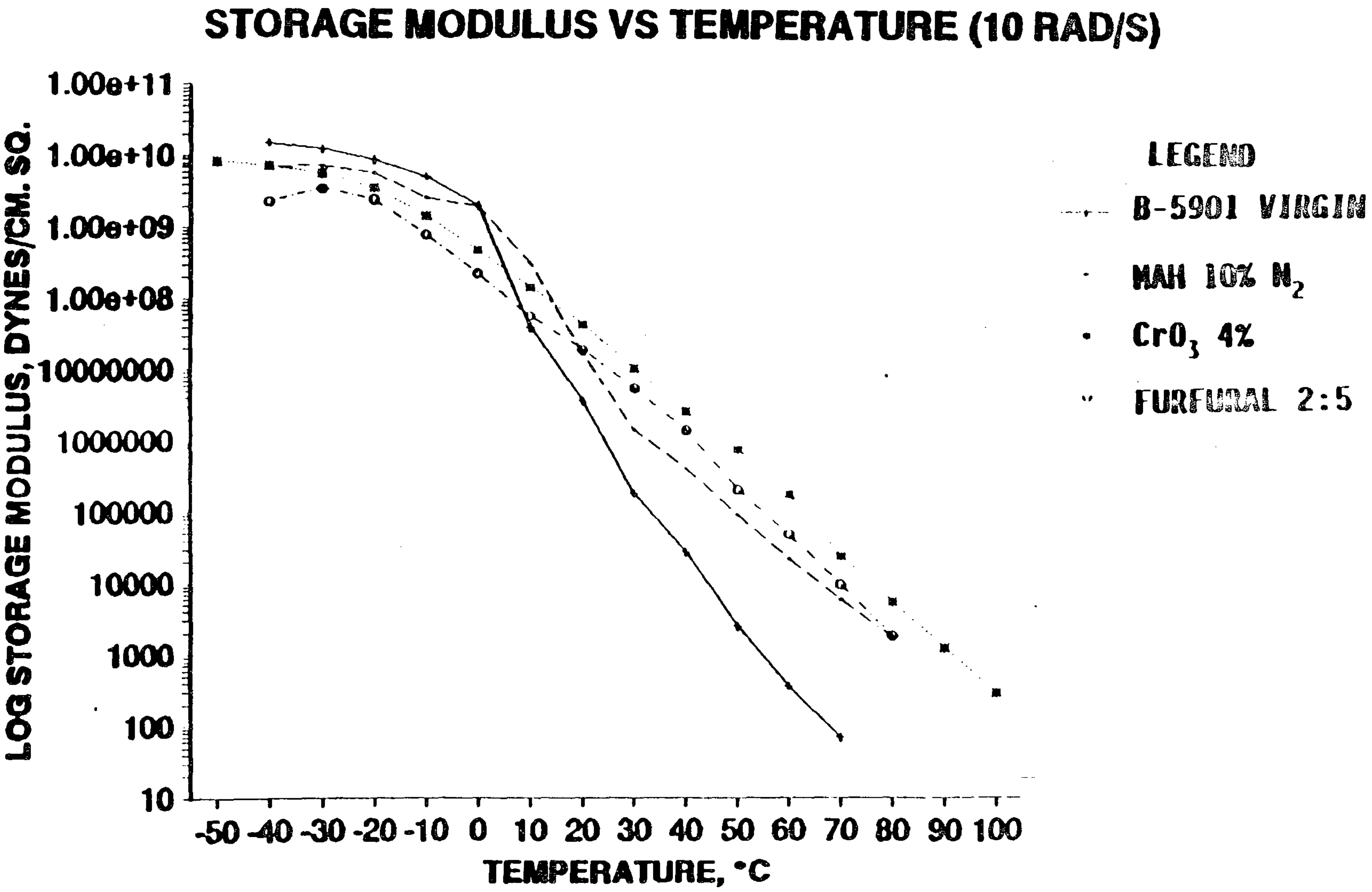

Figure 28. Storage moduli vs temperature of the B-5901 virgin asphalt and its chemically modified versions at 10 radians/second.

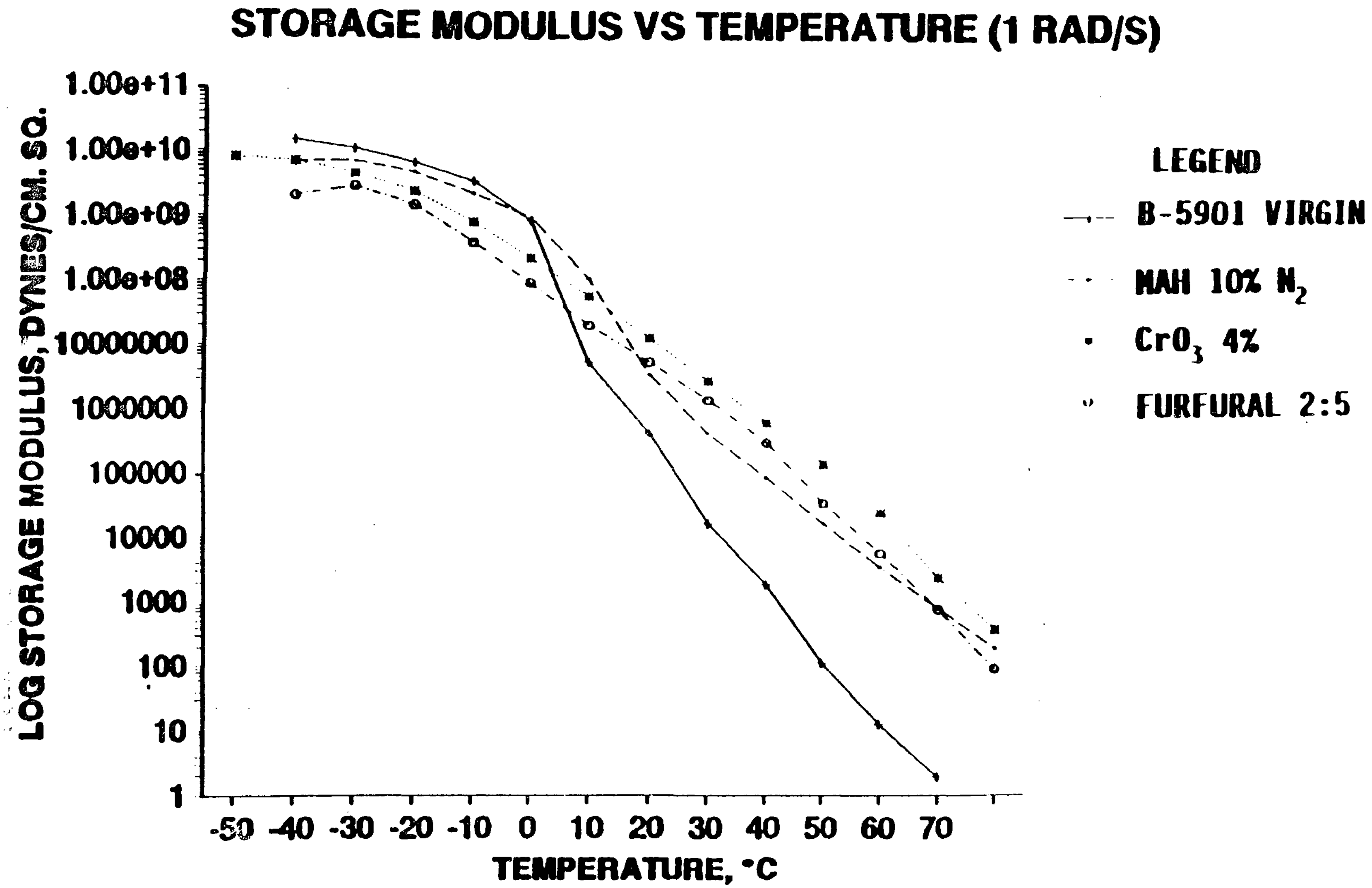

Figure 29. Storage moduli vs temperature of the B-5901 virgin asphalt and its chemically modified versions at 1 radian/second.

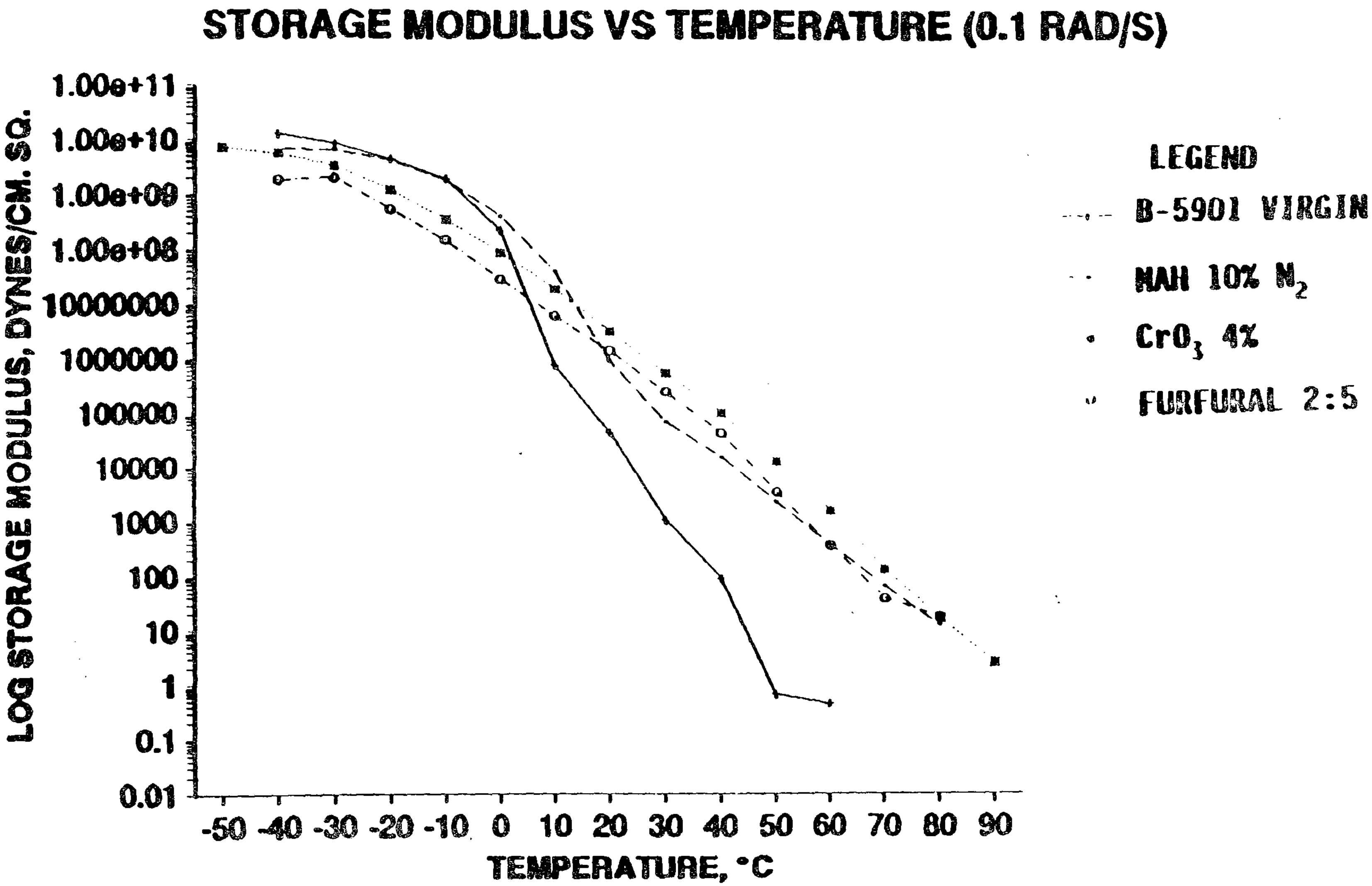

Figure 30. Storage moduli vs temperature of the B-5901 virgin asphalt and its chemically modified versions at 0.1 radian/second.

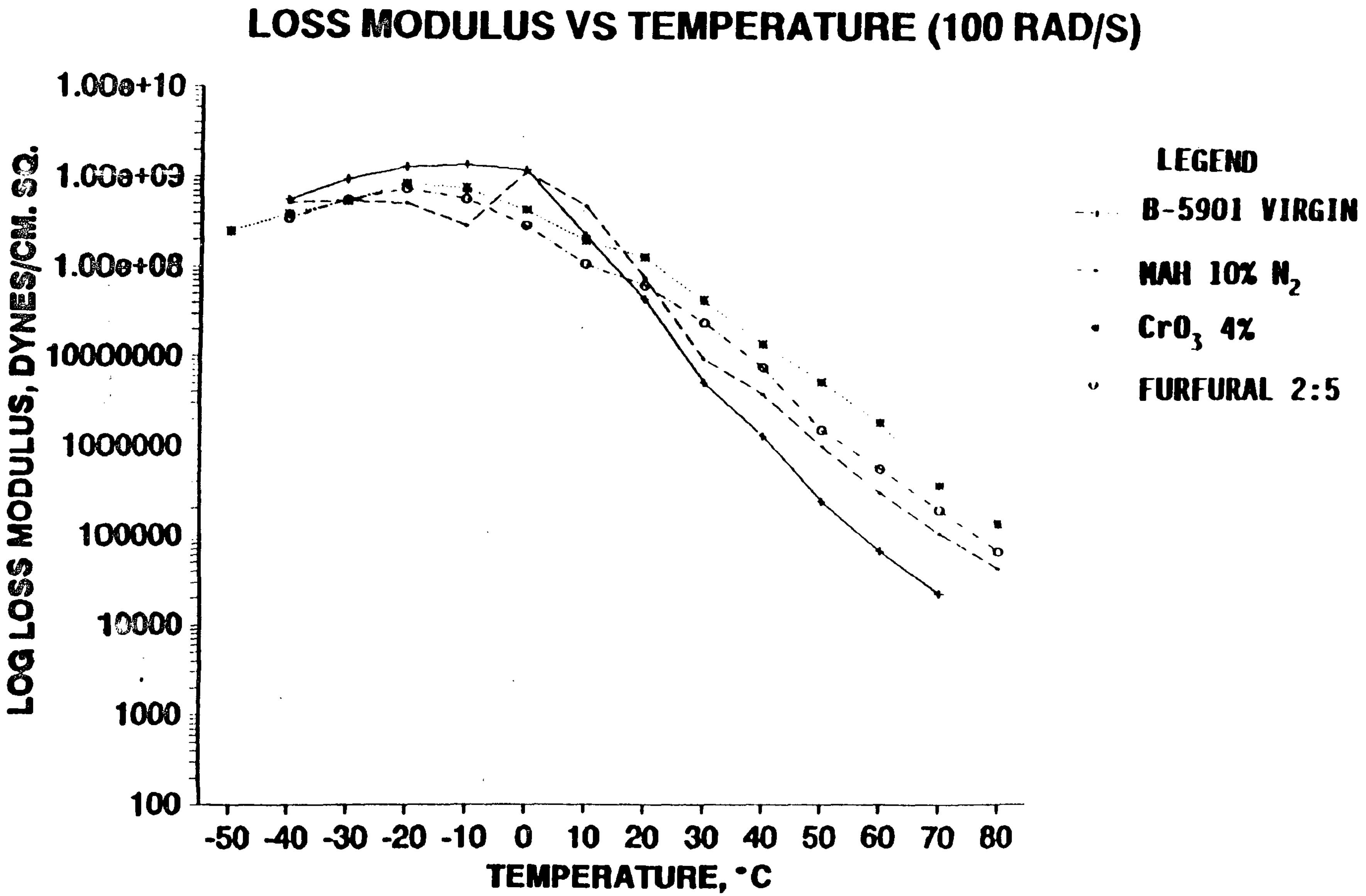

Figure 31. Loss moduli vs temperature of the B-5901 virgin asphalt and its chemically modified versions at 100 radians/second.

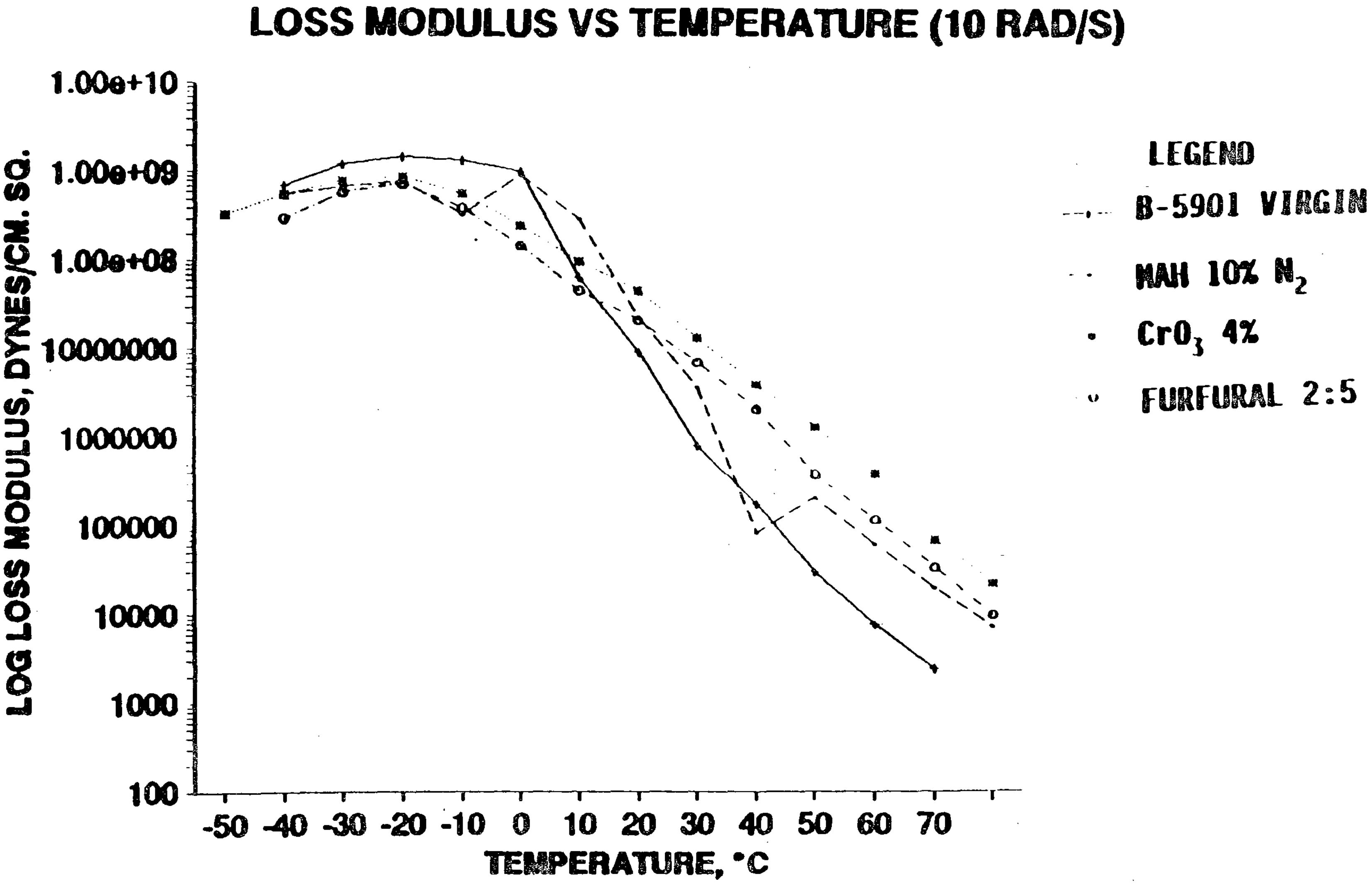

Figure 32. Loss moduli vs temperature of the B-5901 virgin asphalt and its chemically modified versions at 10 radians/second.

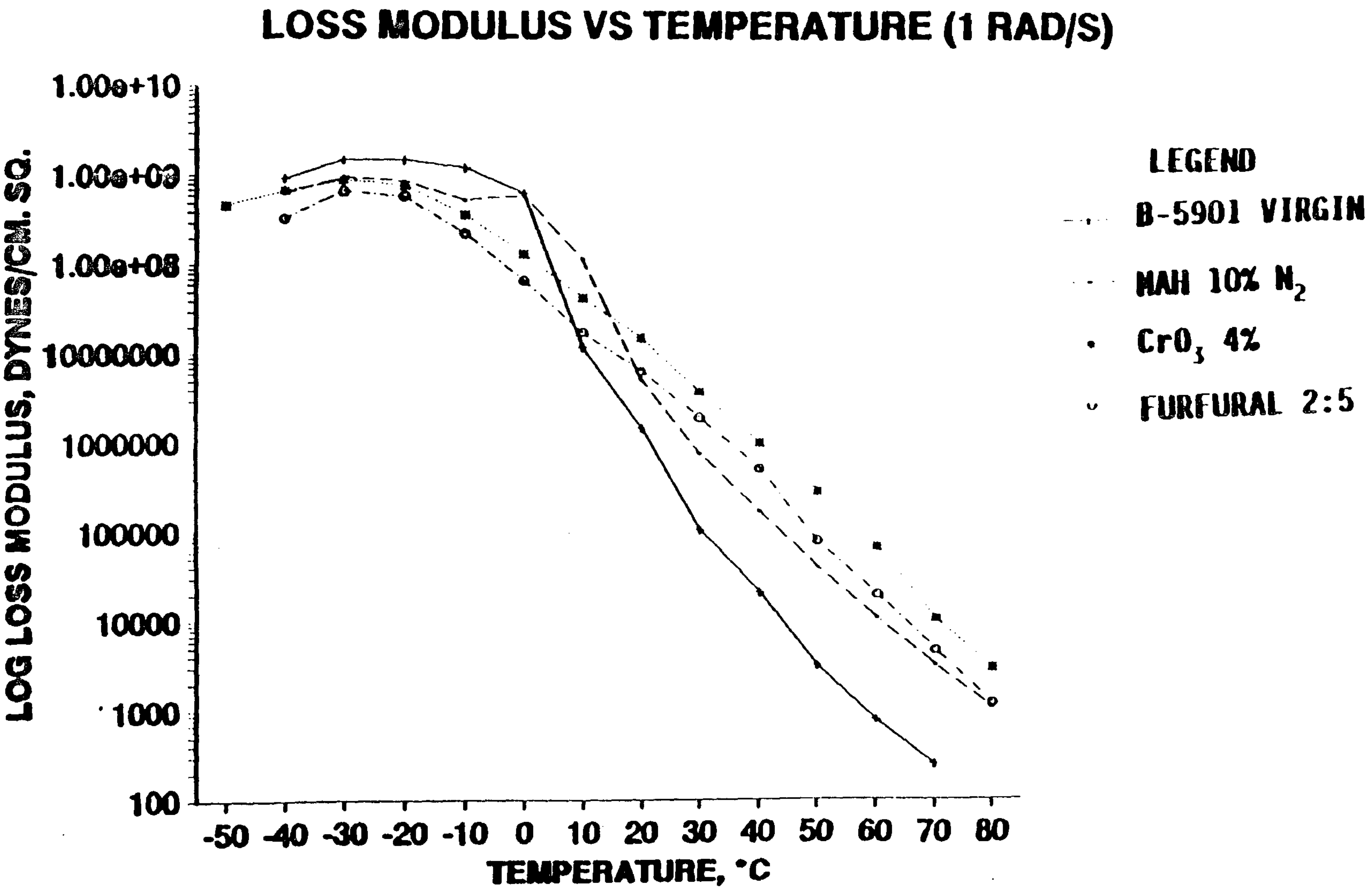

Figure 33. Loss moduli vs temperature of the B-5901 virgin asphalt and its chemically modified versions at 1 radian/second.

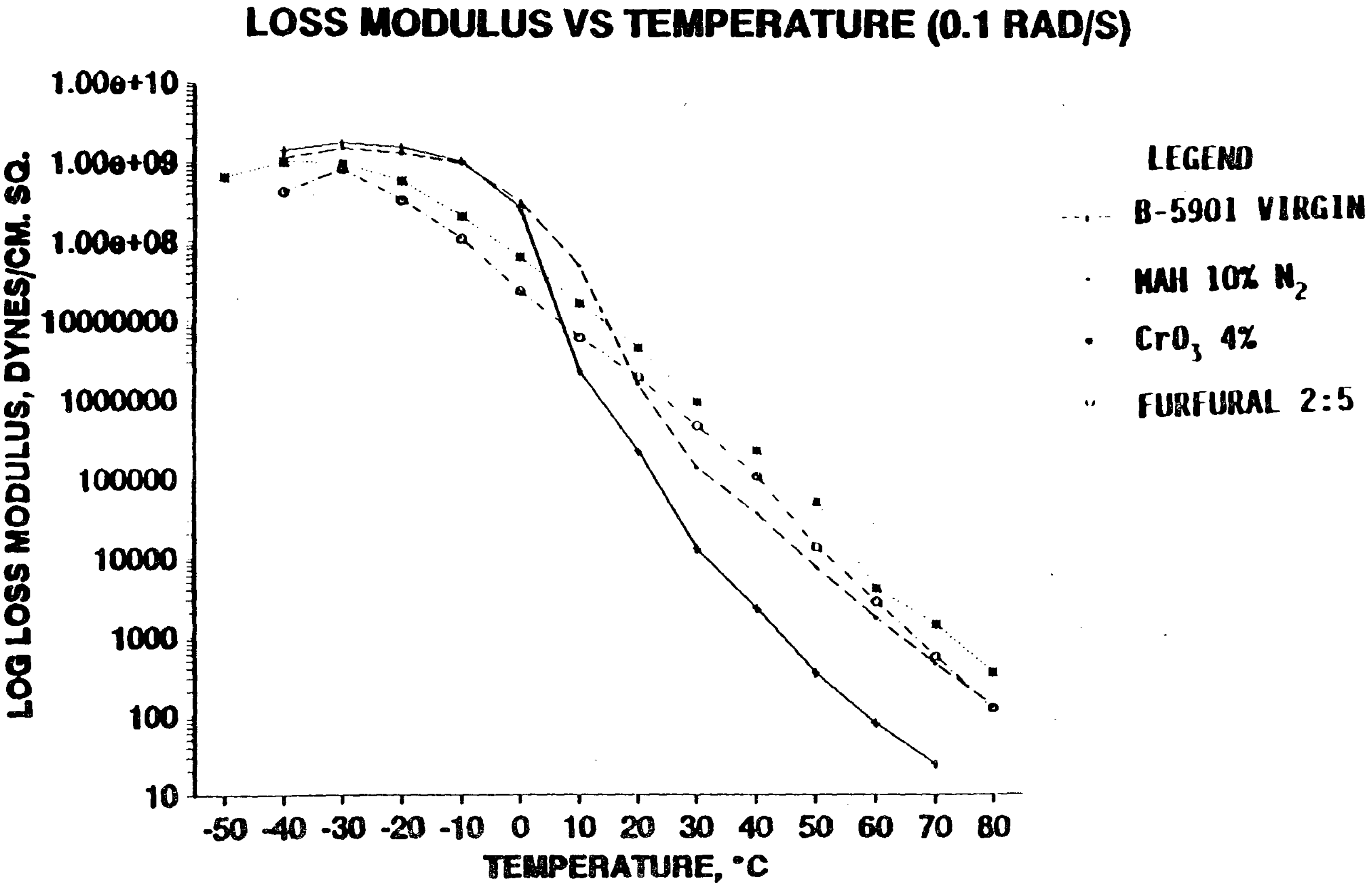

Figure 34. Loss moduli vs temperature of the B-5901 virgin asphalt and its chemically modified versions at 0.1 radian/second.

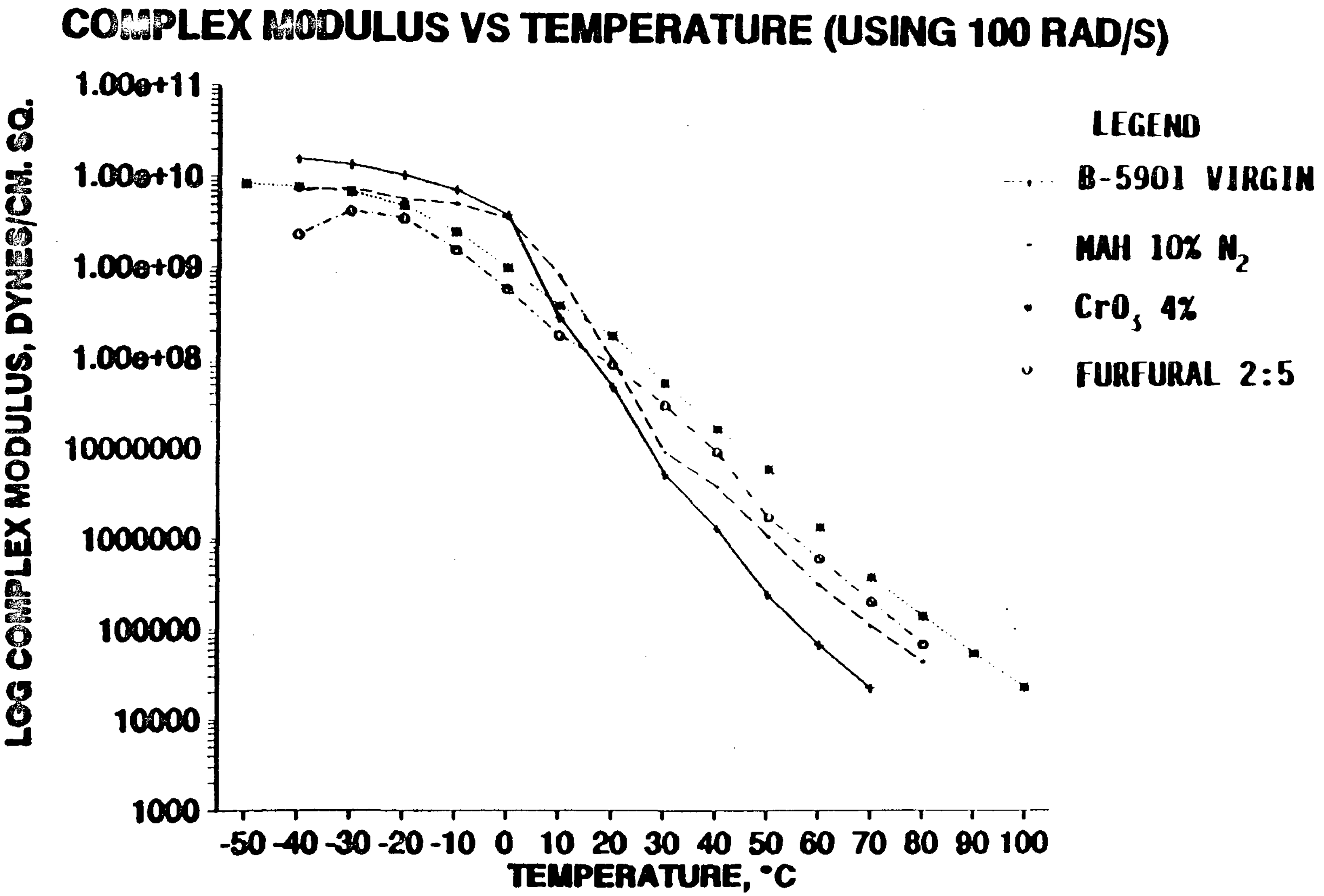

Figure 35. Complex moduli vs temperature of the B-5901 virgin asphalt and its chemically modified versions at 100 radians/second.

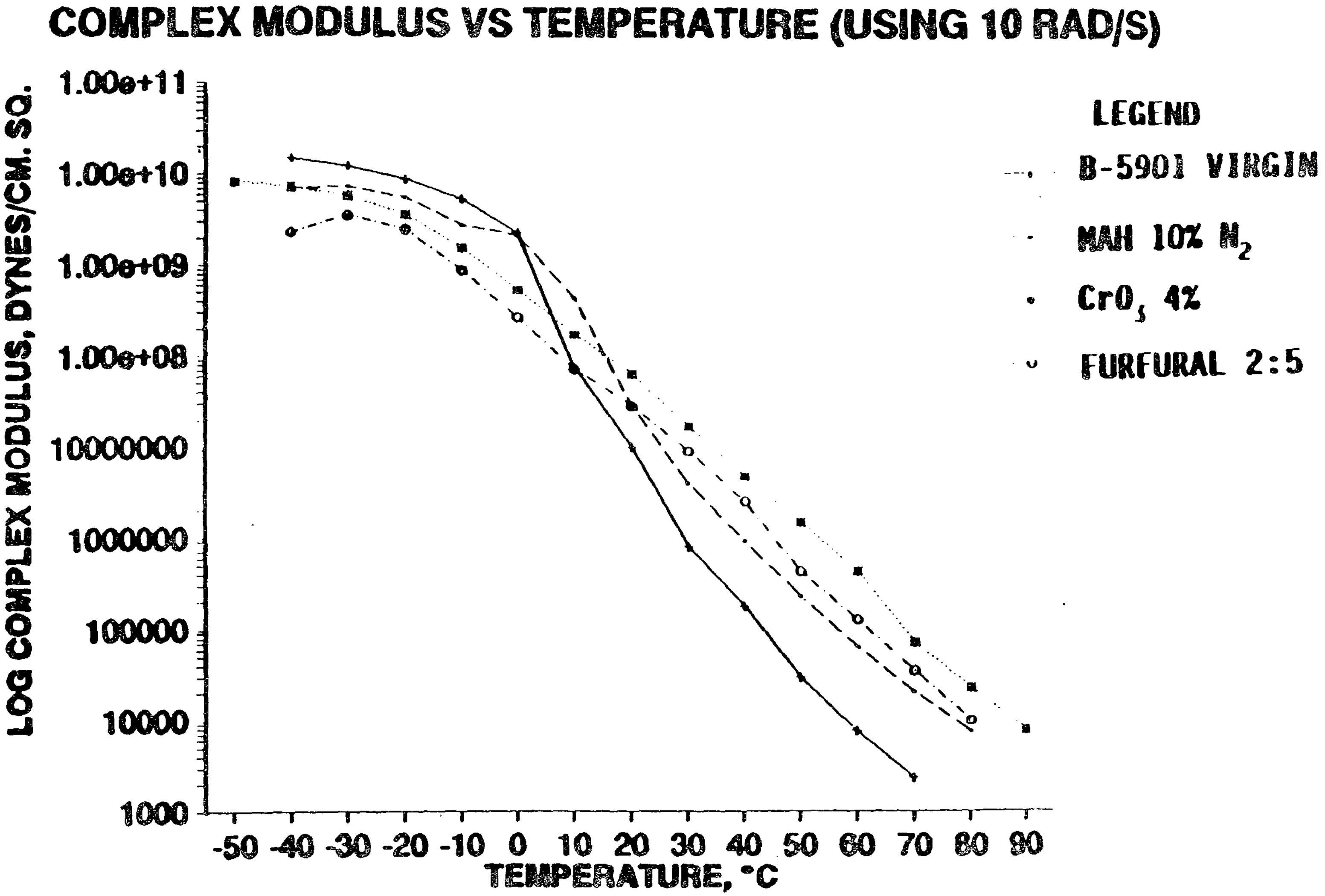

Figure 36. Complex moduli vs temperature of the B-5901 virgin asphalt and its chemically modified versions at 10 radians/second.

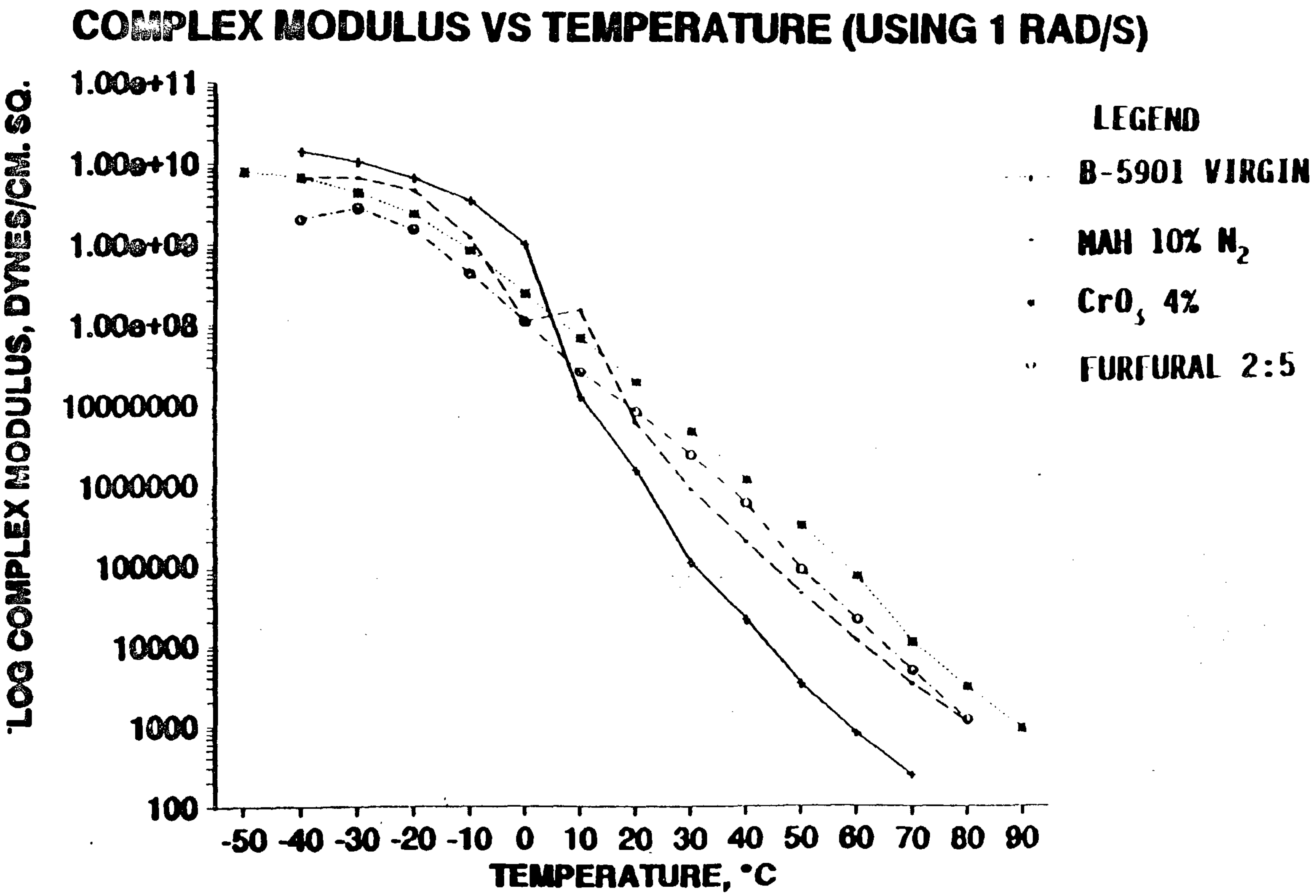

Figure 37. Complex moduli vs temperature of the B-5901 virgin asphalt and its chemically modified versions at 1 radian/second.

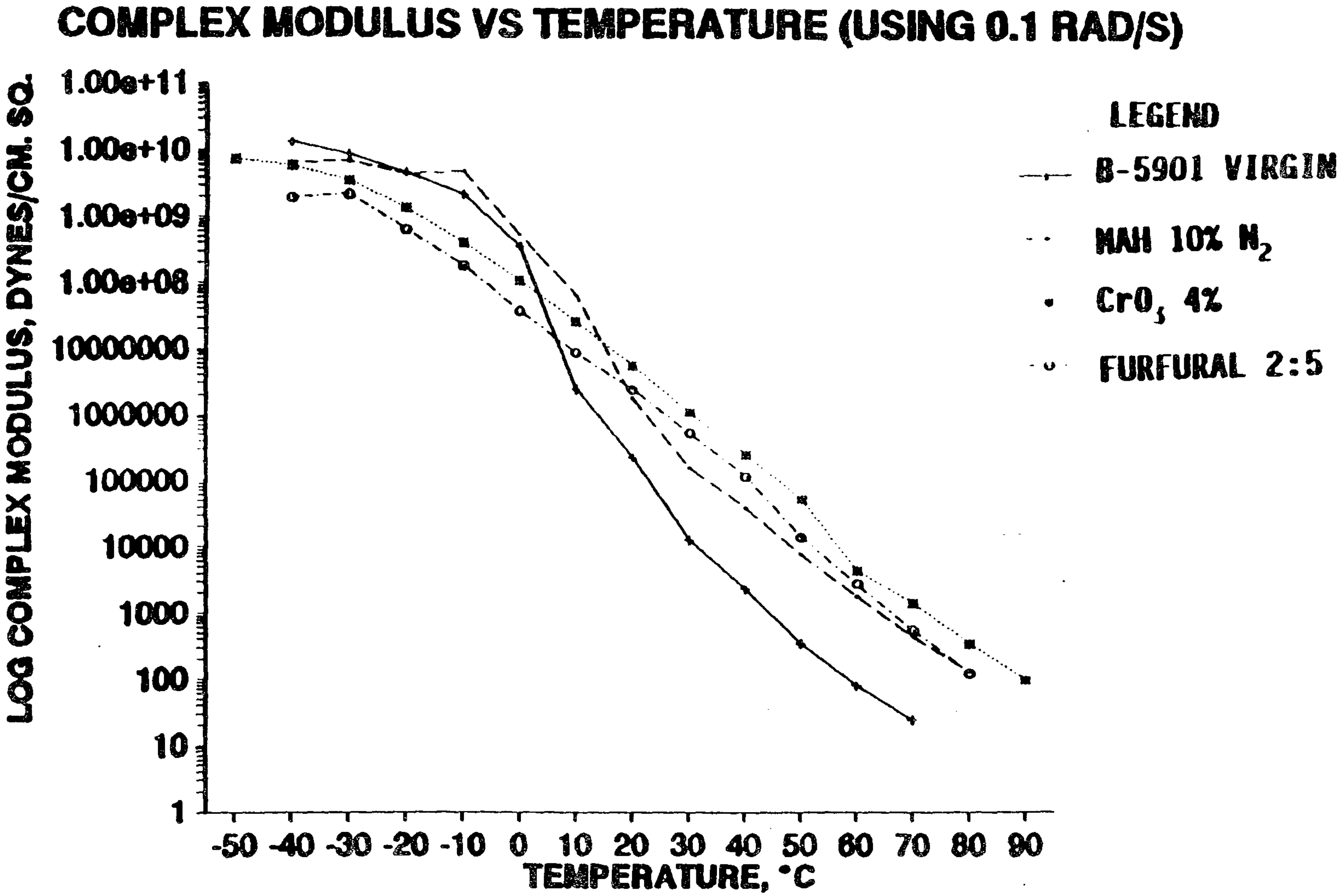

Figure 38. Complex moduli vs temperature of the B-5901 virgin asphalt and its chemically modified versions at 0.1 radian/second.

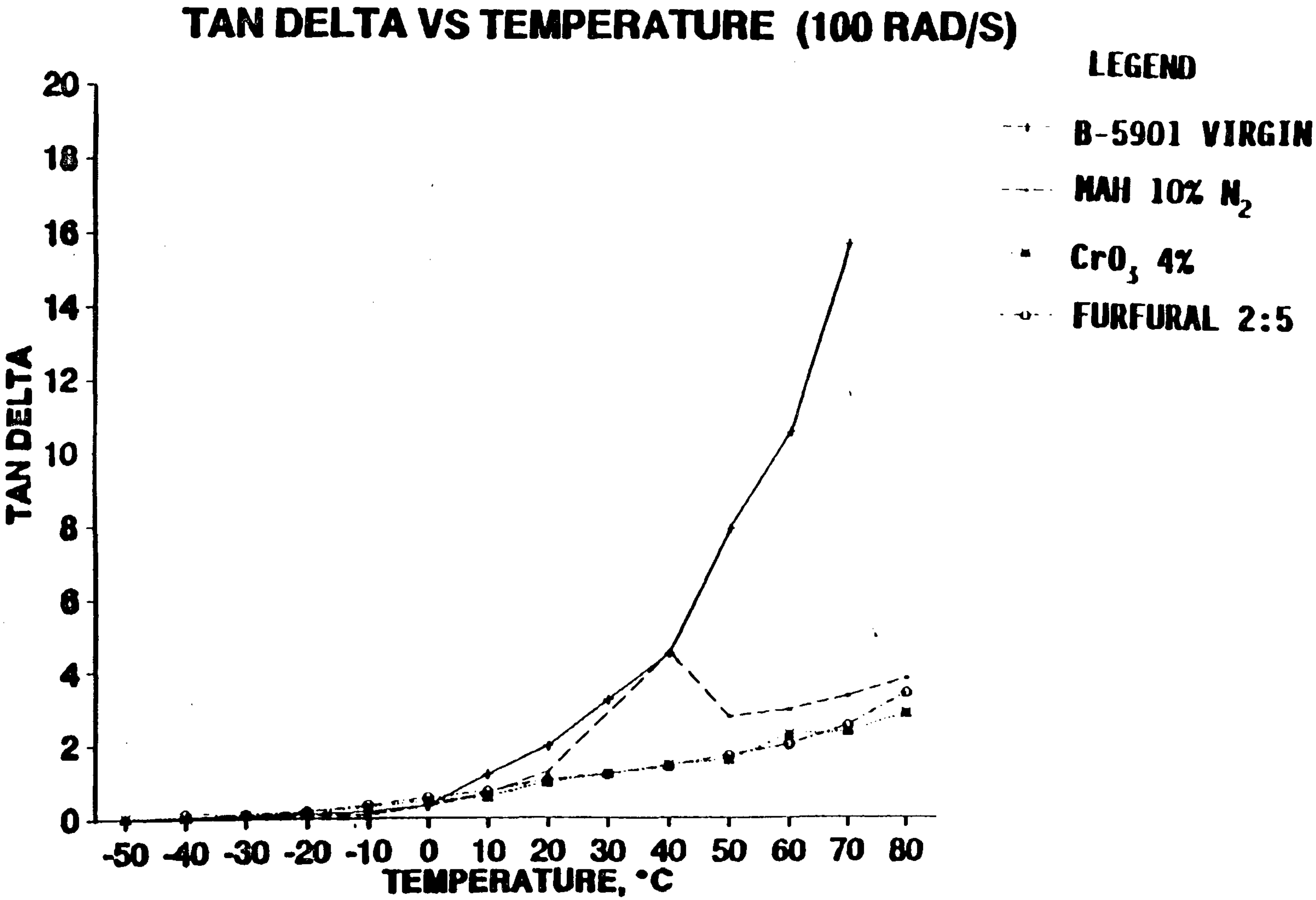

Figure 39. Tan delta vs temperature of the B-5901 virgin asphalt and its chemically modified versions at 100 radians/second.

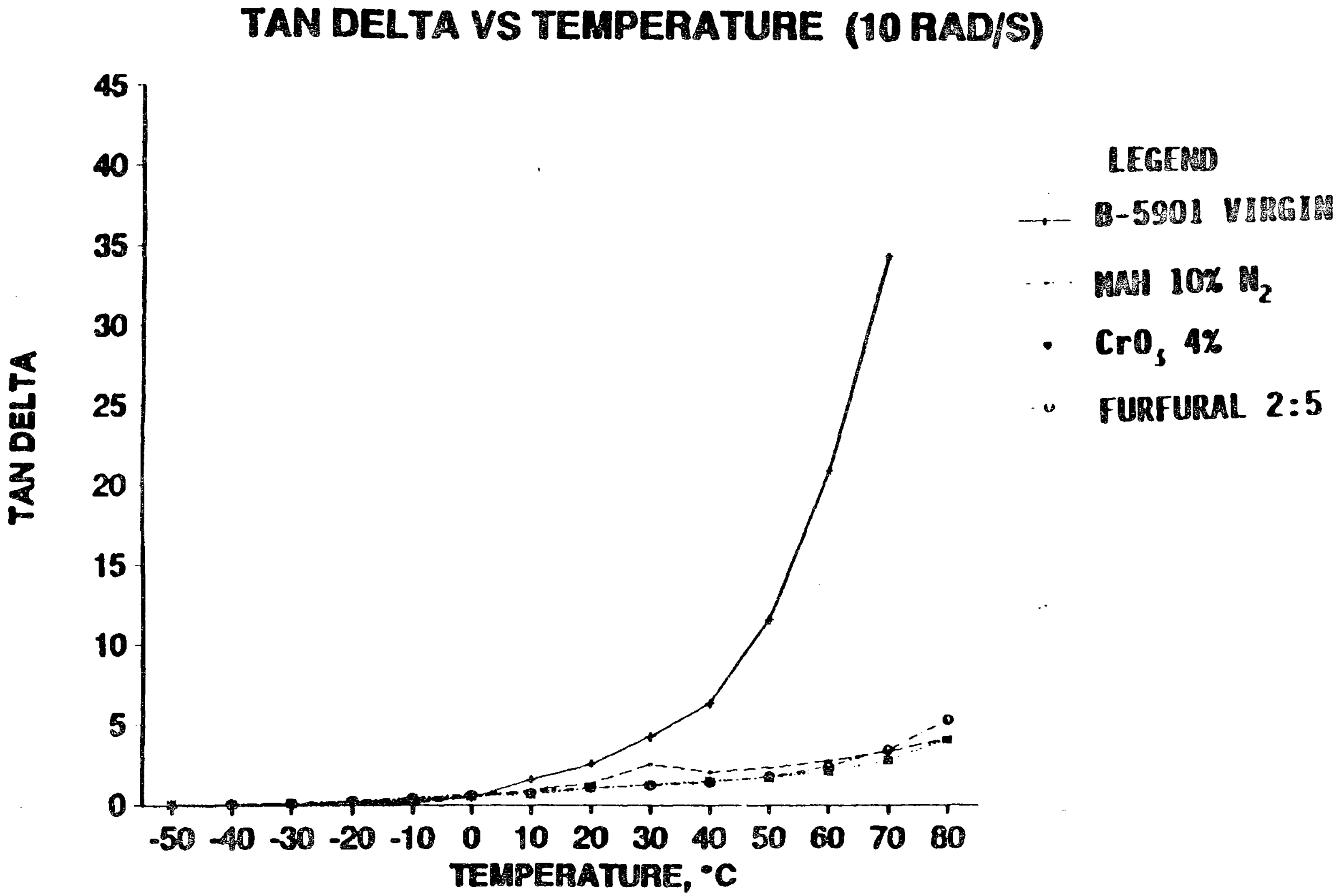

Figure 40. Tan delta vs temperature of the B-5901 virgin asphalt and its chemically modified versions at 10 radians/second.

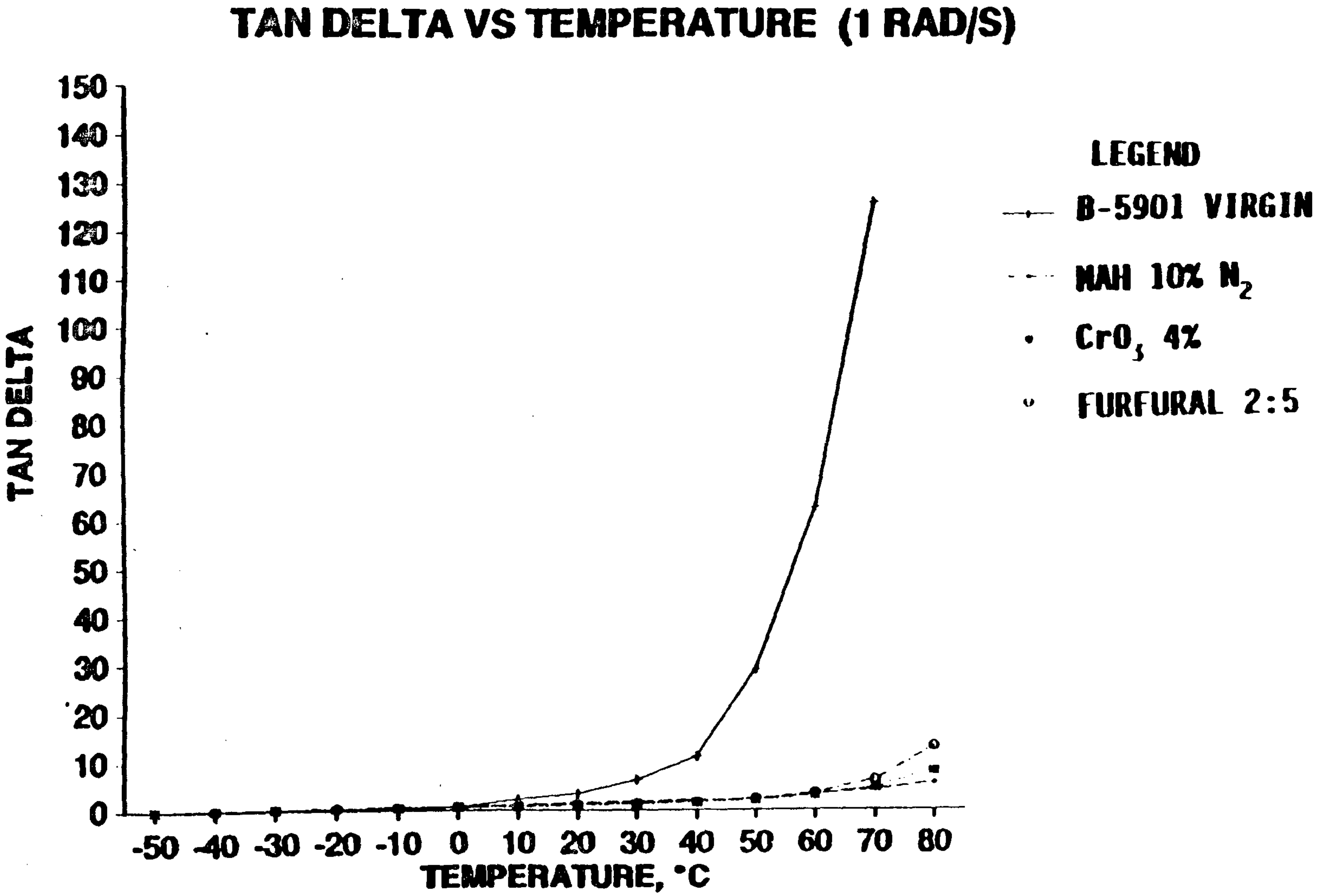

Figure 41. Tan delta vs temperature of the B-5901 virgin asphalt and its chemically modified versions at 1 radian/second.

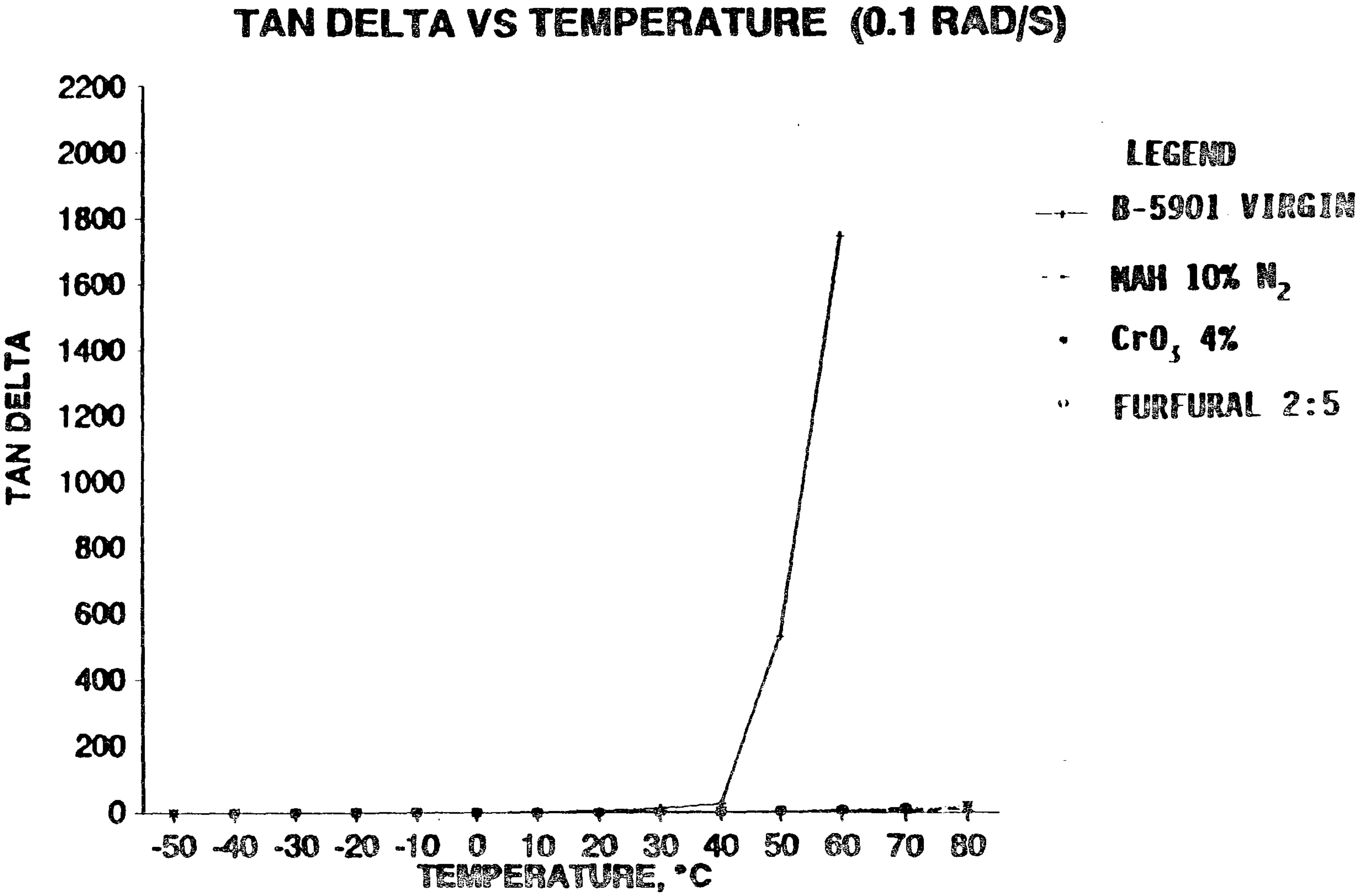

Figure 42. Tan delta vs temperature of the B-5901 virgin asphalt and its chemically modified versions at 0.1 radian/second.

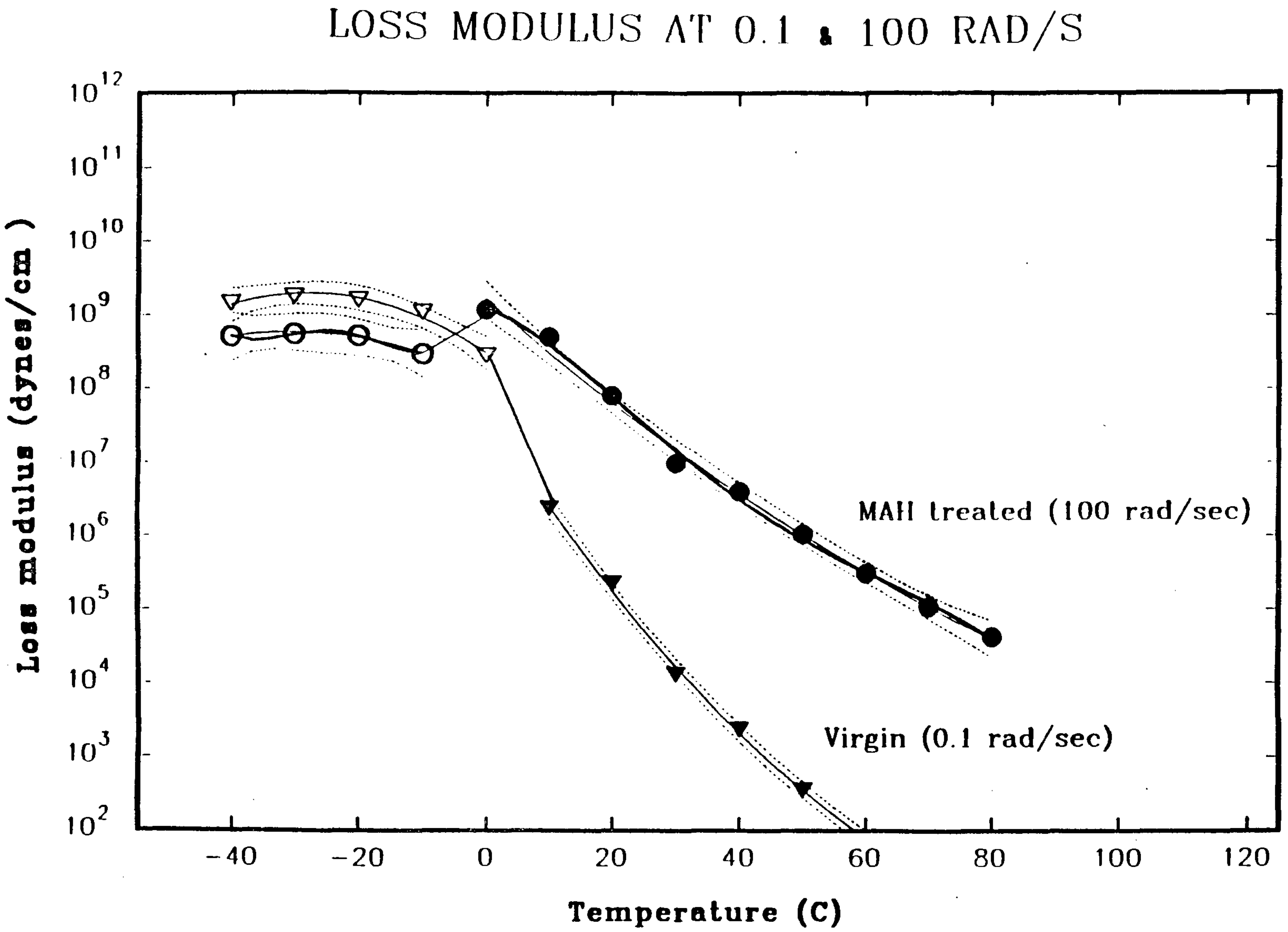

Figure 43. The loss modulus as a function of temperature for the virgin and MAH modified asphalt at 0.1 and 100 rad/sec respectively (the dotted lines on either side of the best fit curve indicate the 95% confidence limits for the fit).

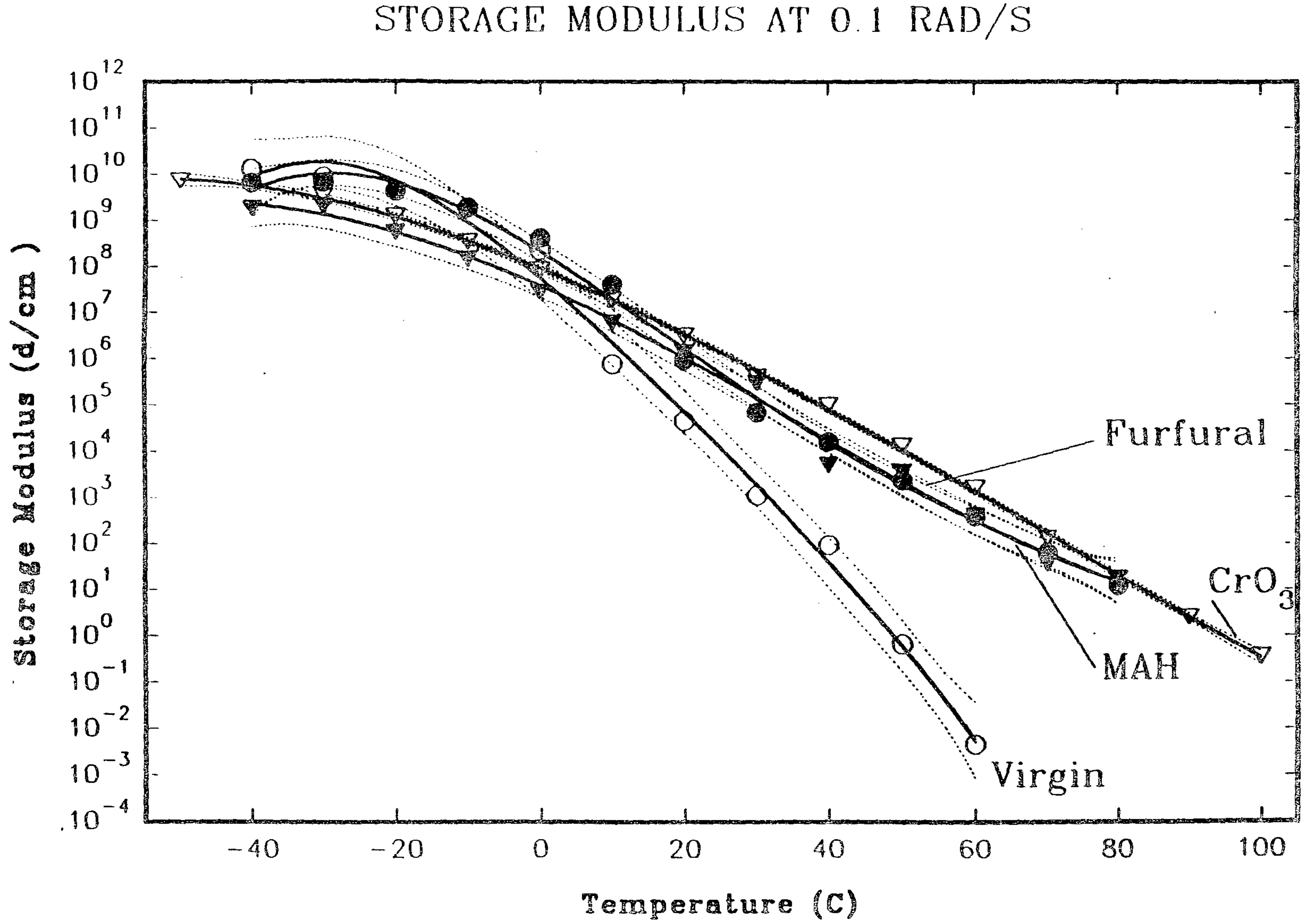

Figure 44. The storage modulii as a function of temperature for virgin and modified asphalts at 0.1 radians/second (the dotted lines on either side of the best fit curve indicate the 95% confidence limits for the fit).

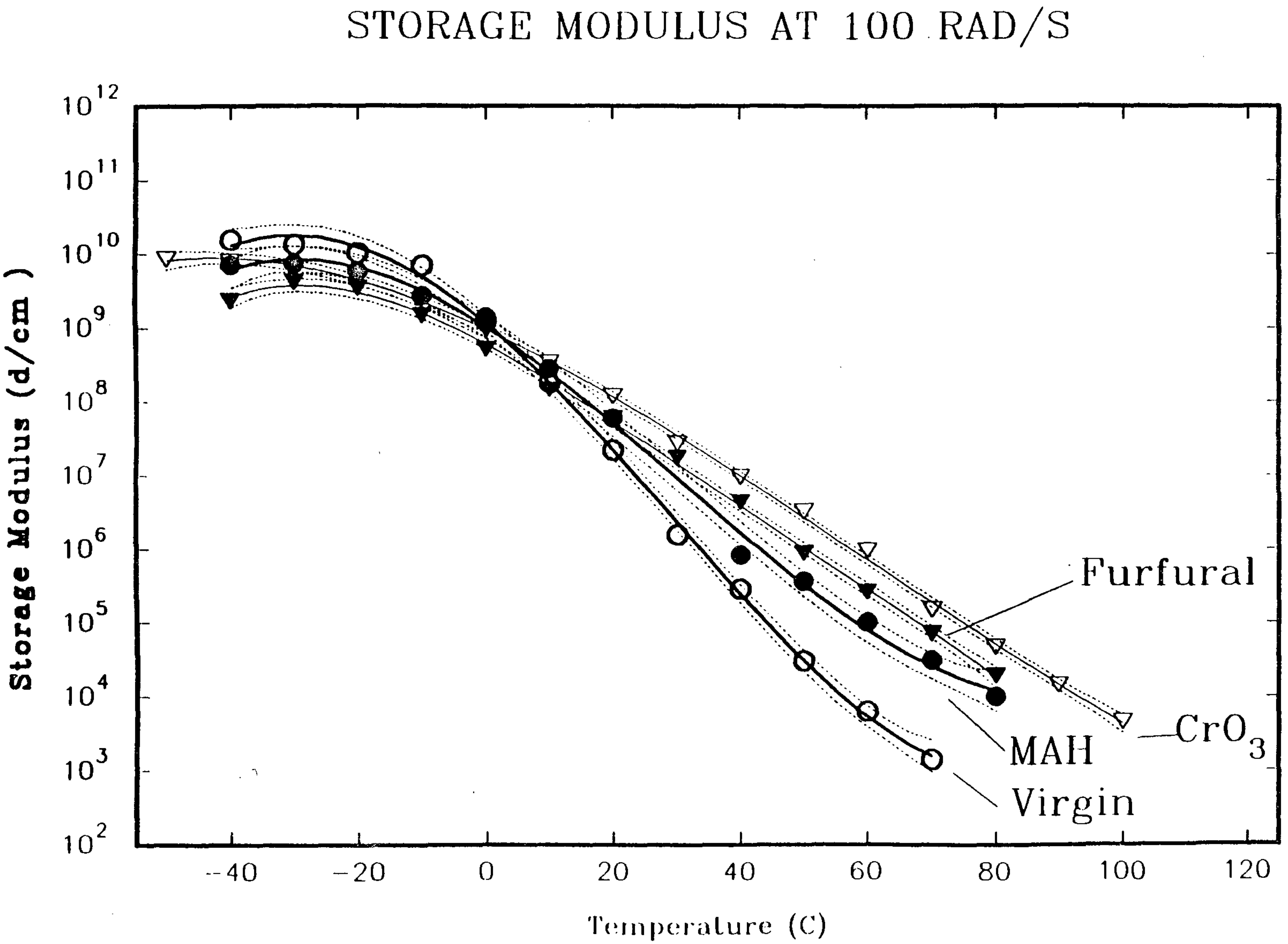

Figure 45. The storage modulii as a function of temperature for virgin and modified asphalts at 100 radians/second (the dotted lines on either side of the best fit curve indicate the 95% confidence limits for the fit).

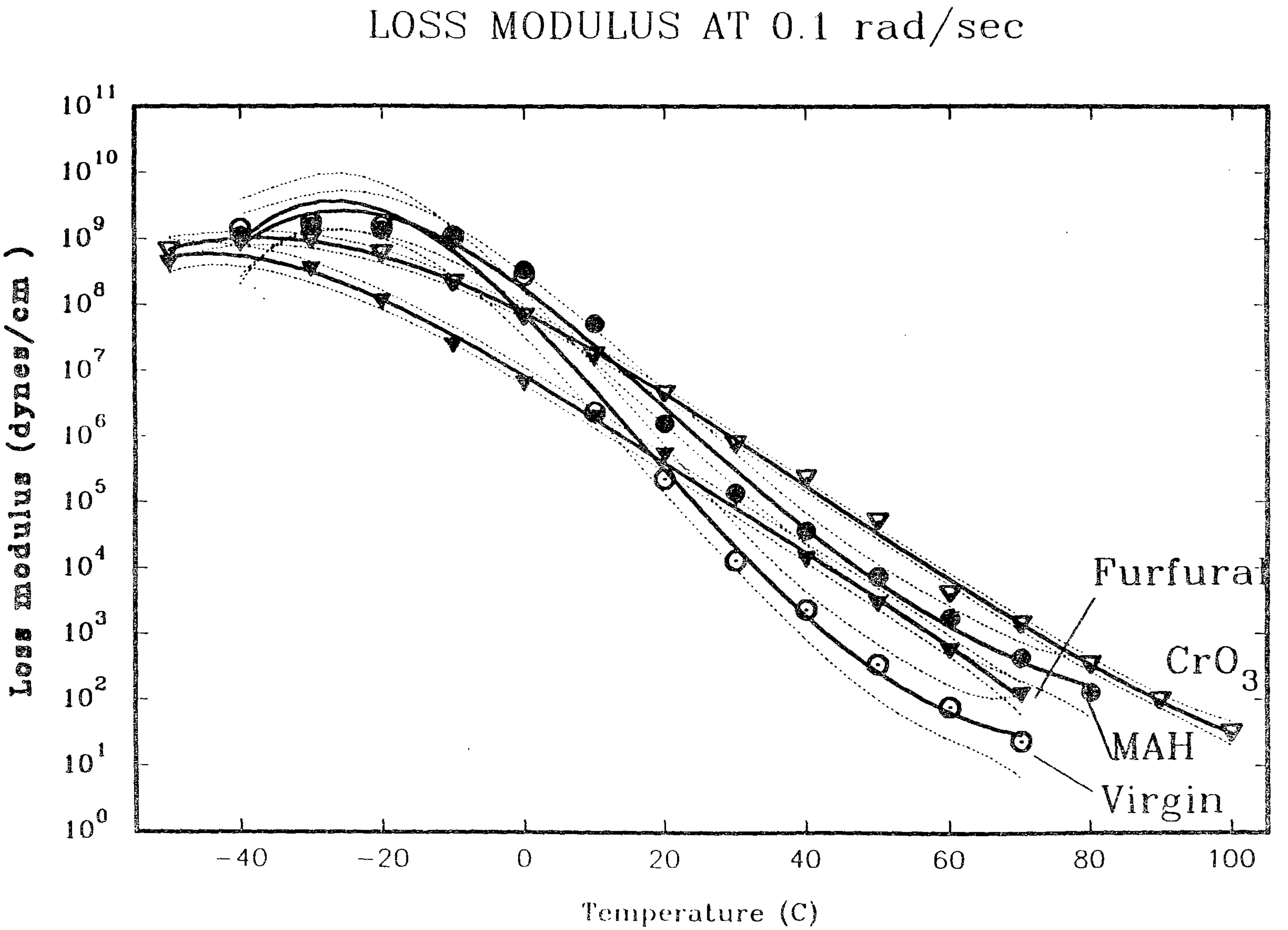

Figure 46. The loss modulii as a function of temperature for virgin and modified asphalts at 0.1 radians/second (the dotted lines on either side of the best fit curve indicate the 95% confidence limits for the fit).

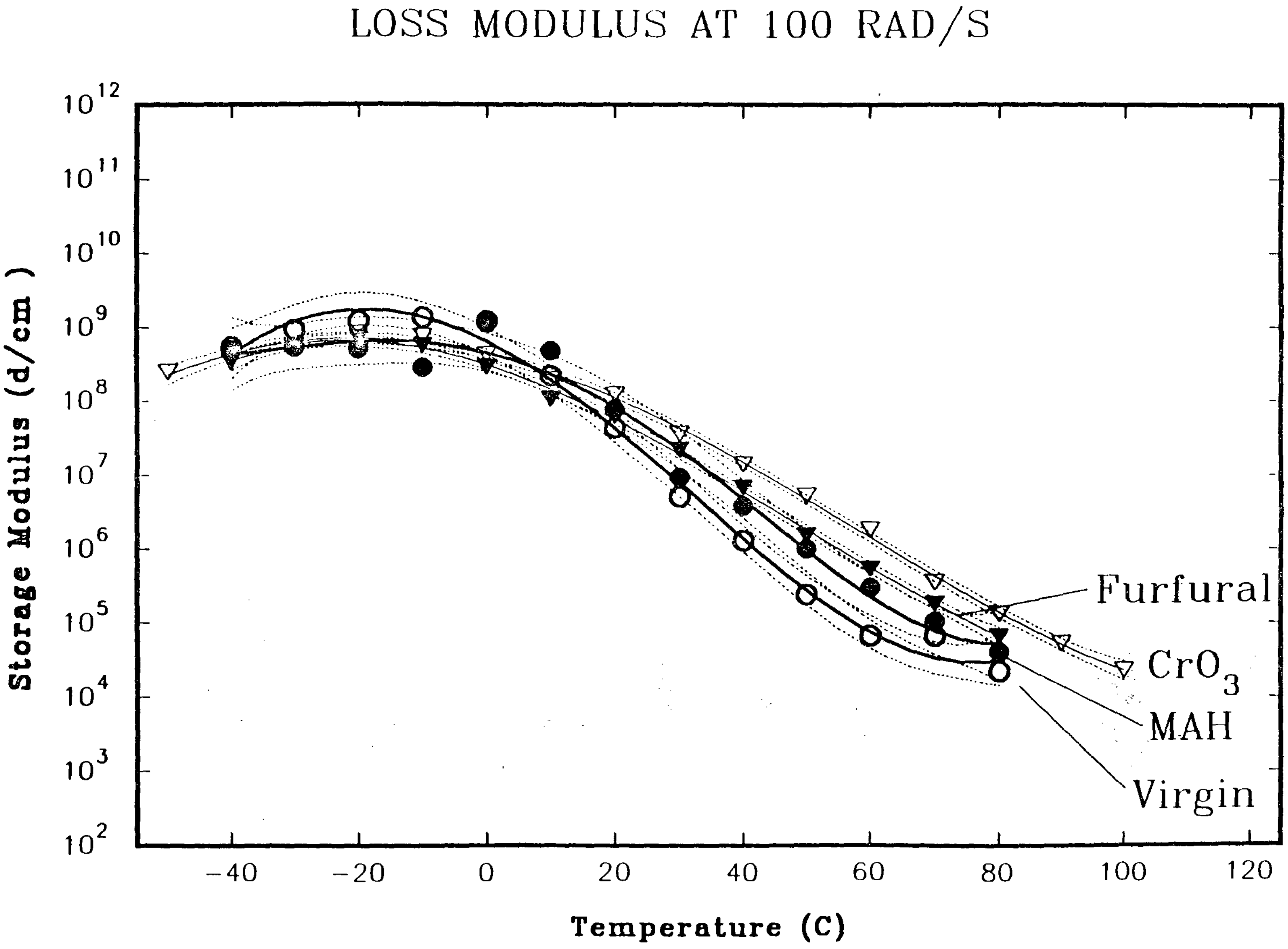

Figure 47. The loss modulii as a function of temperature for virgin and modifies asphalts at 100 radians/second (the dotted lines on either side of the best fit curve indicate the 95% confidence limits for the fit).

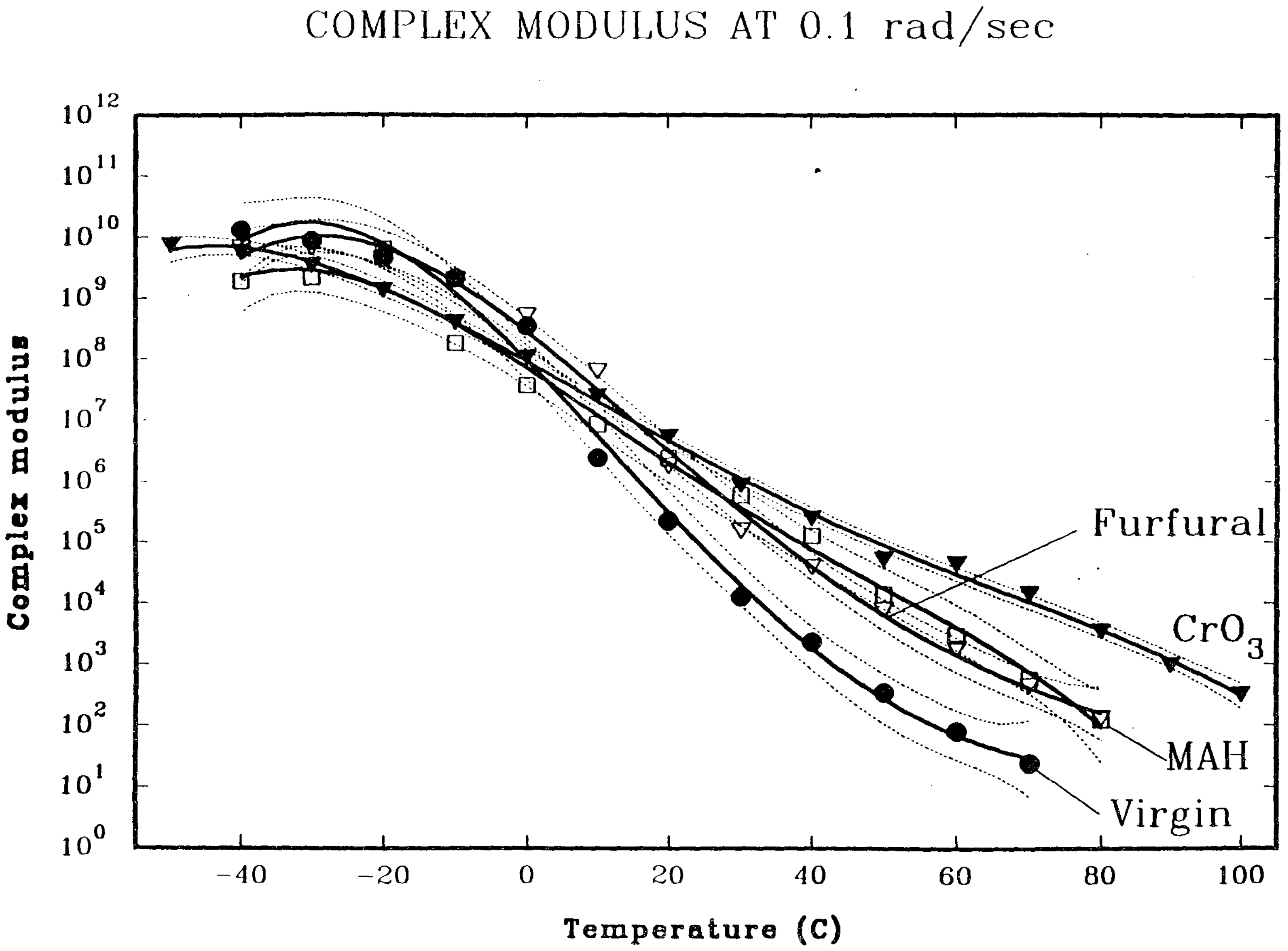

Figure 48. The complex modulii as a function of temperature for virgin and modified asphalts at 0.1 radians/second (the dotted lines on either side of the best fit curve indicate the 95% confidence limits for the fit).

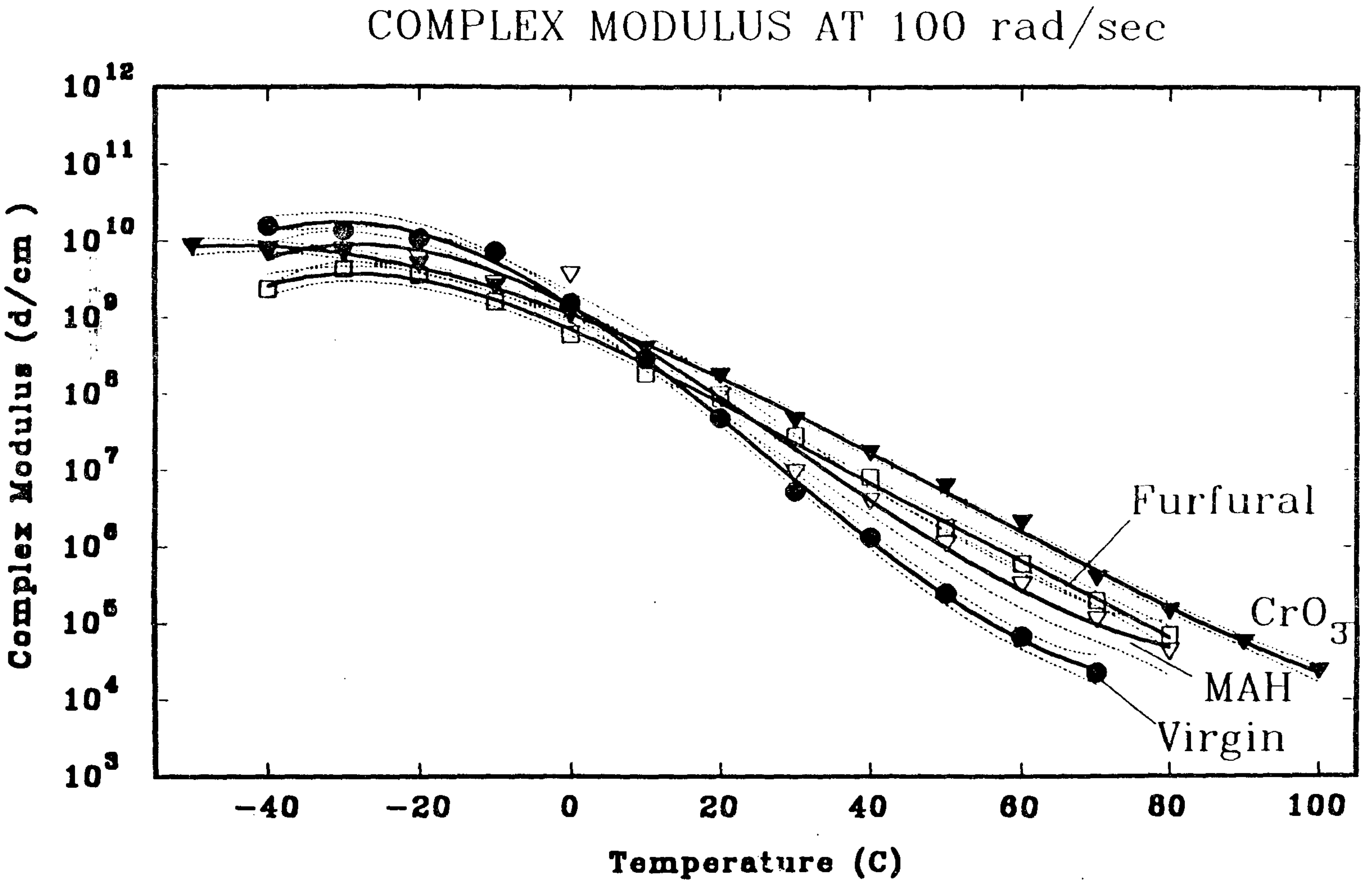

Figure 49. The complex modulii as a function of temperature for virgin and modified asphalts at 100 radians/second (the dotted lines on either side of the best fit curve indicate the 95% confidence limits for the fit).

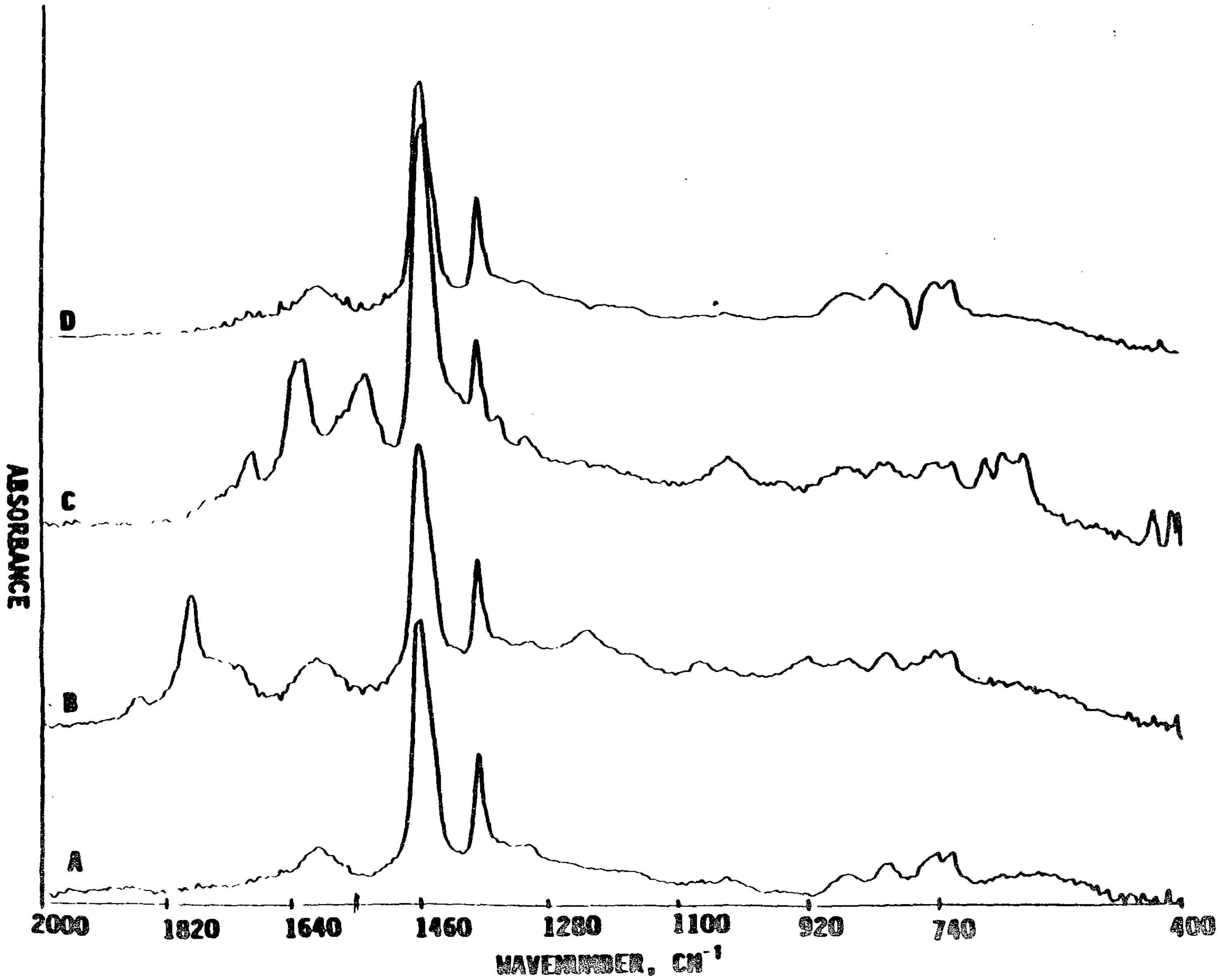

Figure 50. Infrared spectra of A) B-5901 virgin asphalt and its reaction products with B) MAH 10% N_2 C) CrO_3 4% and D) Furfural 2:5 using thin films on the KBr discs.

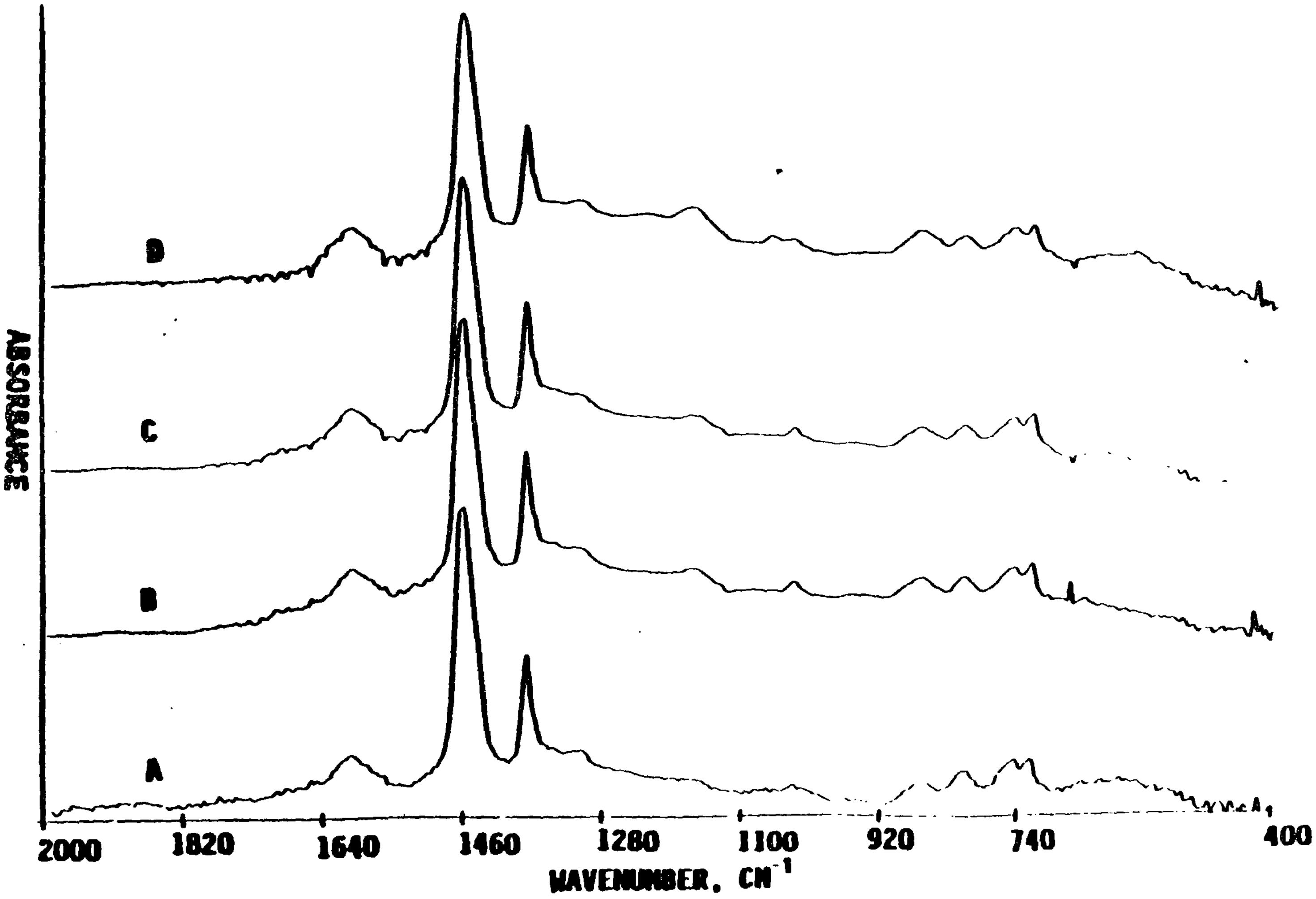

Figure 51. Infrared spectra of A) B-5901 virgin asphalt and its B) Nitrated C) Nitrated-reduced and D) Sulfonated products using thin films on the KBr discs.

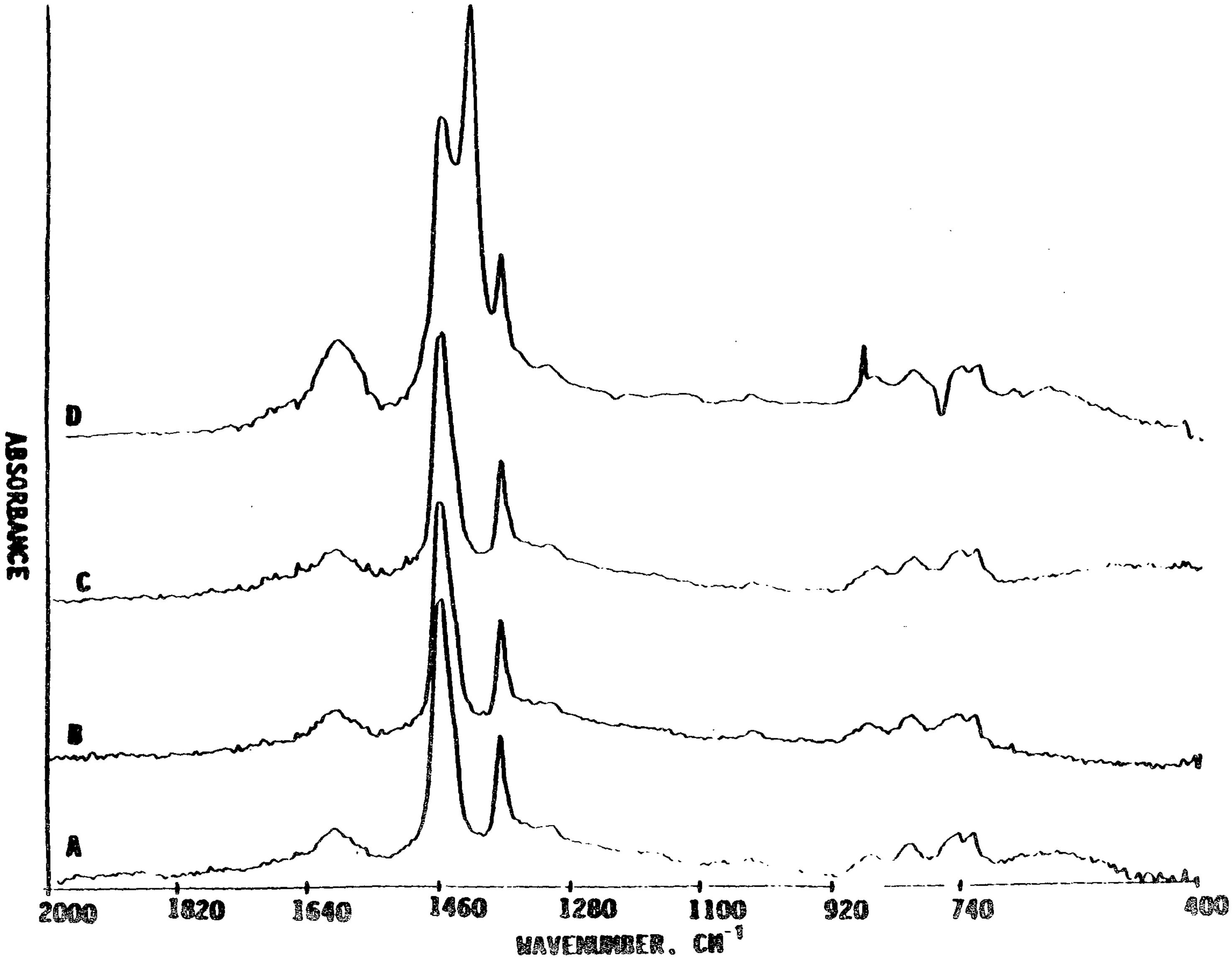

Figure 52. Infrared spectra of A) B-5901 virgin asphalt and its reaction products with B) HCl gas C) Oxalic acid and D) KOH using thin films on the KBr discs.

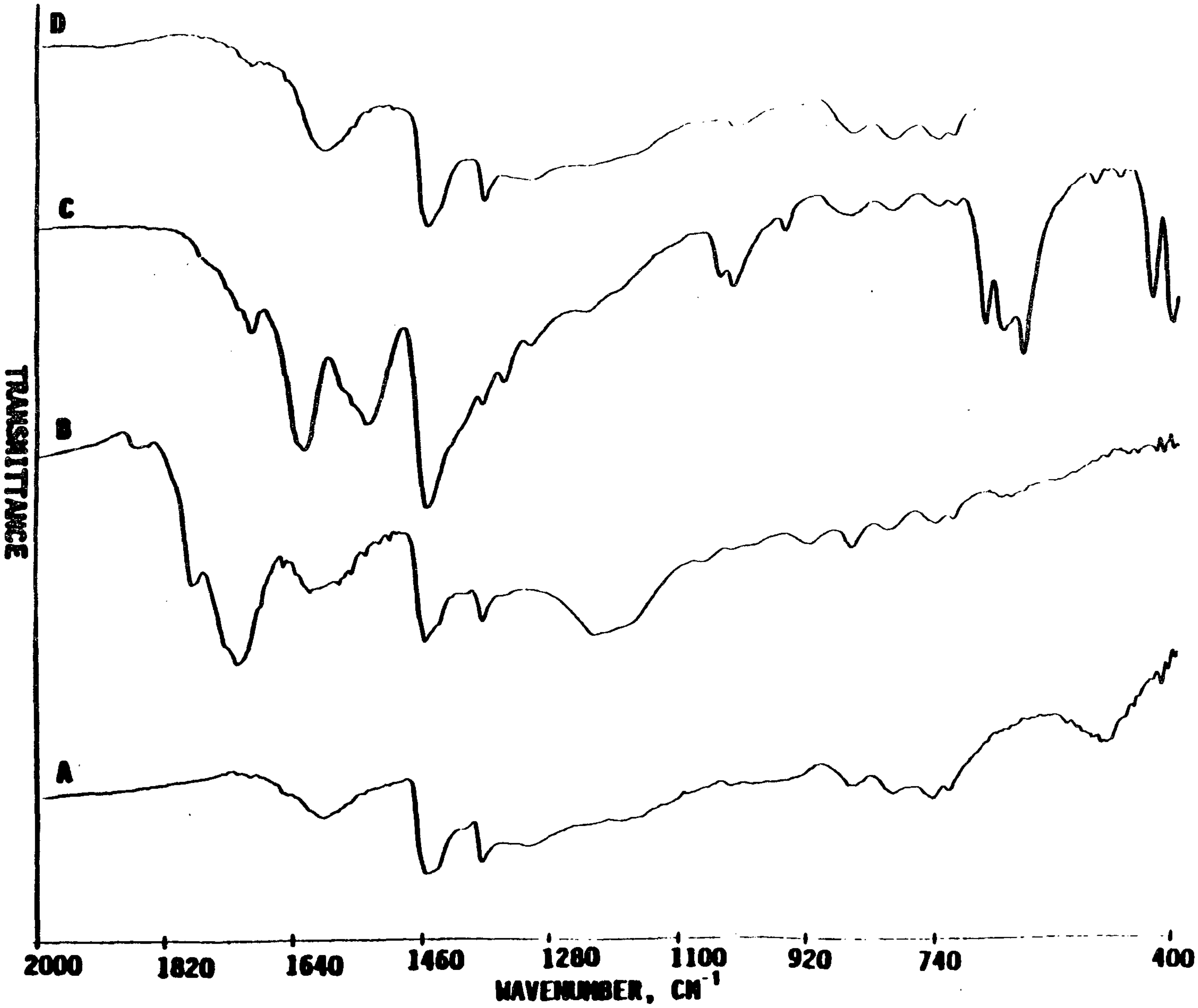

Figure 53. Infrared spectra of asphaltenes from A) B-5901 virgin asphalt and its reaction products with B) MAH 10% N_2 C) CrO_3 4% D) Furfural 2:5 using KBr pellets.

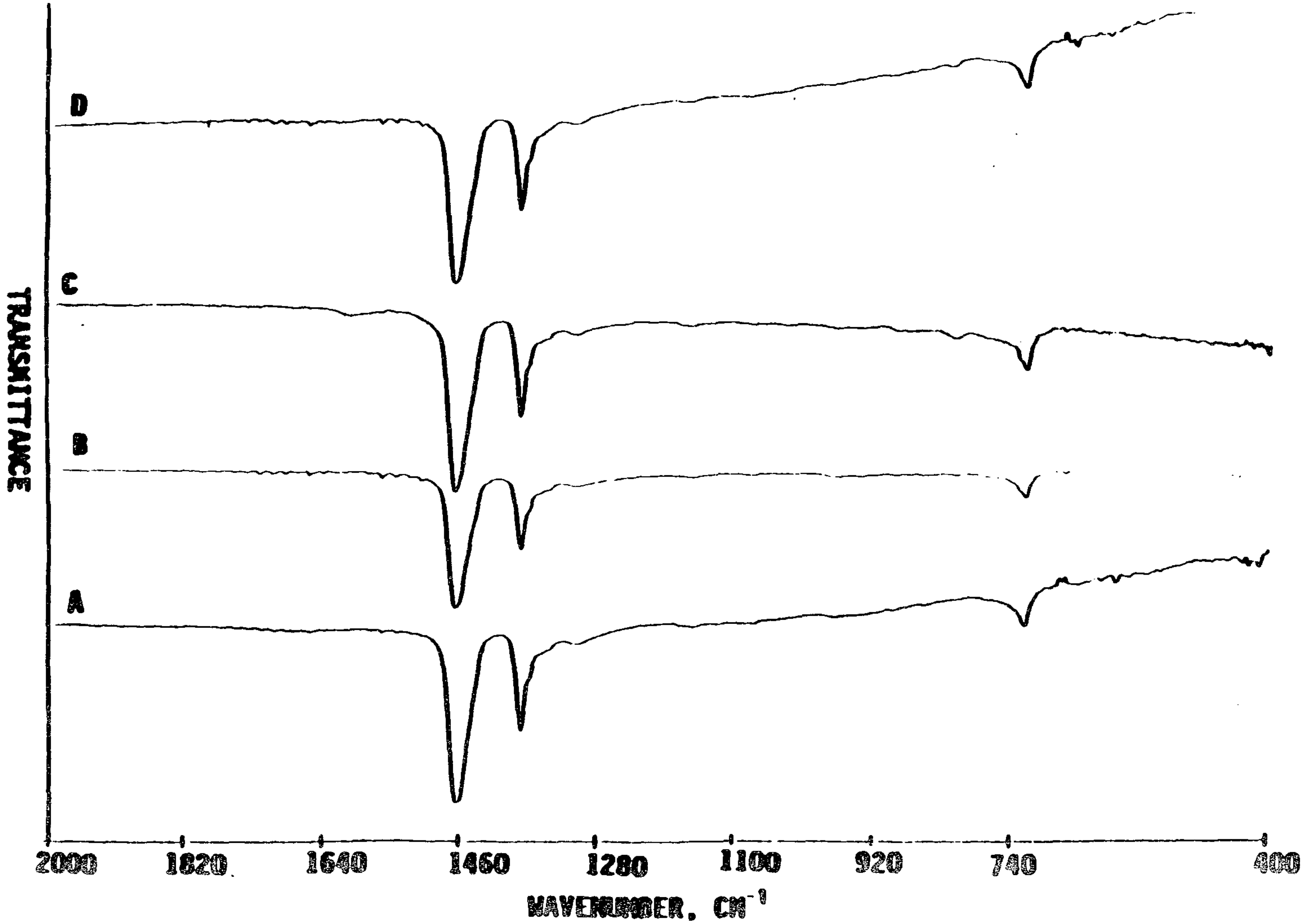

Figure 54. Infrared spectra of saturates fractions from A) B-5901 virgin asphalt and its reaction products with B) MAH 10% N_2 C) CrO_3 4% and D) Furfural 2:5 using thin films on KBr discs.

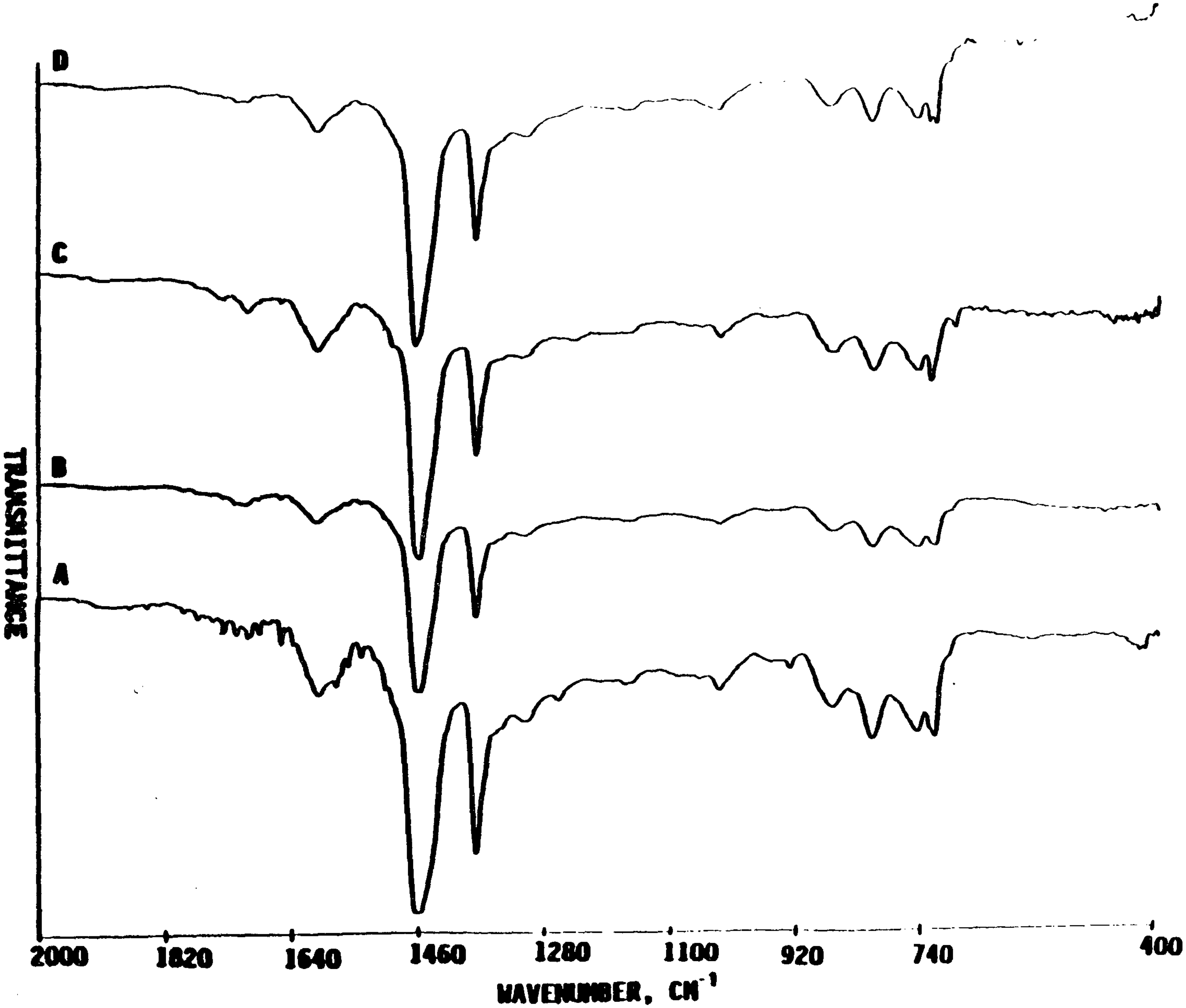

Figure 55. Infrared spectra of Naphthene-aromatics from A) B-5901 virgin asphalt and its reaction products with B) MAH 10% N_2 C) CrO_3 4% and D) Furfural 2:5 using thin films on KBr discs.

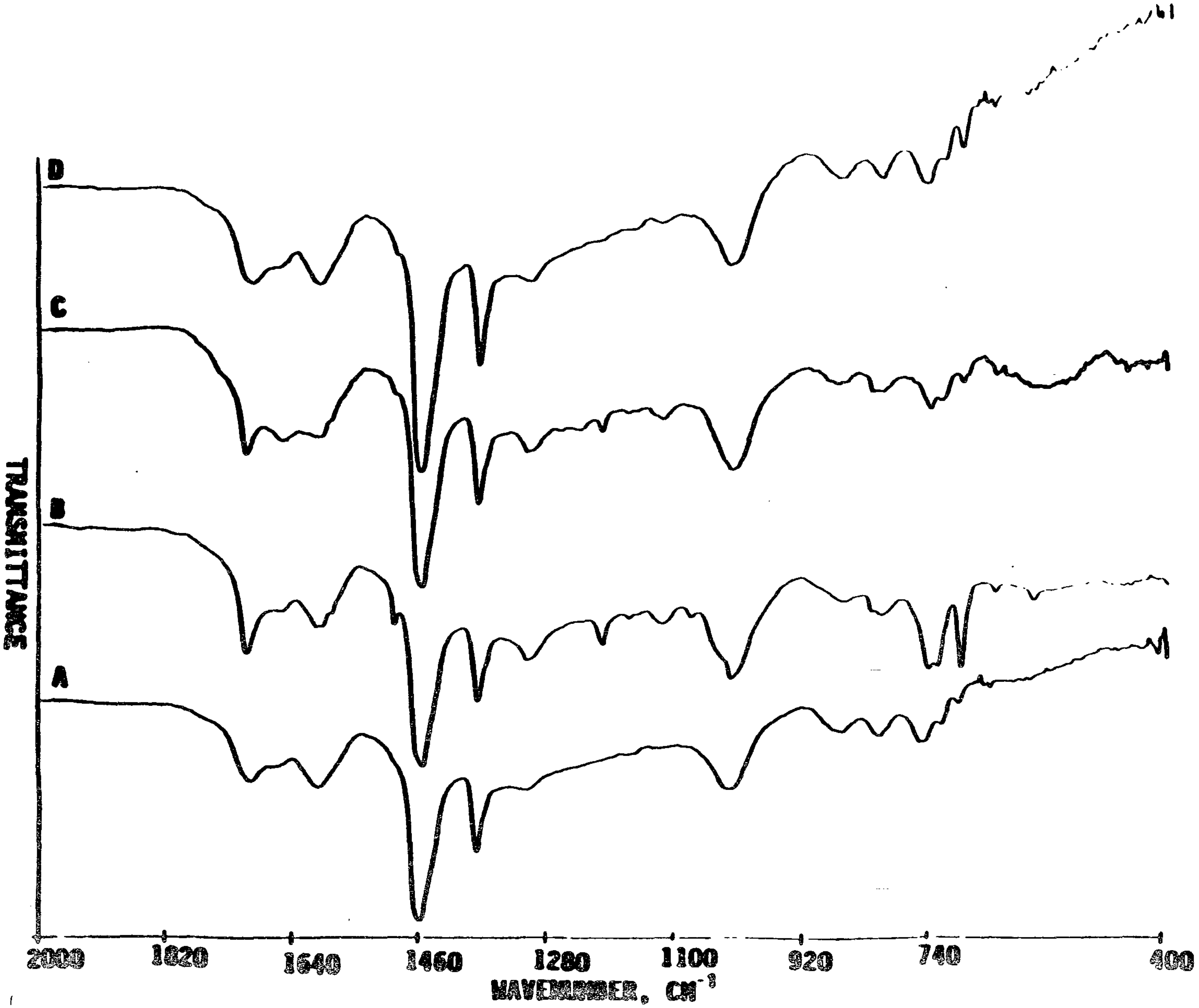

Figure 56. Infrared spectra of the polar-aromatics from A) B-5901 virgin asphalt and its reaction products with B) MAH 10% N_2 C) CrO_3 4% D) Furfural 2:5 using either a thin film on KBr disc or a KBr pellet.

APPENDIX A

This appendix contains data that were obtained in the laboratory during the performance of this project. In addition, a number of computed variables (PVN, PI, LST and aging index) are presented here.

Table 13. Penetrations, viscosities, softening points and specific gravities of all the virgin asphalts and their modified versions used in the study.

Sample	Penetrations			Viscosities		Soft. Pt.	Sp. Gr.
	77 °F	60 °F	50 °F	275 °F	140 °F	°F	
		dmm		cst	poise		
B-5901 Virgin	140	52	25	232	603	113	1.013
Virgin	132	52	29	230	607	115	1.013
Virgin	145	56	27	231	629	115	1.013
MAH 10% N_2	65	31	16	909	4922	138	1.029
MAH 10% N_2	57	26	10	1047	10156	144	1.030
MAH 10% N_2	60	31	18	742	6084	140	1.014
MAH 10% N_2	58	30	10	1417	9626	140	-----
MAH 5%	65	28	19	593	4871	136	1.025
MAH 2%	88	35	22	316	1800	125	1.015
MAH 2.5% N_2 LT	94	42	23	413	1550	126	1.015
NOMAH N_2	119	46	26	263	816	117	1.015
NOMAH N_2	127	51	28	228	630	115	1.013
NOMAH N_2	133	55	27	238	674	115	1.046
MAH 10% Air	58	28	17	1026	11394	140	1.024
NOMAH AIR 150 °C	108	46	24	252	756	116	1.014
NOMAH Air	98	39	24	297	1103	118	1.014
MAH 10% 175 °C	54	26	17	1276	13012	147	1.020
NOMAH 175 °C	138	51	28	232	637	113	1.013
CrO_3 0.5%	77	35	21	396	2064	128	1.020
CrO_3 0.5%	99	41	20	312	1311	119	1.022
CrO_3 1%	96	40	16	325	1140	120	1.025
CrO_3 2%	73	32	16	389	1965	126	1.033
CrO_3 2%	57	27	17	497	3979	135	1.031
CrO_3 4%	47	22	11	567	6347	138	1.045

Table 13. Penetrations, viscosities, softening points and specific gravities of all the virgin asphalts and their modified versions used in the study (continued).

Sample	Penetrations			Viscosities		Soft. Pt.	Sp. Gr.
	77 °F	60 °F	50 °F	275 °F	140 °F	°F	
	dmm			cst	poise		
CrO_3 4%	46	17	14	661	10740	143	1.047
CrO_3 4%	34	22	10	794	16361	148	1.049
CrO_3 4%	37	17	11	786	16264	146	-----
CrO_3 4% 72 h	54	21	14	609	14156	142	1.051
CrO_3 4% Neat	161	62	29	242	---	114	1.004
$NOCrO_3$	133	50	29	253	781	118	1.015
$NOCrO_3$	112	45	23	240	905	117	1.014
$NOCrO_3$	120	47	25	268	833	114	1.014
$NOCrO_3$	193	77	43	243	669	112	1.015
HCl gas	82	31	20	471	8272	131	1.018
HCl gas	100	40	25	279	973	117	1.015
HCl gas	77	36	20	444	3400	127	1.016
HCl gas	73	32	19	399	2505	127	-----
HCl acid 1 ml	93	42	25	314	1368	124	1.015
HCl acid 5 ml	74	34	21	764	2592	124	1.017
Furfural 2:5	53	27	17	546	9903	142	1.017
Furfural 2:5	58	31	18	535	6822	139	1.019
Furfural 2:5	48	25	17	1096	13837	143	1.019
Furfural 1:5	67	32	20	441	3432	131	1.018
Furfural 1:1	94	41	24	335	1517	123	1.015
Furfural 0.5:2.5	72	33	20	418	3050	131	1.019
Furfural 0.5:1	109	43	27	288	1048	120	1.015
Furfural 0.5:1	91	43	24	393	2109	127	1.019
Furfural-Oxalic acid	98	42	23	435	1726	125	1.012
Furfural-NH_4OH	153	58	31	229	604	115	1.014
Oxalic acid	142	50	28	294	719	112	1.009
Oxalic acid	127	53	30	234	602	114	1.014
Nitration Neat H	104	44	23	361	1085	122	1.089
Nitration 1:1 A	57	28	22	778	9467	140	1.018
Nitration 1:1 A	60	31	21	661	7052	139	1.018
Nitration 1:1 A	50	27	15	889	19943	147	1.021

Table 13. Penetrations, viscosities, softening points and specific gravities of all the virgin asphalts and their modified versions used in the study (continued).

Sample		Penetrations			Viscosities		Soft. Pt.	Sp. Gr.
		77 °F	60 °F	50 °F	275 °F	140 °F	°F	
			dmm		cst	poise		
	Nitration 1:1 H	67	32	21	540	6380	136	1.018
	Nitration CaO A	68	32	18	517	3904	131	1.018
	Nit.-reduction A	43	22	15	1344	42374	153	1.022
	Sulfonation 2 ml H	46	24	18	1279	95195	161	1.021
	Sulfonation 1 ml A	89	38	24	438	2712	127	1.016
	Sulfonation 1 ml H	64	32	20	625	8785	141	1.018
	Sulfonation 0.5 ml H	112	48	27	294	1161	120	1.015
	KOH 1%	92	39	24	351	1372	125	1.021
	KOH 4% R 6 h	58	33	23	903	8552	139	1.038
	KOH 4% A 24 h	97	40	23	321	1298	122	1.034
	KOH 7.5%	82	32	21	955	10025	139	1.061
	Sulphanilic acid H	150	56	30	233	650	114	1.015
	Triethylamine A	106	43	24	284	1014	119	1.015
	Triethylamine H	107	42	26	275	977	119	1.015
C-8613	Virgin	112	39	23	234	763	121	1.010
	MAH 10% N_2	53	22	13	1267	6113	141	1.030
	CrO_3 4%	49	20	12	475	4925	138	1.046
	Furfural 2:5	59	25	14	403	3075	132	1.013
C-8615	Virgin	102	35	21	220	804	123	1.020
	MAH 10% N_2	53	22	14	526	4740	140	1.037
	CrO_3 4%	35	15	8	692	12629	147	1.051
	Furfural 2:5	48	22	11	616	5707	141	1.013
C-8561	Virgin	157	54	29	234	665	113	1.018
	MAH 10% N_2	70	34	18	619	4283	135	1.034
	CrO_3 4%	35	17	12	872	17465	148	1.050
	Furfural 2:5	60	28	18	465	2433	127	1.017
C-9040	Virgin	137	43	12	239	610	116	1.012
	MAH 10% N_2	67	35	8	551	2385	128	1.020
	CrO_3 4%	34	15	11	1280	13389	143	1.066

Table 13. Penetrations, viscosities, softening points and specific gravities of all the virgin asphalts and their modified versions used in the study (continued).

Sample	Penetrations 77 °F	60 °F	50 °F	Viscosities 275 °F	140 °F	Soft. Pt.	Sp. Gr.
		dmm		cst	poise	°F	
Furfural 2:5	52	22	13	426	3078	131	1.016
C-9041 Virgin	212	79	43	195	411	108	1.017
MAH 10% N_2	71	35	25	1302	12228	144	1.039
MAH 6% N_2	100	45	25	469	2313	127	1.027
MAH 4% N_2	95	43	27	415	2205	125	1.027
MAH 4% N_2	102	47	26	407	1966	124	1.026
MAH 4% N_2	111	47	27	349	1243	122	1.023
MAH 3% N_2	117	49	28	297	1132	121	1.023
MAH 2% N_2	126	50	30	295	994	118	1.022
CrO_3 4%	47	23	15	788	11831	143	1.049
CrO_3 2%	70	34	7	494	3379	132	1.034
CrO_3 1.5%	132	51	31	285	961	117	1.025
CrO_3 1.5%	85	36	24	408	2279	126	1.030
CrO_3 1.5%	92	41	24	368	1727	125	1.029
CrO_3 1.5%	86	60	23	408	2150	131	1.021
CrO_3 1.5% Neat	173	66	35	225	476	118	1.021
CrO_3 1%	106	47	16	348	1303	122	1.025
CrO_3 0.5%	109	46	28	354	1492	122	1.022
Furfural 2:5	70	33	22	440	4277	131	1.010
Furfural 2:5	73	37	25	383	3607	129	1.021
Furfural 2:5	67	33	22	450	4125	131	1.022
Furfural 2:5	72	37	24	427	3959	132	1.021
Furfural 1:5	92	47	27	339	1635	125	1.018
Furfural 1:5	77	40	23	783	3307	128	1.021
Furfural 0.5:2.5	111	49	30	289	1264	119	1.020
Furfural 0.5:2.5	112	49	29	307	1176	121	1.019
Furfural 0.75:4	71	36	24	391	4019	133	1.018
C-9042 Virgin	78	36	7	401	1923	125	1.027

Table 14. Thin film oven test data of all the virgin asphalts and their modified versions used in the study.

Sample	TFOT %	Penetration 77 °F dmm	Viscosity 275 °F cst	Viscosity 140 °F poise
B-5901 Virgin	0.14	84	329	1312
Virgin	0.12	85	322	1623
Virgin	0.10	87	312	1364
MAH 10% N_2	0.33	46	566	4812
MAH 10% N_2	0.79	46	1927	47660
MAH 10% N_2	0.59	45	1768	36025
MAH 10% N_2	----	--	1097	12955
MAH 5%	0.47	50	838	15018
MAH 2%	0.28	62	466	4074
MAH 2.5% LT	1.04	61	522	4546
NOMAH N_2	0.06	72	369	1934
NOMAH N_2	0.06	85	325	1502
NOMAH N_2	0.07	81	338	1499
MAH 10% Air	0.33	42	1649	43558
NOMAH Air	0.02	79	335	1568
NOMAH Air	0.05	62	413	2823
MAH 175 °C	0.22	45	1661	31519
NOMAH 175 °C	0.023	88	326	1456
CrO_3 0.5%	0.17	55	543	4693
CrO_3 0.5%	0.52	53	486	4738
CrO_3 1%	0.28	49	618	6063
CrO_3 2%	0.71	42	685	9004
CrO_3 2%	0.29	43	721	10267
CrO_3 4%	0.27	28	1297	56668
CrO_3 4%	0.86	27	1410	72191
CrO_3 4%	0.31	28	1331	72358
CrO_3 4%	----	--	----	-----
CrO_3 4% 72 h	0.98	28	1400	67753
CrO_3 4% Neat	0.17	95	326	1265

Table 14. Thin film oven test data of all the virgin asphalts and their modified versions used in the study (continued).

Sample	TFOT Loss %	Penetration 77 °F dmm	Viscosity 275 °F cst	Viscosity 140 °F poise
NOCrO$_3$	0.37	75	356	1809
NOCrO$_3$	0.14	75	375	2183
NOCrO$_3$	0.82	77	364	1372
HCl gas	0.41	49	637	7597
HCl gas	0.14	72	345	2464
HCl gas	0.58	55	695	9704
HCl gas	----	--	---	----
HCl acid 1 ml	0.26	75	425	2680
HCl acid 5 ml	0.37	70	1455	3734
Furfural 2:5	0.37	59	718	13282
Furfural 2:5	0.44	53	738	14759
Furfural 2:5	0.45	53	845	18301
Furfural 1:5	0.24	58	606	8255
Furfural 1:1	0.16	70	465	3294
Furfural 0.5:2.5	0.38	66	526	4753
Furfural 0.5	0.22	76	405	2444
Furfural 0.5	0.36	67	660	6269
Furfural-oxalic acid	0.26	68	598	3720
Furfur.-NH$_4$OH	0.16	91	336	1354
Oxalic acid	0.22	85	323	1573
Oxalic acid	0.23	85	333	1511
Nitration Neat 2 ml H	0.56	53	576	4664
Nitration 1:1 ABSON	0.26	42	1207	29422
Nitration 1:1 A	0.20	45	997	24502
Nitration 1:1 A	0.18	40	1605	67740
Nitration 1:1 H	0.52	49	957	35967
Nit. CaO A	0.13	49	768	12242
Nit. reduction A	0.24	36	2207	189892
Sulfonation 2 ml H	0.96	39	2391	177450

Table 14. Thin film oven test data of all the virgin asphalts and their modified versions used in the study (continued).

Sample		TFOT Loss %	Penetration 77 °F dmm	Viscosity 275 °F cst	Viscosity 140 °F poise
	Sulfonation 1 ml A	0.33	56	657	7452
	Sulfonation 1 ml H	0.68	53	1541	20329
	Sulfonation 0.5 ml H	0.17	72	449	3074
	KOH 1%	0.15	71	421	2301
	KOH 4% R 6 h	0.15	57	736	4749
	KOH 4% A 24 h	0.25	77	394	2187
	KOH 7.5%	0.25	54	1076	12440
	Sulphanilic acid H	0.61	92	302	1261
	Triethylamine A	0.20	73	404	2439
	Triethylamine H	0.14	72	366	2069
C-8613	Virgin	0.09	71	315	1555
	MAH 10% N_2	0.47	40	1170	23065
	CrO_3 4%	1.45	30	943	29134
	Furfural 2:5	0.33	49	531	5659
C-8615	Virgin	0.17	62	307	1807
	MAH 10% N_2	0.47	40	823	16907
	CrO_3 4%	0.38	28	1103	42015
	Furfural 2:5	0.81	45	604	9719
C-8561	Virgin	0.22	91	320	1285
	MAH 10% N_2	1.04	47	991	13562
	CrO_3 4%	0.28	28	1291	38036
	Furfural 2:5	0.55	57	592	6079
C-9040	Virgin	0.07	87	280	1070
	MAH 10% N_2	0.90	44	654	5273
	CrO_3 4%	0.45	28	1334	23845
	Furfural 2:5	0.76	52	500	4130
C-9041	Virgin	0.27	121	285	990
	MAH 10% N_2	0.74	51	1790	28371
	MAH 6% N_2	0.50	66	733	7397

Table 14. Thin film oven test data of all the virgin asphalts and their modified versions used in the study (continued).

Sample	TFOT Loss %	Penetration 77 °F dmm	Viscosity 275 °F cst	Viscosity 140 °F poise
MAH 4% N_2	0.50	64	660	6655
MAH 4% N_2	0.79	65	609	5439
MAH 4% N_2	0.45	74	511	3390
MAH 3% N_2	0.01	91	368	1883
MAH 2% N_2	0.43	82	419	2521
CrO_3 4%	0.48	38	1277	43844
CrO_3 2%	0.25	47	803	12280
CrO_3 1.5%	0.25	78	404	2115
CrO_3 1.5%	0.27	54	626	6365
CrO_3 1.5%	0.42	62	549	4732
CrO_3 1.5%	0.45	56	639	6050
CrO_3 1.5% Neat	0.30	102	314	1308
CrO_3 1%	0.40	69	513	3424
CrO_3 0.5%	0.34	68	475	3030
Furfural 2:5	0.79	70	584	6064
Furfural 2:5	0.35	72	431	15866
Furfural 2:5	0.75	71	683	7009
Furfural 2:5	0.65	67	634	6782
Furfural 1:5	0.40	75	471	3501
Furfural 1:5	0.70	74	1281	3876
Furfural 0.5:2.5	0.44	84	439	2672
Furfural 0.5:2.5	0.45	85	418	2415
Furfural 0.75:4	0.94	74	533	4057
C-9042 Virgin	0.14	47	598	5171

Table 15. PVN, PI, LST and aging index data of all the virgin asphalts and their modified versions used in the study.

Sample	PVN (77-275 °F)	PVN′ (77-140 °F)	PI	LST °C	Aging Index 275 °F	Aging Index 140 °F
B-5901 Virgin	-0.69	-0.78	-1.36	-43.37	1.42	2.18
Virgin	-0.77	-0.87	-0.59	-52.01	1.40	2.67
Virgin	-0.66	-0.67	-1.19	-45.61	1.35	2.17
MAH 10% N_2	0.47	0.20	0.02	-51.17	0.62	0.98
MAH 10% N_2	0.51	0.71	-1.29	-35.88	1.84	4.69
MAH 10% N_2	0.09	0.28	1.04	-60.54	2.38	5.92
MAH 10% N_2	0.96	0.68	-1.27	-36.05	----	----
MAH 5%	-0.13	0.19	0.73	-58.80	1.41	3.08
MAH 2%	-0.72	-0.35	-0.06	-53.92	1.47	2.26
MAH 2.5% N_2 100 °C	-0.25	-0.40	-0.06	-54.42	1.26	2.93
NOMAH N_2	-0.68	-0.71	-0.63	-50.60	1.40	2.37
NOMAH N_2	-0.83	-0.89	-0.56	-51.91	1.43	2.38
NOMAH N_2	-0.71	-0.74	-0.85	-48.88	1.42	2.22
MAH 10% Air	0.51	0.85	0.85	-58.41	1.61	3.82
NOMAH Air	-0.85	-0.95	-0.49	-51.05	1.33	2.07
MAH 10% 175 °C	1.24	1.56	-0.84	-47.84	1.30	2.42
MAH 10% 175 °C	0.72	0.86	1.22	-61.19	1.30	2.42
NOMAH 175 °C	-0.71	-0.74	-0.93	-48.48	1.41	2.29
CrO_3 0.5%	-0.53	-0.42	0.44	-57.67	1.37	2.27
CrO_3 0.5%	-0.61	-0.49	-0.86	-45.92	1.56	3.61
CrO_3 1%	-0.59	-0.69	-1.51	-38.11	1.90	5.32
CrO_3 2%	0.61	-0.55	-0.52	-46.74	1.76	4.58
CrO_3 2%	-0.52	-0.22	0.92	-58.93	1.45	2.58
CrO_3 4%	-0.53	-0.06	-0.21	-45.35	2.29	8.93
CrO_3 4%	-0.35	0.41	0.79	-55.52	2.13	6.72
CrO_3 4%	-0.41	0.34	1.16	-53.90	1.68	4.42
CrO_3 4%	-0.34	0.46	0.87	-53.21	----	----
CrO_3 4% 72 h	-0.30	0.94	0.08	-50.16	2.30	4.79
CrO_3 4% Neat	-0.45	----	-1.31	-45.16	1.35	----
$NOCrO_3$	-0.61	-0.57	-0.65	-51.43	1.41	2.32
$NOCrO_3$	-0.89	-0.69	-0.83	-47.54	1.56	2.41

Table 15. PVN, PI, LST and aging index data of all the virgin asphalts and their modified versions used in the study (continued).

Sample	PVN (77-275 °F)	PVN′ (77-140 °F)	PI	LST °C	Aging Index 275 °F	Aging Index 140 °F
NOCrO$_3$	-0.64	-0.67	-0.79	-48.66	----	----
NOCrO$_3$	-0.21	-0.08	-0.53	-56.56	1.50	2.05
HCl gas	-0.21	1.14	-0.21	-51.67	1.35	0.92
HCl gas	-0.78	-0.80	-0.06	-55.34	1.24	2.53
HCl gas	-0.36	0.100	0.24	-55.45	1.57	2.85
HCl gas	-0.58	-0.30	0.20	-54.50	----	----
HCl acid 1 ml	-0.67	-0.55	0.37	-59.06	1.35	1.96
HCl acid 5 ml	0.38	-0.24	0.64	-59.31	1.90	1.44
Furfural 2:5	-0.46	0.56	1.38	-62.38	1.32	1.34
Furfural 2:5	-0.40	0.34	1.25	-62.16	1.38	2.16
Furfural 2:5	0.38	0.72	1.99	-66.64	0.77	1.32
Furfural 1:5	-0.52	-0.12	1.01	-61.68	1.37	2.41
Furfural 1:1	-0.56	-0.42	0.10	-56.32	1.39	2.17
Furfural 0.5: 2.5	-0.52	-0.12	0.53	-57.87	1.26	1.56
Furfural 0.5:1	-0.63	-0.58	-0.11	-55.71	1.41	2.33
Furfural 0.5:1	-0.36	-0.12	0.32	-58.18	1.68	2.97
Furfural-Oxalic acid	-0.12	-0.21	-0.27	-52.60	1.36	2.15
Furfural-NH$_4$OH	-0.61	-0.63	-0.92	-49.55	1.46	2.24
Oxalic acid	-0.28	-0.55	-1.06	-47.22	1.10	2.19
Oxalic acid	-0.79	-0.94	-0.26	-55.43	1.42	2.51
Nitration Neat	-0.33	-0.62	-0.51	-50.40	1.60	4.30
Nitration 1:1 H	0.10	0.64	2.47	-73.78	1.55	3.11
Nitration 1:1 A	-0.07	0.43	1.91	-69.10	1.51	3.47
Nitration 1:1 A	0.14	1.15	1.07	-58.54	1.81	3.40
Nitration 1:1 H	-0.23	0.51	1.19	-63.68	1.77	5.64
Nit. CaO A	-0.28	0.04	0.33	-55.01	1.49	3.14
Nit.- Reduction A	0.52	1.61	1.88	-64.08	1.64	4.48
Sulfonation 2 ml	0.54	2.51	2.64	-71.77	1.87	1.86
Sulfonat. 1 ml A	-0.22	0.11	0.33	-58.29	1.50	2.75
Sulfonat. 1 ml H	-0.08	0.76	1.22	-63.29	2.47	2.31
Sulfonat. 0.5 ml H	-0.57	-0.42	-0.16	-55.28	1.53	2.65

Table 15. PVN, PI, LST and aging index data of all the virgin asphalts and their modified versions used in the study (continued).

Sample	PVN (77-275 °F)	PVN′ (77-140 °F)	PI	LST °C	Aging Index 275 °F	Aging Index 140 °F
KOH 1%	-0.52	-0.56	0.18	-56.94	1.20	1.68
KOH 4% R 6 h	0.33	0.56	4.06	-84.35	0.82	0.56
KOH 4% A 24 h	-0.59	-0.54	-0.25	-52.71	1.23	1.68
KOH 7.5%	0.84	1.34	0.03	-54.18	1.13	1.24
Sulphanilic acid H	-0.60	-0.57	-0.97	-48.70	1.30	1.94
Triethylamine A	-0.68	-0.67	-0.45	-51.38	1.42	2.44
Triethylamine H	-0.72	-0.68	-0.19	-54.55	1.33	2.12
C-8613 Virgin	-0.93	-0.88	-0.92	-46.65	1.35	2.04
MAH 10% N_2	0.69	0.09	-0.11	-47.90	0.92	3.77
CrO_3 4%	-0.73	-0.24	-0.08	-47.27	1.99	5.92
Furfural 2:5	-0.78	-0.43	-0.23	-47.72	1.32	1.84
C-8615 Virgin	-1.12	-0.97	-0.93	-45.78	1.40	2.25
MAH 10% N_2	-0.52	-0.16	0.21	-51.23	1.56	3.57
CrO_3 4%	-0.55	0.14	-0.37	-40.82	1.59	3.33
Furfural 2:5	-0.40	-0.13	-0.31	-44.56	0.98	1.70
C-8561 Virgin	-0.54	-0.47	-1.29	-45.28	1.37	1.93
MAH 10% N_2	0.01	0.18	0.23	-54.16	1.60	3.17
CrO_3 4%	-0.26	0.44	1.71	-59.89	1.48	2.18
Furfural 2:5	-0.56	-0.63	0.93	-59.76	1.27	2.50
C-9040 Virgin	-0.67	-0.80	-3.23	-20.06	1.17	1.75
MAH 10% N_2	-0.20	-0.49	-2.32	-25.43	1.19	2.21
CrO_3 4%	0.20	0.15	1.28	-55.93	1.04	1.78
Furfural 2:5	-0.82	-0.61	-0.01	-48.66	1.17	1.34
C-9041 Virgin	-0.47	-0.50	-0.92	-52.56	1.46	2.41
MAH 10% N_2	1.10	1.28	1.89	-71.45	1.37	2.32
MAH 6% N_2	0.02	0.14	0.04	-56.19	1.56	3.20
MAH 4% N_2	-0.23	-0.00	0.63	-62.25	1.59	3.02
MAH 4% N_2	-0.17	-0.00	0.14	-57.55	1.50	2.77
MAH 4% N_2	-0.31	-0.36	-0.13	-55.53	1.46	2.73
MAH 3% N_2	-0.50	-0.37	-0.20	-55.22	1.24	1.66
MAH 2% N_2	-0.43	-0.39	-0.27	-55.36	1.42	2.54

Table 15. PVN, PI, LST and aging index data of all the virgin asphalts and their modified versions used in the study (continued).

Sample	PVN (77-275 °F)	PVN′ (77-140 °F)	PI	LST °C	Aging Index 275 °F	Aging Index 140 °F
CrO_3 4%	-0.09	0.54	1.31	-60.22	1.62	3.71
CrO_3 2%	-0.31	-0.06	-2.78	-20.58	1.63	3.63
CrO_3 1.5%	-0.43	-0.35	-0.34	-54.99	1.42	2.20
CrO_3 1.5%	-0.38	-0.15	0.54	-60.07	1.53	2.79
CrO_3 1.5%	-0.44	-0.32	0.22	-57.31	1.49	2.74
CrO_3 1.5%	-0.37	-0.20	0.74	-61.21	1.57	2.81
CrO_3 1.5% Neat	-0.49	-0.69	-0.92	-50.69	1.40	2.75
CrO_3 1%	-0.37	-0.39	-1.77	-35.73	1.47	2.63
CrO_3 0.5%	-0.31	-0.19	0.10	-58.02	1.34	2.03
Furfural 2:5	-0.48	0.18	1.19	-64.30	1.33	1.42
Furfural 2:5	-0.64	0.07	1.75	-70.42	1.13	4.40
Furfural 2:5	-0.49	0.07	1.48	-66.54	1.52	1.70
Furfural 2:5	-0.49	0.15	1.61	-68.74	1.48	1.71
Furfural 1:5	-0.57	-0.38	0.91	-64.60	1.39	2.14
Furfural 1:5	0.47	0.07	1.02	-63.49	1.64	1.17
Furfural 0.5:2.5	-0.61	-0.34	0.37	-61.19	1.52	2.11
Furfural 0.5:2.5	-0.50	-0.41	0.17	-58.99	1.36	2.05
Furfural 0.75:4	-0.63	0.14	1.68	-69.26	1.36	1.01
C-9042 Virgin, Ac-20	-0.50	-0.47	-3.03	-18.38	1.49	2.69

APPENDIX B

This appendix contains the HP-GPC data of all the virgin asphalts and their modified versions obtained using a Photo-diode Array detector at 340 nm. The percentages of LMS, MMS and SMS are presented in table 15.

Table 16. High pressure-gel permeation chromatography data for the virgin asphalts and their chemically modified versions.

Sample		LMS %	MMS %	SMS %
B-5901	Virgin	21.59	45.20	33.20
	Virgin	21.47	45.51	33.02
	Virgin	22.68	45.91	31.41
	Virgin	22.15	45.50	32.35
	MAH 10% N_2	25.84	44.49	29.67
	MAH 10% N_2	25.39	44.08	30.53
	CrO_3 4%	34.51	39.69	25.80
	CrO_3 4%	34.35	39.67	25.98
	Furfural 2:5	20.87	45.29	33.83
	Furfural 2:5	20.65	45.54	33.81
	Furfural 2:5	20.60	45.40	34.00
C-8613	Virgin	21.52	47.56	30.93
	Virgin	21.28	47.89	30.83
	Virgin	21.87	48.10	30.03
	Virgin	21.86	47.87	30.27
	MAH 10% N_2	27.97	44.44	27.60
	MAH 10% N_2	27.93	44.38	27.69
	MAH 10% N_2	27.46	44.50	28.04
	MAH 10% N_2	28.03	44.83	27.15
	CrO_3 4%	31.49	43.25	25.26
	CrO_3 4%	31.50	43.09	25.41
	CrO_3 4%	32.28	42.56	25.16
	CrO_3 4%	32.01	42.94	25.05
	Furfural 2:5	20.07	48.20	31.73
	Furfural 2:5	20.10	48.20	31.68
	Furfural 2:5	19.62	48.26	32.12
C-8615	Virgin	24.68	43.33	31.99
	Virgin	24.39	43.16	32.45
	Virgin	23.74	43.84	32.42
	Virgin	24.09	43.35	32.56
	MAH 10% N_2	26.47	42.98	30.55
	MAH 10% N_2	25.76	43.66	30.87
	MAH 10% N_2	24.95	42.96	32.10
	MAH 10% N_2	25.50	43.07	31.43
	CrO_3 4%	31.65	39.94	28.41

Table 16. High pressure-gel permeation chromatography data for all the virgin asphalts and their chemically modified versions (continued).

	Sample	LMS %	MMS %	SMS %
	CrO_3 4%	31.88	39.74	28.38
	CrO_3 4%	32.05	39.36	28.59
	CrO_3 4%	32.37	39.01	28.62
	Furfural 2:5	24.47	43.15	32.39
	Furfural 2:5	24.41	43.06	32.54
	Furfural 2:5	24.44	43.06	32.50
	Furfural 2:5	24.76	43.06	32.19
C-8561	Virgin	22.91	43.95	33.14
	Virgin	22.43	44.88	32.69
	Virgin	22.58	44.85	32.56
	MAH 10% N_2	30.23	41.30	28.48
	MAH 10% N_2	30.06	41.69	28.25
	MAH 10% N_2	30.25	40.85	28.90
	MAH 10% N_2	30.01	41.21	28.78
	CrO_3 4%	31.79	40.63	27.58
	CrO_3 4%	32.53	40.14	27.33
	CrO_3 4%	33.46	39.52	27.02
	CrO_3 4%	33.05	39.99	26.96
	Furfural 2:5	22.01	44.59	33.39
	Furfural 2:5	21.65	44.53	33.83
	Furfural 2:5	21.82	44.44	33.74
C-9040	Virgin	19.19	49.14	31.68
	Virgin	19.27	49.15	31.58
	Virgin	19.33	48.96	31.71
	Virgin	19.16	49.21	31.62
	MAH 10% N_2	24.70	46.40	28.90
	MAH 10% N_2	24.81	46.78	28.41
	MAH 10% N_2	23.44	47.56	29.00
	MAH 10% N_2	24.02	47.68	28.30
	CrO_3 4%	28.85	44.84	26.32
	CrO_3 4%	29.00	44.32	26.69
	CrO_3 4%	29.61	44.14	26.25
	CrO_3 4%	29.36	44.56	26.08
	Furfural 2:5	19.33	49.21	31.46
	Furfural 2:5	19.55	48.82	31.63
	Furfural 2:5	20.86	49.08	30.06
	Furfural 2:5	21.09	49.09	29.82
C-9041	Virgin	22.98	44.39	32.63
	Virgin	23.25	44.23	32.52
C-9041	Virgin	23.75	43.80	32.46
	Virgin	23.82	43.65	32.54
	MAH 10% N2	32.26	39.39	28.35
	MAH 10% N_2	33.07	38.92	28.01
	MAH 10% N_2	32.37	39.33	28.30

Table 16. High pressure-gel permeation chromatography data for all the virgin asphalts and their chemically modified versions (continued).

Sample	LMS %	MMS %	SMS %
MAH 4% N_2	27.17	41.85	30.98
MAH 4% N_2	27.06	41.97	30.97
MAH 4% N_2	28.07	41.31	30.63
MAH 4% N_2	27.34	41.54	31.13
MAH 3% N_2	26.88	42.51	30.61
MAH 3% N_2	26.39	42.06	31.55
MAH 3% N_2	26.55	42.14	31.31
MAH 3% N_2	26.75	42.19	31.06
CrO_3 4%	32.32	38.90	27.78
CrO_3 4%	32.65	39.23	28.12
CrO_3 4%	32.49	38.80	28.71
CrO_3 4%	32.15	39.25	28.61
CrO_3 2%	29.78	40.11	30.10
CrO_3 2%	29.60	40.85	29.56
CrO_3 2%	29.99	41.26	28.75
CrO_3 1.5%	27.92	41.74	30.34
CrO_3 1.5%	28.20	41.58	30.23
CrO_3 1.5%	27.64	41.89	30.47
CrO_3 1.5%	27.39	41.90	30.71
CrO_3 1%	26.61	42.09	31.30
CrO_3 1%	27.30	41.63	31.07
CrO_3 1%	26.73	42.34	30.93
Furfural 2:5	22.94	43.42	33.65
Furfural 2:5	22.92	43.27	33.80
Furfural 2:5	22.15	44.44	33.41
Furfural 2:5	22.28	44.80	32.91

APPENDIX C

This appendix contains the data obtained with a Cone and Plate Viscometer.

Table 17. Cone and plate viscosity data at 0.05 and 0.01 sec^{-1} rate of shear.

Test Material	Temperature	Viscosities in poises	
		at 0.05 sec^{-1}	at 0.01 sec^{-1}
Virgin B-5901			
	60 °F (15.6 °C)	6.20×10^6	6.30×10^6
	77 °F (25 °C)	3.50×10^5	3.60×10^5
	100 °F (37.8 °C)	2.26×10^4	2.26×10^4
	140 °F (60 °C)	6.13×10^2	6.13×10^2
B-5901 Virgin-2			
	60 °F (15.6 °C)	6.00×10^6	8.2×10^6
	77 °F (25 °C)	6.50×10^5	9.60×10^5
	100 °F (37.8 °C)	5.80×10^4	8.70×10^4
	140 °F (60 °C)	6.07×10^2	6.07×10^2
B-5901 MAH 10% N_2			
	60 °F (15.6 °C)	2.95×10^7	6.15×10^7
	77 °F (25 °C)	5.60×10^6	1.18×10^7
	100 °F (37.8 °C)	7.30×10^5	1.60×10^6
	140 °F (60 °C)	7.05×10^3	7.05×10^3
B-5901 NOMAH N_2			
	60 °F (15.6 °C)	5.80×10^6	9.10×10^6
	77 °F (25 °C)	9.40×10^5	1.29×10^6
	100 °F (37.8 °C)	5.80×10^4	1.12×10^5
	140 °F (60 °C)	6.30×10^2	6.30×10^2
B-5901 MAH 10% Air 150 °C			
	60 °F (15.6 °C)	1.04×10^7	3.10×10^7
	77 °F (25 °C)	4.70×10^6	1.30×10^7
	100 °F (37.8 °C)	1.10×10^6	2.50×10^6
	140 °F (60 °C)	1.13×10^4	1.13×10^4
B-5901 NOMAH Air 150 °C			
	60 °F (15.6 °C)	9.70×10^6	1.10×10^7
	77 °F (25 °C)	7.30×10^5	8.60×10^5
	100 °F (37.8 °C)	4.60×10^4	4.80×10^4
	140 °F (60 °C)	7.56×10^2	7.56×10^2
B-5901 MAH 5%			
	77 °F (25 °C)	3.30×10^6	9.90×10^6
	86 °F (30 °C)	2.12×10^6	4.70×10^6
	95 °F (35 °C)	1.03×10^6	2.33×10^6

Table 17. Cone and plate viscosity data at 0.05 and 0.01 sec^{-1} rate of shear (continued).

Test Material	Temperature	Viscosities in poises	
		at 0.05 sec^{-1}	at 0.01 sec^{-1}
	104 °F (40 °C)	5.70 X 10^5	1.83 X 10^6
	140 °F (60 °C)	4.87 X 10^3	4.87 X 10^3
B-5901 MAH 2%			
	68 °F (20 °C)	4.12 X 10^6	9.00 X 10^6
	77 °F (25 °C)	1.85 X 10^6	3.00 X 10^6
	86 °F (30 °C)	8.10 X 10^5	1.40 X 10^6
	95 °F (35 °C)	2.19 X 10^5	3.30 X 10^5
	104 °F (40 °C)	1.10 X 10^5	2.20 X 10^5
	140 °F (60 °C)	1.80 X 10^3	1.80 X 10^3
B-5901 MAH 10% N_2 175 °C			
	60 °F (15.6 °C)	1.50 X 10^7	3.00 X 10^7
	77 °F (25 °C)	2.75 X 10^6	6.00 X 10^6
	100 °F (37.8 °C)	4.50 X 10^5	8.90 X 10^5
	140 °F (60 °C)	1.30 X 10^4	1.30 X 10^4
B-5901 NOMAH N_2 175 °C			
	60 °F (15.6 °C)	4.70 X 10^6	6.00 X 10^6
	77 °F (25 °C)	4.27 X 10^5	5.38 X 10^5
	100 °F (37.8 °C)	4.65 X 10^4	7.20 X 10^4
	140 °F (60 °C)	6.37 X 10^2	6.37 X 10^2
B-5901 CrO_3 0.5%			
	60 °F (15.6 °C)	4.37 X 10^6	1.75 X 10^7
	77 °F (25 °C)	1.02 X 10^6	1.80 X 10^6
	100 °F (37.8 °C)	9.30 X 10^4	1.10 X 10^5
	140 °F (60 °C)	1.31 X 10^3	1.31 X 10^3
B-5901 CrO_3 1%			
	60 °F (15.6 °C)	1.20 X 10^7	1.90 X 10^7
	77 °F (25 °C)	1.30 X 10^6	1.57 X 10^6
	100 °F (37.8 °C)	1.10 X 10^5	1.28 X 10^5
	140 °F (60 °C)	1.14 X 10^3	1.14 X 10^3
B-5901 CrO_3 2%			
	60 °F (15.6 °C)	1.39 X 10^7	2.73 X 10^7
	77 °F (25 °C)	3.20 X 10^6	4.20 X 10^6
	100 °F (37.8 °C)	2.50 X 10^5	2.50 X 10^5
	140 °F (60 °C)	1.96 X 10^3	1.96 X 10^3
B-5901 CrO_3 4%			
	77 °F (25 °C)	1.60 X 10^7	2.35 X 10^7
	100 °F (37.8 °C)	1.27 X 10^6	2.10 X 10^6

Table 17. Cone and plate viscosity data at 0.05 and 0.01 sec^{-1} rate of shear (continued).

Test Material	Temperature	Viscosities in poises	
		at 0.05 sec^{-1}	at 0.01 sec^{-1}
	140 °F (60 °C)	1.07 X 10^4	1.07 X 10^4
B-5901 CrO_3 4% 72 h			
	60 °F (15.6 °C)	1.75 X 10^8	2.75 X 10^8
	77 °F (25 °C)	9.00 X 10^6	1.80 X 10^7
	100 °F (37.8 °C)	1.17 X 10^6	1.70 X 10^6
	140 °F (60 °C)	3.48 X 10^3	3.48 X 10^3
B-5901 $NOCrO_3$ 24 h			
	60 °F (15.6 °C)	7.40 X 10^6	1.10 X 10^7
	77 °F (25 °C)	7.20 X 10^5	8.10 X 10^5
	100 °F (37.8 °C)	6.20 X 10^4	8.00 X 10^4
	140 °F (60 °C)	7.81 X 10^2	7.81 X 102
B-5901 HCl			
	60 °F (15.6 °C)	2.03 X 10^7	3.10 X 10^7
	77 °F (25 °C)	2.37 X 10^6	4.20 X 10^6
	100 °F (37.8 °C)	2.14 X 10^5	2.55 X 10^5
	140 °F (60 °C)	3.40 X 10^3	3.40 X 10^3
B-5901 Furfural 2:5			
	59 °F (14 °C)	5.10 X 10^6	1.20 X 10^7
	68 °F (20 °C)	2.30 X 10^6	6.00 X 10^6
	77 °F (25 °C)	1.40 X 10^6	3.00 X 10^6
	95 °F (35 °C)	2.60 X 10^5	2.80 X 10^5
	140 °F (60 °C)	1.38 X 10^4	1.38 X 10^4
B-5901 Oxalic Acid 5%			
	60 °F (15.6 °C)	6.30 X 10^6	6.70 X 10^6
	77 °F (25 °C)	6.10 X 10^5	6.70 X 10^5
	100 °F (37.8 °C)	4.42 X 10^4	4.60 X 10^4
	140 °F (60 °C)	7.19 X 10^2	7.19 X 10^2
B-5901 Nitration 1:1			
	68 °F (20 °C)	4.20 X 10^6	1.17 X 10^7
	77 °F (25 °C)	2.55 X 10^6	5.70 X 10^6
	86 °F (30 °C)	1.31 X 10^6	2.68 X 10^6
	95 °F (35 °C)	6.90 X 10^5	1.60 X 10^6
	104 °F (40 °C)	2.68 X 10^5	4.50 X 10^5
	140 °F (60 °C)	1.99 X 10^4	1.99 X 10^4
B-5901 Nitration-Reduction			
	77 °F (25 °C)	1.03 X 10^7	2.40 X 10^7
	86 °F (30 °C)	4.80 X 10^6	1.02 X 10^7
	95 °F (35 °C)	2.25 X 10^6	4.10 X 10^6

Table 17. Cone and plate viscosity data at 0.05 and 0.01 sec^{-1} rate of shear (continued).

Test Material	Temperature	Viscosities in poises	
		at 0.05 sec^{-1}	at 0.01 sec^{-1}
	104 °F (40 °C)	1.13 X 10^{6}	1.95 X 10^{6}
	113 °F (45 °C)	5.60 X 10^{5}	8.40 X 10^{5}
	140 °F (60 °C)	4.23 X 10^{4}	4.23 X 104
B-5901 Sulfonation 1 ml H_2SO_4			
	95 °F (35 °C)	6.10 X 10^{5}	1.25 X 10^{6}
	104 °F (40 °C)	3.80 X 10^{5}	9.70 X 10^{5}
	113 °F (45 °C)	2.30 X 10^{5}	6.40 X 10^{5}
	140 °F (60 °C)	8.78 X 10^{3}	8.78 X 10^{3}
B-5901 KOH 7.5%			
	68 °F (20 °C)	1.05 X 10^{7}	1.90 X 10^{7}
	77 °F (25 °C)	5.40 X 10^{6}	9.50 X 10^{6}
	86 °F (30 °C)	2.27 X 10^{6}	3.48 X 10^{6}
	95 °F (35 °C)	8.70 X 10^{5}	1.28 X 10^{6}
	104 °F (40 °C)	3.85 X 10^{5}	6.00 X 10^{5}
	140 °F (60 °C)	1.00 X 10^{4}	1.00 X 10^{4}
C-8613 Virgin			
	68 °F (20 °C)	4.70 X 10^{6}	5.10 X 10^{6}
	77 °F (25 °C)	1.40 X 10^{6}	1.55 X 10^{6}
	86 °F (30 °C)	5.10 X 10^{5}	5.50 X 10^{5}
	95 °F (35 °C)	1.51 X 10^{5}	1.82 X 10^{5}
	104 °F (40 °C)	6.20 X 10^{4}	7.70 X 10^{4}
	113 °F (45 °C)	2.76 X 10^{4}	3.70 X 10^{4}
	140 °F (60 °C)	7.63 X 10^{2}	7.63 X 10^{2}
C-8613 MAH 10% N_2			
	68 °F (20 °C)	1.53 X 10^{8}	2.30 X 10^{8}
	77 °F (25 °C)	6.90 X 10^{6}	1.30 X 10^{7}
	86 °F (30 °C)	2.60 X 10^{6}	4.85 X 10^{6}
	95 °F (35 °C)	1.35 X 10^{6}	2.20 X 10^{6}
	104 °F (40 °C)	4.80 X 10^{5}	6.90 X 10^{5}
	140 °F (60 °C)	6.11 X 10^{3}	6.11 X 10^{3}
C-8613 CrO_3 4%			
	77 °F (25 °C)	5.00 X 10^{6}	9.80 X 10^{6}
	86 °F (30 °C)	2.68 X 10^{6}	5.10 X 10^{6}
	95 °F (35 °C)	9.80 X 10^{5}	1.50 X 10^{6}
	104 °F (40 °C)	3.50 X 10^{5}	3.80 X 10^{5}
	113 °F (45 °C)	1.40 X 10^{5}	2.30 X 10^{5}
	122 °F (50 °C)	5.80 X 10^{4}	1.30 X 10^{5}
	140 °F (60 °C)	4.92 X 10^{3}	4.92 X 103

Table 17. Cone and plate viscosity data at 0.05 and 0.01 sec^{-1} rate of shear (continued).

Test Material	Temperature	Viscosities in poises at 0.05 sec^{-1}	at 0.01 sec^{-1}
C-8613 Furfural 2:5			
	59 °F (15 °C)	1.17 X 10^7	2.90 X 10^7
	68 °F (20 °C)	9.10 X 10^6	1.78 X 10^7
	77 °F (25 °C)	4.25 X 10^6	8.50 X 10^6
	86 °F (30 °C)	1.60 X 10^6	2.25 X 10^6
	95 °F (35 °C)	4.75 X 10^5	4.80 X 10^5
	104 °F (40 °C)	1.52 X 10^5	1.70 X 10^5
	113 °F (45 °C)	7.60 X 10^4	9.70 X 10^4
	140 °F (60 °C)	3.07 X 10^3	3.07 X 10^3
C-8615 Virgin			
	59 °F (15 °C)	7.2 X 10^6	1.2 X 10^7
	68 °F (20 °C)	2.3 X 10^6	2.8 X 10^6
	77 °F (25 °C)	6.4 X 10^5	9.7 X 10^5
	86 °F (30 °C)	2.9 X 10^5	4.1 X 10^5
	95 °F (35 °C)	1.2 X 10^5	1.82 X 10^5
	104 °F (40 °C)	5.1 X 10^4	9.50 X 10^4
	113 °F (45 °C)	1.75 X 10^4	2.50 X 10^4
	140 °F (60 °C)	8.04 X 10^2	8.04 X 102
C-8615 MAH 10% N_2			
	68 °F (20 °C)	1.20 X 10^7	2.18 X 10^7
	77 °F (25 °C)	3.50 X 10^6	8.60 X 10^6
	86 °F (30 °C)	2.40 X 10^6	4.70 X 10^6
	95 °F (35 °C)	9.60 X 10^5	1.13 X 10^6
	104 °F (40 °C)	5.5 X 10^5	7.4 X 10^5
	113 °F (45 °C)	1.52 X 10^5	1.80 X 10^5
	140 °F (60 °C)	4.74 X 10^3	4.74 X 10^3
C-8615 CrO_3 4%			
	68 °F (20 °C)	6.90 X 10^6	2.4 X 10^7
	77 °F (25 °C)	5.65 X 10^6	1.5 X 10^7
	86 °F (30 °C)	3.25 X 10^6	8.2 X 10^6
	95 °F (35 °C)	1.50 X 10^6	2.6 X 10^6
	104 °F (40 °C)	5.70 X 10^5	1.5 X 10^6
	113 °F (45 °C)	2.41 X 10^5	5.40 X 10^5
	122 °F (50 °C)	1.22 X 10^5	2.75 X 10^5
	140 °F (60 °C)	1.26 X 10^4	1.26 X 10^4
C-8615 Furfural 2:5			
	68 °F (20 °C)	6.8 X 10^6	1.75 X 10^7
	77 °F (25 °C)	3.70 X 10^6	9.05 X 10^6
	86 °F (30 °C)	1.80 X 10^6	5.30 X 10^6
	95 °F (35 °C)	8.3 X 10^5	1.8 X 10^6

Table 17. Cone and plate viscosity data at 0.05 and 0.01 sec^{-1} rate of shear (continued)

Test Material	Temperature	Viscosities in poises at 0.05 sec^{-1}	Viscosities in poises at 0.01 sec^{-1}
	104 °F (40 °C)	3.15×10^5	5.8×10^5
	113 °F (45 °C)	1.10×10^5	1.86×10^5
	122 °F (50 °C)	4.90×10^4	8.00×10^4
	140 °F (60 °C)	5.70×10^3	5.70×10^3
C-8561 Virgin			
	68 °F (20 °C)	1.10×10^6	1.22×10^6
	77 °F (25 °C)	3.80×10^5	4.50×10^5
	86 °F (30 °C)	1.35×10^5	1.90×10^5
	95 °F (35 °C)	4.30×10^4	5.00×10^4
	104 °F (40 °C)	2.20×10^4	2.70×10^4
	113 °F (45 °C)	1.08×10^4	1.27×10^4
	140 °F (60 °C)	6.65×10^2	6.65×10^2
C-8561 MAH 10% N_2			
	68 °F (20 °C)	1.60×10^7	3.60×10^7
	77 °F (25 °C)	2.65×10^6	5.90×10^6
	86 °F (30 °C)	1.80×10^6	3.25×10^6
	95 °F (35 °C)	9.90×10^5	1.60×10^6
	104 °F (40 °C)	3.20×10^5	4.60×10^5
	113 °F (45 °C)	1.26×10^5	1.65×10^5
	122 °F (50 °C)	4.05×10^4	5.40×10^4
	140 °F (60 °C)	4.28×10^3	4.28×10^3
C-8561 CrO_3 4%			
	68 °F (20 °C)	2.65×10^7	1.18×10^8
	77 °F (25 °C)	1.00×10^7	2.00×10^7
	86 °F (30 °C)	5.90×10^6	7.90×10^6
	95 °F (35 °C)	2.05×10^6	3.25×10^6
	104 °F (40 °C)	7.50×10^5	9.00×10^5
	113 °F (45 °C)	2.80×10^5	3.50×10^5
	122 °F (50 °C)	1.00×10^5	1.12×10^5
	131 °F (55 °C)	3.95×10^4	5.90×10^4
	140 °F (60 °C)	1.74×10^4	1.74×10^4
C-8561 Furfural 2:5			
	68 °F (20 °C)	6.50×10^6	1.14×10^7
	77 °F (25 °C)	2.33×10^6	4.14×10^6
	86 °F (30 °C)	1.08×10^6	1.20×10^6
	104 °F (40 °C)	2.24×10^5	2.85×10^5
	113 °F (45 °C)	8.00×10^4	1.10×10^5
	122 °F (50 °C)	3.50×10^4	4.60×10^4
	140 °F (60 °C)	2.43×10^3	2.43×10^3

Table 17. Cone and plate viscosity data at 0.05 and 0.01 sec^{-1} rate of shear (continued).

Test Material	Temperature	Viscosities in poises	
		at 0.05 sec^{-1}	at 0.01 sec^{-1}
C-9040 Virgin			
	59 °F (15 °C)	5.60 X 10^6	5.65 X 10^6
	68 °F (20 °C)	1.50 X 10^6	1.54 X 10^6
	77 °F (25 °C)	5.10 X 10^5	5.60 X 10^5
	86 °F (30 °C)	1.72 X 10^5	2.80 X 10^5
	95 °F (35 °C)	6.20 X 10^4	7.90 X 10^4
	104 °F (40 °C)	2.55 X 10^4	3.10 X 10^4
	140 °F (60 °C)	6.10 X 10^2	6.10 X 10^2
C-9040 MAH 10% N_2			
	68 °F (20 °C)	1.10 X 10^7	1.50 X 10^7
	77 °F (25 °C)	2.00 X 10^6	4.00 X 10^6
	86 °F (30 °C)	1.31 X 10^6	1.83 X 10^6
	95 °F (35 °C)	6.90 X 10^5	1.37 X 10^6
	109.4 °F (42 °C)	1.50 X 10^5	2.20 X 10^5
	140 °F (60 °C)	2.38 X 10^3	2.38 X 10^3
C-9040 CrO_3 4%			
	68 °F (20 °C)	6.90 X 10^6	1.50 X 10^7
	77 °F (25 °C)	5.60 X 10^6	1.22 X 107
	86 °F (30 °C)	3.00 X 10^6	5.58 X 10^6
	95 °F (35 °C)	1.26 X 10^6	2.23 X 10^6
	104 °F (40 °C)	4.10 X 10^5	5.40 X 10^5
	113 °F (45 °C)	1.41 X 10^5	1.83 X 10^5
	140 °F (60 °C)	1.33 X 10^4	1.33 X 10^4
C-9040 Furfural 2:5			
	68 °F (20 °C)	5.70 X 10^6	9.60 X 10^6
	77 °F (25 °C)	2.14 X 10^6	3.20 X 10^6
	86 °F (30 °C)	7.75 X 10^5	1.10 X 10^6
	95 °F (35 °C)	1.90 X 10^5	4.30 X 10^5
	104 °F (40 °C)	7.00 X 10^4	1.32 X 10^5
	140 °F (60 °C)	3.07 X 10^3	3.07 X 10^3
C-9041 Virgin			
	68 °F (20 °C)	3.50 X 10^5	3.50 X 10^5
	77 °F (25 °C)	1.27 X 10^5	1.27 X 10^5
	86 °F (30 °C)	4.20 X 10^4	4.20 X 10^4
	95 °F (35 °C)	1.60 X 10^4	1.60 X 10^4
	104 °F (40 °C)	1.40 X 10^4	1.40 X 10^4
	140 °F (60 °C)	4.11 X 10^2	4.11 X 10^2
C-9041 MAH 10% N_2			
	68 °F (20 °C)	1.32 X 10^7	3.20 X 10^7
	77 °F (25 °C)	7.00 X 10^6	1.48 X 10^7

Table 17. Cone and plate viscosity data at 0.05 and 0.01 sec^{-1} rate of shear (continued).

Test Material	Temperature	Viscosities in poises	
		at 0.05 sec^{-1}	at 0.01 sec^{-1}
	86 °F (30 °C)	3.10 X 10^6	6.00 X 10^6
	95 °F (35 °C)	1.53 X 10^6	2.80 X 10^6
	104 °F (40 °C)	8.20 X 10^5	1.65 X 10^6
	113 °F (45 °C)	3.37 X 10^5	6.90 X 10^5
	122 °F (50 °C)	1.25 X 10^5	2.20 X 10^5
	140 °F (60 °C)	1.22 X 10^4	1.22 X 104
<u>C-9041 MAH 4% N_2</u>	59 °F (15 °C)	1.00 X 10^7	1.97 X 10^7
	68 °F (20 °C)	4.90 X 10^6	6.00 X 10^6
	77 °F (25 °C)	1.65 X 10^6	3.20 X 10^6
	86 °F (30 °C)	6.50 X 10^5	9.60 X 10^5
	95 °F (35 °C)	1.53 X 10^5	4.62 X 10^5
	104 °F (40 °C)	1.08 X 10^5	2.30 X 10^5
	113 °F (45 °C)	4.60 X 10^4	9.50 X 10^4
	140 °F (60 °C)	2.20 X 10^3	2.20 X 10^3
<u>C-9041 CrO_3 4%</u>	68 °F (20 °C)	1.90 X 10^8	1.10 X 10^7
	77 °F (25 °C)	3.25 X 10^7	5.20 X 10^7
	86 °F (30 °C)	2.90 X 10^6	5.80 X 10^6
	95 °F (35 °C)	1.50 X 10^6	2.30 X 10^6
	104 °F (40 °C)	6.37 X 10^5	7.20 X 10^5
	113 °F (45 °C)	2.40 X 10^5	3.30 X 10^5
	122 °F (50 °C)	1.30 X 10^4	2.60 X 10^4
	140 °F (60 °C)	1.18 X 10^4	1.18 X 10^4
<u>C-9041 CrO_3 1.5%</u>	68 °F (20 °C)	2.25 X 10^6	4.43 X 10^6
	77 °F (25 °C)	1.00 X 10^6	1.40 X 10^6
	86 °F (30 °C)	3.80 X 10^5	4.40 X 10^5
	95 °F (35 °C)	1.31 X 10^5	1.95 X 10^5
	104 °F (40 °C)	4.50 X 10^4	5.50 X 10^4
	113 °F (45 °C)	3.10 X 10^4	4.10 X 10^4
	140 °F (60 °C)	2.27 X 10^3	2.27 X 10^3
<u>C-9041 Furfural 2:5</u>	68 °F (20 °C)	6.30 X 10^6	1.30 X 10^7
	77 °F (25 °C)	2.45 X 10^6	5.75 X 10^6
	86 °F (30 °C)	1.20 X 10^6	1.82 X 10^6
	95 °F (35 °C)	4.80 X 10^5	6.20 X 10^5
	104 °F (40 °C)	1.90 X 10^5	2.95 X 10^5
	113 °F (45 °C)	9.40 X 10^4	1.50 X 10^5
	140 °F (60 °C)	4.27 X 10^3	4.27 X 10^3

Table 17. Cone and plate viscosity data at 0.05 and 0.01 sec^{-1} rate of shear (continued).

Test Material	Temperature	Viscosities in poises at 0.05 sec^{-1}	 at 0.01 sec^{-1}
C-9041 Furfural 1:5			
	68 °F (20 °C)	2.30×10^6	3.50×10^6
	77 °F (25 °C)	9.46×10^5	1.29×10^6
	86 °F (30 °C)	3.20×10^5	4.80×10^5
	95 °F (35 °C)	1.40×10^5	1.60×10^5
	104 °F (40 °C)	5.63×10^4	1.03×10^5
	113 °F (45 °C)	1.91×10^4	3.40×10^4
	140 °F (60 °C)	1.63×10^3	1.63×10^3
C-9042 Virgin			
	68 °F (20 °C)	2.60×10^6	3.15×10^6
	77 °F (25 °C)	8.40×10^5	1.13×10^6
	86 °F (30 °C)	2.90×10^5	4.90×10^5
	95 °F (35 °C)	1.25×10^5	2.50×10^5
	104 °F (40 °C)	7.00×10^4	1.35×10^5
	140 °F (60 °C)	1.92×10^3	1.92×10^3

APPENDIX D

This appendix contains the Rheometrics DMA data obtained at frequencies of 100, 10, 1 and 0.1 radians/sec. and at temperatures from -50 to 80 °C. The data are complex viscosity, storage modulus, loss modulus, complex modulus and tan delta in tables 18 through 37.

Table 18. Complex viscosity of the B-5901 virgin asphalt.

Temperature °C	100 Rad/S	Complex viscosity in poise 10 Rad/S	1 Rad/S	0.1 Rad/S
-40	1.567×10^{8}	1.517×10^{9}	1.434×10^{10}	1.303×10^{11}
-30	1.363×10^{8}	1.243×10^{9}	1.079×10^{10}	8.695×10^{10}
-20	1.067×10^{8}	8.894×10^{8}	6.850×10^{9}	4.686×10^{10}
-10	7.310×10^{7}	5.397×10^{8}	3.660×10^{9}	2.181×10^{10}
0	3.897×10^{7}	2.309×10^{8}	1.046×10^{9}	3.545×10^{9}
0	1.535×10^{7}	5.904×10^{7}	1.917×10^{8}	3.927×10^{8}
10	2.878×10^{6}	7.490×10^{6}	1.309×10^{7}	2.439×10^{7}
20	4.884×10^{5}	1.002×10^{6}	1.563×10^{6}	2.253×10^{6}
30	5.378×10^{4}	8.163×10^{4}	1.092×10^{5}	1.289×10^{5}
40	1.337×10^{4}	1.793×10^{4}	2.149×10^{4}	2.321×10^{4}
50	2.461×10^{3}	3.007×10^{3}	3.307×10^{3}	3.496×10^{3}
60	6.808×10^{2}	7.675×10^{2}	8.045×10^{2}	8.032×10^{2}
70	2.251×10^{2}	2.404×10^{2}	2.454×10^{2}	2.429×10^{2}

Table 19. Complex viscosity of the B-5901 MAH 10% N_2 asphalt.

Temperature		Complex viscosity in Poise		
°C	100 Rad/S	10 Rad/S	1 Rad/S	0.1 Rad/S
-40	7.100 X 10^{7}	7.190 X 10^{8}	6.825 X 10^{9}	6.646 X 10^{10}
-30	7.535 X 10^{7}	7.357 X 10^{8}	6.843 X 10^{9}	6.713 X 10^{10}
-20	5.883 X 10^{7}	5.700 X 10^{8}	4.815 X 10^{9}	4.405 X 10^{10}
-10	2.751 X 10^{7}	2.655 X 10^{8}	2.306 X 10^{9}	2.065 X 10^{10}
-10	5.215 X 10^{7}	2.817 X 10^{8}	1.252 X 10^{9}	4.881 X 10^{9}
0	3.584 X 10^{7}	2.171 X 10^{8}	1.136 X 10^{9}	5.228 X 10^{9}
0	1.711 X 10^{7}	7.268 X 10^{7}	2.737 X 10^{8}	9.013 X 10^{8}
10	8.506 X 10^{6}	4.351 X 10^{7}	1.570 X 10^{8}	6.361 X 10^{8}
10	3.848 X 10^{6}	1.407 X 10^{7}	3.990 X 10^{7}	1.197 X 10^{8}
20	9.786 X 10^{5}	2.828 X 10^{6}	6.257 X 10^{6}	1.793 X 10^{7}
30	9.433 X 10^{4}	3.976 X 10^{5}	8.933 X 10^{5}	1.553 X 10^{6}
40	3.934 X 10^{4}	9.383 X 10^{4}	1.994 X 10^{5}	3.965 X 10^{5}
50	1.080 X 10^{4}	2.308 X 10^{4}	4.535 X 10^{4}	7.773 X 10^{4}
60	3.166 X 10^{3}	6.521 X 10^{3}	1.180 X 10^{4}	1.785 X 10^{4}
70	1.099 X 10^{3}	2.079 X 10^{3}	3.376 X 10^{3}	4.484 X 10^{3}
80	4.479 X 10^{2}	7.672 X 10^{2}	1.111 X 10^{3}	1.333 X 10^{3}
80	4.230 X 10^{2}	7.527 X 10^{2}	1.118 X 10^{3}	1.335 X 10^{3}

Table 20. Complex viscosity of the B-5901 CrO_3 4% asphalt.

Temperature	Complex viscosity in poise			
°C	100 Rad/S	10 Rad/S	1 Rad/S	0.1 Rad/S
-50	8.581 X 10^{7}	8.374 X 10^{8}	7.989 X 10^{9}	7.425 X 10^{10}
-40	7.892 X 10^{7}	7.342 X 10^{8}	6.921 X 10^{9}	5.771 X 10^{10}
-30	6.944 X 10^{7}	5.815 X 10^{8}	4.499 X 10^{9}	3.467 X 10^{10}
-20	4.954 X 10^{7}	3.696 X 10^{8}	2.510 X 10^{9}	1.357 X 10^{10}
-10	2.570 X 10^{7}	1.571 X 10^{8}	8.753 X 10^{8}	4.101 X 10^{9}
0	1.045 X 10^{7}	5.443 X 10^{7}	2.560 X 10^{8}	1.076 X 10^{9}
0	2.165 X 10^{7}	1.005 X 10^{8}	4.826 X 10^{8}	1.821 X 10^{9}
0	2.201 X 10^{7}	1.073 X 10^{8}	4.748 X 10^{8}	1.887 X 10^{9}
10	3.904 X 10^{6}	1.741 X 10^{7}	6.997 X 10^{7}	2.513 X 10^{8}
10	6.646 X 10^{6}	2.755 X 10^{7}	1.015 X 10^{8}	3.475 X 10^{8}
10	6.660 X 10^{6}	2.747 X 10^{7}	1.018 X 10^{8}	3.398 X 10^{8}
20	1.840 X 10^{6}	6.298 X 10^{6}	1.999 X 10^{7}	5.502 X 10^{7}
20	1.711 X 10^{6}	6.013 X 10^{6}	1.900 X 10^{7}	5.391 X 10^{7}
30	5.459 X 10^{5}	1.703 X 10^{6}	4.760 X 10^{6}	1.087 X 10^{7}
30	4.526 X 10^{5}	1.571 X 10^{6}	4.623 X 10^{6}	8.647 X 10^{6}
40	1.693 X 10^{5}	4.806 X 10^{5}	1.213 X 10^{6}	2.497 X 10^{6}
50	6.196 X 10^{4}	1.532 X 10^{5}	3.269 X 10^{5}	5.320 X 10^{5}
60	2.060 X 10^{4}	4.325 X 10^{4}	7.568 X 10^{4}	4.413 X 10^{4}
60	1.395 X 10^{4}	2.711 X 10^{4}	5.220 X 10^{4}	7.981 X 10^{4}
60	1.099 X 10^{4}	2.396 X 10^{4}	4.466 X 10^{4}	6.609 X 10^{4}
70	3.880 X 10^{3}	7.296 X 10^{3}	1.131 X 10^{4}	1.439 X 10^{4}
80	1.426 X 10^{3}	2.328 X 10^{3}	3.077 X 10^{3}	3.481 X 10^{3}
90	5.541 X 10^{2}	7.936 X 10^{2}	9.335 X 10^{2}	9.789 X 10^{2}
100	2.339 X 10^{2}	3.010 X 10^{2}	3.265 X 10^{2}	3.175 X 10^{2}

Table 21. Complex viscosity of the B-5901 Furfural 2:5 asphalt.

Temperature °C	Complex viscosity in Poise 100 Rad/S	10 Rad/S	1 Rad/S	0.1 Rad/S
-40	2.347 X 10^{7}	2.348 X 10^{8}	2.082 X 10^{9}	1.914 X 10^{10}
-30	4.293 X 10^{7}	3.600 X 10^{8}	2.923 X 10^{9}	2.177 X 10^{10}
-20	3.593 X 10^{7}	2.578 X 10^{8}	1.598 X 10^{9}	6.449 X 10^{9}
-20	9.020 X 10^{7}	5.813 X 10^{8}	3.262 X 10^{9}	1.497 X 10^{10}
-10	1.611 X 10^{7}	9.010 X 10^{7}	4.540 X 10^{8}	1.844 X 10^{9}
-10	4.188 X 10^{7}	2.231 X 10^{8}	1.030 X 10^{9}	3.625 X 10^{9}
0	5.996 X 10^{6}	2.723 X 10^{7}	1.135 X 10^{8}	3.713 X 10^{8}
0	1.262 X 10^{7}	5.599 X 10^{7}	2.240 X 10^{8}	8.072 X 10^{8}
10	1.829 X 10^{6}	7.327 X 10^{6}	2.661 X 10^{7}	8.610 X 10^{7}
10	3.133 X 10^{6}	1.178 X 10^{7}	4.347 X 10^{7}	1.304 X 10^{8}
20	8.694 X 10^{5}	2.839 X 10^{6}	8.480 X 10^{6}	2.379 X 10^{7}
30	3.108 X 10^{5}	9.052 X 10^{5}	2.427 X 10^{6}	5.296 X 10^{6}
30	2.820 X 10^{5}	8.792 X 10^{5}	2.470 X 10^{6}	5.947 X 10^{6}
40	9.381 X 10^{4}	2.539 X 10^{5}	6.133 X 10^{5}	1.170 X 10^{6}
40	8.116 X 10^{4}	2.435 X 10^{5}	6.258 X 10^{5}	1.278 X 10^{6}
50	1.779 X 10^{4}	4.349 X 10^{4}	8.958 X 10^{4}	1.409 X 10^{5}
60	6.220 X 10^{3}	1.280 X 10^{4}	2.156 X 10^{4}	2.817 X 10^{4}
60	6.018 X 10^{3}	1.281 X 10^{4}	2.197 X 10^{4}	2.954 X 10^{4}
70	2.064 X 10^{3}	3.527 X 10^{3}	4.930 X 10^{3}	5.556 X 10^{3}
70	1.989 X 10^{3}	3.498 X 10^{3}	4.929 X 10^{3}	5.693 X 10^{3}
80	6.972 X 10^{2}	1.002 X 10^{3}	1.210 X 10^{3}	1.240 X 10^{3}

Table 22. Storage modulus of the B-5901 virgin asphalt.

Temperature	Storage modulus in dynes/cm. sq. at			
°C	100 Rad/S	10 Rad/S	1 Rad/S	0.1 Rad/S
-40	1.566 X 10^{10}	1.515 X 10^{10}	1.430 X 10^{10}	1.295 X 10^{10}
-30	1.360 X 10^{10}	1.237 X 10^{10}	1.069 X 10^{10}	8.521 X 10^{9}
-20	1.059 X 10^{10}	8.771 X 10^{9}	6.679 X 10^{9}	4.428 X 10^{9}
-10	7.180 X 10^{9}	5.226 X 10^{9}	3.445 X 10^{9}	1.904 X 10^{9}
0	3.703 X 10^{9}	2.067 X 10^{9}	8.203 X 10^{8}	2.217 X 10^{8}
0	1.223 X 10^{9}	4.290 X 10^{8}	1.192 X 10^{8}	1.832 X 10^{7}
10	1.830 X 10^{8}	3.928 X 10^{7}	5.272 X 10^{6}	7.552 X 10^{5}
20	2.207 X 10^{7}	3.594 X 10^{6}	4.289 X 10^{5}	4.310 X 10^{4}
30	1.585 X 10^{6}	1.850 X 10^{5}	1.708 X 10^{4}	1.057 X 10^{3}
40	2.901 X 10^{5}	2.768 X 10^{4}	1.912 X 10^{3}	9.090 X 10^{1}
50	3.074 X 10^{4}	2.582 X 10^{3}	1.143 X 10^{2}	6.600 X 10^{-1}
60	6.395 X 10^{3}	3.668 X 10^{2}	1.286 X 10^{1}	4.528 X 10^{-3}
70	1.425 X 10^{3}	6.991 X 10^{1}	1.948 X 10^{0}	000000

Table 23. Storage modulus of the B-5901 MAH 10% N_2 asphalt.

Temperature	Storage modulus in dynes/cm. sq. at			
°C	100 Rad/S	10 Rad/S	1 Rad/S	0.1 Rad/S
-40	7.083 X 10^9	7.166 X 10^9	6.794 X 10^9	6.551 X 10^9
-30	7.516 X 10^9	7.324 X 10^9	6.776 X 10^9	6.541 X 10^9
-20	5.861 X 10^9	5.646 X 10^9	4.733 X 10^9	4.205 X 10^9
-10	2.736 X 10^9	2.633 X 10^9	2.240 X 10^9	1.818 X 10^9
-10	4.485 X 10^9	2.458 X 10^9	1.044 X 10^9	3.746 X 10^8
0	3.400 X 10^9	1.961 X 10^9	9.544 X 10^8	4.043 X 10^8
0	1.405 X 10^9	5.757 X 10^8	2.041 X 10^8	6.111 X 10^7
10	6.999 X 10^8	3.160 X 10^8	1.043 X 10^8	3.908 X 10^7
10	2.789 X 10^8	9.723 X 10^7	2.581 X 10^7	6.907 X 10^6
20	6.104 X 10^7	1.678 X 10^7	3.463 X 10^6	9.013 X 10^5
30	0000	1.456 X 10^6	4.291 X 10^5	6.734 X 10^4
40	8.443 X 10^5	4.069 X 10^5	8.765 X 10^4	1.530 X 10^4
50	3.673 X 10^5	9.115 X 10^4	1.686 X 10^4	2.275 X 10^3
60	1.013 X 10^5	2.209 X 10^4	3.562 X 10^3	3.763 X 10^2
70	3.153 X 10^4	5.944 X 10^3	7.985 X 10^2	6.392 X 10^1
80	1.135 X 10^4	1.798 X 10^3	1.942 X 10^2	1.251 X 10^1
80	1.012 X 10^4	1.718 X 10^3	1.967 X 10^2	1.236 X 10^1

Table 24. Storage modulus of the B-5901 CrO_3 4% asphalt.

Temperature °C	Storage modulus in dynes/cm. sq. at 100 Rad/S	10 Rad/S	1 Rad/S	0.1 Rad/S
-50	8.577 X 10^9	8.366 X 10^9	7.975 X 10^9	7.396 X 10^9
-40	7.883 X 10^9	7.319 X 10^9	6.886 X 10^9	5.680 X 10^9
-30	6.923 X 10^9	5.760 X 10^9	4.405 X 10^9	3.328 X 10^9
-20	4.884 X 10^9	3.588 X 10^9	2.386 X 10^9	1.220 X 10^9
-10	2.456 X 10^9	1.464 X 10^9	7.918 X 10^8	3.497 X 10^8
0	9.522 X 10^8	4.817 X 10^8	2.184 X 10^8	8.605 X 10^7
0	1.865 X 10^9	8.549 X 10^8	3.990 X 10^8	1.422 X 10^8
0	1.899 X 10^9	9.168 X 10^8	3.928 X 10^8	1.467 X 10^8
10	3.358 X 10^8	1.440 X 10^8	5.511 X 10^7	1.853 X 10^7
10	5.363 X 10^8	2.151 X 10^8	7.564 X 10^7	2.332 X 10^7
10	5.357 X 10^8	2.135 X 10^8	7.552 X 10^7	2.323 X 10^7
20	1.318 X 10^8	4.295 X 10^7	1.280 X 10^7	3.077 X 10^6
20	1.186 X 10^8	4.011 X 10^7	1.208 X 10^7	3.071 X 10^6
30	3.464 X 10^7	1.044 X 10^7	2.736 X 10^6	5.274 X 10^5
30	2.728 X 10^7	9.379 X 10^6	2.639 X 10^6	3.934 X 10^5
40	9.605 X 10^6	2.669 X 10^6	6.219 X 10^5	9.627 X 10^4
50	3.268 X 10^6	7.688 X 10^5	1.393 X 10^5	1.274 X 10^4
60	9.537 X 10^5	1.806 X 10^5	2.449 X 10^4	1.598 X 10^3
60	3.541 X 10^5	1.088 X 10^5	1.648 X 10^4	1.485 X 10^3
60	4.513 X 10^5	1.018 X 10^5	1.481 X 10^4	1.212 X 10^3
70	1.514 X 10^5	2.448 X 10^4	2.410 X 10^3	1.283 X 10^2
80	4.704 X 10^4	5.563 X 10^3	3.820 X 10^2	1.686 X 10^1
90	1.434 X 10^4	1.254 X 10^3	5.996 X 10^1	2.527 X 10^0
100	4.509 X 10^3	2.922 X 10^2	8.782 X 10^0	3.603 X 10^{-1}

Table 25. Storage modulus of the B-5901 Furfural 2:5 asphalt.

Temperature		Storage modulus in dynes/cm. sq.		
°C	100 Rad/S	10 Rad/S	1 Rad/S	0.1 Rad/S
-40	2.322 X 10^9	2.328 X 10^9	2.055 X 10^9	1.866 X 10^9
-30	4.258 X 10^9	3.551 X 10^9	2.844 X 10^9	2.015 X 10^9
-20	3.519 X 10^9	2.471 X 10^9	1.482 X 10^9	5.498 X 10^8
-20	8.056 X 10^9	5.384 X 10^9	2.927 X 10^9	1.269 X 10^9
-10	1.507 X 10^9	8.100 X 10^8	3.902 X 10^8	1.475 X 10^8
-10	3.720 X 10^9	1.971 X 10^9	8.735 X 10^8	2.817 X 10^8
0	5.226 X 10^8	2.275 X 10^8	9.106 X 10^7	2.829 X 10^7
0	1.059 X 10^9	4.569 X 10^8	1.752 X 10^8	5.918 X 10^7
10	1.471 X 10^8	5.704 X 10^7	2.000 X 10^7	5.956 X 10^6
10	2.416 X 10^8	8.798 X 10^7	3.126 X 10^7	8.662 X 10^6
20	6.014 X 10^7	1.908 X 10^7	5.414 X 10^6	1.375 X 10^6
30	1.986 X 10^7	5.615 X 10^6	1.399 X 10^6	2.387 X 10^5
30	1.736 X 10^7	5.404 X 10^6	1.440 X 10^6	2.972 X 10^5
40	5.415 X 10^6	1.433 X 10^6	3.085 X 10^5	4.155 X 10^4
40	4.400 X 10^6	1.337 X 10^6	3.159 X 10^5	4.952 X 10^4
50	8.949 X 10^5	2.086 X 10^5	3.506 X 10^4	3.467 X 10^3
60	2.768 X 10^5	4.913 X 10^4	5.810 X 10^3	3.645 X 10^2
60	2.641 X 10^5	4.942 X 10^4	6.032 X 10^3	4.062 X 10^2
70	7.590 X 10^4	9.802 X 10^3	7.818 X 10^2	3.818 X 10^1
70	7.221 X 10^4	9.792 X 10^3	8.079 X 10^2	3.691 X 10^1
80	1.945 X 10^4	1.858 X 10^3	9.320 X 10^1	1.779 X 10^1

Table 26. Loss modulus of the B-5901 virgin asphalt.

Temperature °C	Loss modulus in dynes/cm. sq. at 100 Rad/S	10 Rad/S	1 Rad/S	0.1 Rad/S
-40	5.500×10^8	7.014×10^8	9.302×10^8	1.390×10^9
-30	9.242×10^8	1.203×10^9	1.487×10^9	1.729×10^9
-20	1.277×10^9	1.460×10^9	1.517×10^9	1.534×10^9
-10	1.372×10^9	1.341×10^9	1.234×10^9	1.063×10^9
0	1.213×10^9	1.028×10^9	6.482×10^8	2.767×10^8
0	9.276×10^8	4.054×10^8	1.502×10^8	3.474×10^7
10	2.221×10^8	6.375×10^7	1.199×10^7	2.319×10^6
20	4.357×10^7	9.355×10^6	1.503×10^6	2.211×10^5
30	5.139×10^6	7.948×10^5	1.079×10^5	1.284×10^4
40	1.305×10^6	1.771×10^5	2.140×10^4	2.319×10^3
50	2.442×10^5	2.995×10^4	3.305×10^3	3.496×10^2
60	6.778×10^4	7.665×10^3	8.044×10^2	8.032×10^1
70	2.247×10^4	2.403×10^3	2.453×10^2	2.429×10^1

Table 27. Loss modulus of the B-5901 MAH 10% N_2 asphalt.

Temperature	Loss modulus in dynes/cm. sq. at			
°C	100 Rad/S	10 Rad/S	1 Rad/S	0.1 Rad/S
-40	5.006 X 10^{8}	5.549 X 10^{8}	6.434 X 10^{9}	1.119 X 10^{9}
-30	5.330 X 10^{8}	6.777 X 10^{8}	9.482 X 10^{8}	1.508 X 10^{9}
-20	5.085 X 10^{8}	7.771 X 10^{8}	8.818 X 10^{8}	1.314 X 10^{9}
-10	2.900 X 10^{8}	3.361 X 10^{8}	5.466 X 10^{8}	9.786 X 10^{8}
-10	2.661 X 10^{9}	1.375 X 10^{9}	6.921 X 10^{8}	3.129 X 10^{8}
0	1.131 X 10^{9}	9.306 X 10^{8}	6.152 X 10^{8}	3.315 X 10^{8}
0	9.763 X 10^{8}	4.434 X 10^{8}	1.823 X 10^{8}	6.624 X 10^{7}
10	4.833 X 10^{8}	2.989 X 10^{8}	1.173 X 10^{8}	5.019 X 10^{7}
10	2.652 X 10^{8}	1.016 X 10^{8}	3.043 X 10^{7}	9.771 X 10^{6}
20	7.650 X 10^{7}	2.276 X 10^{7}	5.211 X 10^{6}	1.551 X 10^{6}
30	9.433 X 10^{6}	3.699 X 10^{6}	7.834 X 10^{5}	1.399 X 10^{5}
40	3.842 X 10^{6}	8.453 X 10^{5}	1.791 X 10^{5}	3.658 X 10^{4}
50	1.016 X 10^{6}	2.120 X 10^{5}	4.209 X 10^{4}	7.433 X 10^{3}
60	3.000 X 10^{5}	6.134 X 10^{4}	1.125 X 10^{4}	1.744 X 10^{3}
70	1.052 X 10^{5}	1.991 X 10^{4}	3.280 X 10^{3}	4.438 X 10^{2}
80	4.333 X 10^{4}	7.456 X 10^{3}	1.093 X 10^{3}	1.327 X 10^{2}
80	4.107 X 10^{4}	7.327 X 10^{3}	1.100 X 10^{3}	1.329 X 10^{2}

Table 28. Loss modulus of the B-5901 CrO_3 4% asphalt.

Temperature	Loss modulus in dynes/cm. sq. at			
°C	100 Rad/S	10 Rad/S	1 Rad/S	0.1 Rad/S
-50	2.482×10^8	3.374×10^8	4.688×10^8	6.544×10^8
-40	3.784×10^8	5.613×10^8	6.878×10^8	1.022×10^9
-30	5.360×10^8	7.871×10^8	9.124×10^8	9.715×10^8
-20	8.300×10^8	8.845×10^8	7.787×10^8	5.936×10^8
-10	7.578×10^8	5.695×10^8	3.730×10^8	2.142×10^8
0	4.309×10^8	2.533×10^8	1.335×10^8	6.464×10^7
0	1.100×10^9	5.277×10^8	2.715×10^8	1.138×10^8
0	1.112×10^9	5.577×10^8	2.667×10^8	1.187×10^8
10	1.990×10^8	9.780×10^7	4.311×10^7	1.697×10^7
10	3.924×10^8	1.720×10^8	6.772×10^7	2.577×10^7
10	3.958×10^8	1.728×10^8	6.827×10^7	2.480×10^7
20	1.284×10^8	4.604×10^7	1.535×10^7	4.562×10^6
20	1.234×10^8	4.478×10^7	1.466×10^7	4.431×10^6
30	4.219×10^7	1.345×10^7	3.895×10^6	9.502×10^5
30	3.612×10^7	1.260×10^7	3.795×10^6	7.700×10^5
40	1.394×10^7	3.995×10^6	1.041×10^6	2.304×10^5
50	5.265×10^6	1.325×10^6	2.957×10^5	5.165×10^4
60	1.826×10^6	3.929×10^5	7.160×10^4	4.114×10^3
60	8.055×10^5	2.482×10^5	4.952×10^4	7.841×10^3
60	1.002×10^6	2.168×10^5	4.213×10^4	6.497×10^3
70	3.572×10^5	6.871×10^4	1.105×10^4	1.434×10^3
80	1.346×10^5	2.260×10^4	3.053×10^3	3.477×10^2
90	5.352×10^4	7.834×10^3	9.315×10^2	9.786×10^1
100	2.295×10^4	2.995×10^3	3.264×10^2	3.175×10^1

Table 29. Loss modulus of the B-5901 Furfural 2:5 asphalt.

Temperature °C	Loss modulus in dynes/cm. sq. at 100 Rad/S	 10 Rad/S	 1 Rad/S	 0.1 Rad/S
-40	3.412×10^8	3.007×10^8	3.340×10^8	4.272×10^8
-30	5.483×10^8	5.831×10^8	6.776×10^8	8.247×10^8
-20	7.270×10^8	7.357×10^8	5.986×10^8	3.370×10^8
-20	4.058×10^9	2.189×10^9	1.439×10^9	7.944×10^8
-10	5.708×10^8	3.942×10^8	2.320×10^8	1.108×10^8
-10	1.923×10^9	1.045×10^9	5.450×10^8	2.281×10^8
0	2.939×10^8	1.495×10^8	6.778×10^7	2.405×10^7
0	6.852×10^8	3.235×10^8	1.396×10^8	5.490×10^7
10	1.086×10^8	4.597×10^7	1.755×10^7	6.217×10^6
10	1.995×10^8	7.831×10^7	3.021×10^7	9.747×10^6
20	6.279×10^7	2.101×10^7	6.526×10^6	1.941×10^6
30	2.390×10^7	7.097×10^6	1.983×10^6	4.727×10^5
30	2.223×10^7	6.933×10^6	2.007×10^6	5.152×10^5
40	7.661×10^6	2.095×10^6	5.300×10^5	1.094×10^5
40	6.819×10^6	2.034×10^6	5.401×10^5	1.178×10^5
50	1.537×10^6	3.815×10^5	8.242×10^4	1.366×10^4
60	5.570×10^5	1.182×10^5	2.076×10^4	2.793×10^3
60	5.407×10^5	1.181×10^5	2.112×10^4	2.926×10^3
70	1.919×10^5	3.387×10^4	4.868×10^3	5.543×10^2
70	1.854×10^5	3.357×10^4	4.862×10^3	5.681×10^2
80	6.696×10^4	9.849×10^3	1.206×10^3	1.227×10^2

Table 30. Complex modulus of the B-5901 virgin asphalt.

Temperature		Complex modulus in dynes/cm. sq. at		
°C	100 Rad/S	10 Rad/S	1 Rad/S	0.1 Rad/S
-40	1.567 X 10^{10}	1.517 X 10^{10}	1.434 X 10^{10}	1.303 X 10^{10}
-30	1.363 X 10^{10}	1.243 X 10^{10}	1.079 X 10^{10}	8.695 X 10^{9}
-20	1.067 X 10^{10}	8.894 X 10^{9}	6.850 X 10^{9}	4.686 X 10^{9}
-10	7.310 X 10^{9}	5.397 X 10^{9}	3.660 X 10^{9}	2.181 X 10^{9}
0	3.897 X 10^{9}	2.309 X 10^{9}	1.046 X 10^{9}	3.545 X 10^{8}
0	1.535 X 10^{9}	5.904 X 10^{8}	1.917 X 10^{8}	3.927 X 10^{7}
10	2.878 X 10^{8}	7.490 X 10^{7}	1.309 X 10^{7}	2.439 X 10^{6}
20	4.884 X 10^{7}	1.002 X 10^{7}	1.563 X 10^{6}	2.253 X 10^{5}
30	5.378 X 10^{6}	8.163 X 10^{5}	1.092 X 10^{5}	1.289 X 10^{4}
40	1.337 X 10^{6}	1.793 X 10^{5}	2.149 X 10^{4}	2.321 X 10^{3}
50	2.461 X 10^{5}	3.007 X 10^{4}	3.307 X 10^{3}	3.496 X 10^{2}
60	6.808 X 10^{4}	7.675 X 10^{3}	8.045 X 10^{2}	8.032 X 10^{1}
70	2.251 X 10^{4}	2.404 X 10^{3}	2.454 X 10^{2}	2.429 X 10^{1}

Table 31. Complex modulus of the B-5901 MAH 10% N_2 asphalt.

Temperature	Complex modulus in dynes/cm. sq.			
°C	100 Rad/S	10 Rad/S	1 Rad/S	0.1 Rad/S
-40	7.100 X 10^9	7.190 X 10^9	6.825 X 10^9	6.646 X 10^9
-30	7.535 X 10^9	7.357 X 10^9	6.843 X 10^9	6.713 X 10^9
-20	5.835 X 10^9	5.700 X 10^9	4.815 X 10^9	4.405 X 10^9
-10	5.215 X 10^9	2.817 X 10^9	1.252 X 10^9	4.881 X 10^9
-10	2.751 X 10^9	2.655 X 10^9	2.306 X 10^9	2.065 X 10^8
0	3.584 X 10^9	2.171 X 10^9	1.136 X 10^8	5.228 X 10^8
0	1.711 X 10^9	7.268 X 10^8	2.737 X 10^8	9.013 X 10^7
10	8.506 X 10^8	4.351 X 10^8	1.570 X 10^8	6.361 X 10^7
10	3.848 X 10^8	1.407 X 10^8	3.990 X 10^7	1.197 X 10^7
20	9.786 X 10^7	2.828 X 10^7	6.257 X 10^6	1.793 X 10^6
30	9.433 X 10^6	3.976 X 10^6	8.933 X 10^5	1.553 X 10^5
40	3.934 X 10^6	9.383 X 10^5	1.994 X 10^5	3.965 X 10^4
50	1.080 X 10^6	2.308 X 10^5	4.535 X 10^4	7.773 X 10^3
60	3.166 X 10^5	6.521 X 10^4	1.180 X 10^4	1.785 X 10^3
70	1.099 X 10^5	2.079 X 10^4	3.376 X 10^3	4.484 X 10^2
80	4.479 X 10^4	7.672 X 10^3	1.111 X 10^3	1.333 X 10^2
80	4.230 X 10^4	7.527 X 10^3	1.118 X 10^3	1.335 X 10^2

Table 32. Complex modulus of the B-5901 CrO_3 4% asphalt.

Temperature		Complex modulus in dynes/cm. sq.		
°C	100 Rad/S	10 Rad/S	1 Rad/S	0.1 Rad/S
-50	8.581×10^9	8.374×10^9	7.989×10^9	7.425×10^9
-40	7.892×10^9	7.342×10^9	6.921×10^9	5.771×10^9
-30	6.944×10^9	5.815×10^9	4.499×10^9	3.467×10^9
-20	4.954×10^9	3.696×10^9	2.510×10^9	1.357×10^9
-10	2.570×10^9	1.571×10^9	8.753×10^8	4.101×10^8
0	1.045×10^9	5.443×10^8	2.560×10^8	1.076×10^8
0	2.165×10^9	1.005×10^9	4.826×10^8	1.821×10^8
0	2.201×10^9	1.073×10^9	4.748×10^8	1.887×10^8
10	3.904×10^8	1.741×10^8	6.997×10^7	2.513×10^7
10	6.646×10^8	2.755×10^8	1.015×10^8	3.475×10^7
10	6.660×10^8	2.747×10^8	1.018×10^8	3.398×10^7
20	1.840×10^8	6.298×10^7	1.999×10^7	5.502×10^6
20	1.711×10^8	6.013×10^7	1.900×10^7	5.391×10^6
30	5.459×10^7	1.703×10^7	4.760×10^6	1.081×10^6
30	4.526×10^7	1.571×10^7	4.623×10^6	8.647×10^5
40	1.693×10^7	4.806×10^6	1.213×10^6	2.497×10^5
50	6.196×10^6	1.532×10^6	3.269×10^5	5.320×10^4
60	2.060×10^6	4.325×10^5	7.568×10^4	4.413×10^3
60	1.395×10^6	2.711×10^5	5.220×10^4	7.981×10^3
60	1.099×10^6	2.396×10^5	4.466×10^4	6.609×10^3
70	3.880×10^5	7.296×10^4	1.131×10^4	1.439×10^3
80	1.426×10^5	2.328×10^4	3.077×10^3	3.481×10^2
90	5.541×10^4	7.936×10^3	9.335×10^2	9.789×10^1
100	2.339×10^4	3.010×10^3	3.265×10^2	3.175×10^1

Table 33. Complex modulus of the B-5901 Furfural 2:5 asphalt.

Temperature		Complex modulus in dynes/cm. sq.		
°C	100 Rad/S	10 Rad/S	1 Rad/S	0.1 Rad/S
-40	2.347 X 10^{9}	2.348 X 10^{9}	2.082 X 10^{9}	1.914 X 10^{9}
-30	4.293 X 10^{9}	3.600 X 10^{9}	2.923 X 10^{9}	2.177 X 10^{9}
-20	3.593 X 10^{9}	2.578 X 10^{9}	1.598 X 10^{9}	6.449 X 10^{8}
-20	9.020 X 10^{9}	5.813 X 10^{9}	3.262 X 10^{9}	1.497 X 10^{9}
-10	1.611 X 10^{9}	9.010 X 10^{8}	4.540 X 10^{8}	1.844 X 10^{8}
-10	4.188 X 10^{9}	2.231 X 10^{9}	1.030 X 10^{8}	3.625 X 10^{8}
0	5.996 X 10^{8}	2.723 X 10^{8}	1.135 X 10^{8}	3.713 X 10^{7}
0	1.262 X 10^{9}	5.599 X 10^{8}	2.240 X 10^{8}	8.072 X 10^{7}
10	1.829 X 10^{8}	7.327 X 10^{7}	2.661 X 10^{7}	8.610 X 10^{6}
10	3.133 X 10^{8}	1.178 X 10^{8}	4.347 X 10^{7}	1.304 X 10^{7}
20	8.694 X 10^{7}	2.839 X 10^{7}	8.480 X 10^{6}	2.379 X 10^{6}
30	3.108 X 10^{7}	9.052 X 10^{6}	2.427 X 10^{6}	5.296 X 10^{5}
30	2.820 X 10^{7}	8.792 X 10^{6}	2.470 X 10^{6}	5.947 X 10^{5}
40	9.381 X 10^{6}	2.539 X 10^{6}	6.133 X 10^{5}	1.170 X 10^{5}
40	8.116 X 10^{6}	2.435 X 10^{6}	6.258 X 10^{5}	1.278 X 10^{5}
50	1.779 X 10^{6}	4.349 X 10^{5}	8.958 X 10^{4}	1.409 X 10^{4}
60	6.220 X 10^{5}	1.280 X 10^{5}	2.156 X 10^{4}	2.817 X 10^{3}
60	6.018 X 10^{5}	1.281 X 10^{5}	2.197 X 10^{4}	2.954 X 10^{3}
70	2.064 X 10^{5}	3.527 X 10^{4}	4.930 X 10^{3}	5.556 X 10^{2}
70	1.989 X 10^{5}	3.498 X 10^{4}	4.929 X 10^{3}	5.693 X 10^{2}
80	6.972 X 10^{4}	1.002 X 10^{4}	1.210 X 10^{3}	1.240 X 10^{2}

Table 34. Tan delta of the B-5901 virgin asphalt.

Temperature	Tan delta at			
°C	100 Rad/S	10 Rad/S	1 Rad/S	0.1 Rad/S
-40	3.511 X 10^{-2}	4.630 X 10^{-2}	6.503 X 10^{-2}	1.073 X 10^{-1}
-30	6.798 X 10^{-2}	9.723 X 10^{-2}	1.391 X 10^{-1}	2.029 X 10^{-1}
-20	1.205 X 10^{-1}	1.664 X 10^{-1}	2.271 X 10^{-1}	3.464 X 10^{-1}
-10	1.911 X 10^{-1}	2.565 X 10^{-1}	3.583 X 10^{-1}	5.580 X 10^{-1}
0	3.275 X 10^{-1}	4.973 X 10^{-1}	7.902 X 10^{-1}	1.248 X 10^{0}
0	7.586 X 10^{-1}	9.450 X 10^{-1}	1.261 X 10^{0}	1.896 X 10^{0}
10	1.214 X 10^{0}	1.623 X 10^{0}	2.274 X 10^{0}	3.071 X 10^{0}
20	1.974 X 10^{0}	2.603 X 10^{0}	3.504 X 10^{0}	5.130 X 10^{0}
30	3.242 X 10^{0}	4.296 X 10^{0}	6.313 X 10^{0}	1.215 X 10^{1}
40	4.499 X 10^{0}	6.399 X 10^{0}	1.119 X 10^{1}	2.551 X 10^{1}
50	7.942 X 10^{0}	1.160 X 10^{1}	2.892 X 10^{1}	5.298 X 10^{2}
60	1.060 X 10^{1}	2.089 X 10^{1}	6.255 X 10^{1}	1.774 X 10^{4}
70	1.577 X 10^{1}	3.437 X 10^{1}	1.259 X 10^{2}	1.702 X 10^{35}
80	1.702 X 10^{35}	2.540 X 10^{0}	1.826 X 10^{0}	2.078 X 10^{0}

Table 35. Tan delta of the B-5901 MAH 10% N_2 asphalt.

Temperature		Tan delta at		
°C	100 Rad/S	10 Rad/S	1 Rad/S	0.1 Rad/S
-40	7.067 X 10^{-2}	7.742 X 10^{-2}	9.470 X 10^{-2}	1.708 X 10^{-1}
-30	7.092 X 10^{-2}	9.253 X 10^{-2}	1.399 X 10^{-1}	2.305 X 10^{-1}
-20	8.676 X 10^{-2}	1.376 X 10^{-1}	1.863 X 10^{-1}	3.126 X 10^{-1}
-10	1.060 X 10^{-1}	1.276 X 10^{-1}	2.441 X 10^{-1}	5.382 X 10^{-1}
-10	5.933 X 10^{-1}	5.596 X 10^{-1}	6.632 X 10^{-1}	8.354 X 10^{-1}
0	3.327 X 10^{-1}	4.744 X 10^{-1}	6.446 X 10^{-1}	8.199 X 10^{-1}
0	6.949 X 10^{-1}	7.702 X 10^{-1}	8.933 X 10^{-1}	1.084 X 10^{0}
10	6.905 X 10^{-1}	9.461 X 10^{-1}	1.125 X 10^{0}	1.284 X 10^{0}
10	9.509 X 10^{-1}	1.045 X 10^{0}	1.179 X 10^{0}	1.415 X 10^{0}
20	1.253 X 10^{0}	1.356 X 10^{0}	1.505 X 10^{0}	1.720 X 10^{0}
30	----------	2.54 X 10^{0}	1.826 X 10^{0}	2.078 X 10^{0}
40	4.551 X 10^{0}	2.077 X 10^{0}	2.043 X 10^{0}	2.390 X 10^{0}
50	2.766 X 10^{0}	2.326 X 10^{0}	2.497 X 10^{0}	3.267 X 10^{0}
60	2.962 X 10^{0}	2.777 X 10^{0}	3.159 X 10^{0}	4.636 X 10^{0}
70	3.338 X 10^{0}	3.350 X 10^{0}	4.108 X 10^{0}	6.942 X 10^{0}
80	3.817 X 10^{0}	4.147 X 10^{0}	5.630 X 10^{0}	1.061 X 10^{1}
80	4.057 X 10^{0}	4.265 X 10^{0}	5.594 X 10^{0}	1.076 X 10^{1}

Table 36. Tan delta of the B-5901 CrO_3 4% asphalt.

Temperature °C	Tan delta at 100 Rad/S	10 Rad/S	1 Rad/S	0.1 Rad/S
-50	2.894 X 10^{-2}	4.034 X 10^{-2}	5.878 X 10^{-2}	8.849 X 10^{-2}
-40	4.801 X 10^{-2}	7.669 X 10^{-2}	9.988 X 10^{-1}	1.800 X 10^{-1}
-30	7.742 X 10^{-2}	1.366 X 10^{-1}	2.071 X 10^{-1}	2.920 X 10^{-1}
-20	1.699 X 10^{-1}	2.465 X 10^{-1}	3.263 X 10^{-1}	4.865 X 10^{-1}
-10	3.086 X 10^{-1}	3.890 X 10^{-1}	4.710 X 10^{-1}	6.123 X 10^{-1}
0	4.525 X 10^{-1}	5.259 X 10^{-1}	6.116 X 10^{-1}	7.511 X 10^{-1}
0	5.897 X 10^{-1}	6.173 X 10^{-1}	6.803 X 10^{-1}	7.999 X 10^{-1}
0	5.855 X 10^{-1}	6.083 X 10^{-1}	6.788 X 10^{-1}	8.090 X 10^{-1}
10	5.927 X 10^{-1}	6.790 X 10^{-1}	7.822 X 10^{-1}	9.160 X 10^{-1}
10	7.317 X 10^{-1}	7.993 X 10^{-1}	8.953 X 10^{-1}	1.105 X 10^{0}
10	7.389 X 10^{-1}	8.093 X 10^{-1}	9.041 X 10^{-1}	1.068 X 10^{0}
20	9.745 X 10^{-1}	1.072 X 10^{0}	1.199 X 10^{0}	1.482 X 10^{0}
20	1.041 X 10^{0}	1.116 X 10^{0}	1.214 X 10^{0}	1.443 X 10^{0}
30	1.218 X 10^{0}	1.289 X 10^{0}	1.424 X 10^{0}	1.802 X 10^{0}
30	1.324 X 10^{0}	1.343 X 10^{0}	1.438 X 10^{0}	1.957 X 10^{0}
40	1.451 X 10^{0}	1.497 X 10^{0}	1.675 X 10^{0}	2.394 X 10^{0}
50	1.611 X 10^{0}	1.724 X 10^{0}	2.123 X 10^{0}	4.056 X 10^{0}
60	1.914 X 10^{0}	2.175 X 10^{0}	2.924 X 10^{0}	2.575 X 10^{0}
60	2.275 X 10^{0}	2.281 X 10^{0}	3.006 X 10^{0}	5.281 X 10^{0}
60	2.220 X 10^{0}	2.129 X 10^{0}	2.846 X 10^{0}	5.360 X 10^{0}
70	2.359 X 10^{0}	2.807 X 10^{0}	4.584 X 10^{0}	1.118 X 10^{1}
80	2.862 X 10^{0}	4.063 X 10^{0}	7.991 X 10^{0}	2.062 X 10^{1}
90	3.733 X 10^{0}	6.246 X 10^{0}	1.554 X 10^{1}	3.873 X 10^{1}
100	5.090 X 10^{0}	1.025 X 10^{1}	3.716 X 10^{1}	8.813 X 10^{1}

Table 37. Tan delta of the B-5901 Furfural 2:5 asphalt.

Temperature °C	Tan delta at 100 Rad/S	10 Rad/S	1 Rad/S	0.1 Rad/S
-40	1.469 X 10^{-1}	1.291 X 10^{-1}	1.625 X 10^{-1}	2.290 X 10^{-1}
-30	1.288 X 10^{-1}	1.642 X 10^{-1}	2.383 X 10^{-1}	4.094 X 10^{-1}
-20	2.066 X 10^{-1}	2.978 X 10^{-1}	4.040 X 10^{-1}	6.128 X 10^{-1}
-20	5.038 X 10^{-1}	4.065 X 10^{-1}	4.915 X 10^{-1}	6.258 X 10^{-1}
-10	3.788 X 10^{-1}	4.867 X 10^{-1}	5.947 X 10^{-1}	7.512 X 10^{-1}
-10	5.169 X 10^{-1}	5.299 X 10^{-1}	6.240 X 10^{-1}	8.098 X 10^{-1}
0	5.624 X 10^{-1}	6.571 X 10^{-1}	7.444 X 10^{-1}	8.501 X 10^{-1}
0	6.469 X 10^{-1}	7.080 X 10^{-1}	7.971 X 10^{-1}	9.278 X 10^{-1}
10	7.381 X 10^{-1}	8.058 X 10^{-1}	8.772 X 10^{-1}	1.044 X 10^{0}
10	8.254 X 10^{-1}	8.902 X 10^{-1}	9.665 X 10^{-1}	1.125 X 10^{0}
20	1.044 X 10^{0}	1.101 X 10^{0}	1.205 X 10^{0}	1.411 X 10^{0}
30	1.203 X 10^{0}	1.264 X 10^{0}	1.417 X 10^{0}	1.980 X 10^{0}
30	1.280 X 10^{0}	1.283 X 10^{0}	1.393 X 10^{0}	1.734 X 10^{0}
40	1.415 X 10^{0}	1.462 X 10^{0}	1.718 X 10^{0}	2.632 X 10^{0}
40	1.550 X 10^{0}	1.521 X 10^{0}	1.710 X 10^{0}	2.380 X 10^{0}
50	1.718 X 10^{0}	1.829 X 10^{0}	2.351 X 10^{0}	3.940 X 10^{0}
60	2.012 X 10^{0}	2.405 X 10^{0}	3.572 X 10^{0}	7.663 X 10^{0}
60	2.048 X 10^{0}	2.390 X 10^{0}	3.501 X 10^{0}	7.204 X 10^{0}
70	2.528 X 10^{0}	3.455 X 10^{0}	6.226 X 10^{0}	1.452 X 10^{1}
70	2.567 X 10^{0}	3.429 X 10^{0}	6.018 X 10^{0}	1.539 X 10^{1}
80	3.442 X 10^{0}	5.300 X 10^{0}	1.294 X 10^{1}	6.897 X 10^{0}

APPENDIX E

This appendix contains the various typical types of reactions which are assumed to be occurring when asphalt (virgin) is reacted with each of the following reagents:

1. Maleic anhydride (MAH)
2. Chromium trioxide (CrO_3)
3. Furfural in presence of hydrochloric acid.

REACTIONS WITH MAH:

1. Isoprene reacts with maleic anhydride and forms a Diels-Alder product called 4-methyl-1,2,3,6-tetrahydrophthalic anhydride. The Diels-Alder reactions are highly stereospecific.
2. 2,5-Dimethylfuran reacts with maleic anhydride to form the Diels-Alder adduct.
3. Hydroquinone reacts with maleic anhydride with an elimination of water and formation of a product.
4. Polynuclear aromatic hydrocarbons (PAH) react with maleic anhydride and form a Diels-Alder adduct.

The above reactions are shown on the next page:

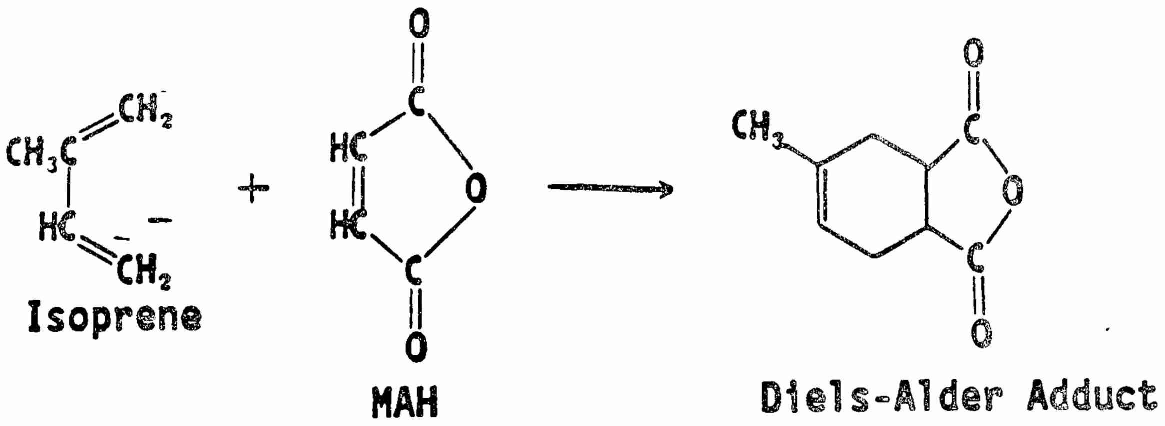
CH₂
CH₃C
HC
CH₂
Isoprene
+
O
C
HC
HC
O
C
O
MAH
CH₃
O
C
O
C
O
Diels-Alder Adduct

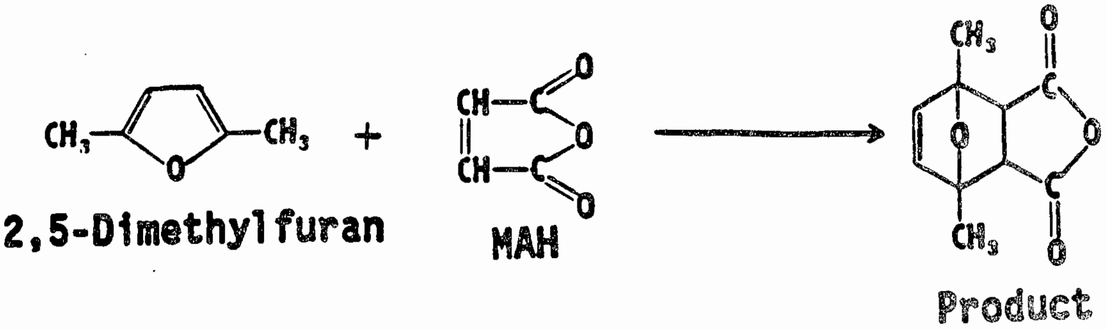
CH₃
O
CH₃
2,5-Dimethylfuran
+
CH
C
O
O
CH
C
O
MAH
CH₃
O
C
O
O
C
O
CH₃
Product

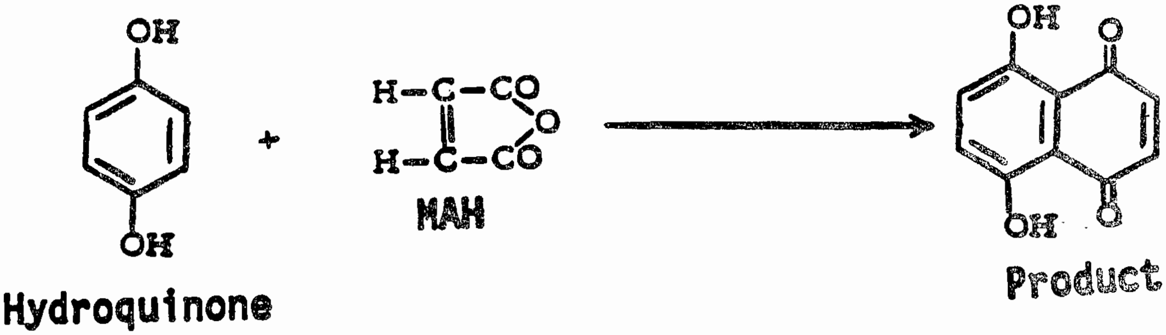
OH
OH
Hydroquinone
+
H—C—CO
O
H—C—CO
MAH
OH
O
OH
O
Product

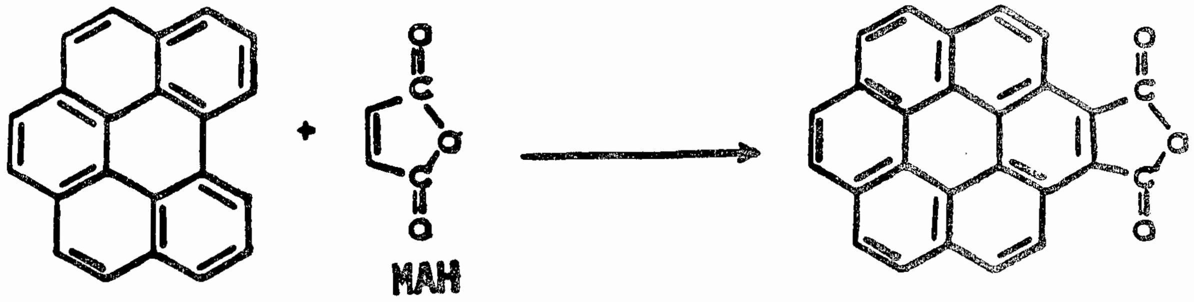
+
O
C
O
C
O
MAH
O
C
O
C
O

PAH

Product

REACTIONS WITH CHROMIUM TRIOXIDE (CrO_3):

1. α-Hydroxy acid is oxidized readily by chromium trioxide to benzophenone and carbon dioxide.
2. Aliphatic side chains attached to aromatic ring systems are more readily oxidized to a carboxyl groups by chromium trioxide.
3. Cyclic ketones are converted into dicarboxylic acid by chromium trioxide.
4. Double bonds are cleaved with chromium trioxide, the products formed, depend on what groups are attached to the olefin.
5. Anthracene oxidizes in the presence of chromium trioxide to form 9,10-anthraquinone.

The above reactions are shown on the next page:

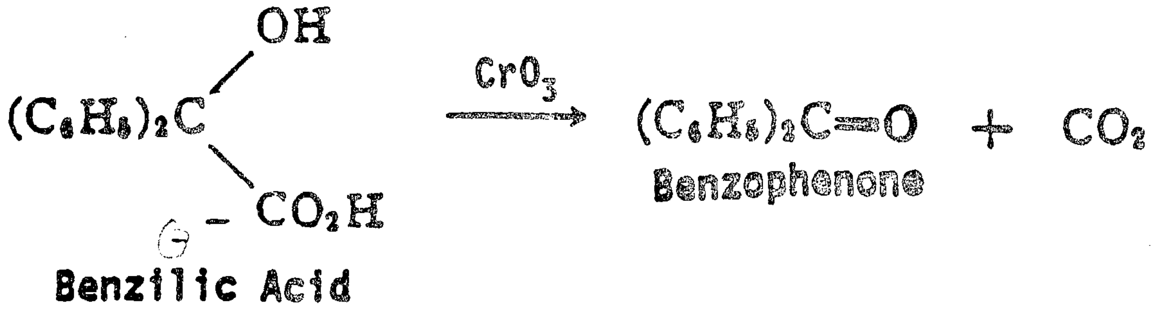

$$(C_6H_5)_2C(OH)CO_2H \xrightarrow{CrO_3} (C_6H_5)_2C{=}O + CO_2$$

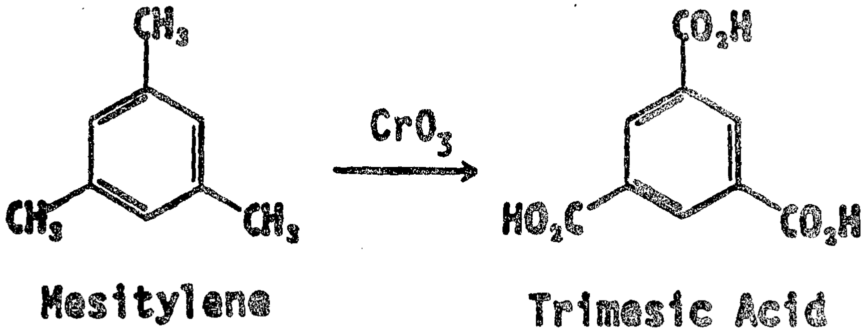

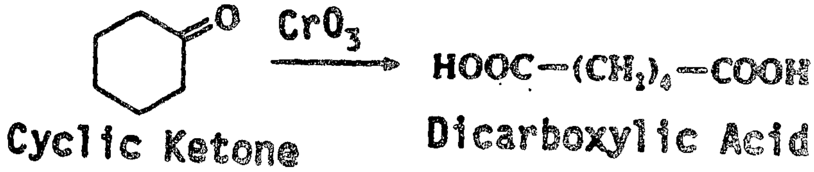

$$\xrightarrow{CrO_3} HOOC{-}(CH_2)_4{-}COOH$$

$$R_2C{=}CHR \xrightarrow{CrO_3} R_2C{=}O + RCOOH$$

Double bond Ketone Acid

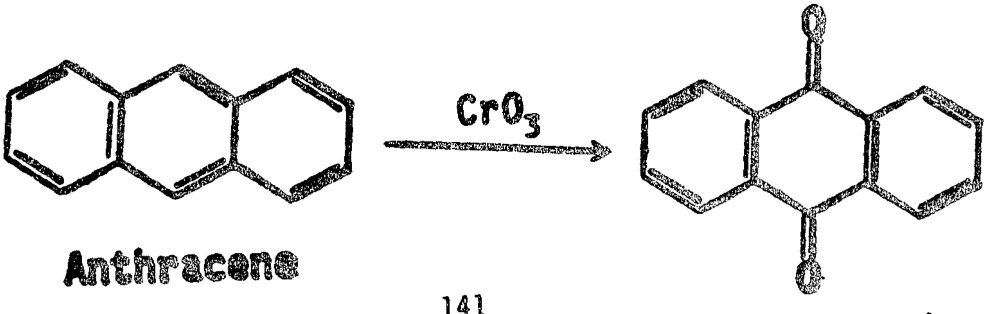

REACTION WITH FURFURAL:

1. Furfural reacts with the phenols and forms the product as shown below:

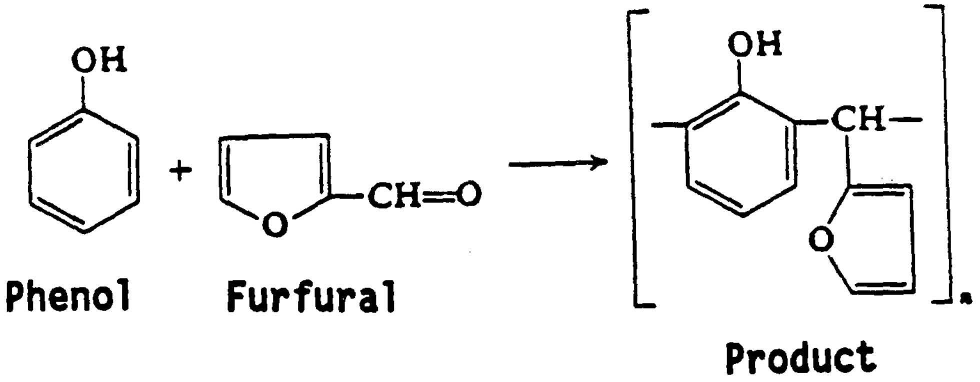

REFERENCES

1. F. N. Finn, K. Nair, and J. Hilliard, "Minimizing Premature Cracking in Asphalt Concrete Pavement," Final Report, National Cooperative Highway Research Program, 9-4, 1973.
2. K. O. Anderson, B. P. Shields, and J. M. Dacyszyn, "Cracking of Asphalt Pavements due to Thermal Effects," Proceedings of the Association of Asphalt Paving Technologists, Vol. 35, 1966, pp. 247-262.
3. R. C. G. Haas, "A Method for Designing Asphalt Pavements to Minimize Low-Temperature Shrinkage Cracking", The Asphalt Institute, College Park, MD., 1973.
4. S. C. Leung and K. O. Anderson, "Evaluation of Asphalt Cements for Low-Temperature Performance," Transportation Research Record, Vol. 1115, 1987, pp. 23-32.
5. P. Jew, J. A. Shimizu, M. Svazic, and R. T. Woodhams, "Polyethylene-Modified Bitumen for Paving Applications," Journal of Applied Polymer Science, Vol. 31, 1986, pp. 2685-2704.
6. V. M. Nadkarni, A. V. Shenoy, and J. Mathew, "Thermomechanical Behavior of Modified Asphalts," Industrial and Engineering Chemistry Product Research and Development, Vol. 24, 1985, pp. 478-484.
7. D. Kumari, B. H. Chollar, J. A. Zenewitz, and J. G. Boone, "Chemical Modification of Asphalts," Preprints, Division of Petroleum Chemistry, American Chemical Society, Vol. 35, No. 3, 1990, pp. 531-540.
8. J. L. Boucher, I-H. Wang, and D. F. Martinez, "Elimination Chemistry in Asphalt," Preprints, Division of Petroleum Chemistry, American Chemical Society, Vol. 35, No. 3, 1990, pp. 550-555.
9. J. L. Boucher, I-H. Wang, R. A. Romaine, "Addition Chemistry in Asphalt," Preprints, Division of Petroleum Chemistry, American Chemical Society, Vol. 35, No 3., 1990, pp. 556-561.
10. J. L. Boucher, I-H. Wang, R. A. Romine,"Nitration Reaction Modification of Asphalts," Preprints, Division of Petroleum Chemistry, American Chemical Society, Vol. 35, No. 3, 1990, pp. 562-567.
11. H. Plancher, S. M. Dorrence, and J. C. Petersen, "Identification of Chemical Types of Asphalt Strongly Adsorbed at the Asphalt-Aggregate Interface and their Relative Displacement by Water," Proceedings of the Association of Asphalt Paving Technologists, Vol. 46, 1977, pp. 151-175.
12. J. C. Petersen, H. Plancher, E. K. Ensley, R. L. Venable and G. Miyake. "Chemistry of Asphalt-Aggregate Interaction: Relationship with Pavement Moisture-Damage Prediction Test," Transportation Research Record, Vol. 843, 1982, pp. 95-104.
13. H. J. Fromm, "The Mechanisms of Asphalt Stripping from Aggregate Surfaces," Proceedings of the Association of Asphalt Paving Technologists, Vol. 43, 1974, pp. 191-219.
14. L. Ciplijauskas, M. R. Piggott and R. T. Woodhams, "Asphalt Ionomers," Polymer Preprint, American Chemical Society, Vol. 19, No. 2, September 1978, pp. 401-406.
15. L. Ciplijauskas, M. R. Piggott and R. T. Woodhams, "Chemically Modified Asphalts for Improved Wet Strength Retention," Industrial and Engineering Chemistry Product Research and Development, Vol. 18, No. 2, 1979, pp. 86-91.

REFERENCES (Continued)

16. "Standard Test Method for Penetration of Bituminous Materials," ASTM D 5-86, Annual Book of ASTM Standards, American Society of Testing and Materials, Vol. 4.03, Philadelphia, PA, 1991.
17. Standard Specifications for Transportation Materials and Methods of Sampling and Testing, Part 11, Penetration of Bituminous Materials, T 49-84, American Association of State Highway and Transportation Officials, Washington, DC, 1986, pp. 73-76.
18. Standard Specifications for Transportation Materials and Methods of Sampling and Testing, Part 11, Kinematic Viscosity of Asphalts, T 201-86, American Association of State Highway and Transportation Officials, Washington, DC, 1986, pp. 721-731.
19. "Standard Test Method for Kinematic Viscosity of Asphalts (Bitumens)", ASTM D 2170-85, Annual Book of ASTM Standards, American Society for Testing and Materials, Vol. 4.03, Philadelphia, PA, 1989.
20. Standard Specifications for Transportation Materials and Methods of Sampling and Testing, Part 11, Viscosity of Asphalts by Vacuum Capillary Viscometer, T 202-84, American Association of State Highway and Transportation Officials, Washington, DC, 1986, pp. 732-739.
21. "Standard Test Method for Viscosity of Asphalts by Vacuum Capillary Viscometer," ASTM D 2171-88, Annual Book of ASTM Standards, American Society for Testing and Materials, Vol. 4.03, Philadelphia, PA, 1989.
22. "Standard Test Method for Softening Point of Bitumen (Ring-and-Ball Apparatus)," ASTM D 36-86 (Reapproved 1989), Annual Book of ASTM Standards, American Society of Testing and Meterials, Vol. 4.03, Philadelphia, PA, 1991.
23. "Standard Test Method for Viscosity of Asphalt with Cone and Plate Viscometer'" ASTM D 3205-86, Annual Book of ASTM Standards, American Socity of Testing and Materials, Vol. 4.03, Philadelphia, PA, 1989.
24. "Standard Test Method for Effect of Heat and Air on Asphaltic Materials (Thin-Film Oven Test)", ASTM D 1754-87, Annual Book of ASTM Standards, American Society of Testing and Materials, Vol. 4.03, Philadelphia, PA, 1989.
25. Standard Specifications for Transportation Materials and Methods of Sampling and Testing, Part 11, Effect of Heat and Air on Asphalt Materials (Thin-Film Oven Test), T 179-83, American Association of State Highway and Transportation Officials, Washington, DC, 1986, pp. 644-647.
26. "Standard Test Method for Recovery of Asphalt from Solution by Abson Method", ASTM D 1856-79 (Reapproved 1984), Annual Book of ASTM Standards, American Society for Testing and Materials, Vol. 4.03, Philadelphia, PA, 1991.
27. N. W. McLeod, "Asphalt Cements: Pen-Vis Number and its Application to Moduli of Stiffness," Journal of Testing and Evaluation, Vol. 4, No. 4, July 1976, pp. 275-282.
28. J. W. Button, J. A. Epps, D. N. Little, and B. M. Gallaway, "Asphalt Temperature Susceptibility and its Effect on Pavements," Transportation Research Record, Vol. 843, 1982, pp. 118-126.

REFERENCES (Continued)

29. J. P. Pfeiffer and P. M. Van Doormaal, "The Rheological Properties of Asphaltic Bitumens," Journal of Institution of Petroleum Technologists, Vol. 22, 1936, pp. 414-440.
30. Design Techniques to Minimize Low-Temperature Asphalt Pavement Transverse Cracking, The Asphalt Institute, College Park, MD., (RR-81-1), 1981.
31. C. Van der Poel, "A General System Describing the Visco-Elastic Properties of Bitumens and its Relation to Routine Test Data." Journal of Applied Chemistry, Vol. 4, 1954, pp. 221-236.
32. P. V. Kandhal and M. E. Wenger, "Asphalt Properties in Relation to Pavement Performance," Transportation Research Record, vol. 544, 1975, pp. 1-13.
33. P. W. Jennings, " High Pressure Liquid Chromatography as a Method of Measuring Asphalt Composition," Research Report No. FHWA-MT-7930, Montana State University, March 1, 1980.
34. T. Marayama, Dynamic Mechanical Analysis of Polymeric Materials, Elsevier Scientific, Amsterdam, 1978.
35. J. D. Ferry, Viscoelastic Properties of Polymers, 3rd edition, John Wiley and Sons, Inc., New York, 1980.
36. H. Plancher, G. Miyake, R. L. Venable and J. C. Petersen, "A Simple Laboratory Test to Indicate the Susceptibility of Asphalt-Aggregate Mixtures to Moisture Damage During Repeated Freeze-Thaw Cycling," Proceedings of the Canadian Technical Asphalt Association, Vol. 25, 1980, pp. 247-262.
37. "Standard Test Methods for Separation of Asphalt into Four Fractions", ASTM D 4124 - 86, Annual Book of ASTM Standards, American Society for Testing and Meterials, Vol. 4.03, Philadelphia, PA, 1989.
38. J. Shim-Ton, K. A. Kennedy, M. R. Piggott and R. T. Woodhams, "Low Temperature Dynamic Properties of Bitumen-Rubber Mixtures," Rubber Chemistry and Technology, Vol. 53, 1980, pp. 88-106.
39. N. W. McLeod, "A 4-year Survey of Low Temperature Transverse Pavement Cracking on Three Ontario Test Roads," Proceedings of the Association of Asphalt Paving Technologists, Vol. 41, 1972, pp. 424-468.
40. H. J. Fromm and W. A. Phang, "Temperature-Susceptibility Control in Asphalt-Cement Specifications," Highway Research Record, Vol. 350, 1970, pp. 30-45.
41. L. J. Bellamy, The Infra-red Spectra of Complex Molecules, John Wiley and Sons, Inc., New York, 1958.
42. H. Plancher, E. L. Green, and J. C. Petersen, "Reduction of Oxidative Hardening of Asphalt by Treatment with Hydrated Lime-A Mechanistic Study," Proceedings of the Association of Asphalt Paving Technologists, Vol. 45, 1976, pp. 1-24.

NTIS does not permit return of items for credit or refund. A replacement will be provided if an error is made in filling your order, if the item was received in damaged condition, or if the item is defective.

Reproduced by NTIS
National Technical Information Service
U.S. Department of Commerce
Springfield, VA 22161

This report was printed specifically for your order from our collection of more than 2 million technical reports.

For economy and efficiency, NTIS does not maintain stock of its vast collection of technical reports. Rather, most documents are printed for each order. Your copy is the best possible reproduction available from our master archive. If you have any questions concerning this document or any order you placed with NTIS, please call our Customer Services Department at (703)487-4660.

Always think of NTIS when you want:
- Access to the technical, scientific, and engineering results generated by the ongoing multibillion dollar R&D program of the U.S. Government.
- R&D results from Japan, West Germany, Great Britain, and some 20 other countries, most of it reported in English.

NTIS also operates two centers that can provide you with valuable information:
- The Federal Computer Products Center - offers software and datafiles produced by Federal agencies.
- The Center for the Utilization of Federal Technology - gives you access to the best of Federal technologies and laboratory resources.

For more information about NTIS, send for our FREE *NTIS Products and Services Catalog* which describes how you can access this U.S. and foreign Government technology. Call (703)487-4650 or send this sheet to NTIS, U.S. Department of Commerce, Springfield, VA 22161. Ask for catalog, PR-827.

Name ______________________________
Address ____________________________
____
____
Telephone __________________________

- Your Source to U.S. and Foreign Government Research and Technology.

U.S. DEPARTMENT OF COMMERCE
Technology Administration
National Technical Information Service
Springfield, VA 22161   (703) 487-4650